Structural and Mechanistic Studies on *E.coli* Porphobilinogen Deaminase and Mutant Variants

By

Sarah Jabeen Awan

A thesis submitted to the University of London for the degree of Doctor of Philosophy in the Faculty of Science

May, 1996

Institute of Ophthalmology, University College London

Supervisors Prof Peter M Shoolingin-Jordan
& Dr Martin J Warren

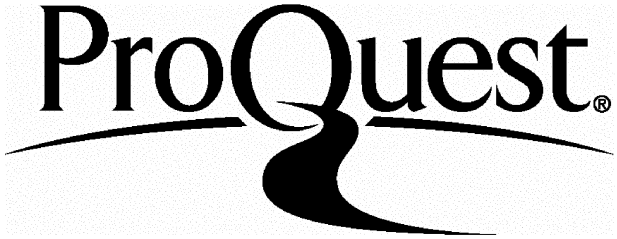

Abstract

Structural and mechanistic studies have been carried out on porphobilinogen deaminase, the third enzyme in the tetrapyrrole biosynthesis pathway. The enzyme catalyses the tetrapolymerisation of porphobilinogen to yield the hydroxymethylbilane product, preuroporphyrinogen. The holoenzyme possesses a novel dipyrromethane cofactor (itself derived from two molecules of porphobilinogen) to which the substrate molecules are bound *via* the enzyme-intermediate complexes ES, ES_2, ES_3 and ES_4 Two aspects of the enzyme have been studied (i) the role of the invariant and catalytically important residue aspartate-84 and (ii) the conversion of apoenzyme (enzyme lacking the cofactor) to holoenzyme.

Three mutants of aspartate-84 were purified and characterised (D84A, D84E and D84N). The D84E mutant was found to exist as free enzyme and also stable enzyme-intermediate complexes. The D84E free enzyme form (E) was crystallised, providing a molecular insight into its catalytic incapacity. Furthermore, the increased stability of the enzyme-intermediate complexes led to the crystallisation of the ES_2 complex, and thus the elucidation of the enzyme in the midst of its catalytic cycle. The D84A and D84N mutants were found to be completely inactive yet existed as ES_2 complexes. An explanation for this phenomenon came from studies on the reconstitution of holoenzyme from apoenzyme.

The apoenzyme was functionally and structurally characterised. Circular dichroism studies revealed considerable secondary structure for the apo-protein, although the apparent susceptibility to modification and denaturation was more indicative of an open conformation. It is proposed that the domains may be tightly packed, but flexible about interdomain hinges due to the absence of the cofactor. The transformation from apoenzyme to holoenzyme was also thoroughly investigated. It was found that whilst the apoenzyme was able to bind porphobilinogen to reconstitute the holoenzyme, probably using the same machinery as employed by holoenzyme for catalysis, the preferred substrate was, in fact, preuroporphyrinogen. This finding gives rise to a new theory on cofactor assembly, and explains the existence of the ES_2 complexes for the catalytically inactive D84A and D84N mutants.

In the Name of Allah, the Most Beneficent, the
Most Merciful.

Allah is the Light of the heavens and the earth.
The parable of His Light is as if ⌈it were⌉ a niche
and within it a lamp,
the lamp is in glass,
the glass as it were a brilliant star,
lit from a blessed tree,
an olive,
neither of the east nor of the west,
whose oil would almost glow forth,
though no fire had touched it.
Light upon Light!
Allah guides to His Light whom He wills.
And Allah sets forth his parables for mankind,
and Allah is All-Knower of everything.

Verily, my prayer, my sacrifice, my living, and
my dying are for Allah, the Lord of all that exists.

Surah An-Nur v.35
Surah Al-An'am v.162

The Holy Qur'an

Acknowledgements

I would like to thank my supervisors, Professor Peter Shoolingin-Jordan and Dr Martin Warren, for giving me the opportunity to undertake this degree and for gentle guidance throughout the research. Their advice, patience and support are gratefully acknowledged.

I am indebted to the following people for their help:

Professor Tom Blundell, Dr Steve Wood and Dr Richard Lambert, previously at Birkbeck College, University of London, for the collaborative crystallography studies; especial thanks are extended to Richard for explaining the complexities of the technique and for hospitality at the Daresbury Laboratories.

Professor Alexander Drake and Dr Giuliano Siligardi, Birkbeck College, University of London, for use of the CD Spectroscopy facilities at the National Chiroptic Centre, and for helpful discussions.

Dr Orval Bateman, Birkbeck College, University of London, for use of the electrospray mass spectrometer.

Professor A. Ian. Scott, Texas A & M University, for the generous gifts of BrPBG and FPBG.

Thanks also to all my friends in the lab who I've had the pleasure of working with: in particular, Sarah and Paul S. for advice and inspiration, and also Russell, El Seed, Sarwar, Chris, Pam, Dave, Josie, Paul O'G., Sue, Ed, Natalie, Richard, Evelyne, Treasa and Seraphina.

Thanks as well to all my other friends who have seen me through the last few years - there are too many to name everyone but I must mention : Saima, Eleni and Kiren, my flatmates; Binoy and Paul, especially for the late-night chauffeuring; Sharena, for the phone-calls; and Wee-Lin, for countless deeds.

I must also thank my relatives for their love and support, especially my brother, Bilal; my sister-in-law, Ayesha; my nephews, Asif and Burhan; my cousin, Zafar; my aunt Aftaab and my uncle Aslam.

Finally, and most importantly, I would like to thank my mother and father for their continual love, prayers and encouragement throughout my life. This thesis is one of the many fruits of their nurturing, and is completed, by the Grace of Allah, with love and respect for them both.

Contents

List of Figures

List of Tables

Abbreviations and Nomenclature

Abbreviations

Å	Angstrom (10^{-10}m)
Abs	Absorption
AIP	Acute intermittent porphyria
5-ALA	5-Aminolaevulinic acid
APS	Ammonium persulphate
ATP	Adenosine triphosphate
BrPBG	Bromoporphobilinogen
CD	Circular dichroism
cpm	Counts per minute
CRIM	Cross reacting immunological material
Da	Dalton
DEAE	Diethylaminoethyl
DNA	Deoxyribonucleic acid
dpm	Disintergrations per minute
DTT	Dithiothreitol
ε_M	Molar extinction coefficient
F_C	Fourier calculated
FPBG	Fluoroporphobilinogen
F_O	Fourier observed
f.p.l.c.	Fast protein liquid chromatography
GSA at	Glutamate semi-aldehyde aminotransferase
k_{cat}	Turnover number
K_m	Michaelis constant
LB	Luria Broth
M_r	Relative molecular mass
NADPH	Nicotinamide adenine dinucleotide phosphate (reduced form)
NEM	N-Ethylmaleimide
n.m.r.	Nuclear magnetic resonance (spectroscopy)
PAGE	Polyacrylamide gel electrophoresis
PBG	Porphobilinogen
PEG	Polyethylene glycol
pKa	Acid dissociation constant
R	Residual index (crystallography)
SDS	Sodium dodecyl sulphate
SRS	Synchroton radiation source
Syn	Synthase
t-RNA	Transfer ribonucleic acid
TAE	Tris-acetate/ethylene diamine tetra acetic acid
TEMED	N, N, N',N'-tetramethylenediamine
Tris	Tris(hydroxymethyl)aminomethane

Amino acids and their abbreviations

Amino Acid	Three Letter code	Single Letter code
Alanine	Ala	A
Arginine	Arg	R
Asparagine	Asn	N
Aspartate	Asp	D
Cysteine	Cys	C
Glutamate	Glu	E
Glutamine	Gln	Q
Glycine	Gly	G
Histidine	His	H
Isoleucine	Ile	I
Leucine	Leu	L
Lysine	Lys	K
Methionine	Met	M
Phenylalanine	Phe	F
Proline	Pro	P
Serine	Ser	S
Threonine	Thr	T
Tryptophan	Trp	W
Tyrosine	Tyr	Y
Valine	Val	V

Nomenclature

The side chains of the pyrrole rings have, in some cases, been given the following abbreviations of single letters for simplicity:

A = $-CH_2COOH$ P = $-CH_2CH_2COOH$
M = $-CH_3$ V = $-CHCH_2$
E = $-CH_2CH_3$

Enzyme intermediate complexes are abbreviated to ES (enzyme with one substrate molecule bound), ES_2 (enzyme with two substrate molecules bound), ES_3 (enzyme with three substrate molecules bound) and ES_4 (enzyme with four substrate molecules bound).

The first and second rings of the dipyrromethane cofactor are referred to as C1 and C2, respectively.

Chapter 1

Introduction

1.1 The Tetrapyrrole Biosynthesis Pathway

1.1.1 Role of Porphobilinogen Deaminase in the Tetrapyrrole Biosynthesis Pathway

Porphobilinogen deaminase is the third enzyme in the tetrapyrrole biosynthesis pathway. The enzyme produces preuroporphyrinogen, a linear tetrapyrrole which is the immediate precursor of the universal template, uroporphyrinogen III, from which all other tetrapyrroles are derived. Modification of the uroporphyrinogen III framework by a range of biosynthetic enzymes results in a variety of essential and complex structures, which have been adopted by nature as prosthetic groups. The modified tetrapyrroles are often referred to as the "pigments of life", and include haem, chlorophyll, sirohaem, factor F_{430} and vitamin B_{12}. The structures of these five modified tetrapyrroles are given in figure 1.1.

Figure 1.1 The Structures of Five Modified Tetrapyrroles, Originating from Uroporphyrinogen III

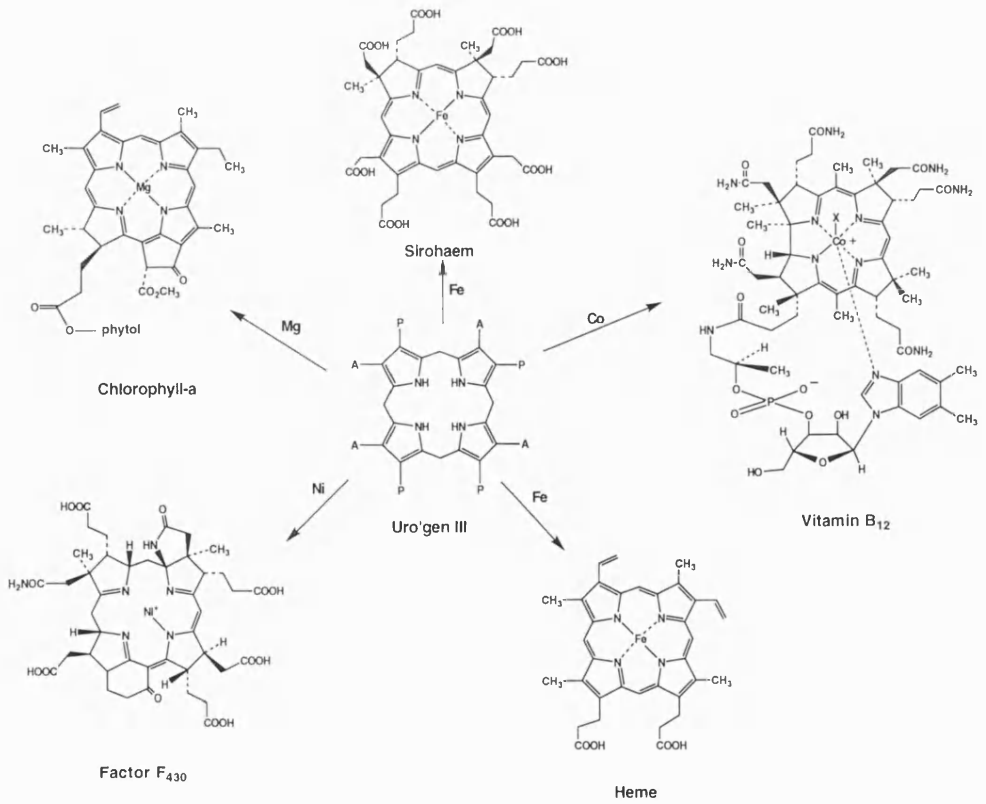

1.2 Biosynthesis of Uroporphyrinogen III

The first real progress made in identifying the intermediates in the tetrapyrrole biosynthesis pathway was made in the 1940's by Shemin, who used himself as an experimental subject to establish that glycine was a precursor of haem (Shemin and Rittenberg, 1945). Over the subsequent years, the pathway has been extensively studied and a considerable understanding of the pathway enzymes and their mechanisms has been acquired. The area has also been the subject of many reviews (Jordan, 1991; Warren and Scott, 1990; Battersby and Leeper, 1990).

The first committed precursor in the tetrapyrrole biosynthetic pathway is 5-aminolaevulinic acid, which is produced by two distinct routes. In mammals and the α-subclass of the purple bacteria, 5-aminolaevulinic acid is synthesised from succinyl CoA and glycine by the catalytic action of 5-aminolaevulinic acid synthase, along the Shemin route in a reaction requiring pyridoxal phosphate (Leeper, 1985). In higher plants and most prokaryotic systems, 5-aminolaevulinic acid is synthesised from the intact carbon skeleton of glutamate. All five carbons of glutamate are incorporated into 5-aminolaevulinic acid, and so this pathway is termed the the C-5 pathway (Beale and Castelfranco, 1974). The two routes for 5-aminolaevulinic acid production can be seen in figure 1.2.

The pyrrole, porphobilinogen, is formed by the condensation of two molecules of 5-aminolaevulinic acid in a Knorr-type reaction (Fabiano and Golding, 1991). The reaction is catalysed by the enzyme 5-aminolaevulinic acid dehydratase (Shemin, 1972). The enzyme is generally found as a homo-octomer and requires either zinc or magnesium for catalytic activity. In this reaction, the first 5-aminolaevulinic acid molecule binds to the enzyme through a lysine group, forming the propionate side chain moiety of the final pyrrole product. The second 5-aminolaevulinic acid molecule then occupies the position next to the reactive amino methyl group, and eventually becomes the acetate side chain moiety. The metal ion is probably required as a Lewis acid in polarizing the carbonyl group.

The final steps, the conversion of the pyrrole units into the cyclised tetrapyrrole structure of uroporphrinogen III, require two enzymes: porphobilinogen deaminase and uroporphyrinogen III synthase (cosynthase).

Figure 1.2 The Two Routes of 5-Aminolaevulinic Acid Production

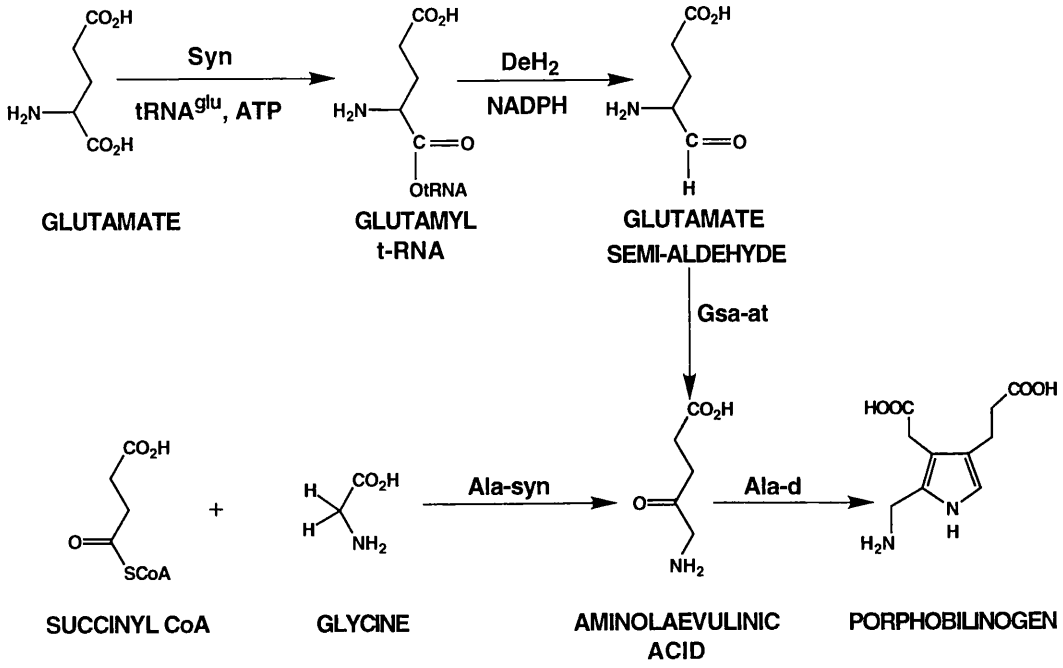

Porphobilinogen deaminase catalyses the head to tail condensation of four molecules of porphobilinogen to yield the linear 1-hydroxymethylbilane, preuroporphyrinogen (the enzyme is sometimes referred to as hydroxymethylbilane synthase). The enzyme catalyses the reaction in a stepwise manner, in which the four substrate molecules are bound sequentially to a novel cofactor. The cofactor is a dipyrromethane that is derived itself from two molecules of the substrate, porphobilinogen, and is covalently attached to the protein through residue cysteine-242 (Jordan and Warren, 1987; Hart *et al.*, 1987). Once attached the dipyrromethane remains bound as a resident cofactor, allowing its free α-position to act as the initiation site for polypyrrole synthesis. The catalytic cycle of the enzyme proceeds *via* covalently bound enzyme intermediate complexes which have

been termed ES, ES_2, ES_3 and ES_4 and are formed by the sequential addition of the substrate-derived pyrrole units. After the fourth substrate ring has been bound, the reaction is terminated and the product, preuroporphyrinogen, is released by hydrolytic cleavage of the bond between the cofactor and the first ring, ring 'a', of the tetrapyrrole. The basic mechanism of porphobilinogen deaminase is depicted in figure 1.3, and is described in more detail later in the chapter.

Figure 1.3 The Reaction Catalysed by Porphobilinogen Deaminase

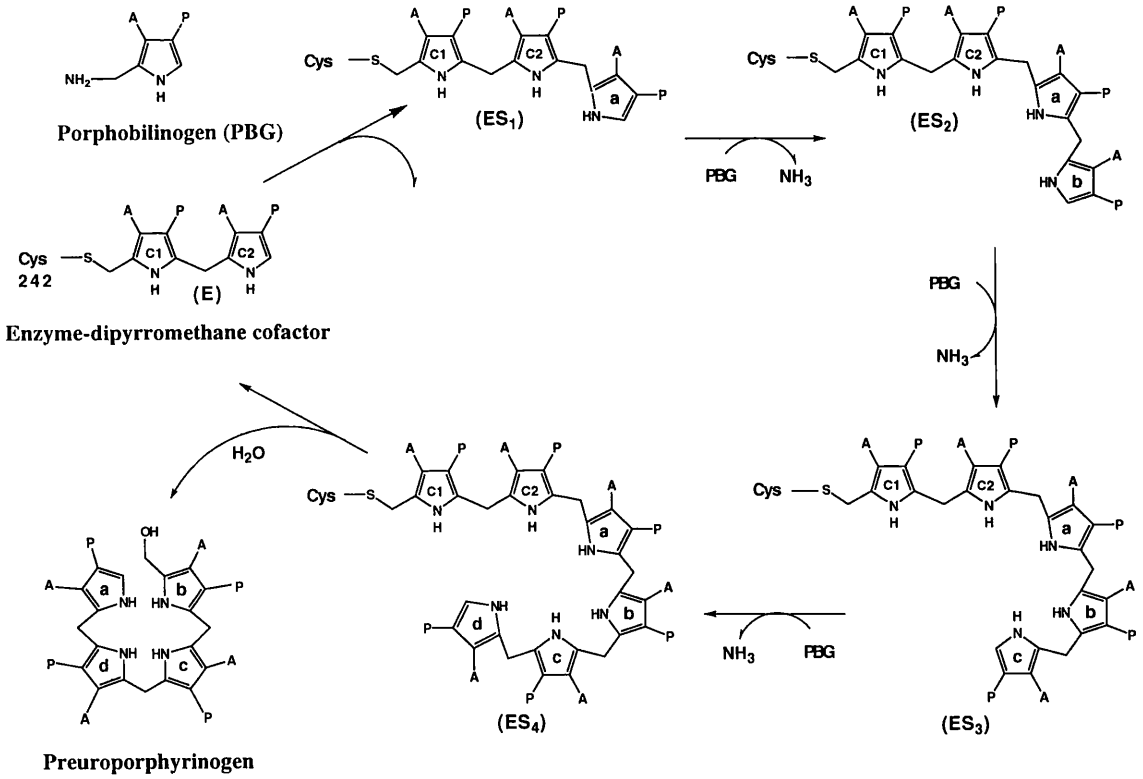

Finally, preuroporphyrinogen is converted to uroporphyrinogen III by the enzyme cosynthase (uroporphyrinogen III synthase). This enzyme rearranges the 'd' ring of preuroporphyrinogen and cyclises the structure to yield the physiologically important uroporphyrinogen III isomer. The mechanism of the enzyme is still unclear, largely because the instability of its substrate makes the enzyme difficult to characterise fully. In the absence of cosynthase, preuroporphyrinogen will cyclise "chemically" without the 'd'

ring rearrangement to yield uroporphyrinogen I. The possible fates of preuroporphyrinogen, in the presence and absence of cosynthase, are illustrated in figure 1.4.

Figure 1.4 The Two Fates of Preuroporphyrinogen

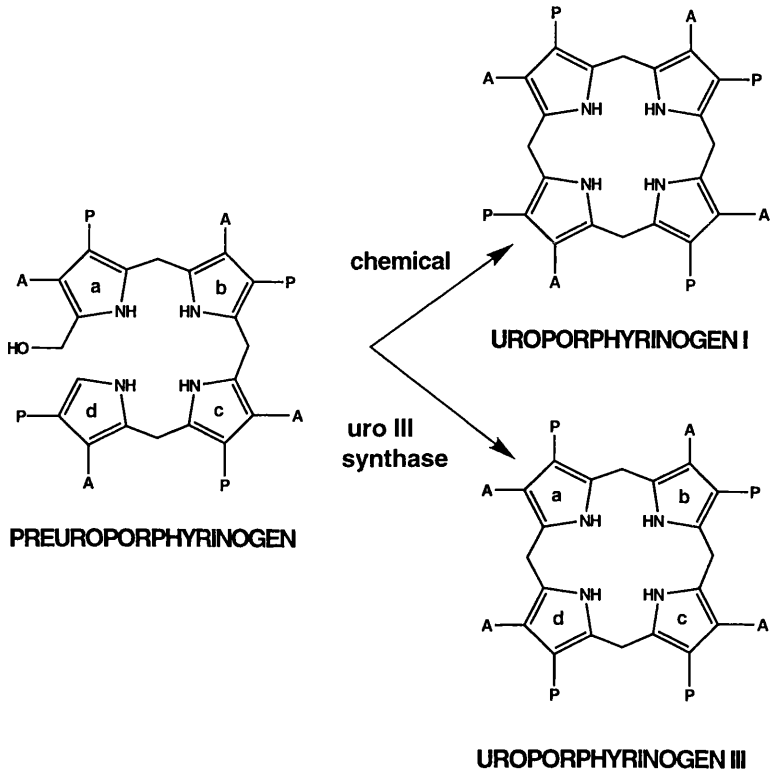

The tetrapyrrole biosynthesis pathway is regulated. The *in situ* substrate concentrations are normally much below the Michaelis constants of all the enzymes, and therefore each reaction can be increased to its maximum velocity if the substrate concentration is raised (Elder, 1982). Particular regulatory functions come from two enzymes, 5-aminolaevulinic acid synthase and porphobilinogen deaminase, as they exhibit approximately ten-fold lower relative activities than the remaining enzymes of the pathway (Hayashi, 1987). 5-Aminolaevulinic acid synthase would appear to be especially important in control as the rate limiting enzyme, as it is noted to be induced under conditions of haem requirements.

In animal and yeast cells, the enzymes of the uroporphyrinogen III biosynthesis pathway are distributed between the mitochondrial and cytosolic compartments (Elder, 1976; Labbe-Bois and Labbe, 1989). The first step of 5-aminolaevulinic acid production is found to occur *via* the enzyme 5-aminolaevulinic acid synthase in the mitochondrion, and the subsequent three steps take place in the cytoplasm. In photosynthetic eukaryotes, however, the enzymes for the production of uroporphyrinogen III, beginning with the synthesis of 5-aminolaevulinic acid from glutamate, are found to be localised almost exclusively in the plastids (Kannangara *et al.*, 1988; Fuesler *et al.*, 1984). (The enzyme cosynthetase has not been studied for its subcellular localisation and therefore cannot be included). In contrast, the phyloflagellate bacteria, *Euglena gracilis*, has been shown to possess both 5-aminolaevulinic acid synthase as well as the C_5 pathway of synthesis (Beale *et al.*, 1981). This posed the interesting possibility of the presence of two separate pathways for uroporphyrinogen III biosynthesis, requiring a duplication of the enzymes, one set of which would not be plastid-localised (Weinstein and Beale, 1983). Subsequent studies suggest, however, that there is evidence for only one pathway for uroporphyrinogen III biosynthesis (Shashidhara and Smith, 1991).

1.3 Prokaryotic Gene Organisation

A considerable amount of the study of the pathway has been carried out on enzymes purified from, and overexpressed in, *E. coli*. The genes coding for the tetrapyrrole biosynthesis enzymes in *E. coli* are prefixed *hem* and are dispersed throughout the genome. The gene names are given in table 1.1. The *hemC* gene, which encodes for porphobilinogen deaminase, is located adjacent to the *cyaA* gene on the *E. coli* K12 chromosome and is part of an operon which also includes the *hemD* gene (Thomas and Jordan, 1986).

1.4 Eukaryotic Gene Organisation

The *hem* genes in mammals have been mapped mainly on the human chromosome using classical family linkage studies. The first human *hem* gene mapped was that encoding for porphobilinogen deaminase (Meisler *et al.*, 1980). Human porphobilinogen deaminase is found to exist as two

Table 1.1 The *hem* Genes found in *E. coli* , Encoding for the Enzymes of the Uropohyrinogen III Biosynthesis Pathway

Locus	Enzyme
hemA	Glutamyl-tRNA reductase
hemL	Glutamate 1-semialdehyde aminotransferase
hemB	5-Aminolaevulinic acid dehydratase
hemC	Porphobilinogen deaminase
hemD	Uroporphyrinogen III synthase

isoenzymes, a housekeeping and erythroid form, both encoded by a single gene which is regulated by two promoters. The structural gene is made up of 15 exons which extend over 10kb of DNA on the long arm of chromosome 11 (Yoo *et al.*, 1993; Wang *et al.*, 1981), specifically located on band 11q23 (Tunnacliffe and McGuire, 1990). The two forms of the enzyme are produced by transcription from two separate promoters: a ubiquitous promoter, resulting in the house-keeping enzyme and a downstream erythroid-specific promoter (Chretien *et al.*, 1988; Grandchamp *et al.*, 1987; Raich *et al.*, 1986). The ubiquitous housekeeping protein is longer and consists of 361 amino acid residues (encoded by exons 1, 3-15), whereas the erythroid enzyme is 17 residues shorter (encoded by exons 2-15).

The genes for the remaining enzymes of the uroporphyrinogen III biosynthesis pathway have also been mapped in humans. The genes are located as follows: 3pter for 5-aminolaevulinic acid synthase, 9q34 for 5-aminolaevulinic acid dehydratase, and 10q25.2 for cosynthase.

1.5 Porphobilinogen Deaminase, as Isolated from a Number of Sources

Porphobilinogen deaminase has been purified from a number of prokaryotic and eukaryotic organisms, including *Rhodobacter sphaeroides* (Jordan and Shemin, 1973), *Escherichia coli* (Hart *et al.*, 1986; Thomas and Jordan, 1986; Jordan *et al.*, 1988), *Euglena gracilis* (Williams *et al.*, 1981),

Chlorella regularis (Shioi *et al.*, 1980), human erythrocytes (Anderson and Desnick, 1980), rat liver (Mazzetti and Tomio, 1988) and yeast (Correa-Garcia *et al.*, 1991). The enzyme has also been isolated from plant sources, including spinach (Higuchi and Bogorad, 1975), pea (*Pisum sativum L.*) (Spano and Timko, 1991) and Thame cress (*Arabidopsis thaliana*) (Jones and Jordan, 1994). In all cases, the purified enzyme is found to be monomeric, with a molecular mass ranging from 34,000 to 44,000 Da and an optimal pH between 8.0 and 8.5.

The cloned cDNAs and nuclear genes encoding porphobilinogen deaminase have also been isolated and sequenced from a variety of organisms, including *E.coli* (Thomas and Jordan, 1986), human erythrocytes (Raich *et al.*, 1986), rat spleen (Stubnicer *et al.*, 1988), *Erwinia chrysanthemi*, Danchin and Lanzen, 1988), mouse (Beaumont *et al.*, 1989), *E.gracilis* (Sharif *et al.*, 1989), *Bacillus subtilis* (Petricek *et al.*, 1990), yeast (Keng *et al.*, 1992), pea (*P.sativum L.*) (Witty *et al.*, 1993), *Pseudomonas aeruginosa*, Sonsteby *et al.*, 1994), Thame cress (*A.thaliana*) (A.G. Smith), *Chlorobium josuii* (Fujino *et al.*), *Chlorobium vibrioforme* (Majumder and Wyche), *Yersinia intermedia* (Glaser and Danchin) and *Mycobactrium leprae* (Robinson and Smith). The primary sequences of porphobilinogen deaminase isolated from these sources can be seen in figure 1.5. Despite the highly divergent sources of the enzyme, the primary sequences are seen to display considerable similarities. A number of conserved residues are prominent, which clearly must play an important role in substrate binding, catalysis or structure. The functions of the conserved residues are better understood in light of the resolved three-dimensional crystal structure of porphobilinogen deaminase (Louie *et al.*, 1992), and are dealt with in detail later in the chapter.

Figure 1.5 The Sequence Alignments of Porphobilinogen Deaminase from a Number of Sources

The numbering system shown applies only to the sequence derived from *E. coli*. The sources and abbreviations are as follows: *Escherichia coli* (*E. coli*), rat, mouse, human, *Arapidopsis thaliana* (arab), pea, *Pseudomonas aeruginosa* (pseu), *Euglena gracilis* (euggr), *Bacillus subtilis*, (bascu), *Chlorobium vibrioformes* (chlvi), yeast, *Chlorobium josui* (chljo), *Yersinia intermedia* (yerin), *Erwinia chrysanthemi* (erwch), and *Mycobacterium leprae* (mylep).

Invariant or highly conserved residues are marked with *.

```
                                        1                                  24
                                                 *     * *  *  *
ecoli ----------  ----------  -----MLDNV  LRIATRQSPL  ALWQA-HYVK
rat   ----------  ----------  -------MRV  IRVGTRKSQL  ARIQTDTVVA
mouse ----------  MSGNGNAATT  AEENGSKMRV  IRVGTRKSQL  ARIQTETVVA
human ----------  MSGNGNAAAT  AEENSPKMRV  IRVGTRKSQL  ARIQTDSVVA
arab  ----------  --------CV  AVEQKTRTAI  IRIGTRGSPL  ALAQAYETRE
pea   ----------  -----SLAVE  QQTQQNKTAL  IRIGTRGSPL  ALAQAHETRD
pseu  ----------  ----------  -----MSSRE  IRIATRQSAL  ALWQAEYVNS
euggr TKPADLQEVS  GGRIWSLAST  TGSNIGAGKT  VRVATRKSPL  AMWQAEFIQS
bacsu ----------  ----------  ------MMRT  IKVGSRRSKL  AMTQTKWVIQ
chlvi ----------  ----------  ----------  ----------  ----------
yeast ----------  ----------  -----MGPET  LHIGGRKSKL  AVIQSNHVLK
chljo ----------  ----------  ---MVFDMKK  IRIGSRDSKL  AIIQSELIMS
yerin ----------  ----------  -----MLDKI  IRIATRQSPL  ALWQA-HYVQ
erwch ----------  ----------  -----MVDTI  LRIATRQSPL  ALWQA-HFVQ
mylep ----------  ----------  ---------M  IRIGTRGSLL  ATTQAALVRD

     25                                                          70
                                    **       *   * *   ** **    *
ecoli DKLMASHPGL  ----VVELVP  MVTRGDVILD  TPLAKVGGKG  LFVKELEVAL
rat   -MLKTLYPGI  Q----FEIIA  MSTTGDKILD  TALSKIGEKS  LFTKELENAL
mouse -MLKALYPGI  Q----FEIIA  MSTTGDKIVD  TALSKIGEKS  LFTKELENAL
human T-AKASYPGL  Q----FEIIA  MSTTGDKILD  TALSKIGEKS  LFTKELEHAL
arab  -KLKKKHPEL  VEDGAIHIEI  IKTTGDKILS  QPLADIGGKG  LFTKEIDEAL
pea   -KLMASHTEL  AEEGAIQIVI  IKTTGDKILS  QPLADIGGKG  LFTKEIDEAL
pseu  TGLEQAHPGL  T----VTLLP  MTSRGDKLLD  APLAKIGGKG  LFVKELETAL
euggr -ELEALWPGI  T----VELQP  MSTRGDKILD  STLAKVGGKG  LFVKELETAL
bacsu -KLKEINPSF  ----AFEIKE  IVTKGDRIVD  VTLSKVGGKG  LFVKEIEQAL
chlvi ----------  ---MNISLKL  VKTTGDVLLD  SPLSKIGDMG  LFTKDIEKHL
yeast --LIEEKYPD  YD---CKVFT  LQTLGDQIQF  KPLYSFGGKA  LWTKELEDHL
chljo AIRKYDPDIE  -----LELIT  MKTTGDKILD  KTLDKIEGKG  LFVKELDNAL
yerin HLLQANHPGL  Q----VELVP  MVTRGDIILD  TPLAKVGGKG  LFVKELELAL
erwch QRLEACHPGL  ----RVELVP  MVTRGXLLLD  TPLAKVGGKG  LFVKELELAL
mylep ALIANGHPA-  ------ELVI  VNTAGDQ--S  SASIDSLGVG  VFTTALRAAI
```

```
     71                                                                 113
                *    *** ** *     *           *    *
ecoli LEN----RAD  IAVHSMKDVP  VEFPQGLGLV  TICEREDPRD  AFV---SNNY
rat   EKNE----VD  LVVHSLKDVP  TILPPGFTIG  AICKRENPCD  AVVFEGKFIG
mouse EKNE----VD  LVVHSLKDVP  TILPPGFTIG  AICKRQNPCD  AVVFHPKFIG
human EKNE----VD  LVVHSLKDLP  TVLPPGFTIG  AICKRENPHD  AVVFHPKFVG
arab  ING----HID  IAVHSMKDVP  TYLPEKTILP  CNLPREDVRD  AFI--CLTAA
pea   ING----DID  IAVHSMKDVP  TYLPEETILP  CNLPREDVRD  AFI--SLSAA
pseu  LEG----AAD  IAVHSMKDVP  MDFPEGLGLY  TICEREDPRD  AFV--SNTYA
euggr LEN----RSD  IAVHSTKDVP  MELPEGLVLG  VICKRHDPCD  AIVFPKGSNL
bacsu LNEE----ID  MAVHSMKDMP  AVLPEGLVIG  CIPEREDPRD  ALI---SKNR
chlvi LAGE----ID  LAVHSLKDVP  TVRRKAWLSP  RSPSVKTPRR  HHF-------
yeast YHDDPSKKLD  LIVHSLKDMP  TLLPEGFELG  GITKRVDPTD  CLVMPFYSAY
chljo YNNE----VD  ITVHSYKDMP  LEENPELPVV  ALSKREDPRD  AFI--LPQNG
yerin LDG----RAD  IAVHSMKDVP  VAFPEGLGLV  TICEPDDPRD  AFV--SPHFA
erwch LEN----RAD  IAVHSMKDVP  VEF-------  ----------  ----------
mylep EEG----CVD  AAVHSYKDLP  TADDPRFTVA  AIPPRNDPRD  AVVTRDELVL

       114                                                         159
           *         **     **  *       * *      *  **  *** **
ecoli ---DSLDALP  AGSIVGTSSL  RRQCQLAERR  PDLIIRSL-R  GNVGTRLSKL
rat   ---KTLETLP  EKSAVGTSSL  RRVAQLQRKF  PHLEFKSI-R  GNLNTRLRKL
mouse ---KTLETLP  EKSAVGTSSL  RRVAQLQRKF  PNLEFKSI-R  GNLNTRLRKL
human ---KTLETLP  EKSVVGTSSL  RRAAQLQRKF  PHLEFRSI-R  GNLNTRLRKL
arab  ----TLAELP  AGSVVGTASL  RRKSQILHKY  PALHVEENFR  GNVQTRLSKL
pea   ----SLADLP  AGSVIGTASL  RRKSQILHRY  PSLTVQDNFR  GNVQTRLRKL
pseu  ----SLADLP  AGSVVGTSRL  GRQAQLLARR  PDLQIRFL-R  GNVNTRLAKL
euggr ---KSLEDLP  HGARVGTSSL  RRQCQLLLKR  PDLKFLEL-R  GNVNTRLAKL
bacsu ---VKLSEMK  KGAVIGTSSL  RRSAQLLIER  PDLTIKWI-R  GNIDTRLQKL
chlvi QVRQGVDGPS  AEAKMATSSL  RRMSQLLSLR  PDLEIMDI-R  GNLNTRFKKF
yeast ---KSLDDLP  DGGIVGTSSV  RRSAQLKRKY  PHLKFESV-R  GNIQTRLQKL
chljo ---------E  NGEPIGSSSL  RRQLQLKELF  PGCKTAPI-R  GNVQTRLKKL
yerin ----HIDDLP  AGSIVGNSSL  RRQCQLRERR  PDLIIRDL-R  GNVGTRLAKL
erwch ----------  ----------  ----------  ----------  ----------
mylep ------AELP  AGSLVGTSSP  RRAAQLRALG  LGLEIRPL-R  GNLDTRLNRV

    160                                                         203
                   ** **  *                                *  ***
ecoli D-NGEYDAI-  ILAVAGLKRL  GLESRI-RAA  LPPEI--VSL  PAVGQGAVGI
rat   DEQLEFSAI-  ILAVAGLQRM  GWQNRV-GQI  LHPEE---CM  YAVGQGALAV
mouse DELQEFSAI-  VLAVAGLQRM  GWQNRV-GQI  LHPEE---CM  YAVGQGALAV
human DEQQEFSAI-  ILATAGLQRM  GWHNRV-GQI  LHPEK---CM  YAVGQGALGV
arab  -QGGKVQAK-  LLALAGLKRL  SMTENV-ASI  LSLDE---ML  PAVAQGAIGI
pea   S-EGVVKAT-  LLALAGLKRL  NMTENV-TST  LSIDD---ML  PAVAQGAIGI
pseu  D-AGEYDAI-  ILAAAGVIRL  GFESRI-RSS  ISVDD---SL  PAGGQGAVGI
euggr D-SGDYDAI-  ILAAAGLKRL  GFSDRVLPGE  TNIIDMNVMC  PAAGQGALSI
bacsu E-TEDYDAI-  ILAAAGLSRM  GWKQDVVTE-  --FLEPERCL  PAVGQGALAI
chlvi D-EGDFDAM-  MLAYAGVYRL  EFSDRI-TEI  LPHET---ML  PAVGQGALGI
yeast DDPKSPYQCI  ILASAGLMRM  GLENRI-TQR  FHSDT---MY  HAVGQGALGI
chljo D-SGEFSAI-  VLAAAGIKRL  GLESRI-GRY  FSVDE---IL  PAASQGIIAV
yerin D-NGDYHAI-  ILAVAGLNRL  GLASRI----  ----------  ----------
erwch ----------  ----------  ----------  ----------  ----------
mylep SSGD--LDAI  VVARAGLARP  GRLDEV----  TETLDPVQMV  PAPAQGAIAV
```

```
    204                                                                253
        *  *                          **          ***     *
ecoli ECRLDDSRTR  ELLAALNHHE  TALRVTAERA  MNTRLEGGCQ  VPIGSYAELI
rat   EVRAKDQDIL  DLVGVLHDPE  TLLRCIAERD  FLRHLEGGCS  VPVAVHTVMK
mouse EVRAKDQDIL  DLVSVLHDPE  TLLRCIAERA  FLRHLEGGCS  VPVAVHTVIK
human EVRAKDQDIL  DLVGVLHDPE  TLLRCIAERA  FLRHLEGGCS  VPVAVHTAMK
arab  ACRTDDDKMA  TYLASLNHEE  TRLAISCERA  FLETLDGSCR  TPIAGYASKD
pea   ACRSNDDKMA  EYLASLNHEE  TRLAISCERA  FLTTLDGSCR  TPIAGYASRD
pseu  ECRTADSDLH  ALLEPLHHTD  TALRVTAERA  LNKRLNGGCQ  VPIACYAIRE
euggr ELRTNDPEIA  ALLEPLHHIP  DAVTVACERA  MNRRLNGGCQ  VPISGFAQLK
bacsu ECRESDEELL  ALFSQFTDEY  TKRTVLAERA  FLNAMEGGCQ  VPIAGYSVLN
chlvi ETRTDDAETR  EIVRVLNDDN  TEMCCRAERA  LLRHLQGGCQ  IPIGSFGSYI
yeast EIRKGDTKMM  KILDEICDLN  ATICCLSERA  LMRTLEGGCS  VPIGVESKYN
chljo QGRVGENF--  DFLKLFHSEE  SLCISLAERT  FVREMNGGCS  TPIAAYATIQ
yerin ----------  ----------  ----------  ----------  ----------
erwch ----------  ----------  ----------  ----------  ----------
mylep ECRAGDSRLV  AVLAALDDAD  TRAAVTAERV  LLAELEAGCS  APVGAIAQVV

      254                         283
                 *    *
ecoli --DGEIWLRG  LVGAPDGSQI  IRGERRGA--  ----------  ----------
rat   --DGQLYLTG  GVWSLDGSDS  MQETMQATIQ  VPVQQEDGPE  DDPQLVGITA
mouse --DGQLYLTG  GVWSLDGSDS  MQETMQATIQ  VPVQQEDGPE  DDPQLVGITA
human --DGQLYLTG  GVWSLDGSDS  IQETMQATIH  VPAQHEDGPE  DDPQLVGITA
arab  -EEGNCIFRG  LVASPDGTKV  LETSRKGPYV  ----------  ----------
pea   -KDGNCLFRG  LVASPDGTRV  LETSRIGSYT  ----------  ----------
pseu  --GDQLWLRG  LVGQPDGTQL  LRAEGR----  ----------  ----------
euggr --GGQLRMEA  RVGSVTGKGP  LIIQSKTFRL  PWSGRTWPQL  ----------
bacsu --GQDEIMTG  LVASPDGKII  FKETVT----  ----------  ----------
chlvi --DGTLKLLA  FVGSVDGKTG  LRNEVTKAVK  ----------  ----------
yeast EETKKLLLKA  IVVDVEGTEA  VEDEIEMLIE  ----------  ----------
chljo -GSEIILKGL  YCNETTGELR  KECVSGNRNN  ----------  ----------
yerin ----------  ----------  ----------  ----------  ----------
erwch ----------  ----------  ----------  ----------  ----------
mylep ESIDGEGRVF  EELSLRGCVA  ALDGSDVIRA  ----------  ----------

          284                                       313
                    *
ecoli -------PQD  AEQMGISLAE  ELLNNGAREI  LAEVYNGDAP  A--
rat   RNIPRGAQLA  AENLGISLAS  LLLNKGAKNI  LDVARQLNDV  R--
mouse RNIPRGAQLA  AENLGISLAS  LLLNKGAKNI  LDVARQLNDV  R--
human RNIPRGPQLA  AQNLGISLAN  LLLSKGAKNI  LDVARQLNDA  H--
arab  -------YED  MVKMGKDAGQ  ELLSRAGPGF  FGN-------  ---
pea   -------YED  MMKIGKDAGE  ELLSRAGPGF  FNS-------  ---
pseu  -----APLAD  AEALGVRVAE  DLLEQGAEAI  LEAVYGEAGH  P--
euggr -------QKE  SEALGVEVAD  MLLADGAQAY  LDEAYASRTL  GWA
bacsu -------GND  PEEVGKRCAA  LMADKGAKDL  IDRVKRELDE  DGK
chlvi ------TPEE  AEAVGIELAE  ILLSMGAEKI  LADIRKTC--  ---
yeast -----NVKED  SMACGKILAE  RMIADGAKKI  LDEINLDRIK  ---
chljo ----------  ----------  -PVELGYELV  KKMKSSKSI-  ---
yerin ----------  ----------  ----------  ----------  ---
erwch ----------  ----------  ----------  ----------  ---
mylep --SGISTSGR  AFELGLAVAV  ELFELGAREL  MWGARSDRAR  GS-
```

1.6 Characterisation of *E. coli* Porphobilinogen Deaminase

A major breakthrough in the study of porphobilinogen deaminase came from the cloning and sequencing of the gene encoding the enzyme, *hemC*, from *E. coli* (Thomas and Jordan, 1986). Whilst the enzyme is found to be ubiquitous, its expression is low and accounts for only 0.01% of the total soluble protein. The identification of the gene encoding the enzyme allowed genetically engineered strains to be produced, which yielded almost 100 times the porphobilinogen deaminase found in the wild-type *E. coli*.

The porphobilinogen deaminase enzyme was subsequently purified and characterised (Jordan *et al.*, 1988). The enzyme was found to have a native molecular mass of 32000±2000 Da, as determined by gel filtration chromatography and 35,000 Da as determined by denaturing polyacrylamide gel electrophoresis. The gene sequence gave an estimated molecular mass of 33857 Da. The enzyme was found to have a pH optimum between 8.4 and 9, becoming inactive below pH 6.0 and irreversibly inactive below pH 4.0. The enzyme had a specific activity of 43μmol of porphobilinogen/hr/mg of protein, and a K_m for porphobilinogen of 19±7μM at its pH optimum. The isoelectric point of the enzyme had an average value of 4.5. The enzyme was found to be able to retain its structure and activity on heat treatment at 60°C, reflecting the stable nature of its tertiary structure.

Another significant advancement in the understanding of porphobilinogen deaminase came from the identification of the unique dipyrromethane cofactor (Jordan and Warren, 1987; Hart *et al.*, 1987). The cofactor was found to be derived from two molecules of the substrate, porphobilinogen, and was covalently linked to the active site residue cysteine-242 *via* a thioether bond (Jordan *et al.*, 1988; Miller *et al.*, 1988). Isotopic labelling of the cofactor indicated that, once bound to the enzyme, the cofactor remained permanently attached as a resident primer and was not turned over (Jordan and Warren, 1987; Hart *et al.*, 1987, Scott *et al.*, 1988). Further proof for the presence of the cofactor came from its reaction with Ehrlich's reagent, which resulted in the characteristic spectrum of a dipyrromethane. On binding two molecules of the substrate, the enzyme was found to exhibit a reaction with Ehrlich's reagent typical of a tetrapyrromethane, which established that the cofactor interacted covalently with the substrate. The dipyrromethane cofactor has been found in all the deaminase samples

obtained from each of the major biological groups studied (Warren and Jordan, 1988; Hart *et al.*, 1990).

The binding of substrate to the enzyme was investigated thoroughly using radiolabelling experiments (Jordan and Seehra, 1980; Battersby *et al.*, 1978, 1979a, b and c). The experiments showed that the binding of substrate was sequential and ordered, with the pyrrole rings binding one at a time in the order of rings a, b, c and then d. The enzyme was also shown to form *via* discernible intermediate forms, representing the enzyme with one, two, three and four substrate molecules attached to the active site during the catalytic cycle. This was shown first by Anderson and Desnick (1980), who isolated deaminase from human erythrocytes in the form of free enzyme and four enzyme-intermediate complexes E, ES_2, ES_3 and ES_4. The introduction of fast protein liquid chromatography subsequently allowed enzyme-intermediate complexes to be isolated from purified *E. coli* deaminase (Warren and Jordan, 1988). The ES forms had been generated by the addition of substrate to the enzyme. However, the fourth enzyme-intermediate complex, ES_4, has not yet conclusively been observed for *E. coli* porphobilinogen deaminase, and this appears to be a difference between the human and *E. coli* porphobilinogen deaminase.

Several other studies have contributed to the understanding of the structure and function of porphobilinogen deaminase, including amino acid modification experiments and site directed mutagenesis. The inhibition of the enzyme by pyridoxal phosphate suggested an important role for lysine residues in the active site (Miller *et al.*, 1989), and site-directed mutagenesis studies of the highly conserved arginine residues also confirmed their role in substrate binding and catalysis (Jordan and Woodcock, 1991; Lander *et al.*, 1991). Studies on the apoenzyme form of porphobilinogen deaminase, which lacks the cofactor, also gave clues to the importance of the cofactor in stabilising the tertiary structure (Scott *et al.*, 1989; Hart *et al.*, 1988). Additionally, a number of substrate analogues and inhibition studies furthered the understanding of the enzyme mechanism (Frydman, 1974; Scott *et al.*, 1989; Clemens *et al.*, 1994; etc.). However, the most recent, and perhaps most enlightening major advancement came with the determination of the three-dimensional crystal structure of the enzyme (Louie *et al.*, 1992). The structure allowed many of the speculations about the enzyme to be answered, and provided a model from which further progress could be made.

1.7 The Three-Dimensional Crystal Structure of Porphobilinogen Deaminase

Louie *et al.*, 1996

1.7.1 Introduction

The three dimensional crystal structure of *E.coli* porphobilinogen deaminase has been solved and reported to resolutions of 1.9Å and 1.76Å, along with a variant protein in which the six methionine residues have been replaced with selenomethionine (Jordan *et al.*, 1992; Hadener *et al.*, 1992; Louie *et al.*, 1994). The detailed structures display conformations of the dipyrromethane cofactor in both the reduced (native) and oxidised forms, depending on the level of reducing agent employed during crystallisation, and the two conformations can be used to allow insights into the nature of substrate binding. The analysis of the structure also provides a basis for predicting the catalytic mechanism of porphobilinogen deaminase. The structure and proposed mechanism for the enzyme have recently been reviewed (Louie *et al.*, 1996).

1.7.2.1 General Description of the Tertiary Structure

The refined atomic model of *E.coli* porphobilinogen deaminase at 1.76Å describes residues 3-48, 58-307, the dipyrromethane cofactor, 249 water molecules and one acetate ion. The molecule comprises of 313 amino-acid residues, and the diffuse electron density of the unresolved residues 1, 2, 49-57 and 308-313 is likely to be a result of their high mobility.

The molecule has approximate overall dimensions of 57x43x32Å, with the polypeptide chain folded into three α/β domains of approximately equal size, as shown in the ribbon diagram of the enzyme in figure 1.6. Domain 1, the N-terminal domain, consists of residues 3-99 and 200-217. Domain 2, the central domain, consists of residues 105-193 and is found to have a similar overall topology to domain 1, and is related to it by an approximate two-fold axis (163°). There are few direct interactions between domains 1 and 2, with residues 100-104 and 194-199 providing the segments of roughly antiparallel polypeptide chain that link them together. Domain 3, the C-terminal domain,

runs from residues 222-313 and has a different toplogy to the previous two domains. The cofactor is bound to a cysteine at residue 242 *via* a thioether link, in the cleft formed between domains 1 and 2.

The residues which connect domains 1 and 2, amino acid residues 100-104 and 194-199, may provide a hinge to facilitate the opening of a binding site for the incoming substrate molecules. A hinge would allow sufficient flexibility for up to six pyrrole rings to be accommodated in the active site cleft, and may also regulate the surfaces available for substrate binding and solvent accessibilty.

Figure 1.6 *E. coli* Porphobilinogen Deaminase - Ribbon Diagram

The cofactor is depicted in red. Domain 1 is shown in pink, domain 2 in green and domain 3 in blue.

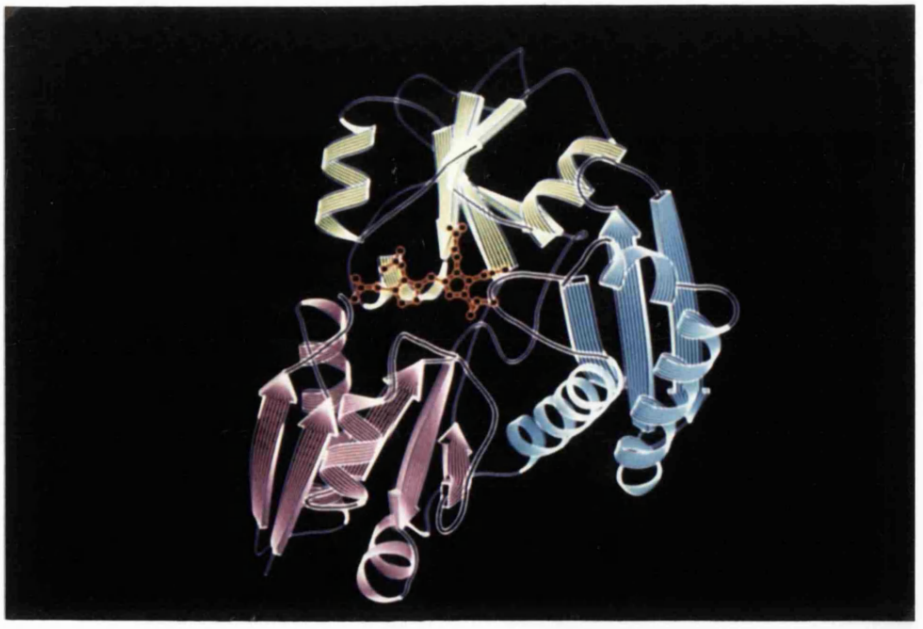

1.7.2.2 Secondary Structure Elements

The overall topology of the porphobilinogen deaminase structure is illustrated in figure 1.7. The structure has been assigned as approximately 38% in a helical conformation, 25% extended, 8% turn and 29% coil.

Figure 1.7 *E.coli* Porphobilinogen Deaminase - Topology Diagram

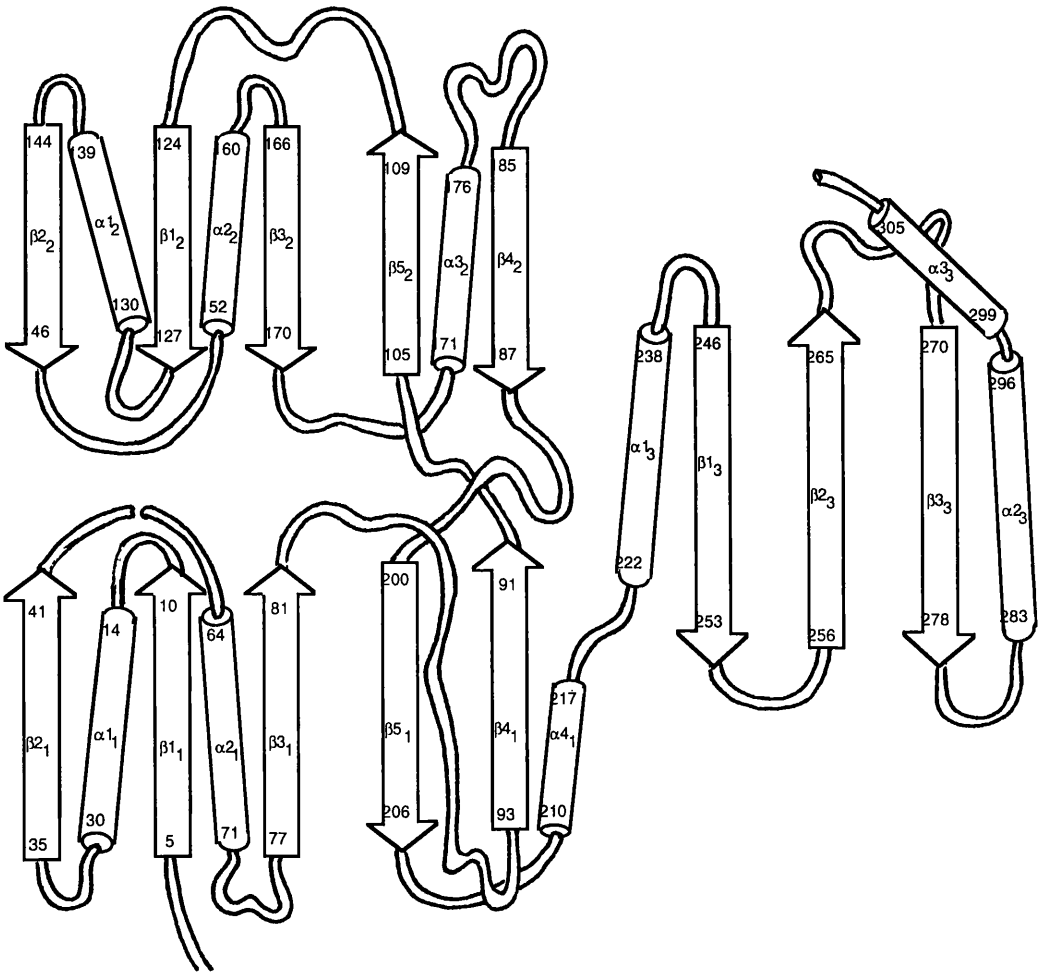

Domains 1 and 2 are both found to consist of a five-stranded β-sheet arrangement with α-helices flanking each of the β-sheets and running approximately parallel with them. The strand in each sheet that immediately

follows a cross-over from the other domain is anti-parallel. The approximate two-fold symmetry between the domains is broken by two prolines in the $\beta 3_1$-$\beta 4_1$ loop, which correspond to the expected position of an α-helix $\alpha 3_2$ in domain 2. Domain 3 has an alternative topology of an open-faced, three-stranded anti-parallel β-sheet with three helices packed in one face. Domain 3 is relatively flat, with a twist of only 25° between strands, in contrast to domains 1 and 2 which have twists of 100-110°. Thirteen reverse turns are observed overall, existing predominantly between elements of secondary structure. The organisation of the polypeptide chain has notable similarities to that of the transferrins and bacterial periplasmic binding proteins (Baker *et al.*, 1987; Spurlino *et al.*, 1991; Louie *et al.*, 1993), and this together with the close resemblance between domains 1 and 2 has strong evolutionary connotations, which are discussed later.

Each domain possesses a distinct hydrophobic core, although the majority of the contacts between the domains are polar. Whilst domains 1 and 2 make few interactions with each other, they both form a complex array of ion pairs and hydrogen bonds with the dipyrromethane cofactor, which lies in a deep cleft between them. The cleft occupies approximately half the width and depth of the protein, and forms the environment of the active site. The positioning of the cofactor near the entrance to the cleft leaves a considerable volume of internal space vacant, in which many well-ordered water molecules are bound.

1.7.2.3 Active Site Details

The floor and ceiling of the active site cleft are formed by the C-termini of the β-sheets, the N-termini of the α-helices and their connecting loops of domains 1 and 2. One face of the helix $\alpha 3_2$ and the interdomain cross-over strands make up the rear wall to define a cavity of approximate dimensions 15x13x12$Å^3$. The dipyrromethane cofactor is covalently attached to the residue cysteine-242, which resides on the α13-β13 loop (residues 241-244) interconnecting a helix in domain 1 with a strand in domain 3. The loop protrudes into the cleft, but makes no direct interactions with either domain. The cofactor is bound to cysteine-242 by a covalent "left-handed spiral" thioether linkage, similar to that of the thioether between the heme group and cysteine-14 in cytochrome C (Louie and Brayer, 1990).

There is a well-defined electron density for the cofactor dipyrrole system in both the oxidised and reduced wild-type porphobilinogen deaminase and in the reduced selenomethionyl variant. Two distinct conformations of the dipyrrole system are observed, as illustrated in figure 1.8. Both conformations occur in the wild-type protein, in which the predominant conformer (80% occupancy) appears to represent the oxidised form of the dipyrrole with the minor conformer (20% occupancy) representing the native (reduced) dipyrromethane. The cofactor of the selenomethionyl variant, crystallised under strong reducing conditions, displays essentially 100% occupancy at the native position.

Figure 1.8 The Two Conformations of the Cofactor

Cofactor ring C1 occupies essentially the same site in the oxidised (yellow) and reduced (brown) state whereas ring C2 occupies different positions.

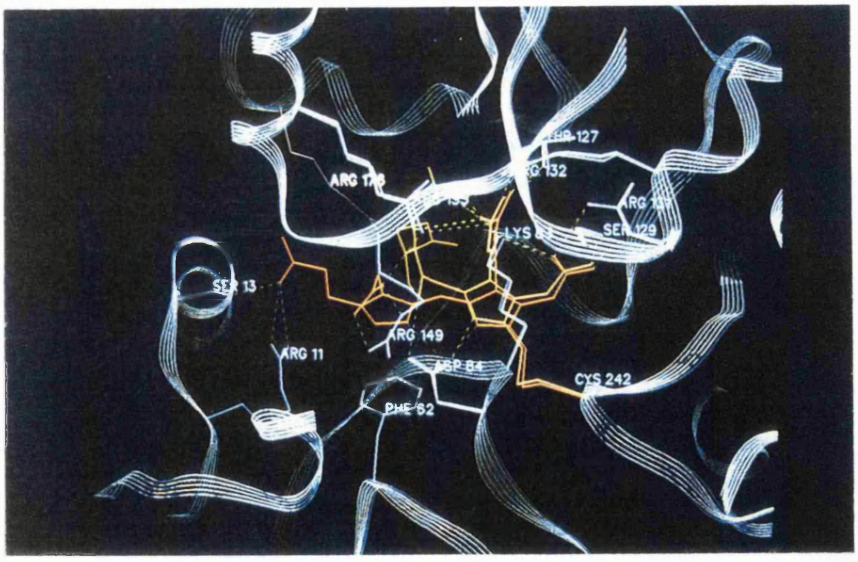

The reduced and the oxidised dipyrroles differ in their conformation about the bridging *meso*-carbon. In the case of the oxidised cofactor, the pyrrole rings are only 11° from coplanarity, whereas the reduced

dipyrromethane pyrrole rings have an interplanar angle of 59° and form a distinct elbow at the methylene group. In the reduced conformer, both rings C1 and C2 are positioned deeper in the active site cleft, with ring C2 displaying the larger shift of ~3.4Å.

The acetate and propionate side groups of the dipyrromethane form the majority of the cofactor-protein interactions. The significance of these interactions is highlighted by the inability of the apoenzyme to incorporate the cofactor analogue, 2-aminomethylpyrrole, in which the side substituents are replaced by hydrogen atoms (Scott *et al.*, 1989). The acidic pyrrole side chains are involved in extensive salt-bridging and hydrogen-bonding with the surrounding protein matrix and with bound water molecules, as depicted in figure 1.9. The polypeptide chain constituents participating in the interactions are : arginyl guanidiniums (arginine-11, arginine-131, arginine-132, arginine-149 and arginine-155), seryl and threonyl hydroxyls (serine-13, serine-81, threonine-127 and serine-129), backbone amide nitrogens (128 N, 150 N, 152 N, 170 N and 199 N) and the amino function of lysine-83. The involvement of the highly conserved arginine residues of the enzyme with the carboxylate-oxygens of the side-chains had previously been predicted (Jordan and Warren, 1987), and the functionality of the enzyme is severely impaired if arginines-131 and -132 are mutated to histidines or leucines (Woodcock and Jordan, 1991; Lander *et al.*, 1991). The side-chain groups, which interact with the cofactor are predominantly invariant, and further take part in hydrogen-bonding with adjacent protein and solvent atoms.

The pyrrole rings themselves also take part in essential interactions, such as the hydrogen bonding of the pyrrole nitrogen hydrogens to the side-chain carboxylic acid group of aspartate-84. In the oxidised cofactor protein, the pyrrole ring C2 is also found to stack against the phenyl ring of phenylalanine-62. Additionally, three of the four carboxylate groups of the cofactor are located very near the N-termini of α-helices.

Overall, the role of the cofactor in both forming an extensive network of interactions which cross-link the three domains and in partially neutralising the electropositivity in the active site cleft satisfactorily explains the compactness and the greater stability of the holoenzyme over the apoenzyme. The active site details showing the reduced conformation of the cofactor are illustrated in figure 1.10.

Figure 1.9 The Interactions of the Cofactor

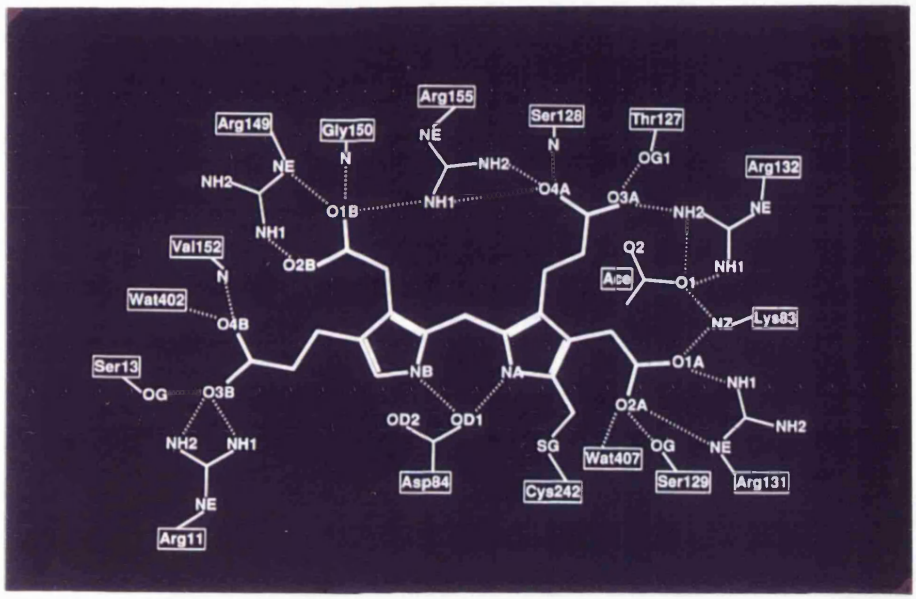

Figure 1.10 Active Site Details

The cofactor is depicted in yellow.

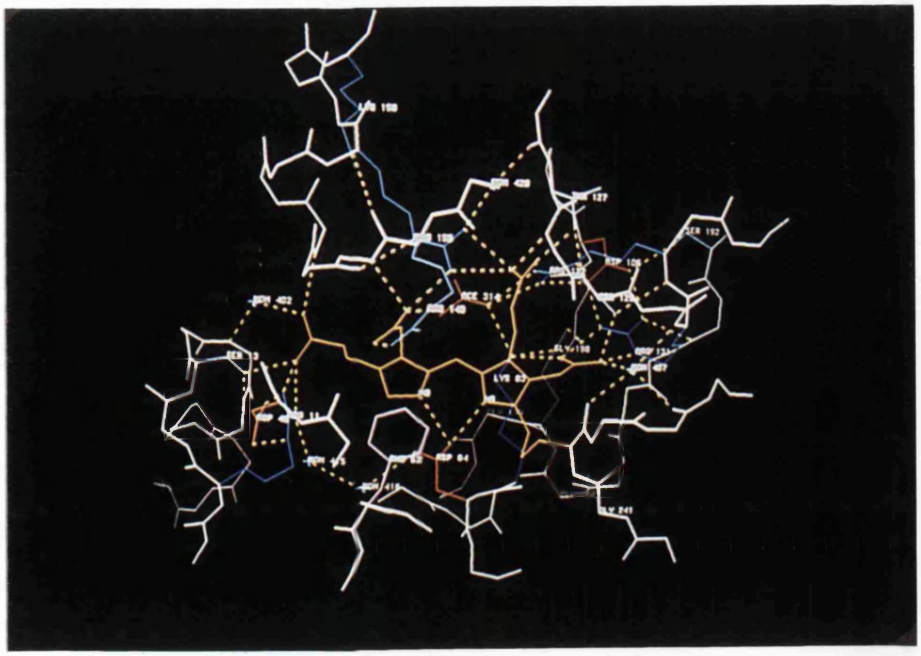

1.7.2.4 Nature of the Oxidation of the Dipyrromethane Cofactor

There is considerable evidence to support the hypothesis that the predominant conformer (80%) of the dipyrrole in the wild-type porphobilinogen deaminase does represent an oxidised form. The initial corroboratory observation for this comes from the effect of reducing agents on the colour of the crystals, the presence of which were found to give rise to colourless crystals. Secondly, the excess lobe of electron density connected to the free α-position of ring C2, which is observed for the predominant conformer, is consistent with the presence of a carbonyl-oxygen atom. Also, the observed near coplanarity of the two rings of the cofactor in the oxidised conformer may signify the presence of a double bond within the bridging methylene group. All these considerations point to an oxidised form of the dipyrromethane such as a dipyromethenone.

Dipyromethanones are strongly chromophoric ($wavelength_{max}$ =390nm) (Jordan and Berry, unpublished results) and undergo a light-induced, internal cis-trans isomerisation, and these properties are consistent with the colour and light-sensitivity of the crystals (Jordan *et al.*, 1992). The carbonyl oxygen of a dipyrromethenone would be appropriately positioned to accept a hydrogen-bond from the carboxylic side group of the aspartate-84 side chain. However, the electron density does not rule out the presence of other forms of dipyrroles. A dipyrromethene, which lacks the carbonyl oxygen, or a dipyrromethanone, could equally well be modelled. It is probable that a mixture of some or all of these dipyrrole systems actually exist.

However, whilst it may be likely that the predominant conformer does represent an oxidised form, the fact that both of the conformations form such considerable interactions with the protein also suggests that the more external position of the C2 ring in the oxidised form may, in fact, represent the binding site of the substrate pyrrole ring.

1.7.3 The Proposed Mechanisms of Action of Porphobilinogen Deaminase

1.7.3.1 The Porphobilinogen Binding Sites

The current structural details of the holoenzyme, together with kinetic studies and other observations, allow many mechanisms to be proposed for substrate binding and catalysis. The observed dipyrrole-protein interactions in the reduced and oxidised wild-type and reduced selenomethionyl forms of porphobilinogen deaminase define at least three binding sites for porphobilinogen moieties within the active site cleft, as described in figure 1.8. The first ring of the cofactor remains positioned similarly in all forms, and the space occupied is referred to as the C1 site. However, the second ring of the cofactor is able to reside in two distinct sites, and it is the position occupied in the reduced forms which is referred to as the C2 site. The position occupied in the oxidised conformer, termed the S site, may closely approximate to the site of substrate binding and polypyrrole-chain elongation.

The binding of an incoming porphobilinogen molecule at the S site would allow the molecule to be appropriately situated to react with the α-free position of the terminal ring of the polypyrrole chain, which has a position deeper in the active site cleft. For the reaction that converts E to ES, this terminal ring would be located at the C2 site. It is possible that the substrate ring may bind in a reverse orientation, as shown in figure 1.11, and therefore the positions of the acetate and proprionate groups would be interchanged. A reverse orientation would then allow the two reacting atoms, the carbon at the free α-position and the amino bearing methyl group of the substrate, to be placed in closer proximity.

The terminal ring of the polypyrrole chain is susceptible to cleavage and hydrolytic release as hydroxyporphobilinogen, particularly in the absence of exogenous porphobilinogen when the S site is free. In this case, the terminal ring will have presumably been occupying an elongation site or the S site. The conformation adopted by the cofactor that directs the ring C2 away from the elongation or substrate-binding site may explain the stability of the dipyrromethane against catalytic turnover.

Figure 1.11 The Proposed Binding of Substrate in a Reverse Orientation

The position of the substrate has been modelled on the observed position of the C2 ring in the oxidised form of the dipyrrole. However, the position of the acetate and propionate groups are interchanged, and thus the aminomethyl group of the substrate porphobilinogen molecule is closer to the nucleophilic free α-carbon of the dipyrromethane cofactor (marked α).

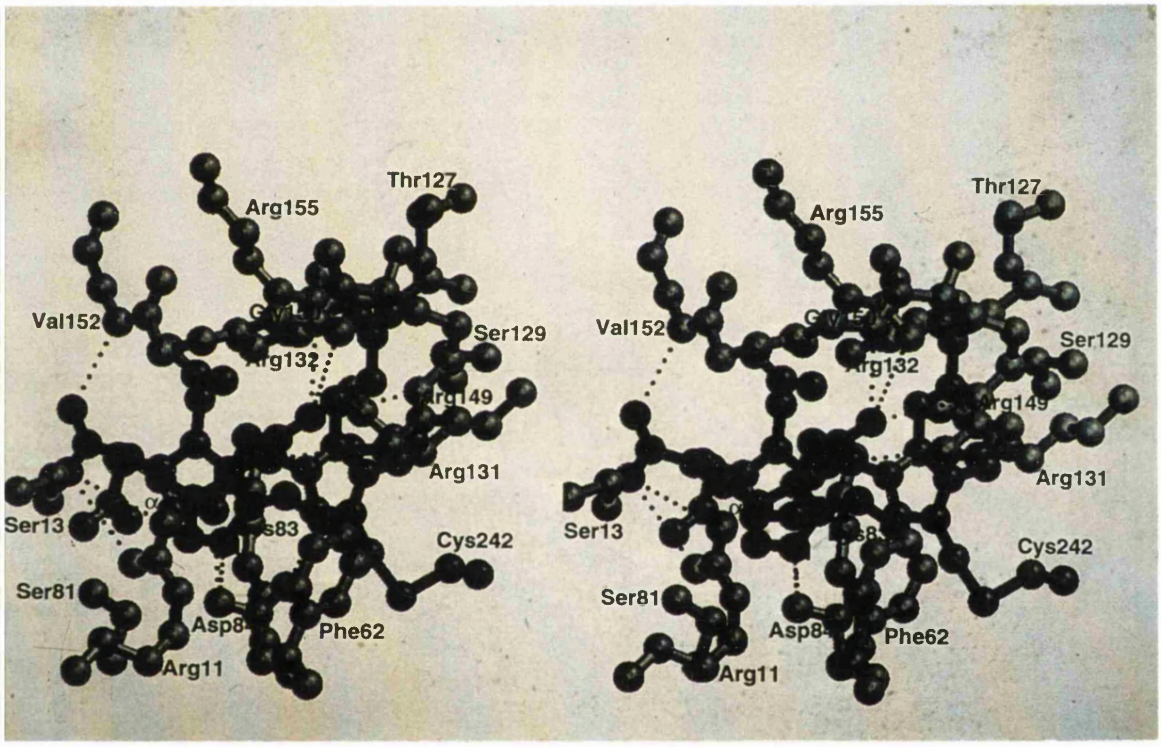

The proposed assignments of the pyrrole binding sites also correlate well with results from site-directed mutagenesis, in which the active site arginine residues have been mutated to histidine or leucine (Jordan and Woodcock, 1991; Lander *et al.*, 1991). The mutagenesis studies indicate that arginines-131 and 132 form key interactions at the C1 site, as replacement of either completely prevents assembly of the dipyrromethane cofactor. The arginines-11,-149 and -155 all form interactions at the proposed S site, and arginine-155 also interacts with the C1 site. Mutagenesis of these residues allows them to retain the ability to assemble the cofactor, although the replacement of arginines-11 and -155 severely inhibits conversion of E to ES and replacement of arginine-149 inhibits all stages of chain elongation,

particularly the ES to ES_2 step. The results of such mutagenesis experiments are therefore equivocal with the proposed S site.

Porphobilinogen would be expected to carry a net negative charge at neutral pH. The excess of positively charged amino-acid side chains, including arginines-11,-131,-132,-149,-155,-176, and lysine-83, within the active site cleft may also play a role in the initial attraction of porphobilinogen to the cleft. Conversely, the lack of acidic side-chains on the protein surface immediately surrounding the active site cleft may also facilitate the binding of porphobilinogen. Such an environment can be described as an example of the Circe effect, which refers to the utilisation of strong attractive forces to lure a substrate into a site in which it undergoes transformation of form and structure (Jencks, 1975).

The interactions between the protein at the S site and the substrate molecules are formed mainly through the acetate and propionate side-substituents. The poor ability of analogs of porphobilinogen, in which the substituents have been modified (Frydman 1974; Clemens *et al.*, 1994), to act as substrates can be easily explained. The limited size of the substrate binding S site, which has only sufficient space to accommodate a single porphobilinogen moiety, explains why the enzyme cannot readily incorporate di- or tripyrromethanes into the 1-hydroxymethylbilane product (Frydman *et al.*, 1976; Battersby and McDonald, 1976; Frydman *et al.*, 1978).

1.7.3.2 The Mechanism of Catalysis of the Ring Couplings

The enzyme appears to have only one active site, indicating no repetition of catalytic machinery and suggesting that the series of ring couplings are not catalysed at (up to) four distinct sites. This conclusion, drawn from structural data, is also consistent with biochemical evidence for a single catalytic site (Warren and Jordan, 1988). Aspartate-84 has been identified as the key catalytic residue, by virtue of the close proximity of its carboxylic acid group to the pyrrole nitrogens of the cofactor. Additional support for the role of the residue comes from mutagenesis studies, as replacement of the aspartate with glutamate leads to an enzyme with less than 1% of the specific activity of the wild-type, and replacement with alanine or asparagine leads to complete catalytic inactivity (Woodcock and Jordan,

1994). The other polar residues present in the active site cleft serve mainly to bind the substrate and growing polypyrrole product.

A model has been proposed for the sequence of reactions involved in ring coupling, based on the role of the residue aspartate-84 (Woodcock and Jordan, 1994), which is illustrated in figure 1.12. The model suggests that initially the side chain carboxylic-acid group of aspartate-84 may be protonated, even though the enzyme is active at high pH, as it is positioned approximately normal to the face of an adjacent phenylalanine 62 and is inaccesible to the external solvent medium. This would allow the two oxygen atoms of aspartate-84 to interact with the hydrogen atoms attached to both pyrrole and primary-amino nitrogens of the porphobilinogen substrate and facilitate the deamination in the following way. Firstly, aspartate-84 would act as a general acid by providing a proton to be taken up by the expelled ammonia molecule (to yield an ammonium molecule) and the resulting carboxylate anion of the aspartate-84 would be able to stabilise the carbocation that may develop at the exocyclic carbon atom; the other oxygen can stabilise the positive charge that develops on the pyrrole nitrogen of the resulting methylene pyrrolenine (Pichon *et al.*, 1992). It has been suggested that the acetate side chain of the substrate ring may lend towards an intramolecular stabilising of the carbocation (Pichon *et al.*, 1992), but this is improbable considering the salt bridges that the acetate forms with the side chains of the active site arginines-11,-149 and-155. After deamination of porphobilinogen, the free oxygen of the aspartate-84 carboxylate group would be able to stabilise a positive charge on the pyrrole nitrogen of the terminal ring of the polypyrrole chain, promoting the generation of a nucleophilic carbon atom at the free α-position of this ring. After carbon-carbon bond formation, the carboxylate group of aspartate-84 could remove the proton from the α-position of the now penultimate ring to complete the ring coupling process.

Figure 1.12 The Role of Aspartate-84 in the Ring Coupling Reaction

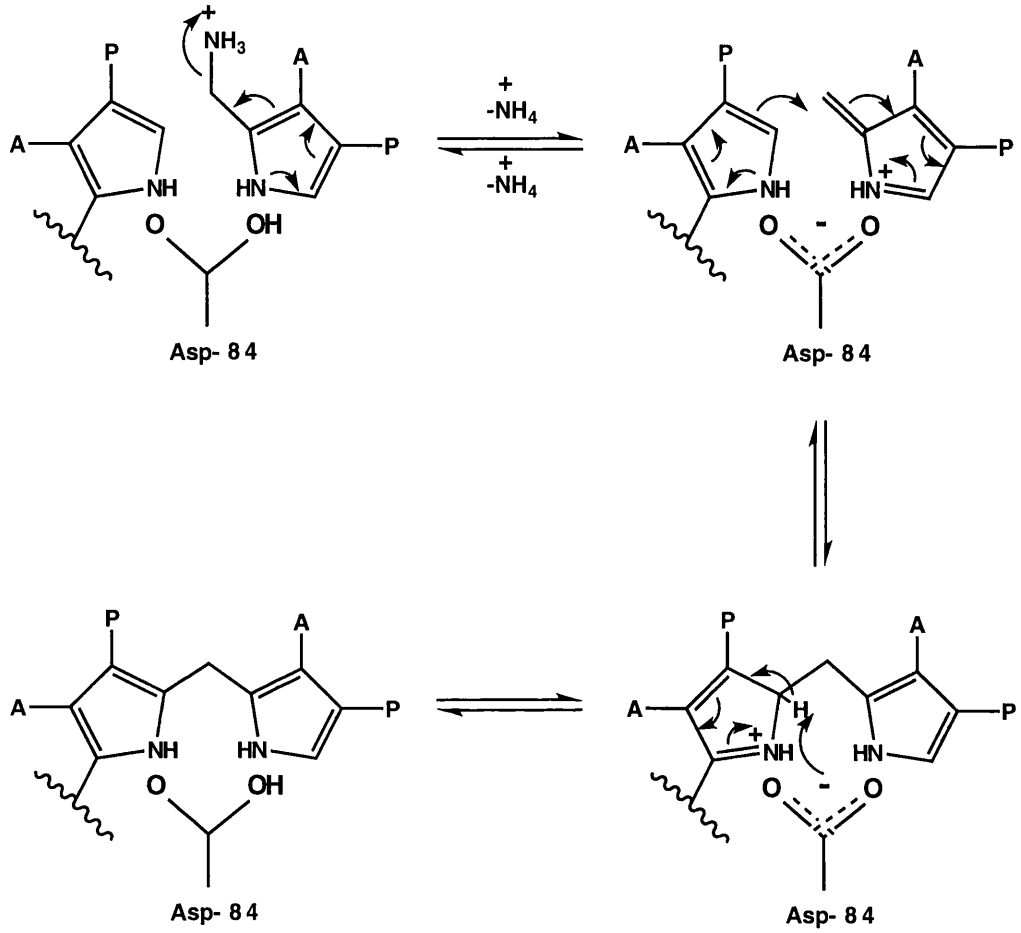

Aspartate-84 is also likely to play a role in initiating the final step in preuroporphrinogen synthesis, responsible for the release of the 1-hydroxy-methylbilane (Woodcock and Jordan, 1994). To fulfil this role, the aspartate-84 carboxylic acid is required to protonate the carbon at the α-position of ring C2 of the dipyrromethane cofactor in the ES_4 complex, and then promote the reversal of a ring coupling reaction to release a tetrapyrrolic methylene pyrrolenine. Lastly, the activation of a water molecule and hydration of the exocyclic carbon-carbon double bond in the methylene pyrrolenine completes

product formation. A water molecule, Wat416, hydrogen bonded to the aspartate-84 side chain, may be the origin of the hydroxyl group in the final 1-hydroxymethylbilane, preuroporphyrinogen.

The proposed mechanism suggests that aspartate-84 is the only residue required to promote the catalysis of all the reaction steps involved in ring coupling. However, it has been observed that mutations of the residue to alanine or asparagine result in enzymes which, although unable to form products, manage to assemble the dipyrromethane cofactor. It is also possible that these mutants are able to bind one or two rings of substrate in a non-catalytic reaction (Woodcock and Jordan, 1994). In addition, amino acid replacements of arginines-131 and-132 at the C1 binding site result in an inactive apoenzyme, and the mutation of lysine-83, which forms salt bridges with both rings C1 and C2 to stabilise a cofactor conformation that directs ring C2 to the rear of the active-site cleft, results in a protein unable to fold. Therefore, the binding of the two reacting rings in the appropriate proximity of these residues must also play an important role in promoting ring coupling.

Further contributions to the promotion of catalysis come from the binding of substrate to the enzyme, as the interactions with the arginine residues would cause the stabilising intramolecular ion-pairs of porphobilinogen to be broken, facilitating the deamination of the incoming pyrrole ring (figure 1.13). As previously mentioned, the pyrrole nitrogens of both rings undergoing coupling and the exocyclic methylene carbon of the deaminated substrate may transiently acquire positive charges during the reaction. The noticeable absence of an α-helix in the segment of polypeptide chain corresponding to 3_1, which disrupts the duplicity between domains 1 and 2, may therefore be explained. The presence of the amino-end of a helix at this position would point at the elongation site, and thus disfavour the generated positive charges.

1.7.3.3 Flexibilty Around the Active Site Cleft

The presence of a single catalytic site in porphobilinogen deaminase requires that the growing polypyrrole chain must be repositioned after each ring-coupling step to allow the α-terminal pyrrole ring to be suitably placed

Figure 1.13 The Intramolecular Ion-Pair of Porphobilinogen

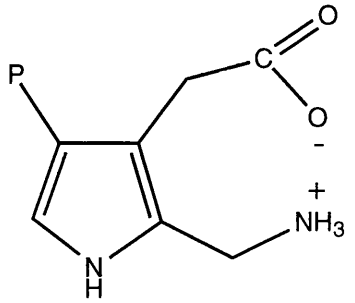

for further reaction in the tetrapolymerisation. Therefore, considerable flexibility in the vicinity of the active site is necessary to allow entry of the substrate, conformational adjustments associated with both attachment of the cofactor and extension of the polypyrrole, and the release of the hydroxymethylbilane product. Such flexibilty is supported by several structural features of the enzyme.

Firstly, the loop which carries the cofactor is found to make few interactions with the rest of the molecule, and is found to have relatively high temperature factors (i.e. thermal motion). Also, cysteine-242, to which the cofactor is attached, is preceeded by two glycine residues that occupy relatively little space and allow considerable flexibility of the loop. Secondly, the main interactions between the protein and the pyrrole rings are made through the acetate and propionate side substituents. The ability of these side groups to change conformations would facilitate favourable protein-polypyrrole interactions to be maintained throughout the course of product elongation. Such adaptibility is apparent in the similar positioning of the ring C1 carboxylate groups in the reduced and oxidised conformers of the cofactor dipyrrole, despite the slightly differing positions of the dipyrrole rings themselves. Thirdly, the loop of the polypeptide chain which comprises residues 48-58, that is thought to be located directly in front of the active site cleft, must be highly mobile at pH 5 as the electron density in this area is poorly resolved. The apparent mobility may point to the presence of a flexible "lid".

A "lid" for the active site may function to form additional binding interactions with the substrate, to modulate the nature of the active site environment, and also to seal off the cleft transiently during catalysis, protecting reactive intermediates from exposure to solvent. A flexible "lid" would therefore suggest a role in an induced fit mechanism, which would be consistent with several observations. Chemical modification by pyridoxal phosphate of both lysine loop residues lysines-55 and-59, or replacement of lysine-59 by glutamate, leads to lowered enzymic activity (Hadener *et al.*, 1990). Furthermore, the presence of the substrates serves to protect the lysines from pyridoxylation (Hart *et al.*, 1984). The ordered polypeptide chain on either side of the "lid" segment is less well defined in the reduced form of the deaminase, the form in which the substrate site is vacant, than in the oxidised form. This indicates that certain interactions upon substrate binding may be important for ordering the "lid" region; such interactions would include salt bridges between aspartate-46 and arginine-11 (arginine-11 in turn salt bridges the propionate of the porphobilinogen moiety), and the stacking of phenylalanine against the pyrrole ring.

Fourthly, further evidence of the flexibility of porphobilinogen deaminase is derived from the location of the active site cleft at the interface between the three domains, which allows maximum interdomain movement. This flexibilty may be important in view of the following factors: a) the cavity between domains 1 and 2 has a large volume capable of holding several pyrrole units; b) there are few direct interactions between domains 1 and 2; c) domains 1 and 2 can potentially hinge or twist open, increasing the interdomain cleft and adjusting the position of each domain's contribution to the active site residues; d) interdomain hinge-opening has been clearly demonstrated in the structurally homologous binding proteins (Louie, 1993); e) domain 3 interacts with the rest of the molecule primarily through hydrogen bonds and salt-bridges, and a movement of domain 3 away from the other two domains would lead to the favourable exposure of hydrophilic surfaces to solvent.

There is considerable biochemical evidence for a change in the relative positioning of domains in the porphobilinogen deaminase molecule during the course of the polymerisation reaction. Protein modification studies with N-ethylmaleimide have shown that the susceptibilty of cysteine-134 to modification increases progressively as the enzyme changes from

holoenzyme through to ES, ES_2 and ES_3 (Warren *et al.*, 1995). Cysteine-134 is located at the interface between domains 2 and 3, and the increased susceptibility to alkylation suggests that its environment changes substantially during the catalytic cycle. Furthermore, a modification of this sulphdryl residue, which is ~18Å distant from the catalytic residue aspartate-84, by N-ethylmaleimide, inactivates and destabilises the protein. There are, in addition, other residues remote from the active site which are essential for chain elongation. The residue arginine-232, upon mutation to histidine, renders an enzyme which inhibits the conversion of ES to ES_2 (Lander *et al.*, 1991). Arginine-232 is ~10Å distant from aspartate-84, but forms hydrogen bonds linking domain 3 to domain 1. The mutagenesis studies suggest that the flexibilty of the enzyme is quite controlled, allowing the domain movement to expand the active site cleft only in a manner which allows optimal positioning of key residues for catalysis. Final evidence for conformational change is derived from the anomolous chromatographic mobilities of ES_2 and ES_3, in which the third enzyme-subtrate complex elutes at a higher salt concentration that might be predicted, suggesting a conformational change occuring upon incorporation of the third pyrrole ring.

1.7.3.4 Manipulation of the Growing Polypyrrole Chain

There are two principal models proposed for the manipulation and accommodation of the growing polypyrrole chain in the enzyme molecule (Louie *et al.*, 1996). The first is that the chain is folded into the large active site cavity, displacing bound water molecules. The calculated volume of the cavity is found to be large enough to accommodate a polypyrrole chain of approximately $3^1/_2$ pyrrole units. Such a model would therefore provide an obvious steric mechanism for preventing the growth of the chain beyond a tetrapyrrole. This model would also satisfy the observations of the precise conservation of residues lining the active site cleft, and the critical replacement of arginine-176, located at the rear left of the cleft, which results in the inhibition of the ES_2 to ES_3 step. An important aspect of this model is that the catalytic and substrate-binding sites are formed by residues primarily from domain 1, whereas the binding sites for the cofactor are formed mainly by domain 2. Thus, as the polypyrrole chain grows within the active site cleft, forming interactions mainly with domain 2, domain 1 would shift position to carry the catalytic site and bound substrate into the appropriate position to

react with the terminal pyrrole ring of the chain (Louie, 1993). This model is described as the 'accommodating active site model' .

The alternative model is termed the 'moving chain model'. This requires that the polypyrrole chain is pulled progressively past the catalytic site, *via* a rigid body movement of all, or part, of domain 3 (to which the cofactor and growing chain is anchored). In this model, the newly extended polypyrrole chain would require repositioning, after every ring addition, to allow the binding sites C1 and C2 to hold the penultimate and terminal rings respectively, causing the displacement of the preceeding ring(s) from the active site. Thus, with every chain extension, the binding interactions of both sites C1 and C2 are broken and subsequently reformed with the suceeding porphobilinogen units of the growing polypyrrole. However, the breakage of numerous, highly specific interactions that occur at each binding site may represent a high energy barrier for each reaction cycle in such a model.

A final, less likely model requires no interdomain movements. As the polypyrrole chain grows, it is accommodated within the active site cleft and then by some means repeatedly attains a conformation that brings the terminal ring into the appropriate position relative to the catalytic and substrate binding sites. However, observations such as the shattering of enzyme crystals on the addition of substrate (Wood, personal communication) suggest that some interdomain movement must take place, and therefore this model is unlikely to be correct.

1.8 Acute Intermittent Porphyria

1.8.1 Introduction

The haem biosynthesis pathway requires, in animals, the action of eight enzymes to produce haem from succinyl CoA and glycine. The reduction in activity of any of these enzymes will lead to a deficiency in haem production and ultimately result in disease. The decrease in activity in the first of these enzymes, the rate controlling 5-aminolaevulinic acid synthase, causes the disorder of hereditary sideroplastic anaemia (Bottomley, 1982). The decrease in activity in any of the remaining seven enzymes of the pathway leads to a group of metabolic disorders known as porphyrias (see Elder and

Path, 1982, for an overview). Porphyrias are brought about by the accumulation of the haem precursors, resulting in characteristic clinical and biochemical features (Bottomley and Muller-Eberhard, 1988). There are seven documented human porphyrias, each representing a defect in one of the enzymes.

The third enzyme in the haem biosynthesis pathway is porphobilinogen deaminase, and the failure of this enzyme to turnover substrate has a two-fold effect upon physiological conditions. Firstly, the pool of tetrapyrroles available for haem synthesis will diminish, limiting the availability of haem for its various functions as a prosthetic group. In humans, the decrease in haem levels will also lessen the regulatory effect that haem has on controlling 5-aminolaevulinic acid synthase, leading to increased concentrations and activity of the enzyme (Kappas, 1983). Secondly, the newly synthesised 5-aminolaevulinic acid synthase and increased activity combine to lead to concentrations of porphobilinogen which are in excess of the malfunctioning enzyme's ability to turn over, resulting in the accumulation of the haem precursors 5-aminolaevulinic acid and porphobilinogen. The human diseased state arising from the deficiency of porphobilinogen deaminase activity is termed acute intermittent porphyria (AIP).

The haem deficiency is thought to manifest itself indirectly. The haem requiring enzyme hepatic tryptophan pyrrolase converts tryptophan to kynurenine, and as activity of this enzyme falls the concentration of

tryptophan will rise, stimulating the synthesis of the neurotransmitter 5-hydroxytryoptamine. The hypothesis is supported by the increased excretion of indoles by AIP patients in their urine (Kappas, 1983). Neurological disorders are also believed to be brought about by the increased concentrations of the haem precursors 5-aminolaevulinic acid and porphobilinogen, and both 5-aminolaevulinic acid and porphobilinogen have been identified in the cerebrospinal fluid of patients with AIP (Sweeney *et al.*, 1970). In support, there are many reports of the effects of *in vitro* administration of the two precursors, although the concentrations used in the majority of cases have not been physiologically significant. A final theory of the possible effect of malfunctioning porphobilinogen deaminase is one where the overactivity of 5-aminolaevulinic acid synthase leads to a depletion in its coenzyme, pyridoxal phosphate. Again, plasma pyridoxal concentrations have been found to be lower in AIP patients, but no correlation has been found between coenzyme concentrations and clinical activity of the disease (Hamfelt and Wetterberg, 1969). It should be noted that all of the above hypotheses are contested, and therefore must remain only theories.

AIP, like most porhyrias, is inherited in an autosomal dominant manner (Kappas, 1989). In affected individuals, the mean activity of the enzyme is 50% of the normal (Strand *et al.*, 1972), which is in keeping with the heterozygous state of these subjects. It is the most common of the porphyrias with an estimated frequency of 1 per 10,000 persons. The frequency of the disorder rises to 1 per 500 amongst psychiatric patients, which is predictable considering the neurological symptons brought on by the malfunctioning enzyme. The disease manifests typically in acute attacks, and in addition to the neurological disorders of psychiatric involvement, peripheral neuritis and paralysis, the symptoms include acute abdominal pain, vomitting and constipation. The elevated amounts of haem precursors result in a diagnostic 'port wine red' colouring of the urine on air oxidation, indicative of the presence of porphobilin, an auto-oxidised product of porphobilinogen. Clinically, haem arginate is administered therapeutically during acute attacks, as exogenous haem will relieve the feedback activation of 5-aminolaevulinic acid synthase. Fortunately, only 10% of known AIP heterozygotes are symptomatic, and the disease is precipitated by factors such as poor diet, alcohol, certain drugs and hormones.

1.8.2 Human AIP Mutations and the Structure of Porphobilinogen Deaminase

The increasing use of polymerase chain reaction (PCR) methods over recent years has allowed the genetic lesions responsible for AIP to be identified. PCR has been employed to amplify mutant DNA for sequence analysis and hence detection of mutations (Picat *et al.*, 1991; Mgone *et al.*, 1992; Delfau *et al.*, 1990; Llewellyn *et al.*, 1992; Scobie *et al.*, 1990). The mutant proteins can be classed according to their enzymic activity and their immunological cross-reactivity, allowing a useful phenotypic characterisation of AIP carriers to be made (Desnick *et al.*, 1985; Nordmann *et al.*, 1990). A positive CRIM status (cross immuno reacting material) indicates a mutant allele which expresses recognisable protein but displays reduced activity, and a CRIM-negative status indicates an unrecognisable protein.

The determination of the three-dimensional structure of *E. coli* porphobilinogen deaminase (Louie *et al.*, 1992) allows the molecular basis of AIP to be better understood. There is 43% identity between the *E. coli* and human sequences of porphobilinogen deaminase (rising to 60% for conserved residues), and the structure of the enzyme from *E. coli* can therefore act as a suitable model for the human enzyme. In this way, the reported human mutations have been analysed for their likely effects on the enzyme structure and catalytic process (Brownlie *et al.*, 1995). The *E. coli* model of the enzyme does have limitations to its use, both in mobile regions and also in "insert" regions where the structure of the human enzyme can only be predicted. However, analysis of intron/extron boundaries indicates that all introns are located in or near to loops connecting secondary structural elements and therefore, overall, the *E.coli* enzyme structure is unlikely to be significantly different to that of the human enzyme.

The mutations of porphobilinogen deaminase identified in AIP sufferers can be classified into one of four types. The first of these, the type 1 mutations, are those which result in frameshifts, incorrect splicing and inappropriate stop codons. These factors easily explain the CRIM-negative status that all but one of the type 1 mutations display. The mutant proteins are predictably unable to fold in a recognisable manner, and may additionally be more susceptible to rapid proteolysis.

Type 2 mutations destabilise the protein structure through steric hindrance or loss of interactions. For example, two mutations of an invariant arginine, R116W and R116T [101], are obviously detrimental to the protein and result in a CRIM-negative status (human numbering, followed by *E.coli* numbering in brackets). The arginine is located on one of two short strands linking domains 1 and 2, and the charged side-chain participates in an ion-pair with a glutamate, E250. The effect of disrupting the R116-E250 salt bridge is also confirmed by the CRIM-negative status of the human E250K mutant. Surprisingly, the site-directed mutations at this position in the *E.coli* enzyme [R101H or R101L] are not disruptive to the enzyme. Type two mutations may also involve mutations in the hydrophobic core, which are deleterious to the protein structure, either because they introduce a buried charge group or lead to large volume change and associated steric clashes, e.g. L177R [159] and A31T [16].

Type 3 mutations involve residues important to the catalytic reaction, and are easily reconciled with the disruption caused. The arginine residues R149, R150, R167 and R173 [131, 132, 149 and 155] all form important interactions with the acetate and propionate side groups of the cofactor and their mutations lead to reduced catalytic activity. A mutation of R149 to histidine or leucine (R149H or R149L) causes the loss of interaction with ring C1 of the cofactor and gives rise to the apoenzyme form. The *E.coli* apoenzyme is unstable, and the human apoenzyme is probably equally rapidly degraded, explaining the CRIM-negative status of R149 mutants. Not all mutants in the catalytic site lead to unrecognisable proteins. The mutation of residue R167, which interacts with the ring C2 side chain when it occupies the hypothesised substrate-binding site, to histidine or leucine (R167H or R167L) leads to an accumulation of the ES intermediate and an elevated K_m. Both mutants R167H and R167L have a CRIM-positive status, as do mutants of R173.

Finally, there are type 4 mutations which have an unknown effect. Such mutations are neither exclusively CRIM-positive nor CRIM-negative. All type 4 mutations are found on the surface of the molecule.

In general, around 85% of unrelated patients with AIP have a CRIM-negative phenotype. The major changes in structure which bring about this phenotype can explain the loss of activity. Of the CRIM-positive mutations,

most occur around the large active site. Here, a number of mutations may occur which would be detrimental for activity but not affect the structure. The high CRIM-positive/activity ratios of some mutants may be satisfied by the presence of stable enzyme-intermediates, which become 'trapped' by the inability of the mutant enzyme to carry the reaction further.

1.9 Comparisons Between Porphobilinogen Deaminase and Periplasmic Binding Proteins

The recent crystal structure determination of porphobilinogen deaminase has shown that this enzyme has the same polypeptide-chain folds as proteins from two classes of binding proteins, the transferrins, in particular, lactoferrin, and the group II periplasmic binding proteins (Louie, 1993). The structural similarities give rise to hypothesis concerning both the molecular evolution of these proteins and the mechanism by which porphobilinogen deaminase catalyses its reaction.

The domains 1 and 2 of porphobilinogen deaminase resemble a number of binding proteins, which also have a core of two topologically similar domains. These binding proteins include the duplicated lobes of transferrins (lactoferrin and serum transferrin) and also the group II periplasmic receptors (the sulphate-, phosphate-, maltodextrin- and lysine/arginine/ornithine binding proteins) (Baker and Lindley, 1992; Quiocho, 1991). Of the 210 carbon atoms in α-helices in domains 1 and 2 of deaminase, 113 are found to be equivalent in the N-lobe of lactoferrin when the two structures are superimposed. Porphobilinogen deaminase and the binding proteins all share the same connectivity within the two rearranged parallel α/β domains and have two interdomain hinge segments. They also have similar lengths of secondary structural elements and similar overall twists of the core β sheets. The N-terminal domains of these proteins share the greatest structural similarity. However, there is no significant sequence identity (less than 12%) between porphobilinogen deaminase and the other proteins. The five residues E-N-R-A-D from porphobilinogen deaminase and the N-lobe of lactoferrin constitute the longest segment of identical sequence between deaminase and any of the binding proteins.

A common feature of deaminase and binding proteins is the binding cleft formed at the interface between the two domains, and the involvement of the amino terminus of one or more α-helices in forming the ligand binding site. For deaminase and several of the binding proteins the ligand is oxyanionic. For example, the active site cleft of deaminase has to provide a binding site for up to twelve carboxylate groups carried on the side substituents of the dipyrromethane and the polypyrrole product; in the transferrins, the initial step in iron ligation is the binding of the essential carbonate anion which provides two coordinate bonds for the ferric ion which is subsequently bound (Anderson *et al.*, 1990).

Despite the lack of sequence homology among porphobilinogen deaminase and the binding proteins, there are several functionally important residues which occur at roughly equivalent positions. These include a serine (residue 129 in deaminase) that both caps the α-12 helix and hydrogen bonds to an acid oxygen on the ligand, an arginine (arg-131 in deaminase) near the amino terminus of this helix which hydrogen bonds to an acid oxygen on the ligand and an aspartate (residue 84 in deaminase) which has diverse roles such as ligand binding, catalysis and domain closure.

The interdomain flexibility inherent in these proteins is also of considerable mechanistic importance to both the binding proteins and porphobilinogen deaminase. In a number of these proteins, both open and closed conformations have been observed crystallographically, the two conformations differing in the width of the interdomain cleft (Rosenberg, 1991; Sack *et al.*, 1989; Oh *et al.*, 1993). Cleft widening is brought about mainly from hinging about the two connecting interdomain strands. In the N-lobe of apo-lactoferrin, exposed basic side chains in the open cleft might serve to attract the carbonate ion, in hololactoferrin a 54° relative rotation of the two domains closes the cleft around the bound ligand and assembles the coordinate sphere for the ferric ion.

In accordance with the considerably larger size of the dipyrromethane cofactor and the tetrapyrrolic chain, the binding cleft in porphobilinogen deaminase has a larger volume than those in the binding proteins. In deaminase, residues mainly from domain 1 form the catalytic and substrate binding sites, whereas residues primarily from domain 2 provide both the binding site for the cofactor and an internal cavity that might serve to

accommodate the growing chain. Therefore, a relative twisting of the two domains provides a possible model for the mechanism by which the terminal ring of the growing chain is carried into the appropriate position to react with the next molecule of porphobilinogen.

To optimise conditions for substrate binding and catalysis, it is important in binding proteins to exclude solvent from the vicinity of the bound ligand in the closed binding cleft. An analogous function in deaminase, to protect reactive intermediates, involves not only cleft closure but movement of the mobile lid. This lid, which is absent in binding proteins, is proposed to close over the active site cleft upon substrate binding (Louie, 1993; Louie, 1995).

The close structural resemblance amongst porphobilinogen deaminase and the binding proteins suggests that these proteins are related by divergent evolution (Louie, 1993). It can be speculated that porphobilinogen deaminase originated from a two domain binding protein specific for an anionic, porphobilinogen-like or perhaps dipyrrolic ligand, and then acquired catalytic groups and possibly the mobile lid. This ancestral porphobilinogen deaminase might have rudimentally catalysed the coupling of porphobilinogen molecules within its binding cleft without covalently attaching the first porphobilinogen to the polypeptide chain. The proposed evolutionary relationship is summarised below in figure 1.14.

Figure 1.14 The Proposed Evolutionary Relationship Among the Group I and Group II Periplasmic Binding Proteins, Porphobilinogen Deaminase and the Transferrins

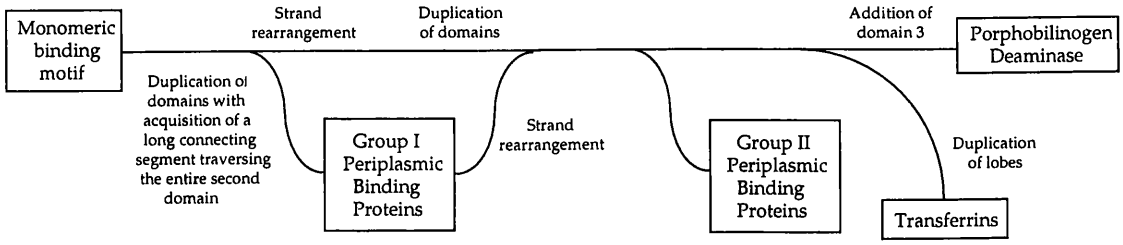

1.10 Aims of the Research

From the foregoing discussion it is clear that although the crystal structure of porphobilinogen deaminase has provided a great deal of valuable information concerning both form and function, it has also produced many questions which need to be addressed. Two questions are of particular importance: Firstly, how does the enzyme self-catalyse the synthesis and insertion of the dipyrromethane cofactor? Does the apoenzyme use the same catalytic machinery employed for preuroporphyrinogen synthesis or are other catalytic groups involved? Secondly, which model is correct for the catalytic cycle of the enzyme, the accommodating active site or the moving chain? Is it possible to obtain a structure of the enzyme in the midst of the cycle, a snapshot of the working enzyme?

i) The Mechanism of Cofactor Assembly

The study of cofactor assembly requires the generation and purification of the "apoenzyme", the form of enyme in which the cofactor is lacking. Once isolated, the apoenzyme can be studied in terms of its structure, stability, and the rate of its conversion to holoenzyme (the form in which the cofactor is present). Preliminary studies on the apoenyme of porphobilinogen deaminase have previously been made (Scott *et al.*, 1989; Hart *et al.*, 1989), and are reviewed in Chapter 5. However, the characterisation of the apoenzyme is comparatively poor and there are a number of unanswered questions. In particular it is suggested, on the basis of nmr evidence, that the apoenzyme is mostly unfolded and only takes on a folded, compact structure on binding the cofactor. How can an unfolded protein promote catalysis? It is much more likely that the cofactor serves to bring the three domains together into a compact structure through their binding to the dipyrromethane. It is more difficult to conceive that the cofactor alone could also promote the folding of structure within the domains. We want to investigate the more likely scenario that the apoenzyme is folded but is flexible around the links between the domains.

In addition, previous work has shown that the maximum conversion to holoenzyme that can be achieved by incubating apoenzyme with porphobilinogen is only around 40%, and this process occurs very

slowly over a period of several hours (Scott *et al.*, 1989; Hart *et al.*, 1989). It would be expected, though, that such a low conversion would be unacceptable *in vivo*, and conditions must exist in which a higher rate of conversion could be achieved. Further , the question of whether the cofactor is bound using the same catalytic machinery as for the binding of substrate has not been addressed. The conversion of apoenzyme to holoenzyme, along with the conformation, stability and inhibition of apoenzyme, were all therefore selected for study.

ii) Substrate Binding and Catalysis

The mechanism by which the enzyme accommodates the growing polypyrrole chain is still one of speculation. It was proposed that valuable evidence regarding this mechanism could be derived from the x-ray crystal structure determination of an enzyme-intermediate complex. To this end the mutant enzyme D84E, in which the catalytically important aspartate-84 had been mutated to glutamate, was chosen for further study based on the fact that the reduced activity of this mutant would provide enzyme-intermediate complexes which would be much more stable than the wild-type equivalents. Once isolated, the highly stable entities would be used for crystallisation and structure determination of the complexes.

The two remaining mutants of aspartate-84, D84A (alanine) and D84N (asparagine), were also chosen for further investigation. The observation that these mutants were catalytically inactive and yet able to exist as ES_2 complexes (Woodcock, 1992) posed an interesting mechanistic enigma. Therefore, the task of establishing the exact nature of these mutants and of providing an explanation for their existence was also undertaken.

Finally, it was hoped that all the observations from the research could be drawn together to provide a clear, overall picture of cofactor assembly, substrate binding and catalysis, and allied conformational changes.

Chapter 2

Materials and Methods

2.1 Materials

PD-10 columns, Sephadex G-75, and all f.p.l.c. equipment and columns were purchased from Pharmacia. Mimetic Orange A6XL column resin was from Affinity Chromatography Limited. Tryptone and yeast extract were obtained from Difco laboratories. All other chemicals were supplied by Sigma Chemical Company, unless stated otherwise.

2.1.1 Bacterial Strains and Vectors

The *E.coli* strains and vectors used are described in Table 2.1.

2.1.2 Media

Luria Broth (LB) Media (Lennox, 1955)

Bacto tryptone	10g
Bacto yeast extract	5g
NaCl	5g

This was made up to 1L with distilled water and autoclaved.

LB Plates

Bacto agar (15g) was added to 1L of the above media before autoclaving and was used to prepare approximately 30 plates.

2xTY Media

Bacto tryptone	16g
Bacto yeast extract	5g
NaCl	5g

This was made up to 1L with distilled water and autoclaved.

Table 2.1 Bacterial Strains and Plasmids Used in this Study

a) Bacterial Strains

Strain	Genotype / Properties	Source
TB1	ara, (lac-proAB), hsdD5, F'[traD36, proA+B+, lacIq, lacZ M15]	Gacesa & Ramji, 1994
JM101	supE, thi-1, (lac-proAB) F'[traD36, proAB, lacIq, Z M15J	Gacesa & Ramji, 1994
SWD84A	as TB1 with pSWD84A	Woodcock & Jordan, 1994
SWD84E	as TB1 with pSWD84E	Woodcock & Jordan, 1994
SWD84N	as TB1 with pSWD84N	Woodcock & Jordan, 1994
MV1190	(dut+, ung+)	Kunkel *et al.*, 1987
RP523	thr-1 leuB6 thi-1 lac Y1 tonA21 supE44 λ- F-, hemB-, heme permeable	Li *et al.*, 1988

b) Vectors and Recombinant

Plasmid	Properties	Plasmid Size (kb)	Source
pBR322	Cloning vector	4.36	Bolivar *et al.*, 1977
pST46	pBR322 with a 2.89kb Sau3A insert from pLC41-4 carrying hemC and hemD	7.24	Thomas & Jordan, 1986
pUC18	Cloning vector	1.68	Messing, 1983
pBM3	pUC18 with a 1.68kb BamHI/SalI fragment carrying hemC	4.38	Mbgeje, 1990
pSWD84A	pUC18 with a 1.68kb BamHI/SalI fragment carrying a hemC mutant of ala for asp at position 84	4.38	Woodcock & Jordan, 1995
pSWD84E	as for pSWD84A, carrying a hemC mutant of glu for asp at position 84	4.38	Woodcock & Jordan, 1995
pSWD84N	as for pSWD84A carrying a hemC mutant of asn for asp at position 84	4.38	Woodcock & Jordan, 1995

2.1.3 Buffers and Solutions

All of the following solutions were sterilised by autoclaving and stored at room temperature unless otherwise stated.

Cell Resuspension Solution

50mM Tris/HCl pH 7.5
10mM EDTA
100µg/ml RNaseA

Cell Lysis Solution

2M NaOH
1% SDS

Neutralisation Solution

1.32M Potassium acetate pH 4.8

TE Buffer

10mM Tris/HCl pH 8.0
1mM EDTA pH 8.0

Column Wash Solution

200mM NaCl
20mM Tris/HCl pH 7.5
5mM EDTA

The solution was diluted with 95% ethanol.

50x TAE

242g Tris/HCl
37.2g Na_2EDTA
57.1ml Glacial acetic acid

$CaCl_2$ Solution (50mM)

$CaCl_2.2H_2O$	7.4g

This was made up to 1l with distilled water, autoclaved and stored at 4°C.

SOC Media

Bacto tryptone	20g
Bacto yeast extract	5g
NaCl	0.5g

This was made up to 950ml with distilled water, and 250mM KCl added (10ml). The solution was adjusted to pH 7.0 with 5N NaOH, made up to a final volume of 1L with distilled water and autoclaved. After cooling, a sterile solution of 1M glucose (20ml) was added.

10x Ligase Buffer

100mM Tris/HCl pH 7.5
50mM $MgCl_2$
50mM DTT
10mM ATP

The $MgCl_2$ and Tris/HCl soltion was sterilised by autoclaving. The DTT and ATP were added subsequently, and the solution filter sterilised and stored at -20°C.

DNA Loading Buffer

0.25% Bromophenol Blue
0.25% xylene cyanol
30% glycerol

This mixture was made in distilled water and autoclaved.

Ethidium Bromide Solution

A stock solution of 10mg/ml was made and was used at a final concentration of 0.5µg/ml.

Preparation of Hemin Solution

Hemin (30mg) was dissolved in 0.2N KOH (400µl), the hemin being added slowly with vortexing between each addition. Next, H_20 (600µl) and 1M Tris/HCl pH7.8 (100µl) was added, followed by ethylene glycol (4.8ml). This solution was mixed by vortexing and centrifuged at 5000g for 5 minutes at 4°C. The insoluble pellet was discarded and the hemin solution used at 1µl/ml. Hemin was required for the growth of the *hemB* derivative of *E.coli.*

2.1.4 Sterilisation

The glassware and plasticware were sterilised by autoclaving at 15 p.s.i. for fifteen minutes.

2.2 Molecular Biology Methods

2.2.1 Digestion of DNA

The restriction enzymes used in this work were purchased from Promega and Pharmacia and came with the required buffers to effect the optimal restriction.

The restriction reactions were carried out in microfuge tubes which in general contained DNA (1µg), restriction enzyme (1µl), 10x buffer (2µl) and water to give a final volume of 20µl. The reactions were incubated at 37°C for 1-3 hours and were terminated by heating the mixture to 80°C for 10 minutes. The reaction mixture was then run on an agarose gel.

2.2.2 Electrophoresis of DNA

The electrophoresis of DNA through an agarose gel was used to separtate, identify and purify DNA fragments. The agarose powder in 1xTAE buffer was melted in a microwave oven. The concentration of agarose used was dependant on the DNA fragment size; the higher the percentage of agarose the smaller the fragments resolved. Routinely a 1% agarose gel was made. The solution was allowed to cool to 50°C before ethidium bromide (10mg/ml) was added to give a final concentration of 0.5mg/ml. The solution was then poured onto a clean gel casting tray, the comb inserted and the gel allowed to set. When the gel had set the comb was removed and the gel placed in a gel tank filled with 1xTAE buffer containing ethidium bromide (0.5µg/ml). The DNA samples, containing loading buffer, were loaded into the wells and the electrophoresis was carried out at 100V for 1 hour.

2.2.3 Visualisation of DNA

The DNA was visualised by placing the gel on a uv-transilluminator.

2.2.4 Determination of DNA Fragment Size

The size of DNA fragments obtained from the restriction digests were estimated by comparing their relative mobilities with fragments of known sizes. The standards routinely used were λ DNA digested with both *Hin*dIII and *Eco*RI, and *Hin*dIII alone (Table 2.2).

Table 2.2 Molecular Size Markers for DNA Agarose Gels

λ-HindIII (kb)	λ-HindIII-EcoRI (kb)
23.130	21.226
9.146	5.148
6.557	4.973
4.361	4.268
2.322	3.530
2.027	2.027
0.564	1.904
0.125	1.584
	1.375
	0.947
	0.831
	0.564
	0.125

2.2.5 Isolation of Plasmid DNA

Plasmid DNA was isolated using the Magic™ Minipreps DNA System (Promega). An overnight culture of *E.coli* (1-3ml) containing the desired plasmid was harvested by centrifugation, and the pellet resuspended in Cell Resuspension Solution (200µl). Cell Lysis Solution (200µl) was added, and the tube inverted several times to give rise to a clear suspension. Next, Neutralisation Solution (200µl) was added, and again the contents mixed by several inversions. The suspension was then centrifuged for 5 minutes and the supernatant transferred to a fresh microfuge tube.

Magic Minipreps DNA Purification Resin (1ml) was added to the supernatant, and the mixture pipetted into a syringe barrel attached to a Magic Minicolumn. The syringe plunger was carefully inserted into the barrel to push the slurry into the Minicolumn. In the same manner, Column Wash Solution (2ml) was added to the Minicolumn. The syringe was removed and the Minicolumn transferred to a microfuge tube in which it was centrifuged for 20 seconds to dry the resin. The Minicolumn was then transferred to a fresh microfuge tube and TE buffer or water (50µl) added. After 1 minute, the

tube was centrifuged for 20 seconds, which led to the elution of the DNA. The DNA was stored at -20°C.

2.2.6 Transformation of DNA into *E.coli*

Using $CaCl_2$ to create competent cells

A bacterial culture of a strain of *E.coli* cells was grown until it had reached an optical density at 600nm of around 0.5. The cells were made competent by resuspending the bacterial pellet from the culture (40ml) in cold 100mM $CaCl_2$ (10ml) at 4°C for a minimum of 45 minutes. After centrifugation for 5 minutes at 4°C, the pellet was resuspended in a solution of 1M $CaCl_2$ (200µl), 50% glycerol (560µl) and H_20 (1240µl). This suspension was aliquoted (200µl) into pre-chilled microfuge tubes and stored at -70°C. For transformation, plasmid DNA (5µl) was added to an aliquot of competent cells and kept on ice for 20 minutes. The cells were then heat shocked at 42°C for 2 minutes. Next, LB media (800µl) was added and the mixture was incubated at 37°C for 20 minutes. The mixture (200µl) was spread on an agar plate containing ampicillin (100µg/ml).

Using electroporation to create competent cells

A bacterial culture of a strain of *E.coli* cells was grown until it had reached an optical density at 600nm of around 0.5. The cells were left on ice for 15 minutes then centrifuged at 4°C for 15 minutes . The pellet was resuspended in distilled water (200µl) and the cells again centrifuged at 4°C for 15 minutes. The distilled water wash was repeated three times. The cells were then resuspended in 10% glycerol and centrifuged in microfuge tubes for 3 minutes. Finally the cells were resuspended in 7% glycerol, frozen in liquid nitrogen and stored at -70°C. For transformation, an aliquot of competent cells (40µl) was added to plasmid DNA (2µl)in a microfuge tube. Within one minute, the mixture was placed in a cuvette and electroporated at 2.5kV. The mixture was then transferred back to a microfuge tube, SOC media (1ml) added and was left shaking at 37°C for one hour. The suspension (250µl) was spread on an agar plate containing ampicillin (100µg/ml).

2.3 Assay Methods

2.3.1 Preparation of Modified Ehrlich's Reagent

Modified Ehrlich's reagent was freshly prepared by dissolving 1g of p-dimethylaminobenzaldehyde in glacial acetic acid (42ml) followed by perchloric acid (70%, 8ml) (Mauzerall and Granick, 1956).

2.3.2 Quantitation of Porphobilinogen

A porphobilinogen solution was mixed with an equal volume of Ehrlich's reagent and the colour left to develop for 15 minutes. The absorption was measured at 555nm and the concentration of porphobilinogen was calculated using the molar extinction coefficient, ε_M= 60200 M^{-1} cm^{-1} (Mauzerall and Granick, 1956).

2.3.3 Determination of Porphobilinogen Deaminase Activity

Porphobilinogen deaminase activity was assayed by measuring the formation of uroporphyrinogen I. An incubation mixture of buffer (100mM phosphate buffer pH 8.0, containing 13mM β-mercaptoethanol and enzyme (total volume 450µl) was warmed to 37°C, as was the substrate, porphobilinogen. A stoichiometric excess of porphobilinogen (50µl) was added to the incubation mixture and kept at 37°C for the required time. The reaction was stopped by the addition of 5N HCl (20µl) to an aliquot of the reaction mixture (80µl). This was then diluted 10-fold with 1N HCl, and benzoquinone (10µl, 0.1% w/v in methanol) added to oxidise the uroporphyrinogen to uroporphyrin. The mixture was left on ice in the dark for 20 minutes. The absorption was measured at 405.5nm and the activity of the enzyme determined using the molar extinction coefficient, ε_M = $5.48 \times 10^5 M^{-1} cm^{-1}$.

2.3.4 Protein Quantitation

Protein concentration was determined by the method of Bradford, 1976. The protein to be quantified was prepared, in varying dilutions, to a final volume of (800µl) with distilled water. Samples for a standard curve were prepared by aliquoting bovine serum albumin at known concentrations to a final volume of 800µl in distilled water. Bradford's Reagent (200µl) was added to each sample, and, after 15 minutes at room temperature, the absorption measured at 595nm. The unknown protein concentration could be determined on comparison to the standard curve.

2.3.5 Purification Procedure

Purification of *E.coli* Porphobilinogen Deaminase

The *E.coli* bacteria overexpressing the porphobilinogen deaminase wild-type, apoenzyme or mutant were grown in LB media containing ampicillin (100µg/ml) overnight at 37°C with shaking (200 rpm), in 2 litre baffled flasks containing 1 litre of media. In the case of apoenzyme, hemin (1µl/ml) was also added. The cells were harvested by centrifugation at 7000xg for 20 minutes.

Sonication of Bacteria

The harvested cells were resuspended in 0.1M phosphate buffer pH 8.0 containing 13mM β-mercaptoethanol (5g cells/ 20ml buffer). The cells were broken by sonication, using a MSE Soniprep ultrasonic disintegrator, at an amplitude of 8 microns in five 1 minute bursts.

Heat Treatment

The sonicate was heated to 60°C and was maintained at this temperature for 10 minutes with gentle stirring. The solution was then cooled on ice and the resulting extract centrifuged (8,000 x g) at 4°C for 15 minutes. The supernatant was collected.

Ammonium Sulphate Fractionation

Solid ammonium sulphate was slowly added to stirring supernatant at room temperature to give a 55% saturation (351g per 1L of solution). The mixture was centrifuged (8,000xg), the supernatant discarded and the precipitate collected. The porphobilinogen deaminase activity was found in the precipitate.

Sephadex G-75 Gel Filtration

The ammonium sulphate pellet was resuspended in 50mM Tris/HCl buffer pH 6.0 containing 13mM β-mercaptoethanol and applied to the top of a vertical column (150cm x 2.5cm) of Sephadex G-75. The column had been equilibriated in 50mM Tris/HCl buffer pH 6.0 containing 13mM β-mercaptoethanol and 0.02% sodium azide, and run at a flow rate of 600ml/min. The gel filtration column was thoroughly washed with the buffer after use. The fractions containing the enzyme were pooled and 2mM dithiothreitol added. The resulting solution was then concentrated in an Amicon ultrafiltration cell fitted with a PM-10 membrane.

Mimetic Orange 1 Affinity Chromatography Column

This step was used for the purification of apoenzyme only. The crude extract of the*E.coli* bacteria containing the porphobilinogen deaminase apoenzyme obtained after sonication and centrifugation, and applied directly to the top of a vertical column (8cm x 1cm) of Mimetic Orange 1 A6XL. The column had been equilibriated in 20mM Tris/HCl pH8.0 (200ml) containing 7mM β-mercaptoethanol, and the same buffer containing increasing salt concentrations was used to elute the apoenzyme.

The apoenzyme was eluted by washing the column with Tris buffer (20mM Tris/HCl pH8.0) (40ml), buffer containing 100mM NaCl (40ml),buffer containing 250mM NaCl (40ml), buffer containing 500mM NaCl (40ml) and buffer containing 1M NaCl (40ml). The fractions containing the purified apoenzyme were then pooled.

The column was washed with 2M NaOH (80ml) and exhaustively with buffer. The column was stored in 25% ethanol (200ml for wash) containing 0.1M NaCl.

PD-10 Column

The purified protein was desalted by gel filtration through a PD-10 column which had been equilibriated against 1mM Tris buffer containing 2mM dithiothreitol. The protein was freeze-dried and stored at -20°C.

2.3.6 Polyacrylamide Gel Electrophoresis

Polyacrylamide gel electrophoresis under denaturing conditions was carried out on a 12% gel. The running gel and stacking gel were made according to the compositions given in table 2.3. The samples were denatured by adding an equal volume of disruption buffer (20% SDS, 1ml; 1M Tris/HCl pH 8, 500ml; glycerol, 600ml; β-mercaptoethanol, 500ml; 0.1% bromophenol blue; distilled water, 7.4ml) and then boiling for ten minutes. Approximately 16µl of sample (8µl protein sample, 8µl disruption buffer) was loaded per well. Each gel was run at a 35mA current until the blue dye had reached the bottom of the gel, stained for protein using Coomassie brilliant blue (0.2% in 10% acetic acid/40% methanol) and destained using 10% acetic acid/40% methanol. The M_r of the protein was determined using protein standards (Table 2.4).

Polyacrylamide gel electrophoresis under non denaturing conditions was carried out as for denaturing conditions but in the absence of SDS and β-mercaptoethanol, at a temperature of 4°C. Enzyme activity on the gel was determined by incubating the gel in a porphobilinogen solution (0.04mM in 0.1M phosphate buffer pH 8.0) at 37°C for up to 90 minutes. This was visualised by examining the fluorescence of the gel on a uv-transilluminator, the fluorescence indicating a porphyrin product. The gel was then stained for protein as above.

Table 2.3 Compositions of Solutions for Denaturing Polyacrylamide Gels

Solution	Volume (ml)	
	Running Gel	Stacking Gel
Acrylamide Bisacrylamide (30%)	3.20	1.00
1.5 M Tris/HCl buffer pH 8.8	2.00	-
0.5 M Tris/HCl buffer pH 6.8	-	1.00
H_2O	2.80	3.00
SDS (10%)	0.08	0.10
TEMED	0.02	0.02
APS	0.10	0.10

Table 2.4 Molecular Weight Markers for Denaturing Polyacrylamide Gels

Protein Standards	Molecular Mass (Da)
Bovine Albumin	66000
Ovalbumin	45000
G3P dehydrogenase	36000
Carbonic anhydrase	29000
Trypsinogen	24000
Soybean trypsin inhibitor	20100
α-lactalbumin	14200

2.3.7 Generation of Porphobilinogen

Porphobilinogen was generated enzymatically according to the method of Jordan and Seehra, 1986. In brief, 5-aminolaevulinic acid dehydratase (500 units) was incubated with 5-aminolaevulinic acid hydrochloride (1g) in 10mM phosphate buffer pH 6.8 (2L) containing 10mM dithiothreitol at 37°C for 17 hours, in the dark and under an atmosphere of nitrogen. The pH of the solution was adjusted to 7.5, and the solution was applied to a column of Dowex 1-X8 (200-400 mesh) acetate. The column was

washed with 1l of water, after which the porphobilinogen was eluted with 1M acetic acid and lyophilised. The porphobilinogen was further purified by recrystallisation from dilute ammonia by adjusting the pH to 5.5 with 0.1M acetic acid. The crystals were filtered, washed with ice-cold methanol and freeze-dried. The crystals were stored at -20°C in the presence of a desiccant.

2.3.8 Reconstitution of Holoenzyme Porphobilinogen Deaminase

Generally, the holoenzyme was reconstituted from the apoenzyme (100µg) by preincubation with a stoichiometric excess of porphobilinogen in 0.1M phosphate buffer pH 8.0 containing 13mM β-mercaptoethanol. The preincubations varied with respect to porphobilinogen concentration, temperature (4°C or 37°C) and length.

Alternatively, the holoenzyme was reconstituted by preincubation of the apoenzyme with preuroporphyrinogen. The preuroporphyrinogen (0.1µmol) was generated by incubating holoenzyme (100µg) with porphobilinogen (0.5µmol) at 37°C in 25mM Tris/HCl pH 9.3 containing 13mM β-mercaptoethanol until all the porphobilinogen had been consumed, followed by removal of the holoenzyme by concentration in an Amicon ultrafiltration cell fitted with a PM-10 membrane, and finally immediate fast-freezing of the preuroporphyrinogen in liquid nitrogen. Preuroporphyrinogen could also be generated in the standard preincubation mix by the addition of a small quantity of holoenzyme (1/50 molar equivalent) to apoenzyme and porphobilinogen.

2.3.9 Purification of Enzyme and Formation and Purification of Enzyme-Intermediate Complexes

The freeze dried enzyme was dissolved in 20mM Tris/HCl buffer (pH 7.5) to give a concentration of 1mg/ml. The solution was applied to a high resolution anion exchange Mono Q HR5/5 column attached to a Pharmacia f.p.l.c. system which had been equilibriated in 20mM Tris/HCl buffer pH 7.5 containing 7mM β-mercaptoethanol.The enzyme was eluted using a linear gradient of sodium chloride (100-350mM, 20ml) at a flow rate of

1ml/min. The absorbance was monitored at 280nm and all fractions eluting from the column which corresponded to peaks in absorbance were collected.

The enzyme-intermediate complexes were generated by mixing stoichiometric amounts of the enzyme (30nmoles) and sustrate (30-1,200nmoles) rapidly at 4°C. The individual complexes were isolated and purified using the f.p.l.c. system, the enzyme eluted using a linear gradient of sodium chloride (100-400mM, 24 ml) at a flow rate of 1ml/min. The complexes were then desalted by gel filtration using a PD10 column equilibriated against mM Tris buffer containing 2mM dithiothreitol, freeze dried and stored at -20°C.

2.3.10 Holoenzyme and Enzyme-Intermediate Complex Detection

The protein solution (1mg/ml) was mixed with an equal volume of Ehrlich's reagent and its spectrum was measured immediately over a range of 350-600nm. The spectra were retaken at intervals over 15 minutes.

2.3.11 Cleavage of Porphobilinogen Deaminase Cofactor

Solid holoenzyme (10mg) was resuspended in 20mM Tris buffer pH 6.0 (6ml) containing dithiothreitol at 2mg/ml and concentrated hydrochloric acid slowly added to a final concentration of 1M. The solution was allowed to stand, in the dark, at room temperature overnight. Protein was collected by centrifugation and resuspended in 50mM phosphate buffer pH 7.2 (35ml) containing 6mM EDTA , 1mM dithiothreitol, 0.1M NaCl and 0.6M urea. The solution was dialysed against the same buffer overnight. Dialysis was continued against 50mM phosphate buffer pH 7.4 containing 6mM EDTA and 13mM β-mercatoethanol for a further 48 hours, with one change of buffer. Finally, the solution was concentrated by ultrafiltration on a PM10 membrane and desalted via gel filtration into 1mM Tris/HCl buffer pH 7.5 containing 2mM dithiothreitol . The solution containing pure apoenzyme was freeze-dried and stored at -20°C.

2.3.12 Treatment of Porphobilinogen Deaminase with Hydroxylamine

A stock solution of 2M hydroxylamine pH 8 was prepared. Hydroxylamine was typically incubated with protein (1mg/ml) in 0.1M phosphate buffer pH 8.0 containing 13mM β-mercaptoethanol at a final concentration of 0.2M.

2.3.13 Inhibition of Porphobilinogen Deaminase Activity

Inhibitor studies were carried out by adding the substrate analogues in stoichiometric equivalents to the enzyme in 0.1M phosphate buffer pH 8.0 containing 13mM β-mercaptoethanol. After incubation, typically at 4°C for 15 minutes, the effects of inhibition were determined either by assay of enzymic activity or by analysis *via* non denaturing polyacrylamide gel electrophoresis.

The inhibitor N-ethylmaleimide (NEM) was incubated with the enzyme at final concentrations of 1, 5, 10 and 50mM in a similar way, but in the absence of reducing agents. The effects of NEM inhibition were also determined by assay of enzymic activity or by analysis *via* non denaturing polyacrylamide gel electrophoresis.

2.3.14 Radioactive Labelling of Enzyme Using 5-Amino-[5-^{14}C] Levulinic Acid

Incorporation of Label and Purification of Enzyme

The *E.coli* bacteria containing the porphobilinogen deaminase mutant D84N were grown in 500ml of LB media containing ampicillin (100μg/ml) and 5-amino-[5-^{14}C] levulinic acid (1μCi) overnight at 37°C with shaking (200rpm).The cells were harvested by centrifugation at 7000xg for 20 minutes. The pellet was resuspended in 0.1M phosphate buffer pH 8.0 containing 13mM β-mercaptoethanol, and partially purified via sonication, heat treatment and centrifugation. The supernatant was then applied to the f.p.l.c. system and thus the protein was loaded in phosphate buffer. The

f.p.l.c. was equilibriated in 20mM Tris/HCl buffer pH 7.5 containing 7mM β-mercaptoethanol.

Determination of ^{14}C Label Incorporation

Scintillation fluid (500µl) and distilled water (400µl) were added to each sample (100µl) to be counted. The counts per minute (cpm) were determined using a β scintillation counter.

2.3.15 Crystallisation and Structure Determination

Crystallisation of Mutant Porphobilinogen Deaminase

Crystallisation of protein was achieved at Birkbeck College, University of London, using the hanging drop method (McPherson, 1982). An ICN Accuflex system was employed to allow a number of conditions to be efficiently screened. A fine matrix search was conducted, beginning with the conditions required for the crystallisation of wild-type enzyme and working away from these in pH and polyethylene glycol (PEG) 4000 concentrations. The wild-type enzyme was known to crystallise optimally in sodium acetate/acetic acid buffer (100mM) pH 5.0 and PEG (9% w/v), at 18°C in total darkness. The hanging drop technique required only 10µg of protein per well.

Monitoring the Stability of Mutant Porphobilinogen Deaminase Enzyme-Intermediate Complexes

To monitor the stability of the enzyme-intermediate complex to crystallisation conditions, a small sample of the protein was retained and resuspended in 1mM Tris buffer containing 2mM dithiothreitol. An equal volume of sodium acetate buffer pH 5.0 was added and the mixture left at room temperature. The sample was subjected to non-SDS polyacrylamide gel electrophoresis immediately, after four hours, overnight and after two weeks.

Crystals of the enzyme were also subjected to SDS and non-SDS gel electrophoresis after a period of several months.

Data Collection of Mutant Porphobilinogen Deaminase

Data were collected from the mutant D84E at Birkbeck College on a MAR research 180mm image plate on a Siemens generator. The D84E substrate complex data were collected on a MAR image plate, initially at Birkbeck College and subsequently at Station 9.5 using sychroton radiation, at the Daresbury Laboratories. The crystals were cooled either at 4°C or -70°C.

Data Processing and Model Building

The data were refined and processed using a series of software programmes. Graphics packages were employed for the model building. A full list of the programmes used together with a brief description of their function is given in Chapter 4. In general, the wild-type structure was widely used to generate phases for the mutant structures and to serve as a reference.

2.3.16 Circular Dichroism Spectroscopy Studies on Porphobilinogen Deaminase

Circular dichroism (CD) spectroscopy studies were carried out at the National Chiroptic Centre at Birkbeck College. The protein was prepared in 20mM Tris/HCl pH 8.0 containing 13mM β-mercaptoethanol, typically at a final concentration of 1.2mg/ml. The CD spectra were obtained using either a JASCO J-720 or J-600 spectropolarimeter, and secondary structure predictions were made using the "Grams" Multiple Component Analysis Software.

2.3.17 Electrospray Mass Determinations of Porphobilinogen Deaminase Mutants

Electrospray mass determinations were carried out at Birkbeck College, after a further purification of the mutant enzyme by dialysis and reverse phase h.p.l.c. Dialysis was carried out overnight at 4°C against distilled water. The dialysed protein was applied to a C18 column attached to a Varian 5000 h.p.l.c. system. The column had been equilibriated in H_2O, and the protein was eluted from the column in a 0-70% gradient of CH_3CN/TFA (100%/0.1%). The purified protein was loaded directly on to a VG Platform

Electrospray Mass Spectrometer (ESMS), and was applied in a continuous phase of CH_3CN (50%).

2.3.18 Dynamic Light Scattering of Porphobilinogen Deaminase

Molecular sizing was carried out using the dynamic light scattering machine, DynaPro-801. Samples were prepared using either a 20nm or 100nm filter.

Chapter 3

Further Characterisation of the Aspartate-84 Mutants of *E. coli* Porphobilinogen Deaminase

3.1 Introduction

The aspartate-84 residue of porphobilinogen deaminase has been mutated to alanine (D84A), glutamate (D84E) and asparagine (D84N) and the properties of the mutant enzymes studied (Woodcock, 1992; Woodcock and Jordan, 1994). A mutation to alanine would not be expected to be structurally disruptive to the protein as alanine is smaller than aspartate and therefore could easily be accommodated in the space occupied by aspartate. However, alanine is of intermediate polarity and cannot participate in hydrogen bonding. Glutamate has the same charge as aspartate and can participiate in hydrogen bonding, but is one carbon-carbon bond longer and therefore may be expected to cause the mutant to function less efficiently. Asparagine has no charge, is of comparable size and shape to aspartate and can participate in hydrogen bonding.

The characterisation of the aspartate-84 mutants has been noted to give two alternative sets of results, which have been classified according to the presence or absence of reducing agent in the purification procedure. In all cases, each mutant migrates as a single protein band of M_r 35,000±3000, similar to that of wild-type protein when subjected to electrophoresis on an SDS polyacrylamide gel.

Electrophoresis under non-denaturing conditions reveals a double protein band profile which is characteristic for *E. coli* deaminase holoenzyme (Jordan *et al.*, 1988). In strong reducing conditions, the D84E mutant is found to migrate similarly to wild-type on a non-SDS polyacrylamide gel, which is expected as the mutant protein retains the same overall charge as the wild-type enzyme. The D84A and D84N mutants migrate with a slightly lower mobility, which again is consistent with their lower net negative charge. The results indicate that the mutants exist in the holoenzyme form, as the mobility of apoenzyme is substantially less than wild-type under non-denaturing conditions (Warren and Jordan, 1988; Scott *et al.* 1989; Jordan and Woodcock, 1991),

The coloured, oxidised forms of these mutants have also been examined by electrophoresis under non-denaturing conditions (Woodcock, 1992). The D84E mutant is still observed to migrate similarly to wild-type enzyme, whilst the D84A and D84N mutants are seen to migrate with a

greater mobility than wild-type. It is suggested in the literature that this indicates a conformational change induced in the protein by the transition from the dipyrromethane to the dipyrromethene structure, or a related chromophore (Woodcock and Jordan, 1994). An alternative explanation for the greater mobility of the D84A and D84N mutants may be the presence of an enzyme-intermediate complex, although it would be difficult to attribute such an existence solely to the absence of reducing agent. An oxidised cofactor would be unable to bind substrate.

The kinetics of the mutants have also been investigated, and the D84E mutant is found to have a specific activity of 0.3μmol/hr/mg, which is less than 1% of the wild type porphobilinogen deaminase (43μmol/hr/mg). The K_m of the D84E mutant, 16±4μM, is similar to that of the wild type, 19±7μM, and indicates that substrate binding has been largely unaffected. The unaltered K_m and the k_{cat}, which is found to be greatly reduced, are consistent with a catalytic role for aspartate-84. The alanine and asparagine mutations leave the enzyme devoid of catalytic activity.

A possible structural explanation for the D84E kinetic data may be the displacement of the carboxyl group to a position less favourable for optimal interaction with the two reacting pyrrole rings at the S and C sites. In a converse mutation for triose phosphate isomerase, the replacement of a key glutamate residue with aspartate leads to a dramatic reduction of k_{cat}/K_m (Knowles, 1991; Blacklow *et al.*, 1991). In the case of the D84A and D84N mutants, the lack of activity is likely to be due to the combined losses of negative charge, the acid group for catalysis and the hydrogen bonding ability.

All three mutants are believed to contain the dipyrromethane cofactor. When the pure enzyme for all mutants is obtained in the absence of reducing agents they are pink on freeze drying, providing evidence that the dipyrromethane cofactor is present and is likely to exist in an oxidised state. The increased oxygen sensitivity of the cofactor in the mutant enzymes compared to wild-type is predictable because of the hydrogen bonds that aspartate-84 forms with the cofactor and their contribution to the stability of the dipyrrole system; the hydrogen bonding is likely to be disrupted to various degrees in the mutants. The reaction of each mutant with modified Ehrlich's reagent further confirms the presence of the cofactor. The reaction of

D84E with Ehrlich's reagent gives a spectrum typical of a dipyrromethane, with an initial maximum absorption at 565nm and an intense purple colour changing with time to give a maximum at 495nm and a yellow colour (Plusec and Bogorad, 1970; Jordan and Warren, 1987). The reaction of the D84E mutant with Ehrlich's reagent occurs faster than that of the wild type. The reaction of D84A and D84N with Ehrlich's reagent give a spectrum with maxima seen initially at both 565 and 495nm, changing to an absorption at 495nm only. The profile of this spectrum is similar to that of a tetrapyrromethane (Radmer and Bogorad, 1972) and, again, raises the possibility of the presence of an enzyme intermediate complex, such as ES_2, for the catalytically inactive D84A and D84N mutants (Woodcock and Jordan, 1994).

The aspartate-84 mutants are found to be thermostable to temperatures of 65°C for ten minutes. This indicates that they are likely to be correctly folded and to have adopted the native tertiary structure. The mutants purified under reducing conditions can be isolated as a single peak on an f.p.l.c. system, with all three mutants eluting at a salt concentration of 240mM NaCl. The D84E mutant can be incubated with the substrate porphobilinogen to produce enzyme intermediate complexes ES, ES_2 and ES_3. When the complexes are made in this way, ES is the major peak observed and is found to be heat stable at 37°C, unlike the wild-type ES complex (Warren and Jordan, 1988). The accumulation of the ES complex indicates that for the D84E mutant the catalytic cycle is impaired for substrate binding and highlights the possible role of aspartate-84 in the tetramerisation reaction. The D84E mutant enzyme-intermediate complex ES_4 has not yet been observed.

When the mutants D84A and D84N are purified in the absence of reducing agents, a different set of results is obtained after analysis by f.p.l.c. Both mutants are found to elute at a higher salt concentration of 260mM NaCl, indicating a more negatively charged species. Elution at 260mM NaCl is more typical of the wild-type ES_2 complex and, again, suggests the presence of an enzyme-intermediate complex. The elution profile of D84E purified in the absence of reducing agent remains unchanged.

In general, the results would appear to suggest that the D84A and D84N mutants exist as the enzyme-intermediate complex ES_2. The literature has suggested that the presence of the complex may be dependant on the

oxidation state of the cofactor (Woodcock and Jordan, 1994). The presence of a complex would also satisfy the observed pink colour of protein purified in the absence of reducing agents, although this explanation would require the D84E mutant also to contain enzyme-intermediate complexes. In addition, if complexes are present it is unlikely that they would only be observed for mutants with an oxidised cofactor. An established procedure for the release of pyrrolic intermediates from native enzyme involves the treatment of the protein with bases related to ammonia (eg. NH_2OH and $NHOCH_3$, Plusec and Bogorad, 1970; Davies and Neuberger, 1973). However, treatment of the D84A and D84N mutants with the amino compound hydroxylamine yields bands of unchanged mobility when examined by denaturing PAGE. This may suggest that either the mutants are not enzyme-intermediate complexes, or that the mutant enzyme-intermediate complexes are oxidised and therefore the reaction to allow release of any pyrrolic intermediates cannot be performed. However, as the reaction to release pyrroles by nitrogenous bases is catalytic, it is more likely that the aspartate-84 mutants cannot perform the reaction simply due to their catalytic inactivity. The two mutants have also been investigated further by treatment with formic acid. Previous work (Warren 1988) has shown that treatment of ES_2 with formic acid will lead to twice as much porphyrin formation as treatment of enzyme alone for native protein. On treating the D84A and D84N mutants with formic acid, no significant increase of porphyrin production is observed in comparison to wild-type. This again implies either that the mutants may not be enzyme-intermediate complexes or that the complexes are oxidised and cannot be released.

A more likely explanation for the two alternative sets of results obtained for the D84A and D84N mutants is the different purification techniques that were used in each case. For mutants purified in the presence of reducing agents, an anion-exchange column was employed (Woodcock and Jordan, 1994). Enzyme-intermediate complexes of these mutants would possibly have remained bound to the column, whilst only the free enzyme form of the mutants would have eluted in the expected fractions. For the D84A and D84N mutants purified in the absence of reducing agents, a gel filtration column was used (Woodcock, 1992). In this case, the protein would have separated on the basis of size and not charge, and therefore any enzyme-intermediate complexes were more likely to have been isolated in this way. It

is probable that the purification of the D84E mutant *via* gel filtration would also have yielded enzyme-intermediate complexes.

The aim for this chapter is to characterise further all three aspartate-84 mutants and to establish the exact nature of the D84A and D84N mutants. It is also proposed that each mutant protein, in particular the enzyme-intermediate complex ES_2 of the D84E mutant, should also be isolated in sufficient quantity for crystallisation purposes.

3.2 Results and Discussion

3.2.1 The D84E Mutant of Porphobilinogen Deaminase

3.2.1.1 General Properties of the D84E Mutant

E. coli cells expressing the mutant D84E porphobilinogen deaminase were grown overnight in 2 litres of LB media with ampicillin (100μg/ml) overnight at 37°C with shaking. The cells were harvested by centrifugation. The mutant enzyme was purified using a slight modification of the existing protocol (Woodcock and Jordan, 1994).

The pelleted bacterial cells were resuspended in a minimum volume of 0.1M phosphate buffer pH 8.0 containing 13mM β-mercaptoethanol. The first step in the purification procedure was to break open the cells by sonication. The sonicate was heat treated and centrifuged. The enzyme was then precipitated from the supernatant using an ammonium sulphate fractionation of 0-55%. After centrifugation, the pellet from the ammonium sulphate fractionation was resuspended in a minimum volume of 20mM Tris/HCl buffer pH 6.0 containing 13mM β-mercaptoethanol and applied to a gel filtration G-75 column which had been equilibriated in the same buffer. The enzyme eluting from the column was more than 90% pure. The enzyme was concentrated to around 10mg/ml by ultrafiltration using a PM10 membrane, which allows only proteins of a molecular mass less than 10,000 Da to pass through. Finally, purified porphobilinogen deaminase was exchanged into 1mM Tris/HCl buffer pH 7.5, containing 2mM dithiothreitol using a PD-10 column, freeze-dried and stored at -20°C.

The solid pure enzyme sample was found to be colourless, which indicated that the enzyme was in a reduced form. Approximately 40mg of pure protein was obtained per prepararation from 2L of media. The purity of the enzyme was studied at various stages of the purification procedure by polyacrylamide gel electrophoresis using a 12% SDS gel. The molecular mass of the protein, 35,000 Da, was determined by comparing the mobility on the gel with that of the molecular mass markers. The specific activity was found to be 0.27μmol/hr/mg.

3.2.1.2 F.P.L.C. of the D84E Mutant Porphobilinogen Deaminase

After purification the mutant D84E porphobilinogen deaminase (~10mg/ml) was applied to a MonoQ HR5/5 column attached to a Pharmacia f.p.l.c. system. The MonoQ column had been equilibriated in 20mM Tris/HCl buffer pH 7.5 containing 7mM β-mercaptoethanol. The purified protein was eluted from the column in the same buffer using a linear salt gradient. The resulting chromatogram is presented in figure 3.1.

Figure 3.1 F.P.L.C. Trace of Purified Mutant D84E Porphobilinogen Deaminase

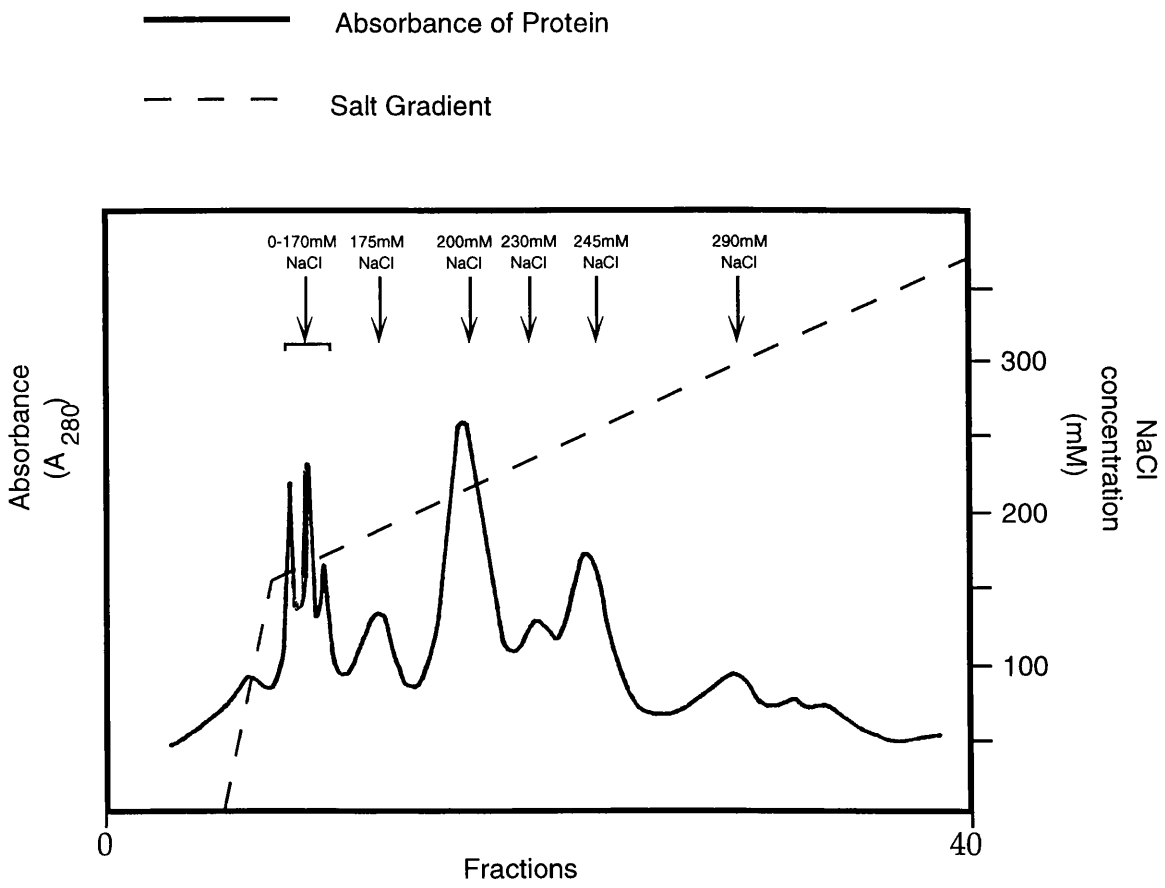

The chromatogram in figure 3.1 shows that the f.p.l.c. system allowed the further separation of protein by anion-exchange. Multiple peaks for protein were observed eluting in 0-170mM NaCl. Five other peaks were

detected, eluting at 175mM NaCl, 200mM NaCl, 230mM NaCl, 245 mM NaCl and 290mM NaCl.

3.2.1.3 Polyacrylamide Gel Electrophoresis of the Peaks Isolated From the F.P.L.C. of D84E

The fractions isolated from the f.p.l.c. of D84E were subjected to electrophoresis on denaturing and non-denaturing polyacrylamide gels, to examine further their deaminase content. The gels are shown in figure 3.2 and 3.3.

The denaturing gels in figure 3.2 show that lanes 1-9 contained little deaminase, lanes 10-18 contained a strong band migrating the same distance as the 36,000 Da band of the molecular mass marker and fractions 19 -22 contained a weaker band migrating the same distance as the 36,000 Da band of the molecular mass marker, as well as several low molecular mass impurities. This indicated that the peaks of protein observed eluting at 200, 230, 245 and 290mM NaCl most likely contained the deaminase. The fractions believed to contain deaminase were subjected to electrophoresis on a non-denaturing gel, the results of which are shown in figure 3.3.

The non denaturing gel in figure 3.3 shows that lanes 10 and 11 contained a protein with the same electrophoretic properties as wild-type holoenzyme. Lanes 12-14 contained a number of bands that migrated to the same distance and beyond the wild-type. Lanes 15 and 16 contained a band of the same mobility of the lower band observed in fractions 12-14. Fractions 17 was too faint to be considered. Fractions 18-20 contained a band that migrated just beyond that seen in fractions 15 and 16.

Figure 3.2 The Denaturing Polyacrylamide Gels of the Fractions Collected from the F.P.L.C. of the D84E Mutant

The lane containing the holoenzyme (wild-type control) and the molecular mass marker are labelled 'WT' and 'Mk' respectively.

All other lanes contain consecutive fractions isolated from the f.p.l.c. column, and are numbered according to the chromatogram shown in figure 3.1.

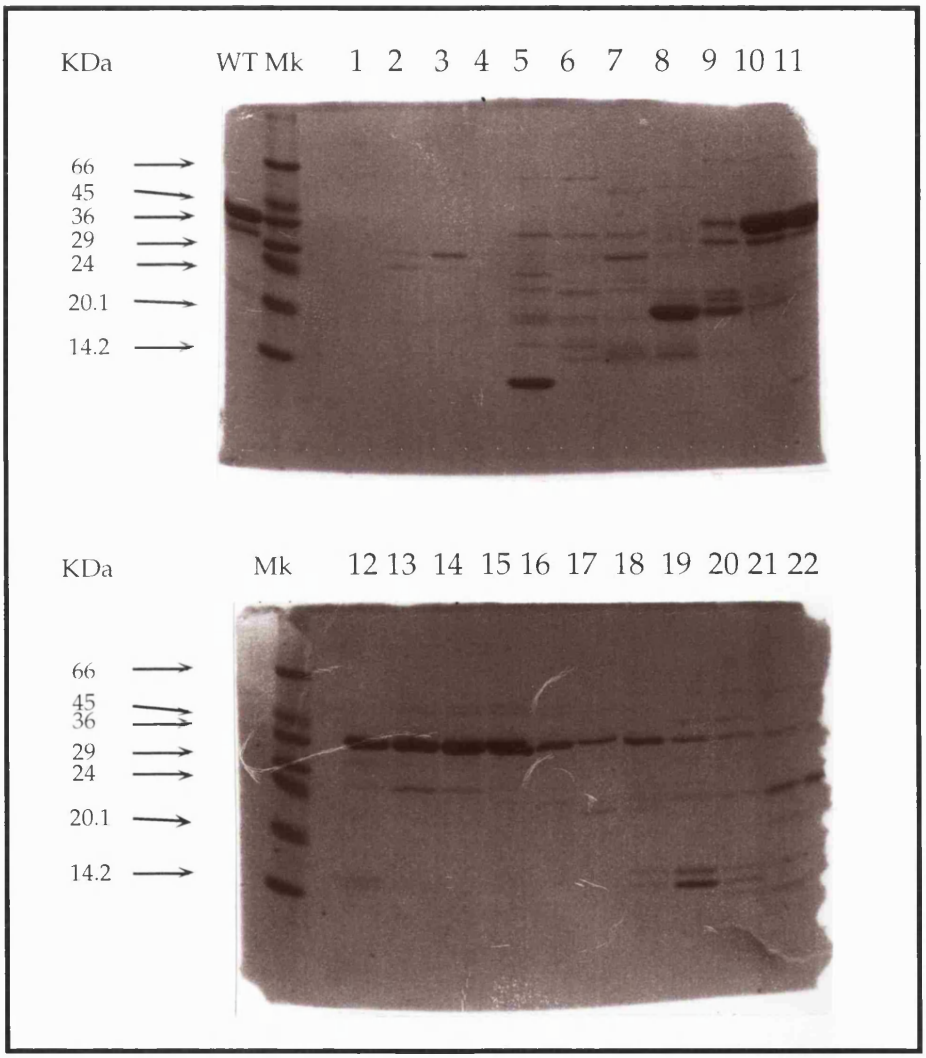

Figure 3.3 The Non-Denaturing Polyacrylamide Gel of Fractions Collected from the F.P.L.C. of the D84E Mutant

The lanes containing the apoenzyme and holoenzyme (wild-type controls) are labelled 'Apo' and 'WT' accordingly. For clarity, the migrations of the apoenzyme and holoenzyme are marked in the figure.

All other lanes contain consecutive fractions isolated from the f.p.l.c. column, and are numbered according to the chromatogram shown in figure 3.1.

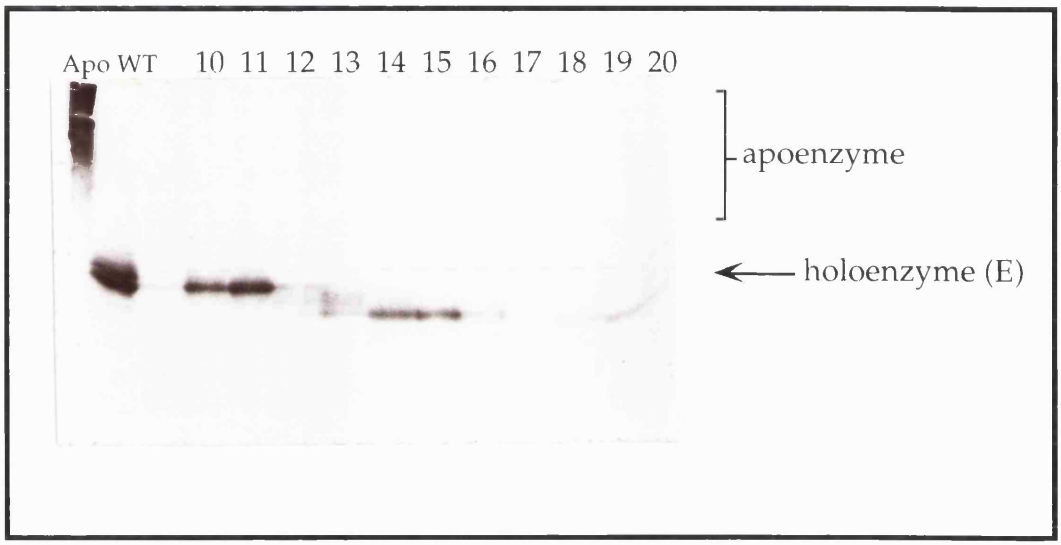

On the basis of (i) their elution profile on the MonoQ column and (ii) their electrophoretic properties, the fractions were assigned as follows: the protein eluting at 200mM NaCl assigned as holoenzyme; the protein eluting at 230mM NaCl assigned as a mixture of holoenzyme, ES and ES_2; the protein eluting at 245mM NaCl assigned as ES_2; and the protein eluting at 290mM NaCl assigned as ES_3.

These results suggest that the D84E mutant exists endogenously in the form of holoenzyme and enzyme-intermediate complexes. The ratio of these complexes varied with each preparation, although in general the ES_2 peak appeared as the largest form for the complexes. This is in contrast to the analysis of wild-type enzyme by f.p.l.c. and gel electrophoresis, where the majority of protein is the holoenzyme, with only a small additional percentage of the enzyme-intermediate complex ES.

3.2.1.4 Polyacrylamide Gel Electrophoresis of the D84E Mutant Enzyme Incubated with Porphobilinogen

The D84E holoenzyme isolated from the MonoQ column was incubated with increasing concentrations of substrate and examined by non-denaturing gel electrophoresis. On the same gel, f.p.l.c.-isolated fractions containing the D84E holoenzyme and naturally present enzyme-intermediate complexes were also subjected to electrophoresis to allow a direct comparison of their electrophoretic properties and further confirm their assignments. The results are shown in figure 3.4.

Figure 3.4 Comparison of the Naturally Present D84E Complexes with the Incubation of the D84E Holoenzyme with Substrate

The lane containing the holoenzyme (wild-type control) is labelled 'WT'. For clarity, the migration of the holoenzyme is marked in the figure.

All other lanes are labelled according to the f.p.l.c.-isolated fraction number they contain, with fraction '10' being taken as holoenzyme. These numbers do not correspond to those described on previous pages as they are from another preparation.

The incubations of holoenzyme with porphobilinogen are labelled 10a, 10b, 10c, 10d and 10e to indicate a 1, 5, 10, 20 and 30 molar excess of porphobilinogen respectively.

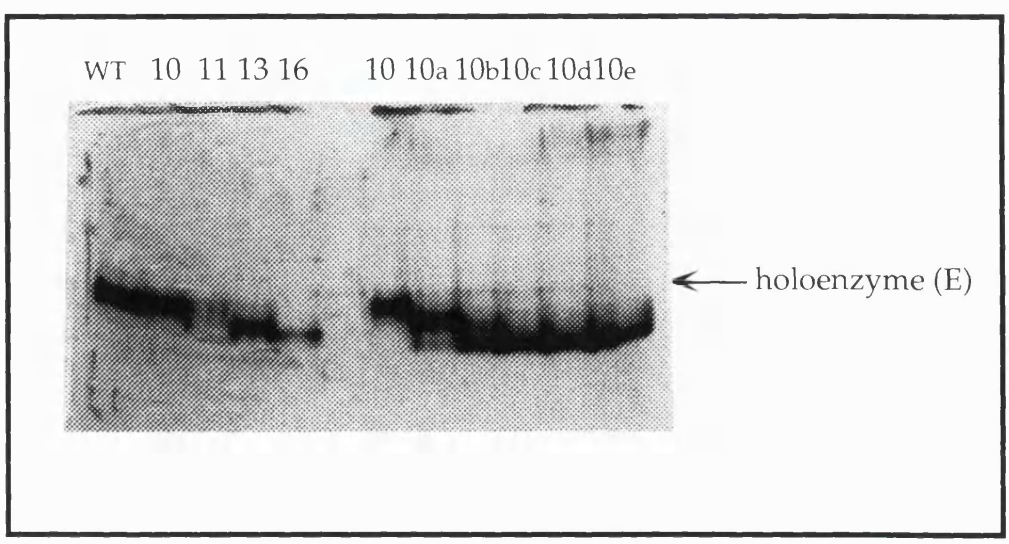

The non denaturing gel in figure 3.4 shows the protein in fraction 10 migrated the same distance as wild-type. Fraction 11 contained a number of protein bands that migrated to the same distance and beyond the wild-type. Fractions 13 contained a band of the same mobility of the lower band observed in fraction 11. Fraction 16 contained a band which migrated just beyond that of fraction 13. Therefore, fraction 10 was assigned to holoenzyme, fraction 11 assigned to a mixture of E, ES and ES_2, fractions 13 assigned to ES_2 and fraction 16 assigned to ES_3

The incubation of the D84E holoenzyme with increasing concentrations of porphobilinogen led to the appearance of a number of bands which appeared to run the same distance, and slightly beyond, as those observed for fractions 10, 11, 13 and 16. The similar migration of the bands produced by incubating D84E holoenzyme with porphobilinogen to those of the proposed naturally present complexes confirms that the peaks observed for D84E, which were isolated in the absence of added substrate, are likely to be enzyme-intermediate complexes. The majority of protein formed from incubating holoenzyme with porphobilinogen migrated beyond the band of fraction 16, suggesting the possibility of an ES_4 complex.

3.2.1.5 Polyacrylamide Gel Electrophoresis of the D84E Mutant Enzyme Purified Using Different Techniques

The naturally present enzyme-intermediate complexes which could be separated on the MonoQ column were available in much higher abundance than those generated by incubation of enzyme with substrate. Such complexes had not been previously been observed for the D84E mutant, and the factors which may have led to their isolation, in this case, are likely to have included the use of gel filtration rather than anion-exchange chromatography. The D84E mutant previously studied (Woodcock and Jordan, 1994) was purified by way of anion-exchange, and it is possible that any complexes which existed in the cell may have been lost at this stage as the increased negative charge of the complexes may have required an increased salt concentration for elution. The use of gel filtration, however, would allow the proteins to be separated on a basis of size and not charge, and therefore the complexes were more likely to elute in the typical fractions anticipated for porphobilinogen deaminase.

The D84E mutant of porphobilinogen deaminase was therefore purified using the two different chromatography techniques of gel filtration and anion-exchange for analysis. Before the samples were further purified by application to the f.p.l.c. system, the protein from each preparation was examined by non denaturing polyacrylamide gel electrophoresis, as shown in figure 3.5.

Figure 3.5 Comparison of Samples of the D84E Mutant, Purified Using Two Different Techniques

Lane 1 contains the holoenzyme (wild-type control). For clarity, the migration of the holoenzyme is marked in the figure.

Lane 2 contains the mutant D84E purified using anion-exchange
Lane 3 contains the mutant D84E purified using gel filtration.

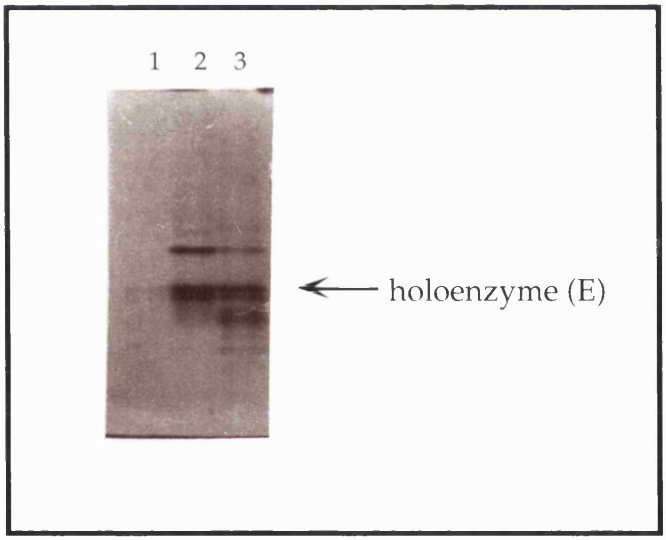

The gel in figure 3.5 shows the wild-type protein (lane 1) migrated, very faintly, with the typical double band profile. The D84E sample purified using anion-exchange (lane 2) migrated with multiple bands, including a double band of similar mobility to wild-type and a single band with lower mobility than wild-type. The D84E sample purified using gel filtration (lane 3) also migrated with multiple bands, identical to those of D84E purified using anion-exchange, as well as bands of higher mobility than wild-type. The band

of low mobility observed for both D84E samples is likely to contain protein other than deaminase, which would be removed from the samples after application to the f.p.l.c. system. The additional bands observed for the D84E sample purified using gel filtration migrated as those expected for enzyme-substrate complexes.

These results indicate that the isolation of the enzyme-substrate complexes of D84E was likely to be a result of the purification technique employed. This result was of importance as the detection of these existing complexes allowed their facile isolation in sufficient quantity for crystallisation purposes. Purification of the naturally present D84E ES_2 complex was subsequently undertaken by employing the gel filtration strategy.

3.2.1.6 Purification of the D84E ES_2 Complex

Enzyme purified from the gel filtration column was applied to the f.p.l.c. and the peak observed eluting as the third deaminase peak (eluting at 285mM NaCl) was isolated as the ES_2 complex. To support the assumption that this peak did indeed contain ES_2, a small quantity of ES_2 was also generated by incubation of D84E holoenzyme with porphobilinogen and isolated *via* f.p.l.c. of the mixture. The two preparations of the complex were then co-injected onto the f.p.l.c. and were found to co-elute.

The purified ES_2 complex was desalted into 1mM Tris buffer containing 2mM dithiothreitol and freeze dried. The lyophilised material was white, which indicated that the cofactor was in a reduced form. To ensure that the ES_2 complex had not been degraded on freeze drying, a small sample of the protein was dissolved and reinjected onto the f.p.l.c. A single peak was observed eluting at 285mM NaCl, and the ES_2 complex was therefore confirmed to be intact and was prepared for crystallisation (Chapter 4).

3.2.1.7 Treatment of the D84E Mutant Enzyme and Enzyme-Intermediate Complexes with Hydroxylamine

The isolated naturally present intermediates of D84E were subjected to treatment with hydroxylamine. Whilst it has been documented that pyrrolic intermediates of wild-type porphobilinogen deaminase are released upon short incubation with hydroxylamine (Plusec and Bogorad, 1970; Davies and Neuberger, 1973), it has also been reported that the D84A and D84N mutants, which may contain enzyme-intermediate complexes, are unchanged on hydroxylamine incubations (Woodcock, 1992). This may be a reflection of their catalytic inactivity, or a conformation that does not allow their release, or an absence of complexes to begin with.

Hydroxylamine was incubated with naturally present holoenzyme and enzyme-intermediate complexes of D84E at a final concentration of 0.2M. This concentration was known to be effective in releasing pyrrolic intermediates of wild-type enzyme. The untreated and treated fractions were analysed by non denaturing polyacrylamide gel electrophoresis, as shown in figure 3.6.

The gel in figure 3.6 shows that all the fractions appear to be unchanged after hydroxylamine treatment when examined by non denaturing polyacrylamide gel electrophoresis. This result may again be a reflection of the lower activity (and thus the greater stability) of naturally present complexes, or a conformation that does not allow their release.

Whilst the majority of the results do indicate that the extra peaks isolated from D84E are enzyme-intermediate complexes, it may require the crystal structure of one of these complexes (see Chapter 4) to satisfy the contention.

Figure 3.6 Non-SDS Gel Comparing Untreated and Hydroxylamine Treated Fractions Containing D84E Mutant Naturally Present Complexes

The lane containing the wild-type holoenzyme (control) is labelled 'WT'. For clarity, the migration of the holoenzyme is marked in the figure.

All other lanes contain fractions isolated from f.p.l.c., with fraction '10' being taken as holoenzyme. The fractions marked with a * are treated with hydroxylamine.

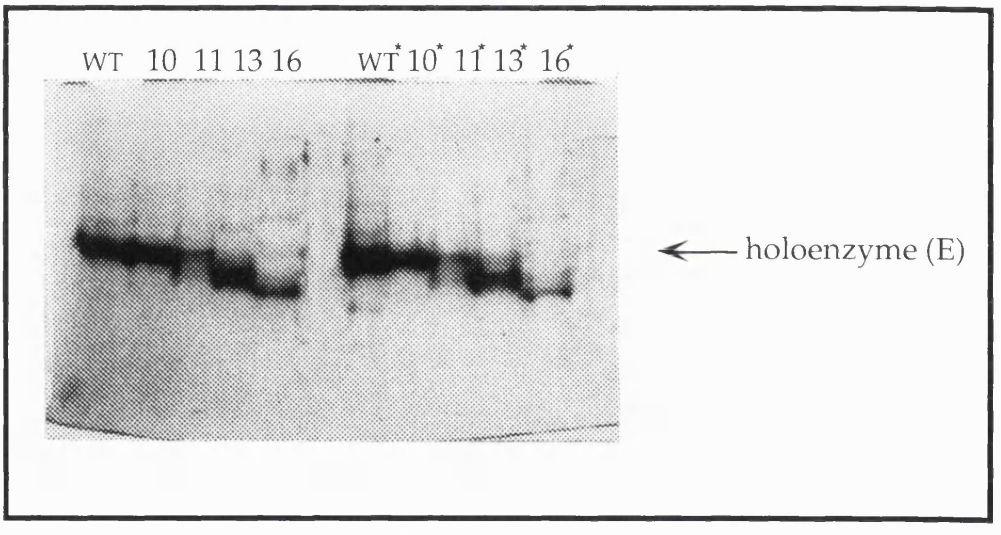

3.2.2 The D84A Mutant of Porphobilinogen Deaminase

3.2.2.1 General Properties of the D84A Mutant

E. coli cells expressing the mutant D84A porphobilinogen deaminase were grown in the same manner as the cells expressing the mutant D84E enzyme. The mutant D84A enzyme was then also purified using the same protocol as that used for the mutant D84E enzyme.

Despite the strong reducing conditions in which the D84A mutant was purified the solid pure enzyme sample was found to be slightly pink, an observation which had only previously been noted for oxidised mutant protein (Woodcock, 1992). Approximately 25mg of pure protein was obtained per prepararation from 2L of media. The purity of the enzyme was studied at various stages of the purification procedure by polyacrylamide gel electrophoresis using a 12% SDS gel. The molecular mass of the protein, 35,000 Da, was determined by comparing the mobility on the gel with that of the molecular mass standards.

3.2.2.2 F.P.L.C. of the D84A Mutant

After purification, the mutant D84A porphobilinogen deaminase (~10mg/ml) was applied to a MonoQ HR5/5 column attached to a Pharmacia f.p.l.c. system. The MonoQ column had been equilibriated in 20mM Tris/HCl buffer pH 7.5 containing 7mM β-mercaptoethanol. The purified protein was eluted from the column in the same buffer using a linear salt gradient. The resulting chromatogram is presented in figure 3.7.

The chromatogram in figure 3.7 shows that the f.p.l.c. system allowed the further separation of protein by anion-exchange. Multiple peaks of protein were observed eluting in 0-180mM NaCl. Two major peaks of protein were also observed eluting at 220mM NaCl with a shoulder at 200mM NaCl; and at 270mM NaCl. Two minor peaks were observed eluting at 290mM NaCl and 320mM NaCl.

Figure 3.7 F.P.L.C. Trace of Purified D84A Mutant Porphobilinogen Deaminase

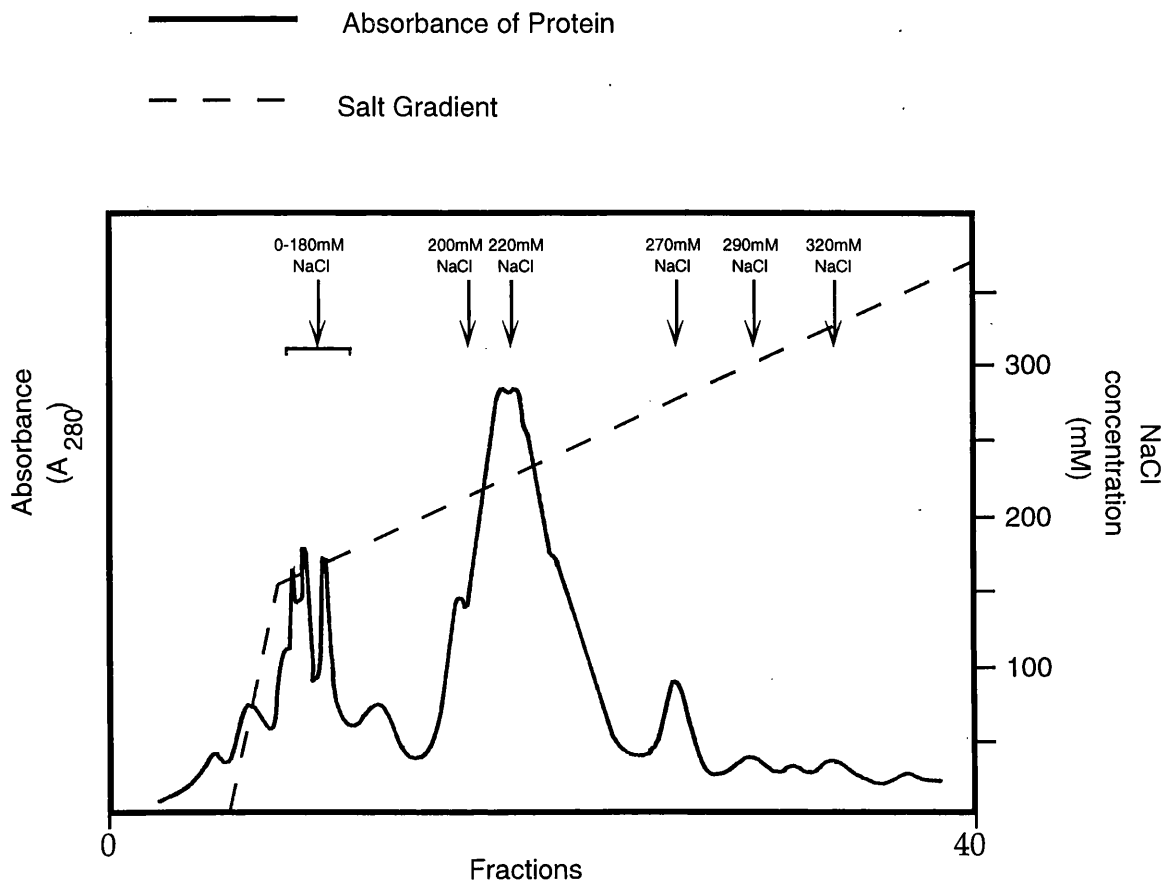

3.2.2.3 Polyacrylamide Gel Electrophoresis of the Peaks Isolated from the F.P.L.C. of D84A

Fractions 1-22 isolated from the f.p.l.c. of D84A were subjected to electrophoresis on denaturing and non-denaturing polyacrylamide gels, the results of which can be seen in figures 3.8 and 3.9.

Figure 3.8 The Denaturing Polyacrylamide Gel of the Fractions Collected from the F.P.L.C. of the D84A Mutant

The lane containing the holoenzyme (wild-type control) and the molecular weight marker are labelled 'WT' and 'Mk' respectively.

All other lanes contain consecutive fractions isolated from the column, and are numbered according to the chromatogram shown in figure 3.7.

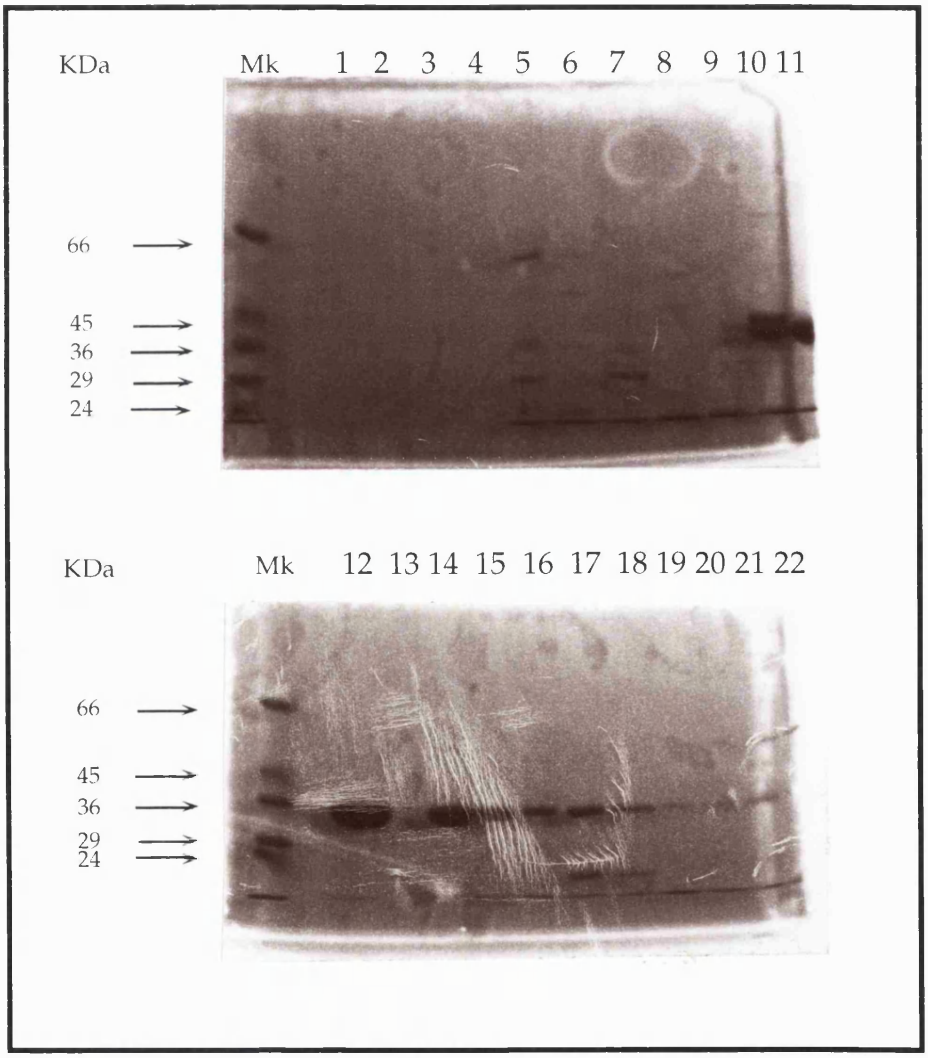

The denaturing gel in figure 3.8 shows that fractions 1-9 contained little deaminase, lanes 10-18 contained a strong band migrating the same distance as the 36,000 Da band of the molecular mass marker and fractions 19 -22 contained a weaker band migrating the same distance as the 36,000 Da band of the molecular mass marker, as well as impurities. This indicated that the two main peaks observed eluting at 220 and 270mM NaCl contained the deaminase enzyme.

The fractions believed to contain deaminase were subjected to electrophoresis on a non-denaturing gel, the results of which are shown in figure 3.9.

Figure 3.9 The Non-Denaturing Polyacrylamide Gel of Fractions Collected from the F.P.L.C. of the D84A Mutant

The lanes containing the apoenzyme and holoenzyme (wild-type controls) are labelled 'Apo' and 'WT' accordingly. For clarity, the migrations of the apoenzyme and holoenzyme are marked in the figure.

All other lanes contain consecutive fractions isolated from the f.p.l.c. column, and are numbered according to the chromatogram shown in figure 3.7.

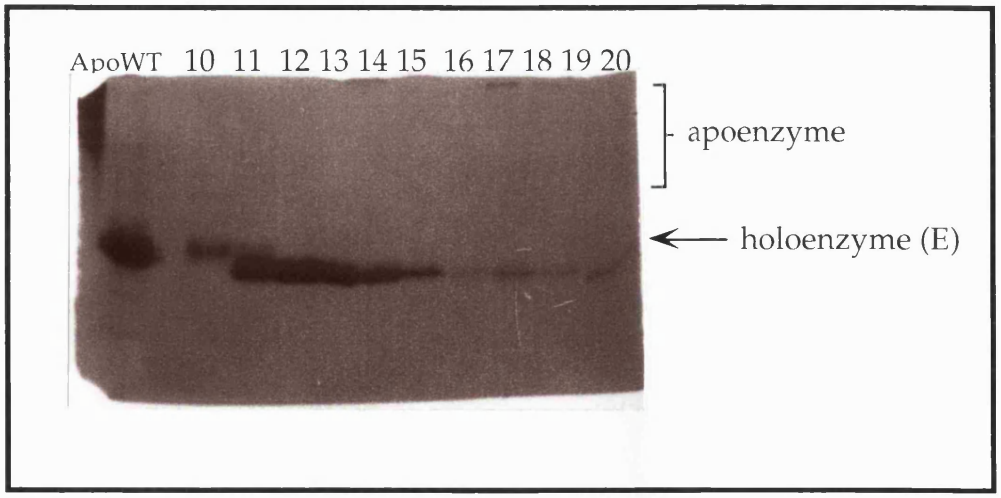

The non denaturing gel in figure 3.9 shows that lane 10 contained a protein with the same electrophoretic properties as the wild-type. Lane 11 contained more than one band that migrated to the same distance and beyond

the wild-type. Lanes 12-18 contained a band of the same mobility that migrated beyond wild-type (fractions 12 and 13 may have contained more than one band, it was difficullt to visualise clearly). Lanes 19 and 20 appeared to contain a band that migrates just beyond that seen in fractions 12-18.

It appeared that D84A contained a number of forms of deaminase. Whilst it cannot be concluded from this data alone whether these were oxidised or reduced states or whether any complexes were present, the mobility of the majority of the enzyme on the non-denaturing gel did suggest a migration similar to that observed for an ES_2 complex.

3.2.3 The D84N Mutant of Porphobilinogen Deaminase

3.2.3.1 General Properties of the D84N Mutant

E. coli cells expressing the mutant D84N porphobilinogen deaminase were grown in the same manner as the cells expressing the mutant D84E enzyme. The mutant D84N enzyme was then also purified using the same protocol as that used for the mutant D84E enzyme.

As with the D84A mutant, the solid pure D84N mutant was found to be slightly pink. Approximately 25mg of pure protein was obtained per prepararation from 2L of media. The purity of the enzyme was studied at various stages of the purification procedure by polyacrylamide gel electrophoresis using a 12% SDS gel. The molecular mass of the protein, 35,000 Da, was determined by comparing the mobility on the gel with that of the molecular mass markers.

3.2.3.2 F.P.L.C. of the D84N Mutant

After purification the mutant D84N porphobilinogen deaminase (10mg/ml) was applied to a MonoQ HR5/5 column attached to a Pharmacia f.p.l.c. system. The MonoQ column had been equilibriated in 20mM Tris/HCl buffer pH 7.5 containing 7mM β-mercaptoethanol. The purified protein was eluted from the column in the same buffer using a linear salt gradient. The resulting chromatogram is presented in figure 3.10.

The chromatogram in figure 3.10 shows that the f.p.l.c. system allowed the further separation of protein by anion-exchange chromatography. Multiple peaks were observed on the chromatogram, eluting at 1mM NaCl, 165mM NaCl, 185mM NaCl, 205mM NaCl, 225mM NaCl with a shoulder at 235mM NaCl, 270mM NaCl and at 290mM NaCl.

Figure 3.10 F.P.L.C. Trace of Purified D84N Mutant Porphobilinogen Deaminase

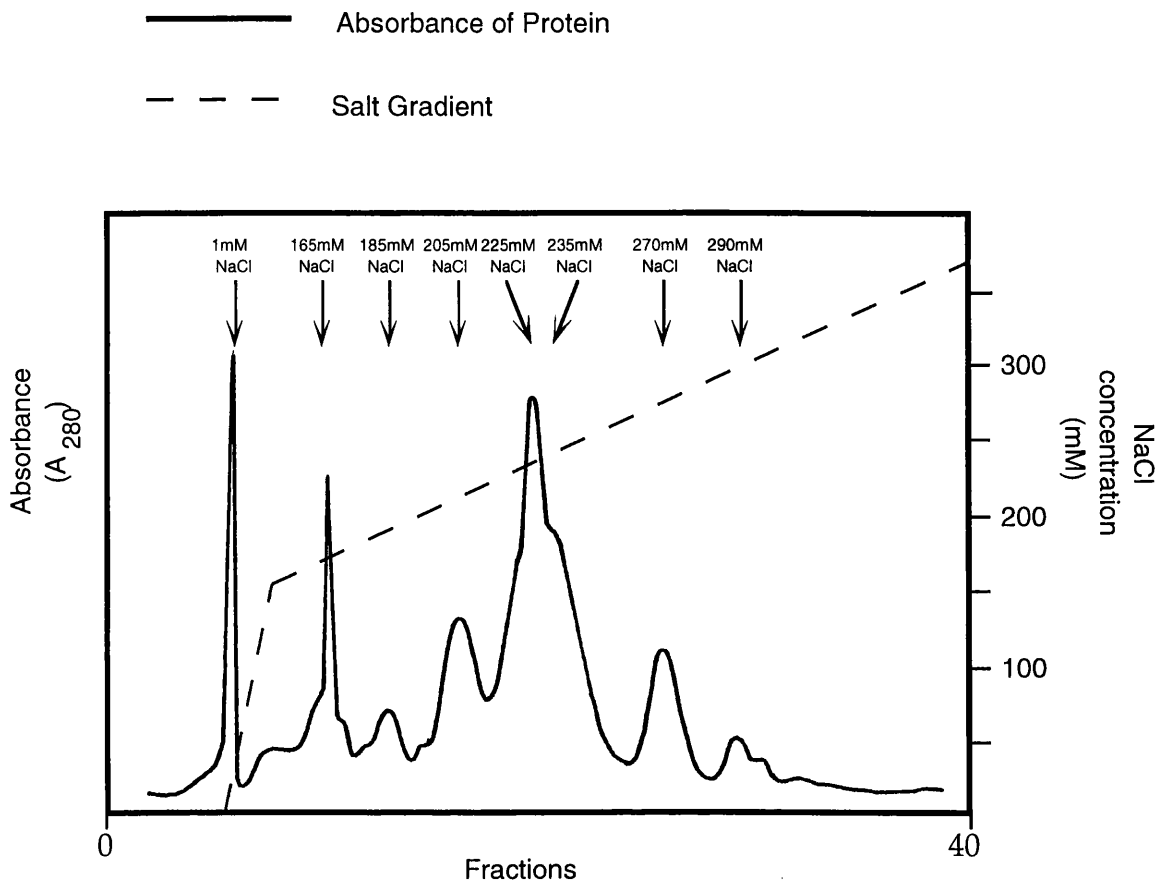

3.2.3.3 Polyacrylamide Gel Electrophoresis of the Peaks Isolated From the F.P.L.C. of D84N

The fractions isolated from the f.p.l.c. of D84E were analysed by denaturing and non denaturing polyacrylamide gel electrophoresis, to examine further their deaminase content. The gels are shown in figures 3.11 and 3.12.

The denaturing gel in figure 3.11 shows that lanes 1-9 contained little deaminase, lanes 10-15 contained a strong band that migrated the same distance as the 36,000 Da band of the molecular weight marker and lanes 16-22 contained a band that migrated the same distance as the 36,000 Da band of

Figure 3.11 The Denaturing Polyacrylamide Gels of the Fractions Collected from the F.P.L.C. of the D84N Mutant

The lane containing the holoenzyme (wild-type control) and the molecular mass marker are labelled 'WT' and 'Mk' respectively.

All other lanes contain consecutive fractions isolated from the f.p.l.c. column, and are numbered according to the chromatogram shown in figure 3.10.

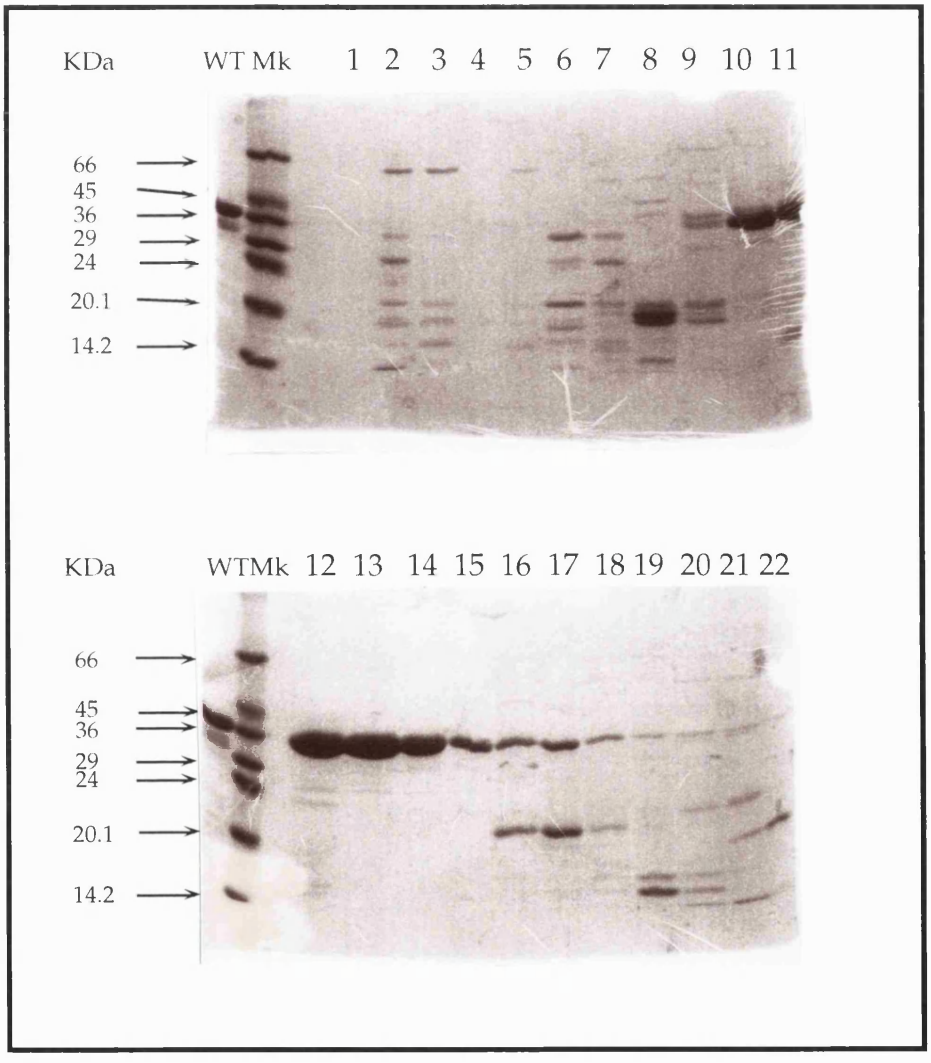

the molecular mass marker, as well as several other proteins. This indicated that the peaks observed on the chromatogram eluting at 205, 225, 270 and

290mM NaCl probably all contained deaminase, although the last two peaks may not have resulted from deaminase alone.

The fractions believed to contain deaminase were then subjected to electrophoresis on a non-denaturing gel, the results of which are shown in figure 3.12.

Figure 3.12 The Non-Denaturing Polyacrylamide Gel of the Peaks Observed from the F.P.L.C. of the D84N Mutant

The lane containing the apoenzyme and holoenzyme (wild-type controls) are labelled 'Apo' and 'WT' accordingly. For clarity, the migrations of the apoenzyme and holoenzyme are marked in the figure.

All other lanes contain consecutive fractions isolated from the f.p.l.c. column, and are numbered according to the chromatogram shown in figure 3.10.

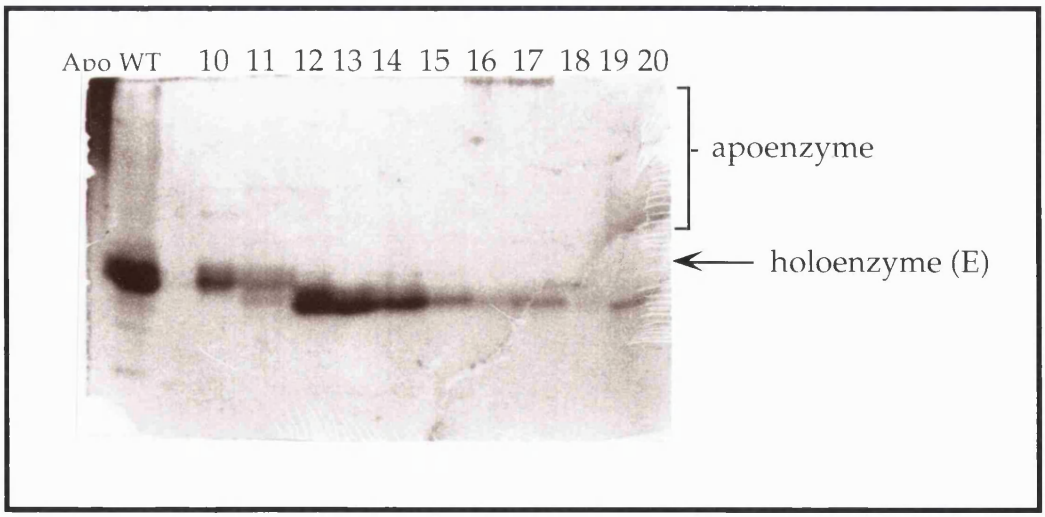

The non denaturing gel in figure 3.12 shows that lane 10 contained a protein with the same electrophoretic properties as wild-type. Lane 11 contained protein with a number of bands that migrated to the same distance and beyond the wild-type. Lanes 12-17 also contained protein with bands that migrated beyond wild-type. Lanes 19 and 20 appeared to contain a protein band that migrated slightly further than those seen in lane 12-17.

It appeared from the electrophoretic properties of the mutant D84N protein that more than one form of deaminase was present, although these forms could not be assigned as enzyme-intermediate complexes from this data alone. To help identify the types of deaminase present for the D84N mutant, the protein was radioactively labelled. The growth of D84N in the presence of 5-amino-[5-^{14}C] levulinic acid would give some indication of the ratio of label in each form.

3.2.4 Radioactive Labelling of the D84N Mutant of Porphobilinogen Deaminase

3.2.4.1 Purification and F.P.L.C. of the ^{14}C Labelled D84N Mutant

E. coli cells harbouring the D84N mutant of porphobilinogen deaminase were grown as normal, in the presence of 5-amino-[5-^{14}C] laevulinic acid. The enzyme was partially purified from the cells *via* sonication, heat treatment and centrifugation. The supernatant was taken and a sample applied to a Mono Q HR5/5 column attached to a Pharmacia f.p.l.c. system and fractions collected. The chromatogram can be seen in figure 3.13.

The chromatogram in figure 3.13 shows that a large peak of protein was observed eluting immediately in the absence of salt, and a second large peak eluted at 170mM NaCl. Minor peaks were also observed at 130mM, 180mM, 185mM, 195mM, 200mM and at 245mM NaCl.

Figure 3.13 F.P.L.C. Trace of Partially Purified ^{14}C Labelled D84N

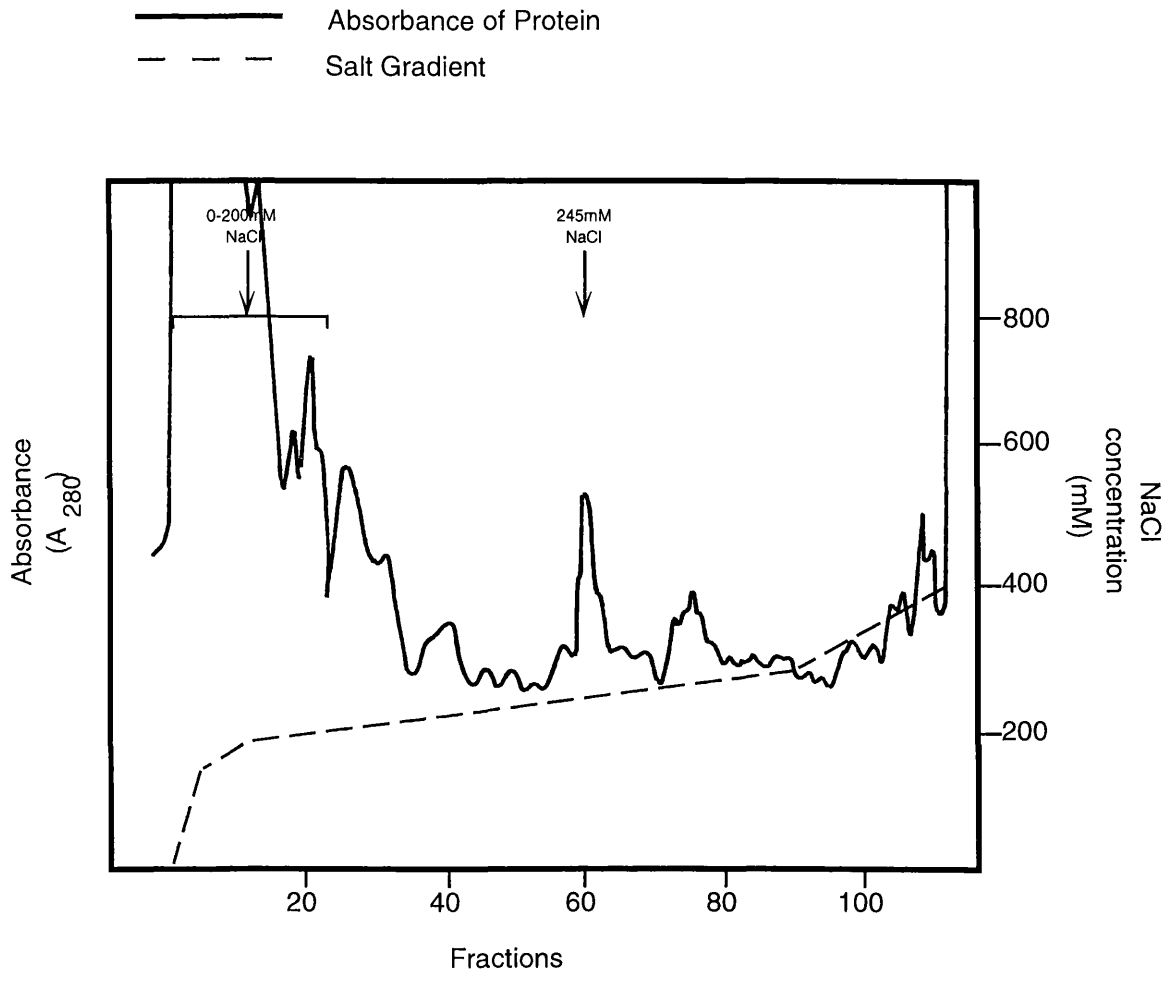

3.2.4.2 Determination of Counts Per Minute for Each Sample of ^{14}C Labelled D84N

The amount of radioactive isotope was determined in each fraction by scintillation counting, and the counts per minute (cpm) can be seen in a bar graph form in figure 3.14.

Figure 3.14 Counts Per Minute of Fractions Eluting from the F.P.L.C. of Partially Purified ^{14}C Labelled D84N

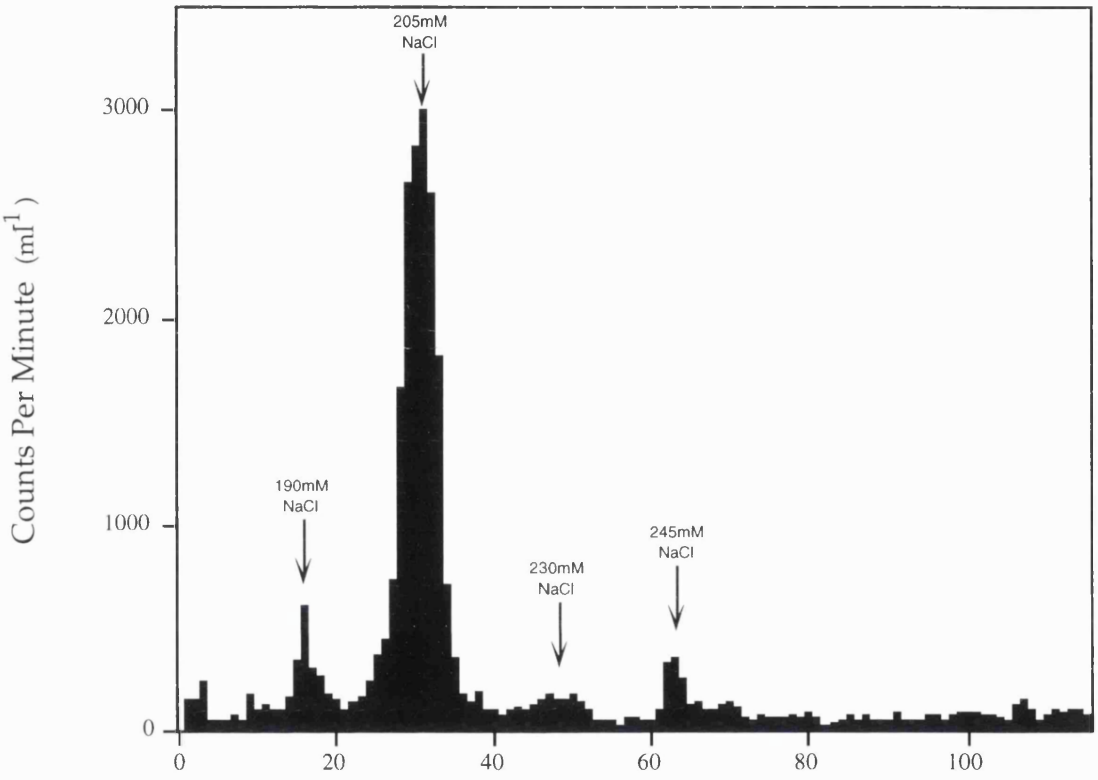

The bar chart in figure 3.14 shows that four peaks of radioactivity were observed, the first in the fractions eluting at 190mM NaCl (fractions 14-19), the second in the fractions eluting at 205mM NaCl (fractions 23-36), the third minor peak in the fractions eluting at 230mM NaCl (fractions 45-52) and the fourth in the fractions eluting at 245mM NaCl (fractions 61-65). The second peak contained approximately six times the amount of radioactivity found in the first, third and fourth peak.

It was noted that the profile of the peaks of radioactivity and the percentage of salt between their elutions was similar to the profile of protein peaks eluting on f.p.l.c. of the unlabelled D84N.

3.2.4.3 Determination of Specific Activity for Each Sample of ^{14}C Labelled D84N

The specific activity was determined for each f.p.l.c. purified fraction of the ^{14}C labelled D84N mutant. A graph of the specific activity can be seen in figure 3.15.

Figure 3.15 Specific Activity of Fractions Eluting from the F.P.L.C. of Partially Purified ^{14}C Labelled D84N

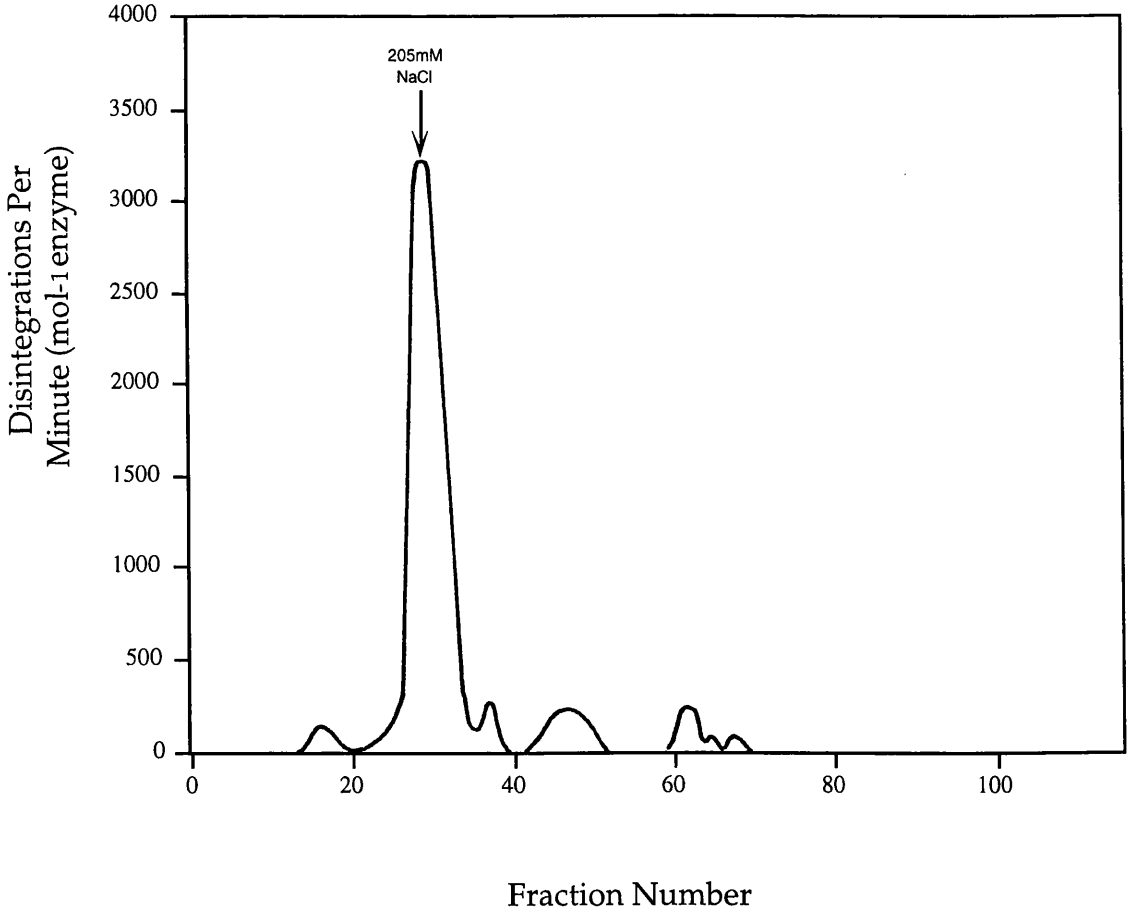

The graph in figure 3.15 shows that a single major peak of specific activity was observed eluting at 205mM NaCl (fraction 25-35).

3.2.4.4 Polyacrylamide Gel Electrophoresis of the Fractions Collected from the F.P.L.C. of the ^{14}C Labelled D84N Mutant

The fractions collected from the f.p.l.c. were then subjected to electrophoresis on denaturing polyacrylamide gels with alternate fractions analysed. A sample of the supernatant before injection onto the f.p.l.c. was also run and is referred to as 'Cr' (crude). The results are shown in figure 3.16.

Figure 3.16 The Denaturing Polyacrylamide Gel Electrophoresis of Fractions Collected from the F.P.L.C. of the Partially Purified ^{14}C Labelled D84N Mutant

The lane containing the molecular mass marker is labelled 'Mk'.

All other lanes contain alternate consecutive fractions isolated from the f.p.l.c. column, and are numbered according to the chromatogram shown in figure 3.13.

Figure 3.16a Fractions 1-25

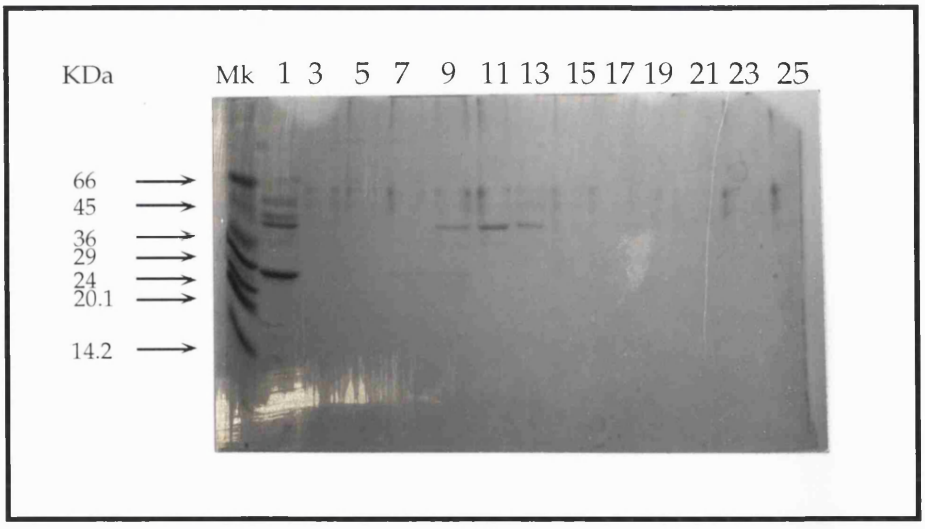

Figure 3.16b Fractions 27-51

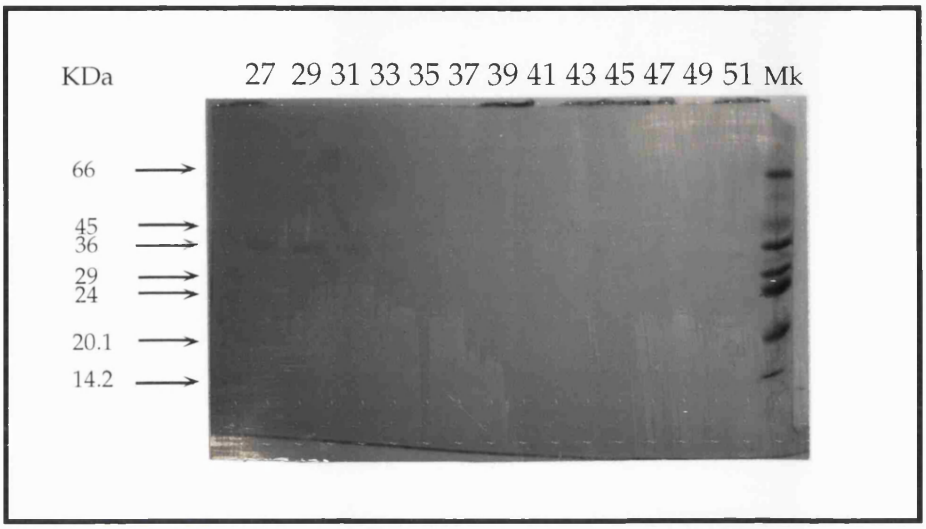

Figure 3.16c Fractions 53-75

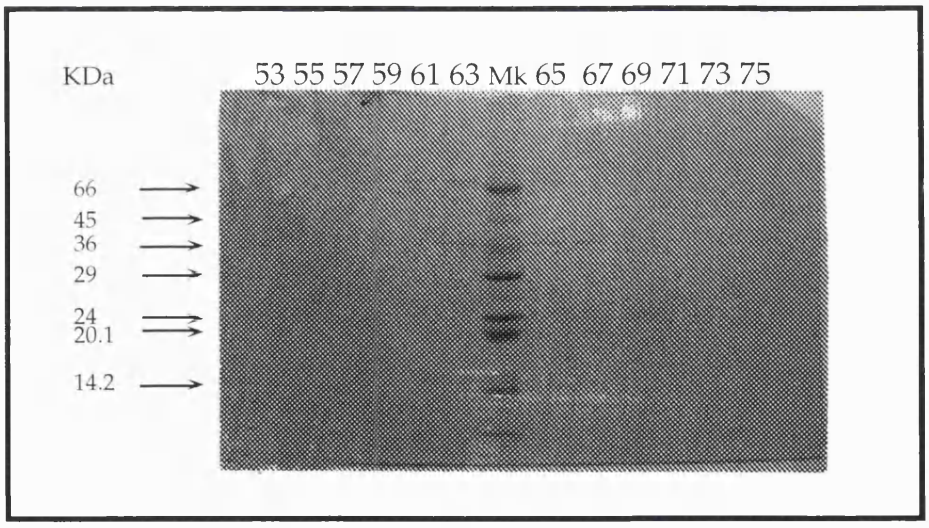

Figure 3.16d Fractions 77-101

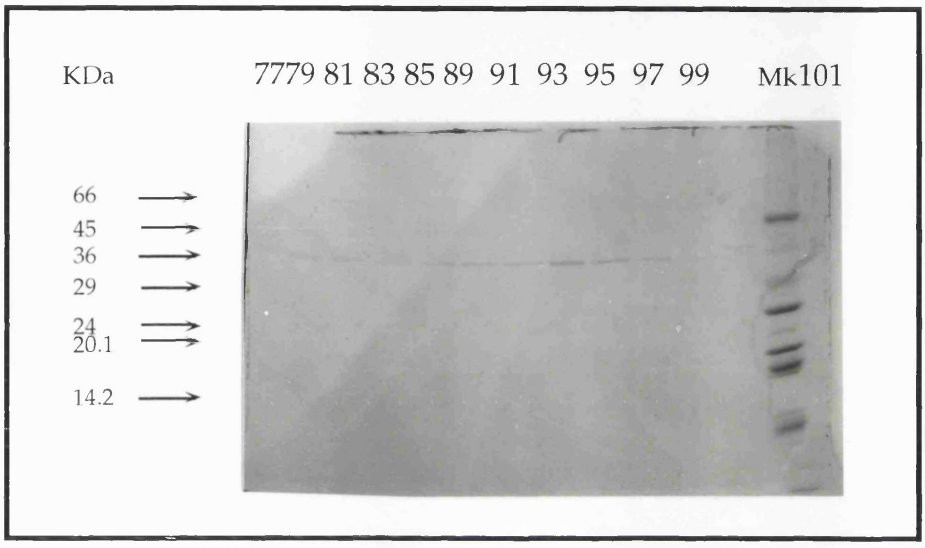

Figure 3.16e Fractions 101-115 and Sample 'Cr'

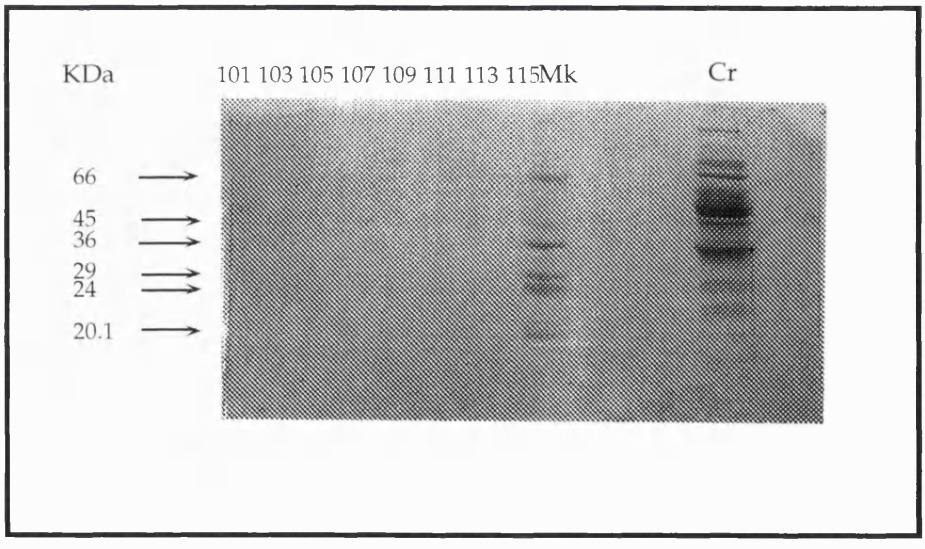

The gels in figure 3.16a-e show that the protein found in lanes 1,7 and 9, 27, 29, 31, 33, 35 and sample 'Cr' corresponded to the 36,000 Da band on the molecular mass marker, indicating that they may all contain the deaminase enzyme. The protein in lanes 27-35 also corresponded to the major peak of radioactivity as seen in figure 3.13. The lanes representing fractions 14-19, 45-

52 and 61-65, which contained the three other radioactive peaks observed, did not appear to correspond to deaminase.

The deaminase containing fractions 27, 29, 31, 33, 35 and 7, 8, 9 were then subjected to non-denaturing polyacrylamide gel electrophoresis, the results of which are shown in figure 3.17.

Figure 3.17 The Non-Denaturing Polyacrylamide Gel of Deaminase-Containing Fractions Collected from the F.P.L.C. of the Partially Purified ^{14}C Labelled D84N Mutant

The lanes contain fractions isolated from the f.p.l.c. column, and are numbered according to the chromatogram shown in figure 3.13.

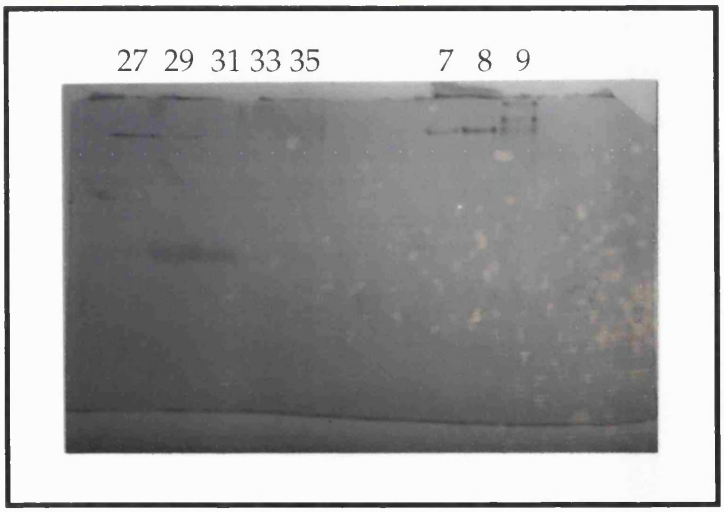

The gel in figure 3.17 shows that the protein in lanes 27, 29, 31, 33 and 35 electrophoresed as two bands, one which barely travelled and remained at the top of the gel and the other which migrated half way down the gel. Fraction 7 also contained these bands in addition to two more which lay in between them.

From comparing bands, peaks and radioactivity it appeared that only one major form of deaminase was present which was found in fractions 27-35. However, it still could not be concluded whether the D84N mutant deaminase existed as holoenzyme or as enzyme-intermediate complex. Fractions 7-9 gave rise to a very large peak on the f.p.l.c. trace, although from the denaturing gel

it could be seen that the deaminase in these fractions was not more than 20% pure. Also, these fractions did not correspond to any peaks in radioactivity.

It was interesting to note that fraction 1, which eluted immediately, also gave rise to a very large peak on the f.p.l.c. trace and presented the strongest band for deaminase on the denaturing gel. As the fraction did not correspond to any radioactivity it was therefore proposed that fraction 1 may contain apoenzyme. The only suggestion against this possibility is the fact that this protein has survived the heat treatment step, and apoenzyme is known to be heat labile (Scott *et al.*, 1989). However, later experiments in this chapter suggest that the apoenzyme form of the asp-84 mutants may be able to withstand heat treatment when present in a crude extract. The holoenzyme can be reconstituted by incubation of the purified apoenzyme with a three-fold molar equivalent of porphobilinogen for a minimum of four hours (Scott *et al*, 1989). To repeat the effect a sample of fraction 1 was incubated with a five molar equivalent of porphobilinogen for twenty four hours at room temperature. The sample was then analysed on a non-denaturing polyacrylamide gel against the other deaminase containing fractions: 7, 8, 9, 29, 30 and 31, and also fraction 1 in the absence of porphobilinogen. The results are shown in figure 3.18.

The gel in figure 3.18 shows that the protein in lanes 7, 8 and 9 could not be seen and the protein in lanes 29, 30 and 31 all gave rise to identical single bands. Both samples of fraction 1 appeared to be identical, migrating as a ladder of bands characteristic for apoenzyme (Scott *et al*, 1989), although this could also have been due to the large number of impurities present in fraction 1.The holoenzyme did not appear to have been reconstituted from fraction 1, but there are several reasons why this may have happened. Results described in Chapters 5 and 7, which were obtained later, indicate that it may not be possible to reconstitute from D84N apoenzyme *in vitro*. It is also possible that this band does not contain the apoenzyme.

Figure 3.18 The Non-Denaturing Polyacrylamide Gel of Fraction 1 Incubated with Porphobilinogen Analysed Against Fractions Collected from the F.P.L.C. of Partially Purified ^{14}C D84N

The lanes contain fractions isolated from the f.p.l.c. column, and are numbered according to the chromatogram shown in figure 3.13.
1 indicates fraction 1 in the absence of porphobilinogen, 1* indicates fraction 1 in the presence of porphobilinogen.

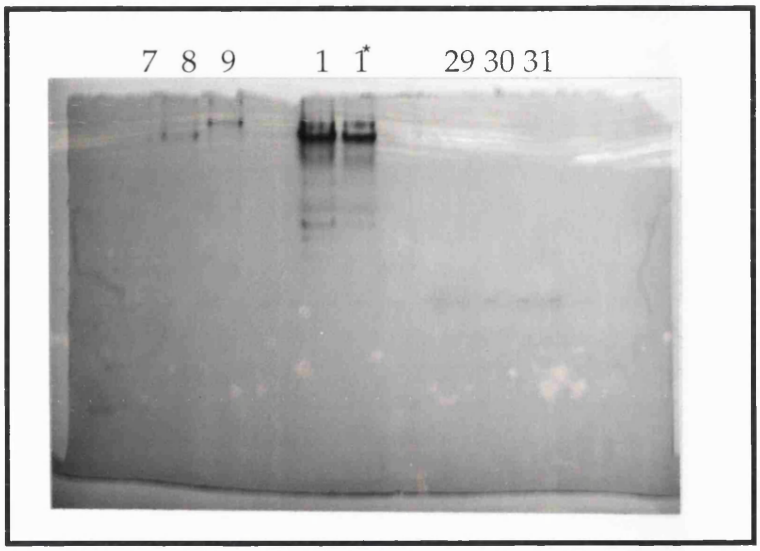

3.2.4.5 Polyacrylamide Gel Electrophoresis Showing the Effect of Heat Treatment on D84N

The possibility of the apoenzyme form existing for the D84N mutant was further investigated. It had been noted that the D84N mutant, when examined by non denaturing gel electrophoresis before application to the f.p.l.c. system, migrated with an additional ladder of bands characteristic of apoenzyme. This suggested the possibility that apoenzyme may have been able to withstand heat treatment in a crude extract. The sample was therefore analysed again by non denaturing gel electrophoresis after a second heat treatment at 60°C for ten minutes. In this case, the sample was not crude but contained >80% pure D84N enzyme. The results are shown in figure 3.19. For

comparison, the effects of heat treating the apoenzyme and holoezyme of wild-type porphobilinogen deaminase are shown on the same gel.

Figure 3.19 The Non-Denaturing Polyacrylamide Gel Showing the Effect of Heat Treating D84N Purified by Gel Filtration.

Lane 1 contains holoenzyme (wild-type control).
Lane 2 contains apoenzyme (wild-type control).
For clarity, the migrations of the apoenzyme and holoenzyme are marked in the figure.
Lane 3 contains heat-treated wild-type holoenzyme.
Lane 4 contains heat-treated wild-type apoenzyme.
Lane 5 contains mutant D84N.
Lane 6 contains heat-treated mutant D84N.

The gel in figure 3.19 shows the characteristic migrations of the holoenzyme and apoenzyme of wild-type (lanes 1 and 2). After heat treatment of these samples it was observed that the bands seen for holoenzyme (lane 3) remained intact, whilst the ladder of bands seen for apoenzyme (lane 4) had mostly disappeared. The sample of D84N before heat treatment (lane 5) migrated as a ladder of bands, with a strong additional band of a higher mobility than that of wild-type holoenzyme. After heat treatment (lane 6), the ladder of bands of D84N has been considerably reduced.

The results suggest that the D84N mutant does contain a large percentage of apoenzyme, which may well be separated out after application to the f.p.l.c. The apoenzyme appears to be able to withstand heat to some degree when in a crude extract, but is denatured more easily in a more pure sample.

3.2.5 Comparisons Between the D84A, D84E and D84N Mutants of Porphobilinogen Deaminase

3.2.5.1 Polyacrylamide Gel Electrophoresis of the D84A, D84E and D84N Mutants

Samples of the first deaminase-containing fraction eluted from the f.p.l.c. of D84A, D84E and D84N were subjected to electrophoresis on a non-denaturing polyacrylamide gel. Therefore, in the case of D84A and D84N, it was not the fractions which contained the majority of the enzyme that were taken but those that gave rise to an earlier smaller deaminase peak (i.e., the fractions which were proposed to contain free enzyme). For comparison, the fractions were run alongside samples of apoenzyme and wild-type deaminase.

The same samples were also incubated with a thirty molar excess of porphobilinogen at 37°C for 10 minutes. These mixtures were subject to electrophoresis on a non-denaturing polyacrylamide gel. The results are shown in figure 3.20.

The non-denaturing gel in figure 3.20 shows apoenzyme appearing as a ladder of bands that migrated behind the wild-type, whilst wild-type migrated with the typical double band profile. The D84A and D84N mutants appeared to have the same mobility, and migrated to the same distance as the higher band (less mobile) of wild-type. The D84E mutant appeared to migrate slightly beyond the D84A and D84N mutants and to a distance in between the double band of wild-type. The mobility of the mutants is consistent with their respective charges, is identical to the mobility previously observed for the mutants purified under reducing conditions and are the results expected for the holoenzyme form of the mutants.

This suggests that the two different mobilities previously observed for the D84A and D84N mutants purified in the presence and absence of reducing agent (Woodcock, 1992), which migrated just behind D84E and much further than D84E respectively, in fact indicated two forms of the enzyme that do not appear independantly of one another but are both present in the cell. In other words, it indicates that the enzyme exists as the holoenzyme form and an

enzyme-intermediate complex form. The complex, in which form the majority of the D84A and D84N enzyme exists, is predicted to be the ES_2 complex and the previous observations of it appearing only in the absence of reducing agents are more likely to be due to the purification technique rather than the oxidation state of the cofactor.

Figure 3.20 The Non-Denaturing Polyacrylamide Gel Comparing the D84A, D84E and D84N Mutants of Porphobilinogen Deaminase

Lane 1 contains apoenzyme (wild-type control).
Lane 2 contains wild-type holoenzyme (wild-type control).
For clarity, the apoenzyme, holoenzyme, and the bands which migrate beyond the holoenzyme are marked in the figure.
Lane 3 contains mutant D84A.
Lane 4 contains mutant D84E.
Lane 5 contains mutant D84N.
Lane 6 contains wild-type apoenzyme incubated with porphobilinogen.
Lane 7 contains wild-type holoenzyme incubated with porphobilinogen.
Lane 8 contains mutant D84A incubated with porphobilinogen.
Lane 9 contains mutant D84E incubated with porphobilinogen.
Lane 10 contains mutant D84N incubated with porphobilinogen.

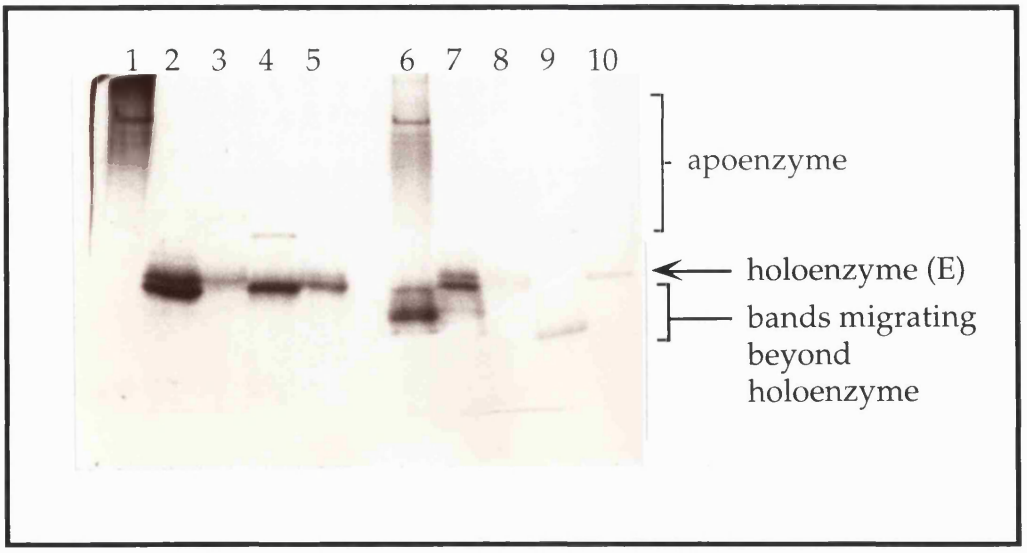

The gel in figure 3.20 also gives details of the effect of substrate incubation with apoenzyme, wild-type holoenzyme and the aspartate-84

mutants. The apoenzyme still appears to electrophorese as a ladder of bands as previously observed (Scott *et al.*, 1989; Hart *et al.*, 1988), and now also contains a number of bands that run beyond the wild-type double band. The wild-type enzyme also displays a number of extra bands that run beyond the double band. The D84A and D84N mutants do not display any extra bands. The D84E mutant displays only one strong band which migrates to the same distance as the lowest new band observed for wild-type.

The wild-type apoenzyme therefore appears to have reconstituted into holoenzyme after incubation at 37°C with porphobilinogen, and has accumulated as enzyme-intermediate complexes. The wild-type has also made enzyme-intermediate complexes on incubation with porphobilinogen. The D84E mutant is found to have turned completely to an enzyme-intermediate complex after 10 minutes incubation at 37°C with porphobilinogen. The D84A and D84N mutants are found to be inactive on incubation with porphobilinogen, in agreement with the fact that they are catalytically inactive. Thus the intriguing question remains as to how these mutants have formed as ES_2 complexes.

3.2.5.2 Spectral Properties of the D84A, D84E and D84N Mutants

It was observed that the D84E, D84A and D84N mutant holenzyme forms were colourless in solution and on freeze drying, whereas the proposed enzyme-intermediate forms of the three mutants were found to be pink in solution and on freeze-drying.

Spectral changes are observed when porphobilinogen deaminase is reacted with Ehrlich's reagent, giving rise to characteristic profiles for the holoenzyme and enzyme-intermediate complexes. The wild-type holoenzyme and mutant D84E holoenzyme, D84E ES_2, D84A and D84N were reacted with Ehrlich's reagent and the spectral changes monitored over a time period of up to 10 minutes. For the D84A and D84N samples, it was the form in which the majority of the protein existed, that is, the proposed ES_2 complex, that was used for the reaction. All enzyme samples were first applied to a PD10 gel filtration column to remove the reducing agent β-mercaptoethanol, which is known to interfere with the Ehrlich's reaction. The spectra can be observed in figure 3.21.

Figure 3.21 Spectra of Wild-Type and Aspartate-84 Mutants of Porphobilinogen Deaminase After Reaction With Ehrlich's Reagent

Spectra observed immediately (0 minutes), 3 minutes, 5 minutes, 7 minutes and 10 minutes

a) wild-type, recorded at 0, 3 and 5 minutes.

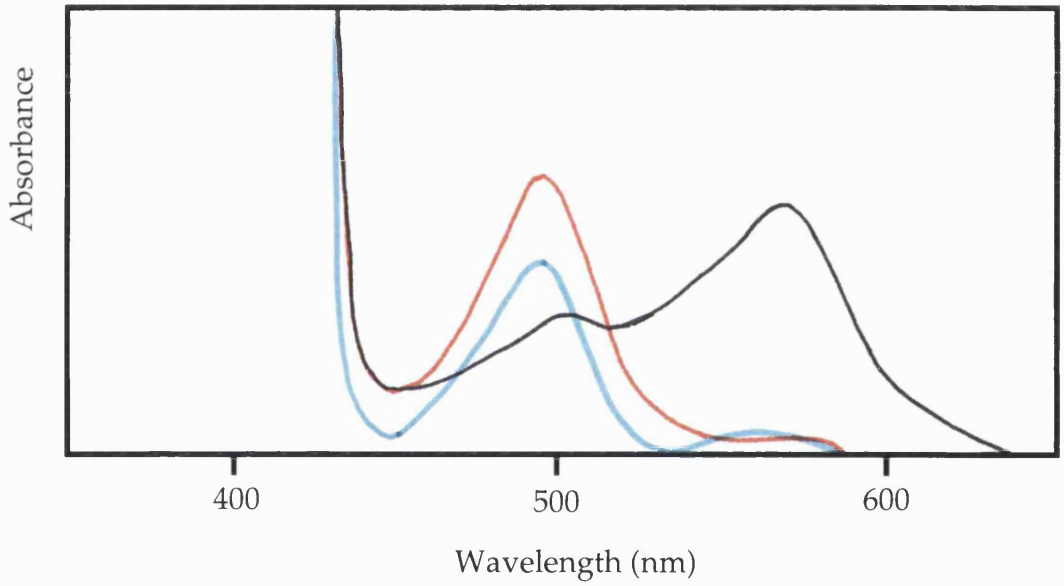

b) D84E holoenzyme, recorded at 0, 5 and 10 minutes.

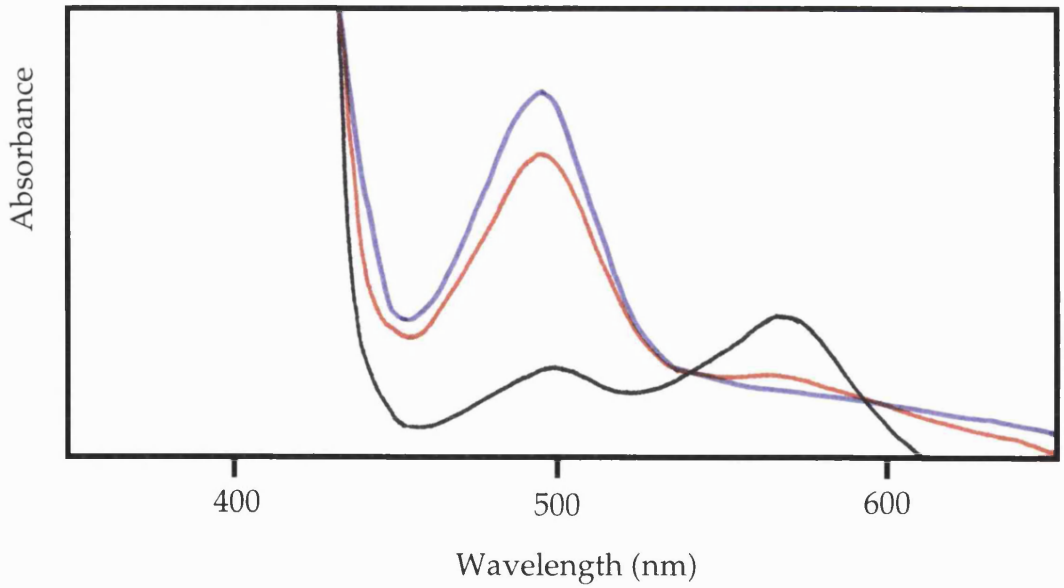

c) D84E enzyme-intermediate complex ES_2, recorded at 0, 3 and 7 minutes.

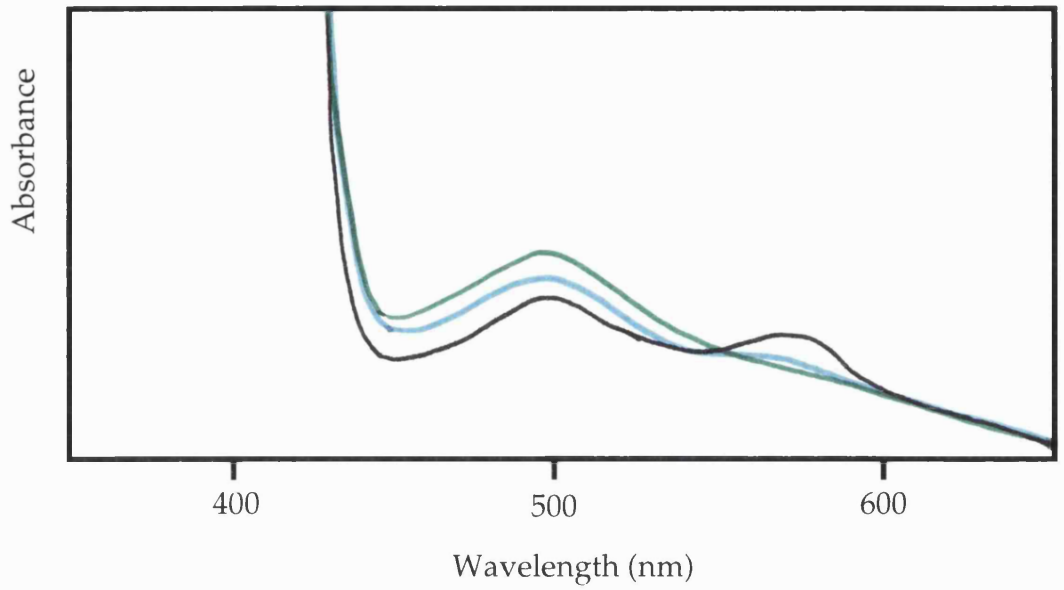

d) D84A , the predominant form, recorded at 0, 5 and 10 minutes.

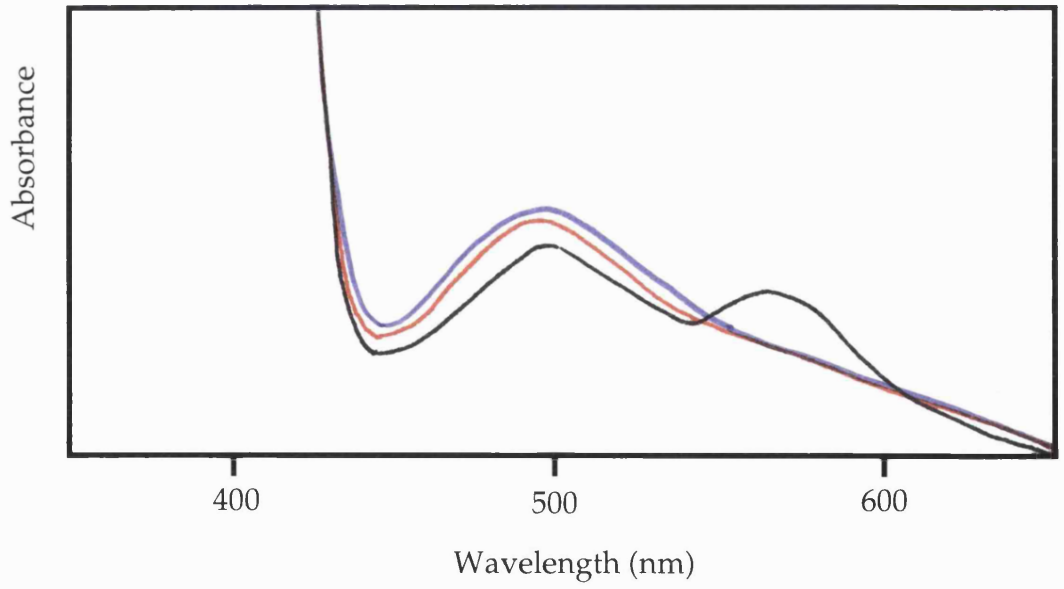

e) D84N , the predominant form, recorded at 0, 3, 7 and 10 minutes.

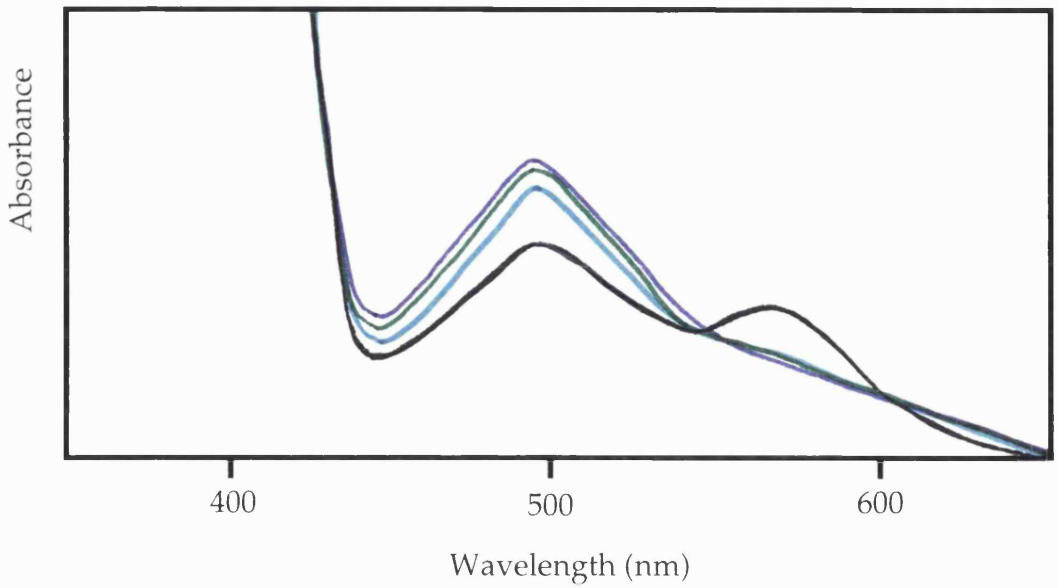

The spectra in figure 3.21a show that the wild-type enzyme was seen to display the typical spectral profile of a dipyrromethane (Plusec and Bogorad, 1970; Jordan and Warren, 1987). An absorption maximum was initially observed at 565nm, changing within three minutes to give a maximum at 495nm. The D84E mutant holoenzyme (figure 3.21b) was found to display a similar profile to wild-type holoenzyme, as had been previously observed (Woodcock and Jordan, 1994). The D84E ES_2 complex (figure 3.21c) gave rise to maxima seen initially at both 565nm and 495nm, changing within three minutes to give a maximum at 495nm only. This result was in keeping with the expected spectral profile for an enzyme-intermediate complex (Warren, 1988). The D84A and D84N mutants (figures 3.21d and e) both gave rise to a spectra similar to the D84E ES_2 complex, again as previously observed (Woodcock and Jordan, 1994).

These results provide further evidence that the extra peaks isolated *via* f.p.l.c. of the aspartate-84 mutants are enzyme-intermediate complexes. They also strongly indicate that the D84A and D84N mutants contain an enzyme-intermediate complex, although the Ehrlich's reaction spectral profiles for the various complexes are known to be very similar and therefore it would not be easy to distinguish which complex was present (Warren 1988).

3.2.6 Electrospray of the D84N Mutant of Porphobilinogen Deaminase

Electrospray mass spectroscopy allows the measurement of the molecular mass of a protein to an accuracy of 0.01%. This technique was therefore employed to establish the molecular mass of the mutant D84N protein and to determine the exact nature of the protein, that is, to determine whether the D84N existed in the form of one of the enzyme-intermediate complexes. The mutant enzyme was first purified further by dialysis and reverse-phase h.p.l.c. The electrospray was carried out in the presence of formic acid, which is known to lead to the release of wild-type enzyme-intermediate complexes. However, it has been shown that D84N is unchanged after treatment with formic acid and therefore it was anticipated that the presence of formic acid would not lead to any breakdown of the enzyme. The sample of D84N subjected to electrospray was largely the predominant form of the enzyme, believed to be ES_2.

The wild-type holoenzyme has a predicted value of 34270 and a reported electrospray value of 34271±3 (Aplin *et al.*, 1991). The predicted molecular mass of D84N holoenzyme would also be 34270. The electrospray mass spectrum for D84N can be seen in figure 3.22.

Figure 3.22 Electrospray Mass Spectrum of the Mutant D84N of Porphobilinogen Deaminase

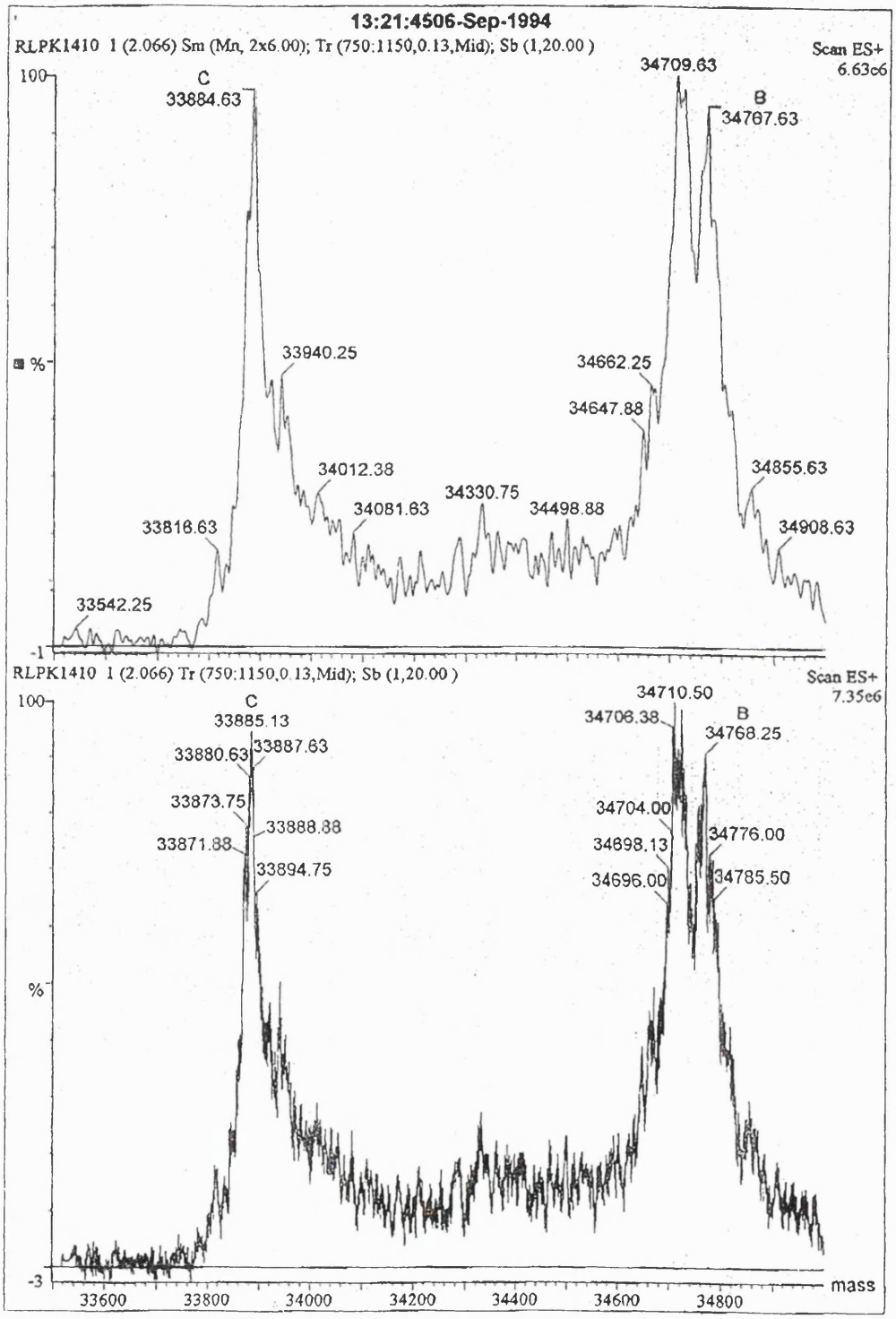

The mass spectrum in figure 3.22 reveals three major peaks for the mutant, with molecular mass of 33882.99±12.67 Da, 34720.69±14.36 Da and 34769.25±17.94 Da. Whilst the standard deviations for these results were found to be high, they were nevertheless substantially lower than the mass of a single molecule of porphobilinogen, which has a predicted molecular mass of 219. Therefore the high standard deviations would not lead to any misassignments. The poor profile was not due to contamination and was likely to be a feature of the protein.

None of the three peaks observed fell in the range of the predicted vaue for holoenzyme, 34270 Da. Predicted values for other states of the porphobilinogen deaminase enzyme are:

apoenzyme	33832 Da
apoenzyme + one pyrrole ring	34051 Da
holoenzyme	34270 Da
enzyme-intermediate complex ES	34489 Da
enzyme-intermediate complex ES_2	34708 Da
enzyme-intermediate complex ES_3	34927 Da
enzyme-intermediate complex ES_4	35146 Da

The peaks observed therefore appear to have a molecular mass of apoenzyme+50 Da, the enzyme-intermediate complex ES_2+18 Da, and the enzyme-intermediate complex ES_2+60 Da. The discrepancies are difficult to explain. They are unlikely to be due to any residual β-mercaptoethanol, molecular mass 78 Da, as the peaks observed for β-mercaptoethanol are usually sharp and characteristic.

Despite the discrepancy between predicted and observed values for the first and third peak, the second peak clearly confirms the presence of the enzyme-intermediate complex ES_2 for the mutant D84N porphobilinogen deaminase. As the D84A mutant has been found to be similar to the D84N mutant in every respect, it is also likely to predominate in an ES_2 enzyme-intermediate complex.

The apparent presence of the apoenzyme may be a consequence of the formic acid. Whilst it has previously been shown that the acid only leads to the release of the intermediate complexes and not the cofactor, this may have been because the cofactor was oxidised. It is unlikely that the presence of

apoenzyme is due to an instability of the cofactor, as the cofactor for the D84N mutant has been shown to be heat stable. It is also possible that the apoenzyme form of the mutant was already present in the sample. However, whilst it has been observed that the apoenzyme form of D84N can be isolated even in the later purification stages of the enzyme, it is still unlikely that it would have been present in this sample as the protein had been f.p.l.c. purified and analysed by non denaturing gel electrophoresis.

3.3 Conclusions

The f.p.l.c. isolation and polyacrylamide gel analysis of the three aspartate-84 mutants has given a clearer insight into their nature. In the case of the D84E mutant, naturally present complexes were identified which were not previously observed. These enzyme-intermediate complexes were found to be considerably more stable than those of wild-type enzyme, and thus proved valuable for crystallisation experiments.

Regarding the D84A and D84N mutants, results were produced in the presence of reducing agents which had only previously been observed for enzyme purified in the absence of reducing agent. This indicates that the oxidation state of the cofactor is not likely to be the basis for the enigmatic characteristics of the D84A and D84N mutants (Woodcock and Jordan, 1994), and the different purification techniques have instead been assigned as the likely cause of the alternative data sets. The results all point towards the existence of the D84A and D84N mutants as ES_2 complexes, but this does not satisfactorily relate with the observed catalytic inactivity of these mutants. Interpretation of results presented in this chapter, in the light of experiments with apoenzyme reported in Chapter 5, has now led to a new hypothesis that explains the existence of ES_2 forms of D84A and D84N mutants. It has now been concluded that the reconstitution of holoenzyme from apoenzyme takes place preferentially with preuroporphyrinogen, and not porphobilinogen. The addition of the 1-hydroxymethylbilane to apoenzyme would initially yield an ES_2 complex, which in the wild-type enzyme would react with two further molecules of porphobilinogen to give holoenzyme (apoenzyme plus cofactor) and the product, pre-uroporphyrinogen. Further details of the cofactor assembly hypothesis are given in Chapter 5.

A mechanism for cofactor assembly involving the addition of preuroporphyrinogen to apoenzyme would satisfy the results observed for the D84A and D84N mutants. Both mutants would be able to bind and react with the highly reactive 1-hydroxymethylbilane, but would not then be able to carry the reaction forwards, or backwards, due to the mutation of the catalytic residue. Such a hypothesis would also therefore suggest that a different mechanism is employed for cofactor assembly and substrate binding since the aspartate-84 residue could not then be considered essential for cofactor assembly. This hypothesis could also explain why the proposed

apoenzyme observed during the purification of radiolabelled D84N was unable to bind porphobilinogen, since this is so unreactive compared with preuroporphyrinogen. It is observed in comparative experiments described in Chapter 5 that the rate of preuroporphyrinogen incorporation is considerably greater than that for porphobilinogen.

Chapter 4

Crystallisation of the Aspartate-84 Mutants of *E. coli* Porphobilinogen Deaminase

4.1 Introduction

The understanding of protein structure and function has been greatly enhanced by X-ray diffraction in single crystals and nuclear magnetic resonance (NMR) spectroscopy in solution. Both techniques allow the precise three-dimensional positions of most of the residues in a protein molecule to be accurately determined. Whilst the techniques yield different types of information due to the different environments, the protein either being tightly packed in a crystal or freely tumbling in solution, the structure of the core of globular proteins derived from X-ray or NMR data is generally found to be very similar (Billeter, 1992).

The recent elucidation of the crystal structure of native *E. coli* porphobilinogen deaminase (Louie *et al.*, 1992) has provided a detailed molecular description of the enzyme and valuable insight into the reaction mechanism, highlighting possible structure-function relationships of the active site components. In particular, the crystal structure revealed the side chain carboxyl group of the invariant aspartate-84 residue to be positioned near the proposed S and C pyrrole binding sites, within hydrogen-bonding distance to the two pyrrole nitrogen hydrogens of the dipyrromethane cofactor , suggesting that the residue was a strong candidate for a catalytic group (figure 4.1). Site-directed mutagenesis studies of the aspartate-84 residue confirmed its role as the likely catalytic residue (Woodcock and Jordan, 1994). Nevertheless, whilst the native structure has contributed greatly to our understanding of the enzyme, the debate over the mechanism of cofactor assembly, substrate binding and the manner in which the enzyme accommodates the growing polypyrrole chain is as yet unresolved. The crystallisation of the catalytic residue mutants, D84A, D84E and D84N, was therefore undertaken to investigate further the role of the invariant aspartate-84 residue.

The porphobilinogen deaminase D84A, D84E and D84N mutants have been described in Chapter 3. The D84A and D84N mutants are found to be catalytically inactive. The D84E mutant is found to possess less than 1% of the activity of the wild-type whilst the K_m of the D84E mutant is similar to that of the wild-type, indicating that catalysis rather than substrate binding has been affected. All three mutants are found to possess the cofactor. The three-dimensional structure of the D84A, D84E and D84N mutants would allow the

structural basis of the decrease in activity to be established, and therefore clarify the role of asp-84 in the mechanism of substrate binding and catalysis. It is anticipated that structural changes would be observed for all three mutants in the vicinity of this residue and possibly also in the surrounding environment.

A three-dimensional structure of each of the enzyme-intermediate complexes of porphobilinogen deaminase is required to describe accurately the chain elongation process. There are three ways in which one catalytic site could be used to accommodate the intermediates of the tetrapolymerisation: either the growing tetrapyrrole is packaged into the cleft, or the domains move with respect to one another and pull the growing chain through the active site, or a combination of both mechanisms. It has been predicted that conformational changes will occur on substrate binding, which is borne out by the observation that native porphobilinogen deaminase crystals shatter upon addition of porphobilinogen (Lambert, personal communication). Furthermore, amino acid modifying experiments have shown that one of the cysteine residues (cysteine-134), which is non-reactive in the E state, becomes exposed and more reactive as substrate is bound (Warren *et al.*, 1995). The crystallisation of one of the enzyme-intermediate complexes would therefore allow the capture of the protein in the midst of its catalytic cycle, and for this purpose the ES_2 complex of the D84E mutant was selected due to its abundance and stability.

There are five stages involved in the determination of the crystal structure: the growing and characterising of crystals, X-ray diffraction data collection, phase determination, model building and atomic refinement and finally the interpretation of the model (Eisenberg and Hill, 1989).

The preparation of X-ray grade crystals often represents the largest obstacle encountered during the process of crystallisation, and there are various well documented techniques for achieving crystallisation of proteins (McPherson, 1982; Blundell and Johnson, 1976). The traditional batch method requires a large quantity of protein and involves the careful manual addition of precipitant to the protein solution or the changing of pH until the protein comes to the limit of its solubility. An alternative method, the hanging drop technique, employs a system in which a drop containing protein and precipitant is allowed to equilibriate in a closed container with a larger

aqueous reservoir whose precipitant concentration is optimal for producing crystals. As the precipitant is the major solute present, vapour diffusion in this closed system results in net transfer of water from the protein solution to the reservoir, until the precipitant concentrations is the same in both solutions. As a result, the precipitant concentration in the protein solution will rise to the optimal level for crystallisation. Whilst the main advantage of the hanging drop technique is that only μg amounts of protein are required, a major disadvantage is that the crystals produced are invariably small.

Once suitable crystals have been grown, the next step is that of X-ray diffraction data collection. X-rays are electromagnetic radiation of wavelengths 0.1-100Å. X-rays in the useful range for crystallography, having a similar wavelength to that of the bond lengths, can be produced by bombarding a metal target with electrons produced by a heated filament and accelerated by an electric field. A high-energy electron collides with a metal target atom and displaces an electron from a low-lying metal orbital. As a result, an electron from a higher orbital drops into the resulting vacancy and emits its excess energy as an X-ray photon. There are three common sources of X-rays: X-ray tubes, rotating anode tubes and particle accelerators.

Synchrotron radiation is generated by particle accelerators, the most powerful source of X-rays. Particle accelerators consist of giant rings in which electrons or positrons circulate at velocities near the speed of light, driven by energy from radio-frequency transmitters and maintained in circular motion by powerful magnets. A charged body like an electron emits energy (synchrotron radiation) when forced into curved motion, and in accelerators the energy is emitted as X-rays. The advantages of synchrotron radiation lie with the ability to collect to a much higher resolution at shorter wavelengths, thereby extending the lifetime of sensitive crystals (Acharya *et al.* 1989). Station 9.6 at the Daresbury Laboratory is a high intensity X-ray protein crystallography experimental station which harnesses monochromatic synchrotron radiation from a beam of electrons which circulate around the Synchrotron Radiation Source (SRS) storage ring. The working apparatus of Station 9.6 can be seen in figure 4.1.

Figure 4.1 Station 9.6 at the Daresbury Laboratories

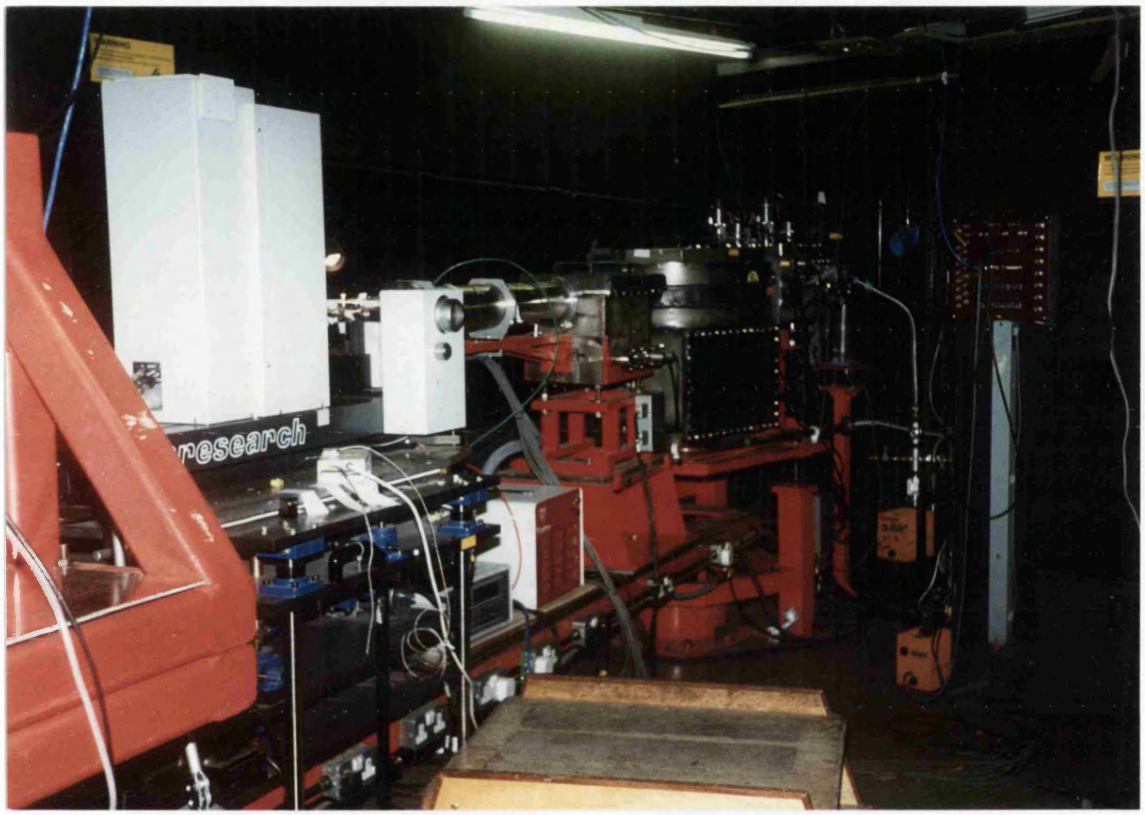

The crystal from which data is to be collected is mounted between an X-ray source and an X-ray detector. The crystal lies in the path of a narrow beam of X-rays and diffracts the source beam into many discrete beams, each of which produces a distinct spot, a reflection, on the detector. The detector used may be film or, more commonly, an image plate.

The raw data produced from crystallography are the reflections which make up the diffraction pattern, and the measurable parameters of the diffraction pattern are the indices and the intensity of each reflection. Both parameters provide valuable information: the indices allow a calculation of the unit cell to be made, and the intensities hold an inverse relationship with the amplitude of the diffracted rays that contribute towards them.

The unit cell is the smallest and simplest volume element that is completely representative of a whole crystal, and the unit cell dimensions are required to devise a strategy of data collection that will give rise to the most identifiable, measurable reflections without overlap. The internal symmetry of the cell provides important information for the same reason. If the cell and its contents are highly symmetrical, then the number of crystal orientations required in order to obtain all the distinct or unique reflections can be reduced. Both the unit cell dimensions and the symmetry are determined from a preliminary diffraction pattern. The unit cell is then assigned a space group to describe its symmetry.

The true diffractors of X-rays are the clouds of electrons in the molecules of the crystal. Diffraction reveals the distribution of electrons of the molecules and therefore an electron density map can provide a description of the surface features and overall shape of all molecules in the unit cell. The goal of data processing is to obtain the mathematical function whose graph is the desired electron density map. To allow the calculation of the electron density map, a full description of the waves of the diffracted rays must first be obtained. Three parameters are therefore required to describe a wave: amplitude, frequency and phase. The amplitude of the diffracted rays can be calculated from the intensity of the reflections, whilst the frequency of the ray corresponds to the frequency of the X-ray source beam. The phase of the wave, however, cannot be measured directly and has to be estimated. The estimation of this parameter is often referred to as the 'phase problem'.

The phase problem is normally solved by labelling the protein with heavy atoms, a method known as isomorphous replacement. This procedure involves the introduction of a single or limited number of heavy atoms per protein molecule without disrupting or significantly altering the crystal lattice. As x-rays are diffracted by the clouds of electrons in the molecules of the crystal, the substantial addition of electrons in the structure due to the heavy atoms causes significant changes in X-ray recorded intensities. These changes are then interpreted to estimate phases. A phase must be calculated for each reflection to be included in the calculation of the electron density map.

Alternatively, the phase of the diffracted ray can be estimated by methods of molecular replacement or anomolous scattering. Molecular

replacement is the simplest method to use when a similar structure is already known. The procedure is most commonly used when a native protein structure has been solved, and phases are required for mutants of the protein or proteins isolated with ligands, such as substrate. Anomolous scattering is the least commonly used method, and employs the characteristic drop in X-ray absorption of heavy atoms at their absorption edge.

Once the wave descriptions, known as structure factors, have been obtained for each reflection, a reversible mathematical process known as a Fourier transform is then applied to convert this information into a three-dimensional electron density map. A crude structure can then be modelled. The process thereon is an iterative one, and requires several cycles of calculations to improve the map, *via* the computation of new phases from the model. The model is also improved by methods of least-squares refinement and solvent flattening and also the application of additional constraints and restraints. Areas of ambiguity in the model can be eliminated from further calculations to avoid biasing the phase improvements.

The progress of the iterative process is constantly monitored to ensure that the structure factor amplitudes that can be calculated from the current model agree with the original amplitudes measured. Other criteria for the model must also be met: the structure must be chemically, stereochemically and conformationally reasonable. The accuracy of the model and its fulfilment of the criteria is judged by various indices, such as the R-factor and the Ramachandran plot.

The electron density maps are often cast in the form of difference Fourier maps. The latest calculated electron density map can be compared with the original density map observed by showing only the differences between the two. Such a map would be referred to as the difference Fourier map F_o-F_c, a map of observed minus calculated electron density. This map would show both positive and negative density, and the negative density would be an indication of where the contribution from the calculated map would be greater than that from the observed map.

A more commonly used difference Fourier map is the $2F_o$-F_c map. This map is everywhere positive, and shows negative density only in areas which are incorrect. Such a map is also advantageous to use when solving the

structure of a mutant protein or protein with a bound ligand, when the native structure is already known. In this case, the observed map would refer to the model obtained from the current data, whilst the calculated map would be that of the known protein structure.

The strategy adopted for structure determination is dependant on various factors and figure 4.2 outlines the path taken for both native and mutant porphobilinogen deaminase. The high resolution model of the native porphobilinogen deaminase was, of course, advantageous in helping to solve the structure of the mutants. Problems were nevertheless encountered along the way, particularly due to the apparent mobility of the substrate rings.

Figure 4.2 The Strategy Adopted for the Protein Structure Determination of Wild-Type and Mutant Porphobilinogen Deaminase

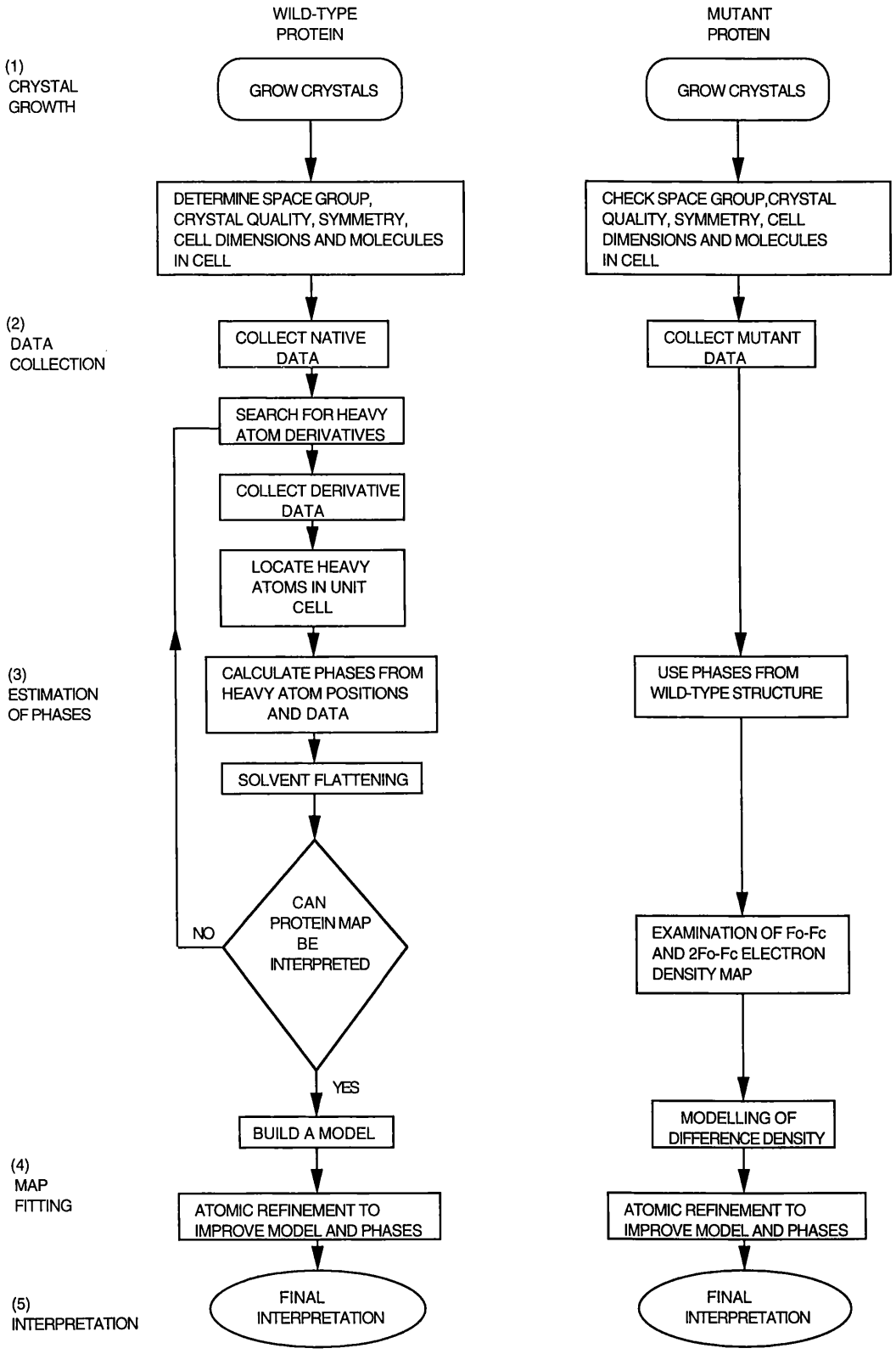

4.2 Results and Discussion

4.2.1 Crystal Growth and Morphology

4.2.1.1 Growth of Mutant Porphobilinogen Deaminase Crystals

The protein was prepared for crystal growth as described in Materials and Methods, with typically only 10μg of protein required per well for a fine matrix search to be conducted. Use of an automated ICN pippetting station enabled the preparation of a large number of rapid and reproducible hanging drop plates. In order to ensure crystals were formed with a reduced cofactor, extensive use of DTT was employed and all solutions were completely degassed. Crystals of D84E were found to form optimally at a pH of 5.1 using an 8% polyethylene glycol solution as a precipitant. The ES_2 derivative crystals formed best at pH 5.3, using an 11% polyethylene glycol 8000 solution. The absence of light was also essential to prevent the crystals becoming deformed and elastic, as previously observed for native porphobilinogen deaminase (Wood, unpublished results). Crystals were only obtained with the D84E protein, the D84A and D84N mutants failed to crystallise.

4.2.1.2 Stability of Mutant Porphobilinogen Deaminase Under Crystallisation Conditions

The D84E mutant was believed to remain stable until crystallisation was achieved and therefore was not monitored in any way. However, a more cautious approach was taken for the D84E ES_2 protein in order to establish whether the enzyme-intermediate complex had remained intact and not broken down to yield holoenzyme or ES. This was important as it is known that native ES complexes decompose to generate the free enzyme (Warren and Jordan, 1988). A sample of freeze-dried D84E ES_2 was therefore resuspended in sodium acetate buffer, pH 5.5 and left at room temperature to simulate the conditions used for crystallisation. A control sample of ES_2 was resuspended in 1mM Tris buffer pH 7.5 containing 2mM dithiothreitol and also left at room temperature. When the two samples were analysed by non-

denaturing PAGE immediately, after four hours and twenty four hours, the complex appeared to have remained intact and the two samples were seen as single bands of the same mobility (results not shown). The two samples were also analysed after two weeks, when no bands were observed which implied that the protein had been degraded (results not shown). The ES_2 crystal itself was analysed by denaturing and non-denaturing PAGE after a number of months, and the complex again appeared intact which implied that crystallisation was achieved before any breakdown of protein (results not shown).

4.2.1.3 Mutant Porphobilinogen Deaminase Crystal Morphology

The D84E crystals displayed the typical tile-like morphology that had previously been observed for deaminase (Jordan *et al.*, 1988) but grew mainly as clusters of tiles stacked together. The crystals were deep red, in contrast to native crystals which are colourless under the same conditions, indicating that the cofactor may have become oxidised, despite the fact that the crystals were grown under strong reducing conditions. Similarly, the D84E ES_2 crystals were also a deep red in colour and grew as clusters of tiles stacked together. The largest well-formed crystal cluster was subsequently separated to yield a tile-like crystal suitable for data collection. Crystals of the D84E ES_2 complex can be seen in figure 4.3.

Figure 4.3 The Crystal Cluster of the D84E ES_2 Mutant of Porphobilinogen Deaminase

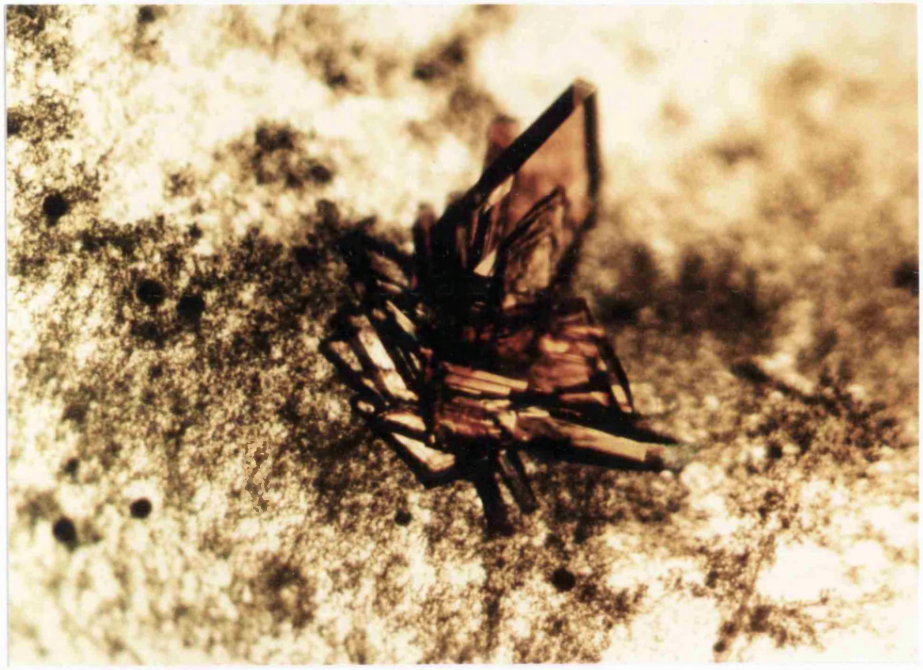

4.2.2 Data Collection

4.2.2.1 Preliminary Data Collection of Mutant Porphobilinogen Deaminase

The previous characterisation of the diffraction pattern of native protein crystals provided information regarding the unit cell. The crystals were known to be orthorhombic, with unit cell dimensions of a=88Å b=76Å, c=50Å, α=90°, β=90°, γ=90°. Data needed only be collection over a 90° rotation as the cell was found to have two planes of symmetry.

The data for both mutant D84E and the mutant ES_2 complex were initially collected at Birkbeck College using the Mar research 180mm image plate fitted to a Siemens generator. However, due to the small size of the crystals of the mutant protein it was necessary to collect a higher resolution data set using synchrotron radiation at the Daresbury Laboratories. Data were collected for both the mutant D84E and the mutant ES_2 complex at Station 9.5 (a similar source to Station 9.6). The monochromator was calibrated to a bromine absorption edge. The cooled crystals (4°C) diffracted out to a resolution of 2.0Å and data were collected over 90°.

4.2.2.2 Cryo-cooling of Crystals of Mutant Porphobilinogen Deaminase Crystals

Subsequently, data were collected for cryo-cooled crystals of D84E and D84E soaked with substrate. It was predicted that D84E soaked with substrate may also provide a means of obtaining an enzyme-intermediate model. It was interesting to note that D84E crystals did not shatter upon the addition of substrate, in contrast to the native protein, and this may be a tribute of the reduced activity of the mutant enzyme. A colour change accompanied the addition of substrate, causing the crystals, but not the surrounding solution, to change from colourless to pink. The low temperature (100K) involved with cryo-crystallography allows the lifetime of the protein crystal to be increased by reducing radiation damage during data collection (Gamblin and Rodgers, 1993). It has also been suggested that cooling may increase the internal order of the parts of the protein which are mobile at room temperature (Petsko,

1995). For porphobilinogen deaminase this would include the substrate rings and the mobile loop. Synchrotron radiation data for D84E and D84E soaked with substrate were collected at Stations 9.5 and 9.6 respectively. As cryo-cooling is a technique not previously applied to porphobilinogen deaminase, the collection of data for the D84E crystal soaked with substrate is described in further detail to highlight some of the associated problems.

The D84E substrate-soaked crystals selected for data collection were rapidly cooled in liquid ethane and stored in liquid nitrogen (100K). The presence of a cryostream was employed and its orientation optimised to allow the temperature of the crystal to be maintained once mounted. The cryostream consisted of low temperature nitrogen gas at fixed pressure surrounded by an outer coaxial sheath of dry air. The flow rate of the warm gas sheath was adjusted visually to minimise turbulence of the cold gas stream. Ideally, the loop containing the crystal would be mounted parallel with the cold gas stream to prevent disruption at the edge of the gas stream; in this case data was to be collected through a 90° rotation and therefore this condition could not be met continuously.The presence of a dry air sheath is also helpful in preventing ice formation on the crystal.

Preliminary data were collected for the mounted crystal of substrate-soaked D84E and the X-ray diffraction pattern was studied. Notable ice rings were observed to have formed on the diffraction pattern, and examination of the crystal revealed that there had been a large build-up of ice on the crystal. Careful removal of the ice from the crystal with tweezers and further collection of data from the crystal showed that the crystal had been spoilt by the ice formation. Data collection from the first crystal was therefore abandoned.

The pressure of the cryostream dry air sheath was readjusted and a second crystal mounted. On data collection it appeared that the stream was now at a more suitable flow rate and no further ice rings were observed on the diffraction pattern. Data was collected over 90° to a resolution of 2.2Å. As data was collected over a period of about 10 hours, the crystal was monitored throughout for ice build up. Figures 4.4 and 4.5 show the crystal with and without ice formation.

Data collection from cryo-cooled crystals was therefore viable but it was necessary to strike a balance between maintaining low temperature and preventing interference with the diffraction pattern. Achieving this balance was not only time-consuming, especially when time was at a premium, but was at the cost of the first choice of crystal. However, these may be teething problems which would not be present for further data collection. The effectiveness of the technique would lie with the structure modelled from the data.

4.2.2.3 Raw Data Collected for Mutant Porphobilinogen Deaminase

The X-ray diffraction oscillation images for the mutant D84E and the D84E ES_2 complex were collected, the image for the D84E ES_2 complex being shown in figure 4.6. The X-ray photograph shows a two-dimensional section through a three-dimensional array of spots. The intensity of each spot was recorded and this information provided the basic experimental data of X-ray crystallographic analysis.

Figure 4.4 The Cryo-Cooled D84E Substrate-Soaked Crystal

The incorrect adjustment of the cryostream has led to ice formation on the crystal.

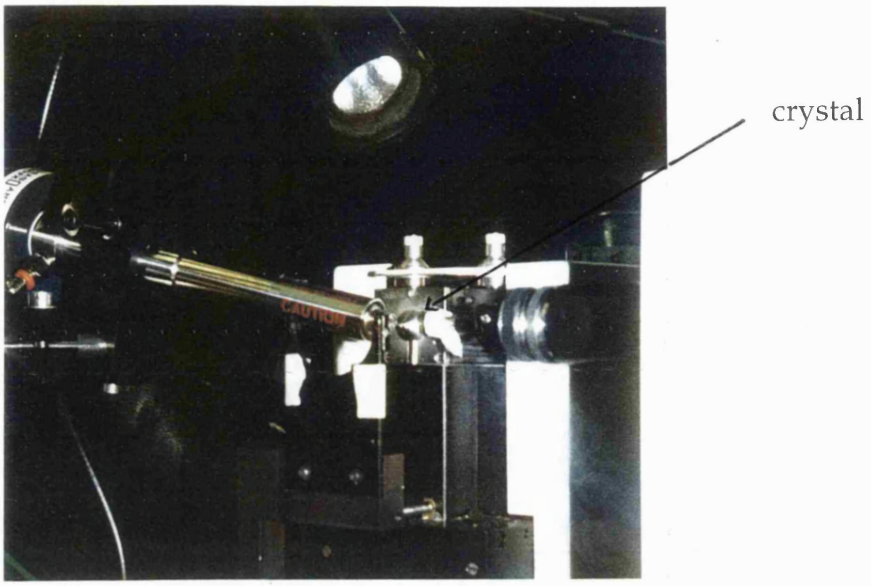

Figure 4.5 The Cryo-Cooled D84E Substrate-Soaked Crystal

The optimal adjustment of the cryostream has prevented ice formation on the crystal.

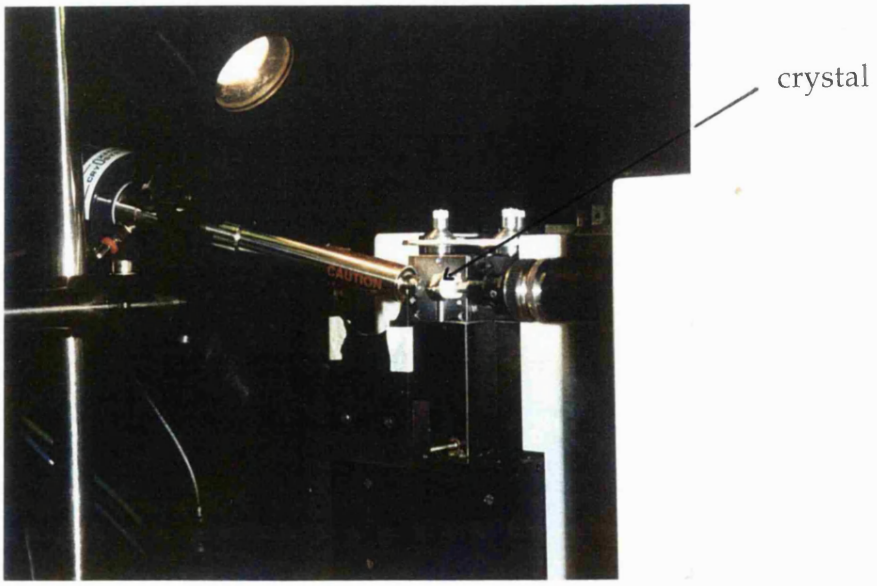

Figure 4.6 Oscillation Images of the Mutant D84E ES_2 Complex

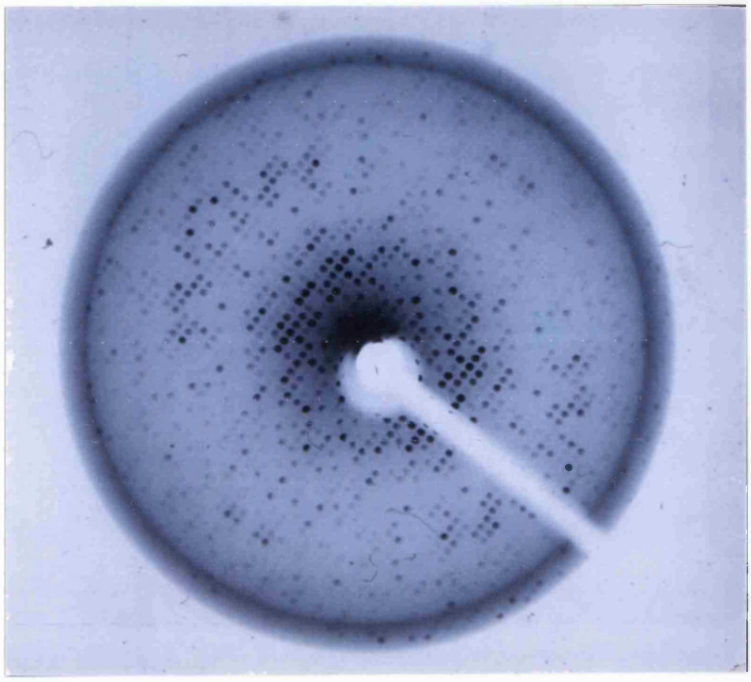

The summary of results for the data collection of the mutant D84E and D84E ES_2 complex is shown in tables 4.1 and 4.2.

Table 4.1 Summary of Data Collection Results for the Mutant D84E

Crystal size	0.1 0.1 0.1mm
Space Group $P2_12_12$	Orthorhombic ∴ 90° data
Data Collection Birkbeck MAR Research Image Plate @ λ = 1.54Å	Oscillation Camera : Film 3°/Oscillation @ 20°C Maximum Resolution 3.0Å
Number of Recorded Measurements 30307	Number of Unique Reflections 5922
R_{merge} 14.3%	91.33% Complete

Table 4.2 Summary of Data Collection Results for the Mutant D84E ES_2 Complex

Crystal size	0.2 0.2 0.1mm
Space Group $P2_12_12$	Orthorhombic ∴ 90° data
Data Collection SRS 9.5 MAR Research Image Plate @ λ = 0.92Å	Oscillation Camera : Film 3°/Oscillation @ 4.0°C Maximum Resolution 2.0Å
Number of Recorded Measurements 70856	Number of Unique Reflections17725
R_{merge} 6.8	81.00% Complete

4.2.3 Data Processing

There are currently a large number of computer programs available which accommodate every step of the data processing. The programs are applied in turn to achieve the final electron density map. An outline of the programs used for the processing of the mutant D84E and D84E ES_2 complex data is shown in table 4.3.

The data from the D84E substrate-soaked crystal is currently undergoing processing by Dr Lambert at Birkbeck College.

4.2.3.1 Electron Density Map Interpretation - Modelling the Structure of the Mutant Porphobilinogen Deaminase D84E Enzyme and the D84E ES_2 Complex

The structure of native *E. coli* porphobilinogen deaminase locates asp-84 on a loop connecting sheet $\beta 3_1$ and sheet $\beta 4_1$ (Louie *et al.*, 1992). With the cofactor in its oxidised form the two pyrrole rings of the cofactor are coplanar and the carboxylate group of the aspartate is able to interact equally with both of the pyrrole ring nitrogen hydrogens of the cofactor. The reduced cofactor structure revealed an orientation of ring C2 of the cofactor which is believed to be the correct *in vivo* conformation. The previously observed positon for ring C2 in the oxidised structure is important since it is likely to represent the approximate position of the substrate binding site. Aspartate-84 was still found to be able to hydrogen bond with both rings of the cofactor in the reduced structure. The interactions of the side chain of the aspartate-84 residue with the cofactor in the reduced structure can be seen in figure 4.7.

Replacement of aspartate-84 with either alanine, glutamate or asparagine produces mutant proteins with subtle amino acids modifications. The D84A mutant lacks both a negative charge and the capacity to form hydrogen bonds and therefore the loss of activity can be explained. The D84N mutant maintains a side chain which can participate in hydrogen bonding, although the negative charge is lost. Again, the loss of activity can be explained, as the side chain can now no longer support the positive charge created by the pyrrole nitrogens during catalysis. The D84E mutant differs from the wild-type enzyme in that an additional methylene group is present

Table 4.3 An Outline of the Programs used for Data Processing

Program	Function
Ips	Control of image plate system
Idxref	Calculates an orientation matrix and missetting angles
Refix	(As above)
Mosflm	Outputs profile fitted intensities of predicted Bragg reflections
Abscale (now part of **Mosflm**)	Applies Lorentz/polarisation corrections and scales A, B and C films
Sortlef	Utility program sorting by Miller index
Rotavata	Calculates statistics and scaling for batches
Agrovata	Applies the scaling to the data set. Calculates R_{merge} value
Truncate	Handles negative reflections and outputs structure factor amplitudes
Simwt	Applies a scaling to account for absent atoms and misplaced atoms in Fourier difference maps
FFT (Fourier)	Generates difference Fourier electron density
Frodo/o	Molecular graphics display package
Restrain	Least squares refinement package

Figure 4.7 Model of Native Reduced Porphobilinogen Deaminase

The model illustrates the reduced cofactor conformation and the interactions with the aspartate-84 residue.

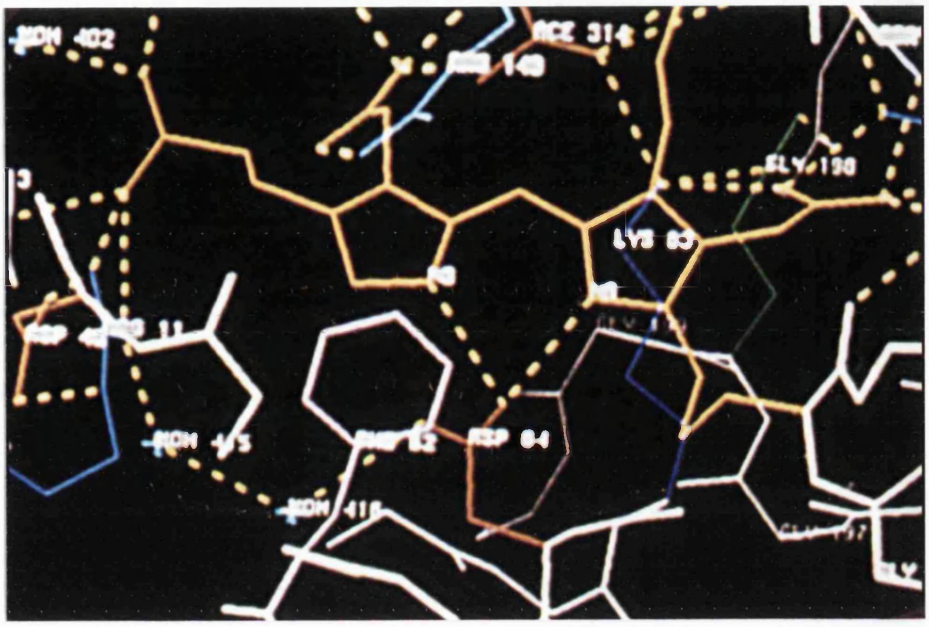

in the side chain. However, the essential carboxylic acid group at the terminus of the side chain is still available for interaction with the cofactor, having a comparable pK_a of 4.07 (pK_a of aspartate side group = 3.9). The glutamate side group carboxylic acid can therefore still provide a negative charge and also participate in hydrogen bonding. The huge loss in activity for the mutant can only then be explained by the loss of the correct spatial location of the amino acid side chain.

4.2.3.2 Preliminary Structure of the Mutant Porphobilinogen Deaminase D84E Enzyme

Phases which had been previously calculated for the 1.9Å structure in which the cofactor was oxidised were used to generate the initial diffrerence Fourier maps with the 3Å data derived from the reduced cofactor crystal. The 2Fo-2Fc difference Fourier electron density map showed changes in the

distribution of electron density. In particular, electron density was observed adjacent to the oxidised C2 location, in the position associated with the reduced structure location of C2 cofactor ring, which confirmed that the cofactor was in a reduced conformation. Additional electron density was also associated with the side chain of the residue aspartate-84. The $2F_o$-F_c map allowed the glutamate residue and the reduced cofactor to be comfortably modelled in the new electron density. The initial Fourier difference map can be seen in figure 4.8.

Figure 4.8 The Mutant D84E Fourier Difference Electron Density $2F_O$-$2F_C$

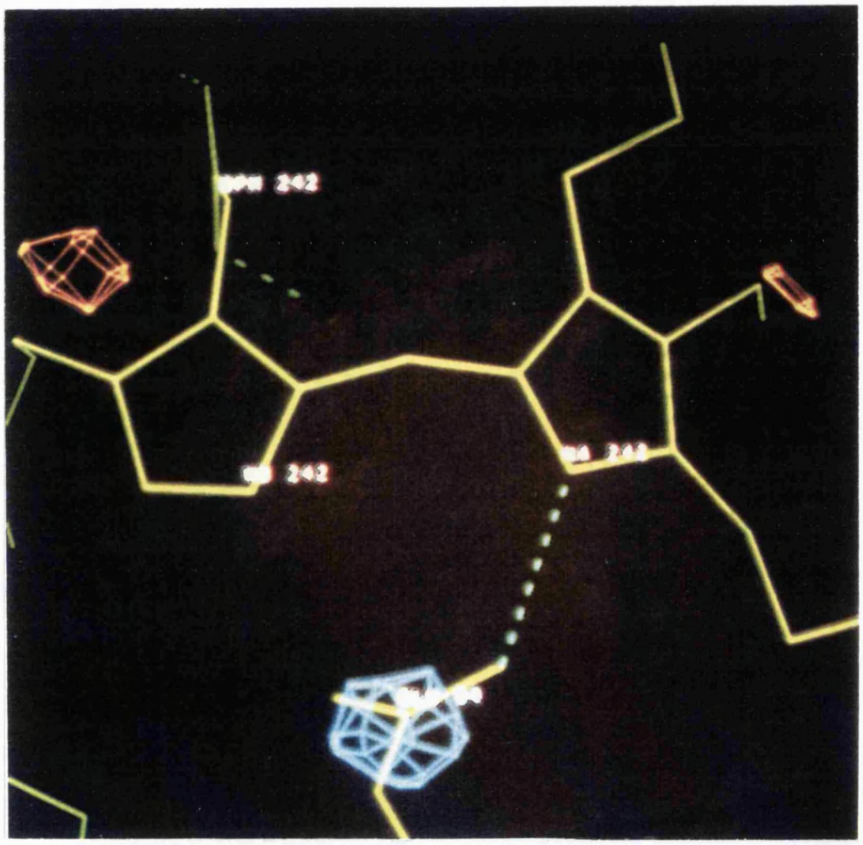

4.2.3.3 Refinement of the Mutant Porphobilinogen Deaminase D84E Enzyme Structure

The preliminary structure of the D84E mutant was then refined. To avoid biasing the structure, the modelled cofactor was omitted together with solvent and the aspartate-84 was replaced with alanine. Two rounds of geometric refinement were then performed to optimise the stereochemistry of the model.

4.2.3.4 Final Structure of the Mutant Porphobilinogen Deaminase D84E Enzyme

The final model of the D84E mutant was produced after the refinement process. The active site can be seen in figures 4.9 and 4.10, illustrating the reduced cofactor conformation and the interaction with the glutamate residue at the mutated position 84. The hydrogen bond interactions between the pyrrole nitrogen hydrogens of the cofactor and the glutamate-84 side chain carboxylate group were found to be modified in that the pyrrole nitrogen hydrogen of ring C2 of the cofactor was seen to have lost its hydrogen bond interactions. Thus, the extension of the residue 84 side chain length by an extra carbon appeared to have caused the position of the carboxylate group to be shifted away from the cofactor C2 ring. The hydrogen bond interaction with the C1 ring was maintained although the angle is changed.

The structure offered some explanation for the reduced activity of the D84E mutant. The absence of hydrogen bonding with ring C2 of the cofactor suggested that glutamate-84 would fail to support a positive charge on the pyrrole nitrogen of the terminal pyrrole ring and thus the generation of a nucleophilic carbon atom at the free α-position of this ring would be considerably less facilitated. In addition, the oxygen of the side group would now no longer be in an optimal position to remove the proton from the α-position of the ring C2 in the last step of ring coupling. The reverse reactions required for product release would also be affected in the same manner.

The structure was limited to only the two rings of the cofactor. It is likely that the loss of hydrogen bonding to the ring C2 of the cofactor also suggests that potential hydrogen bonding to the proposed S1 site would have

Figure 4.9 The Refined Structure of the D84E Mutant

The structure illustrates the reduced conformation of the cofactor.

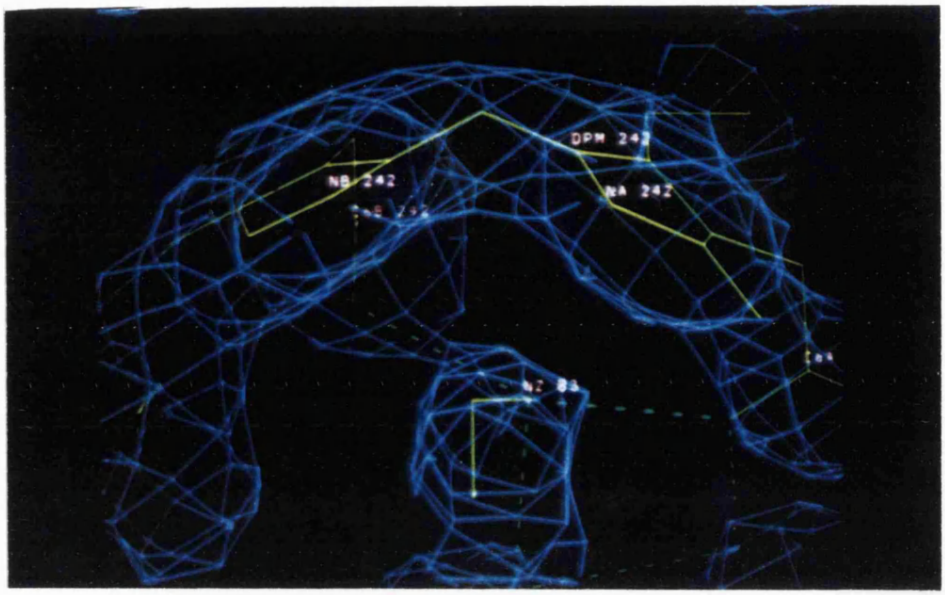

Figure 4.10 The Refined Structure of the D84E Mutant

The structure illustrating the interactions of the cofactor with the glutamate side chain carboxylate group.

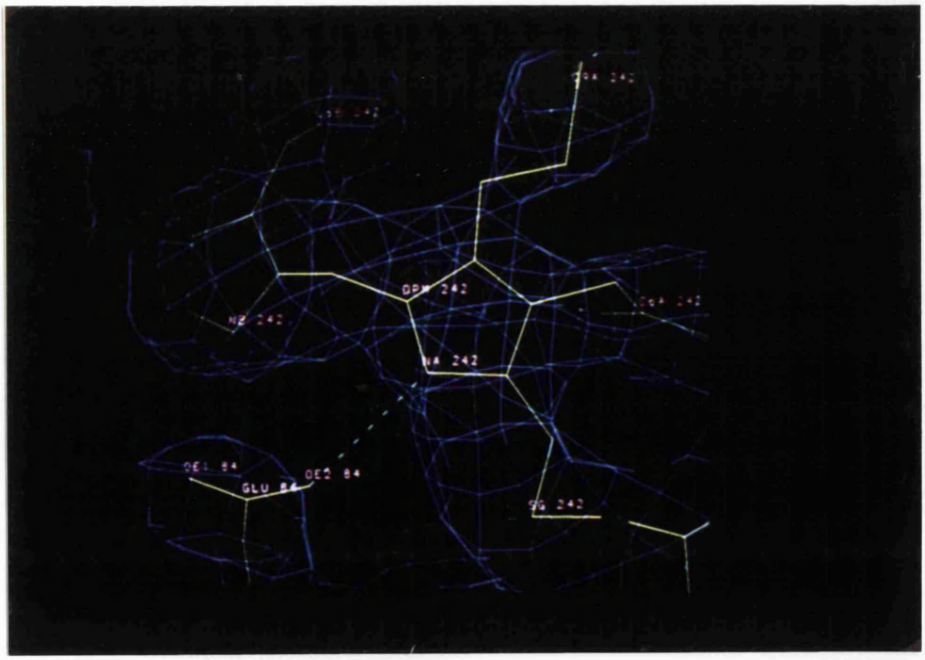

been impaired or lost and therefore interactions from the residue at 84 with the incoming substrate that were present in the native enzyme were also now unlikely to be maintained. Such a loss of interaction would further explain the reduced activity of the mutant. It was anticipated that the structure of the D84E enzyme-substrate intermediate complex would confirm this hypothesis, and allow more detailed explanations of the reduced activity to be derived.

4.2.3.5 Preliminary Structure of the Mutant Porphobilinogen Deaminase D84E ES_2 Complex

In order to calculate the electron density for the D84E ES_2 complex, the initial phases derived from the oxidised wild-type were again used to create the $2F_o$-$2F_c$ and $2F_o$-F_c difference Fourier maps. The initial $2F_o$-F_c maps showed cofactor electron density for both the oxidised and reduced C2 ring positions, together with electron density for the glutamate side chain. Electron density from a possible third ring was also observed adjacent to the C2 ring. This additional electron density was in a position appropriate for interactions between the former free α-postion and the substrate ring.

The preliminary model for the complex can be seen in figure 4.11, although the results are still speculative whilst refinement is in progress. Only one substrate ring has been confidently modelled, the position of the second substrate ring is still tentative.

The structure of the cofactor was observed to be in the reduced cofactor conformation in the initial difference Fourier map. Adjacent to the α-position of the ring C2 of the cofactor was an area of difference electron density sufficient to allow a single pyrrole ring to be modelled comfortably. Density was observed linking the S1 ring to the C2 ring. Preliminary modelling suggests that the acetate side chain of S1 interacts with arginine-11 NH_2, serine-13 OH and a main chain amide nitrogen of the residue at 152. The propionate side chain interacts with glutamine-19 NH_2 and a main chain nitrogen of the residue at 81. The plane of the S1 ring appears to be parallel to the C1 ring. The mutated glutamate-84 residue is unable to hydrogen bond to either rings C2 or S1.

Figure 4.11 The Preliminary Structure of the D84E ES_2 Mutant

The structure illustrates the interactions of the cofactor with the glutamate side chain carboxylate group and the location of the two substrate rings.

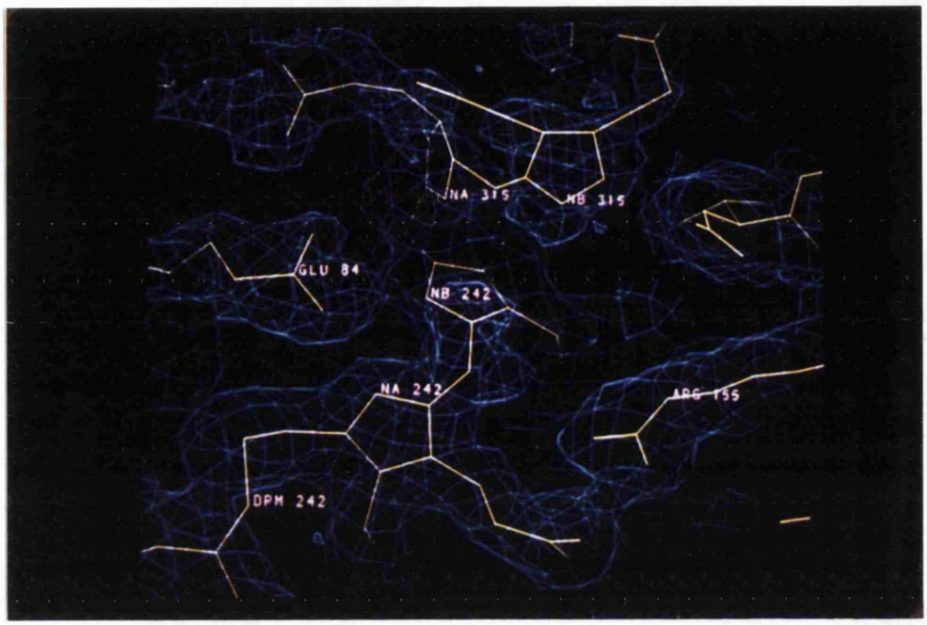

Density adjacent to the putative S1 site indicated a second pyrrole ring, although the density was insufficient to allow its confident modelling. It should be noted, therefore, that the location shown for the S2 ring in figure 4.11 is presented with some caution. The lack of density in this area may be due to either (i) the breakdown of the complex, and therefore the crystal may in fact only be an ES complex, or (ii) the mobility of the S2 ring. The latter possibility is the more likely as the ES_2 complex has not been observed to be less stable than the ES complex for the D84E mutant. In addition, evidence from non denaturing gel electrophoresis suggested that the ES_2 complex is still intact in the crystal. It was the apparent mobility of the second substrate ring that led to the cryo-cooling of subsequent crystals in an attempt to improve resolution of the ring.

The structure indicated, as anticipated, that the hydrogen bonding to the ring S1 had also been lost and thus the glutamate was unable to provide

some of the interactions required by the incoming porphobilinogen molecule for ring coupling. The reduction of activity of the mutant to only 1% of the wild-type could now easily be explained. The glutamate side chain resided in an inappropriate position to support the positive charges of the developing carbocation or the methylene pyrrolenine of the incoming ring. These losses in hydrogen bonding, together with those lost to the terminal ring of the polypyrrole chain (in this case, ring C2) would result in the impediment of every stage of ring coupling that would, in the native enzyme, be catalysed by aspartate-84. Also, it may be possible that the glutamate side chain is not in an environment as hydrophobic as aspartate, and therefore could well be deprotonated. This would prevent glutamate-84 from serving as an acid to protonate the leaving NH_3.

4.2.3.6 Refinement of the Mutant Porphobilinogen Deaminase D84E ES_2 Complex Structure

Initial refinement was performed with cysteine-242 (dipyrromethane cofactor removed) and an alanine replacement at positions 84, 11, 131, 132, 149, 155, 176 and 232. The $2F_o$-F_c map indicated difference electron density derived from the clearly reduced cofactor at position 242, and from glutamate-84 and arginines-11, -131, -132, -149, -155, -176 and -232. The difference map also indicated density into which a third pyrrole ring could be comfortably located.

4.3 Conclusions

The aims of this chapter were to achieve the crystallisation, X-ray diffraction data collection and structure modelling of the mutant D84E enzyme and enzyme-intermediate complex. All of the aims were satisfactorily accomplished, with the exception of the confident modelling of the second substrate ring of the ES_2 complex. The mutant models provided valuable information in confirming the role of the catalytic residue aspartate-84, and provided a structural basis for the severely impaired activity of the mutant D84E enzyme. The preliminary model of the D84E ES_2 complex indicated that no conformational changes had yet taken place to accommodate the substrate rings, although it appeared likely that a change would have to occur for further substrate rings to be bound.

Chapter 5

Characterisation of the Apoenzyme of *E. coli* Wild-Type and Mutant Porphobilinogen Deaminase

5.1 Introduction

The apoenzyme of porphobilinogen deaminase is the form of the enzyme that lacks the dipyrromethane cofactor. The apoenzyme has been prepared using two distinct methods: either *via* the *hem B* strain of *E. coli* , which lacks the enzyme 5-aminolaevulinic acid dehydratase and therefore cannot produce porphobilinogen (Scott *et al.*, 1989), or by treating pure holoenzyme with dilute acid to cleave the dipyrromethane cofactor (Hart *et al.*, 1988). The lack of reaction when treating the purified apoenzyme with Ehrlich's reagent confirms the absence of cofactor in enzyme purified from both sources (Hart *et al.*, 1988; Scott *et al.*, 1989) and preliminary characterisation of the wild-type apoenzyme has been reported.

The apoenzyme is found to be sensitive to denaturation by 6M urea and heat treatment at 60°C (Scott *et al.*, 1989) and therefore is predicted to exist in a conformationally unstable state. As a consequence, apoenzyme isolated from the *hemB* strain is purified using essentially the same protocol for holoenzyme but omitting the heat treatment step. The stability of the porphobilinogen deaminase holoenzyme to both urea and heat treatment indicates that it is the presence of the dipyrromethane cofactor which confers stability allowing the formation of a stable, native tertiary structure. The three-dimensional crystal structure of the holoenzyme provides some understanding about the increased stability, as the side chains of the cofactor form a number of salt bridges and hydrogen bonds with the surrounding protein matrix (Louie *et al.*, 1992). The apoenzyme must therefore undergo a conformational change on binding the cofactor.

When subjected to electrophoresis under denaturing conditions, the apoenzyme is observed to have a mobility that appears to equal that of the holoenzyme. However, when analysed under non-denaturing conditions the apoenzyme displays no active bands that correspond to the same mobility of holoenzyme but, instead, contains a major protein band migrating slightly behind that of holoenzyme as well as a characteristic ladder of bands of decreasing electrophoretic mobility. Analysis of the ladder of bands demonstrates that they do contain porphobilinogen deaminase, but are not aggregates of the protein. The nature of the protein in these bands remains obscure (Scott *et al.*, 1989). When examined by urea polyacrylamide gel electrophoresis the ladder of bands is found to have been replaced by three

closely spaced bands of low mobility indicating that the apoenzyme has completely unfolded in the presence of urea.

The apoenzyme can be reconstituted to afford a holoenzyme with about 50% of the native catalytic activity by incubation with a three-fold molar excess of porphobilinogen at 4°C for 5-6 hours (Hart *et al.*, 1988; Scott *et al.*, 1989). Further incubation is not found to improve the recovery of activity. On analysis by non denaturing gel electrophoresis, incubation of apoenzyme with a three fold molar excess of porphobilinogen is seen to lead to a reduction in the ladder of bands, together with the appearance of new bands corresponding to holoenzyme and ES_2.

The apoenzyme has also been analysed by ^{13}C-NMR spectroscopy (Hart *et al.*, 1988; Scott *et al.*, 1989). Apoenzyme at pH 8 is found to exist in a conformationally mobile state similar to the semi-unfolded state of holoenzyme at pH 12. Moreover, apoenzyme reconstituted with porphobilinogen displays a ^{13}C-NMR spectrum containing broad peaks characteristic of native holoenzyme at pH 8. This further substantiates the possibility that the difference in stability between apoenzyme and holoenzyme is due to a change in conformation brought about by the presence of cofactor.

The apoenzyme reconstituted with porphobilinogen has been examined by anion-exchange using an f.p.l.c. system (Hart *et al.*, 1988). The elution profile shows the characteristic peaks for holoenzyme, ES, ES_2 and ES_3 as well as several smaller peaks which are not normally seen on adding substrate to deaminase. Reconstituted holoenzyme has also been found to be indistinguishable from native enzyme with regards to its u.v. spectrum, its reaction with Ehrlich's reagent and K_m for porphobilinogen. The apoenzyme can therefore be seen to catalyse the covalent binding of two porphobilinogen units to generate its own dipyrromethane cofactor, with no requirement for additional enzymes.

The manner in which the apoenzyme binds the two porphobilinogen rings is still one of contention. The mechanism may be similar to that of the binding of substrate rings to the cofactor, although an alternative mechanism would better explain the permanent attachment of the cofactor. Some clues towards the manner of cofactor binding have arisen as a result of substrate analogue studies with the apoenzyme (Scott *et al.*, 1989). The analogues,

aminomethylpyrrole (in which the acidic side chains are removed) and aminomethyldipyrromethane, give rise to the typically observed banding patterns when incubated with apoenzyme and examined by gel electrophoresis, but reconstitute to less than 5% activity of that seen with porphobilinogen. The studies therefore signify the importance of the acetate and propionate side chain for recognition, and suggest that the cofactor is made by binding porphobilinogen one molecule at a time rather than forming the dipyrromethane prior to attachment.

Other clues to the mechanism of cofactor assembly have come from the finding that D84A and D84N mutants that have no catalytic activity exist as enzyme-substrate complexes, suggesting that the apoenzyme may be able to interact with a preformed pyrrole system as well as with porphobilinogen. Central to the elucidation of cofactor assembly is the isolation of pure and reconstitutable apoenzyme for detailed studies with putative cofactor precursor molecules and inhibitors.

5.2 Results and Discussion

5.2.1 The Apoenzyme of Native *E. coli* Porphobilinogen Deaminase, as Synthesised Using the *hemB* Strain

5.2.1.1 Expression of the Apoenzyme of Native Porphobilinogen Deaminase

The porphobilinogen deaminase expression plasmid BM3 was constructed by ligation of a *Bam*HI-*Sal*I restriction fragment containing the *hemC* gene into the *Bam*HI-*Sal*I restriction sites of pUC18 (Mbgeje, 1990). The apoenzyme was purified from *hem B* derivatives of *E.coli* transformed with plasmid BM3, which were grown in the presence of haem. The *hemB* strain, is unable to synthesise porphobilinogen as it lacks the enzyme 5-aminolaevulinic acid dehydratase and therefore the porphobilinogen-derived cofactor would be expected to be absent in deaminase expressed in this strain. All DNA manipulations were carried out using standard techniques as described in Materials and Methods.

5.2.1.2 Purification of the Apoenzyme of Native Porphobilinogen Deaminase

The *hem B* derivative of *E.coli* transformed with plasmid BM3 was grown overnight in LB media containing ampicillin (100μg/ml) and haemin (5μg/ml) at 37°C. The presence of haemin was essential for growth due to the lack of the enzyme 5-aminolaevulinic acid dehydratase. The cells were harvested by centrifugation, resuspended in 100mM phosphate buffer pH 8.0 containing 13mM β-mercaptoethanol and broken by sonication.

When purifying native holoenzyme, the proceeding step would be that of heat treatment at 60°C for ten minutes. However, the instability of apoenzyme to heat at this temperature requires this step to be omitted. As a result, a valuable purification step is lost and additional steps were necessary to achieve the isolation of a protein that appeared homogeneous when analysed by denaturing polyacrylamide gel electrophoresis.

A number of affinity chromatography columns were therefore investigated for their ability to bind crude apoenzyme. Affinity chromatography columns are available in kits, which allow a number of different columns to be sampled for their specific protein binding capacities. Such columns have been employed before for the purification of porphobilinogen deaminase (Jones and Jordan, 1995). The Mimetic Orange 1 A6XL column was found to hold the highest affinity for apoenzyme, and allowed the purification of the protein to at least 90% homogeneity in a single step. The standard protocol steps for the purification of porphobilinogen deaminase, ammonium sulphate precipitations and anion-exchange chromatography, were therefore no longer required.

The sonicated cells of apoenzyme were centrifuged to remove cell debris and the supernatant was applied to a Mimetic Orange 1 A6XL column (2.5x15cm) equilibriated in 20mM Tris/HCl pH 7.5 containing 13mM β-mercaptoethanol. The protein was eluted using Tris buffer containing increasing concentrations of NaCl as described in the Materials and Methods. The fractions eluted from the column were examined by denaturing polyacrylamide gel electrophoresis, as shown in figure 5.1. The earlier fractions eluted from Tris/HCl buffer and Tris/HCl buffer containing 100mM and 250mM NaCl contained bands which corresponded to impurities. The protein fractions eluted from Tris/HCl buffer containing 500mM and 1M NaCl were found to contain only a band which migrated to the same distance as wild-type porphobilinogen deaminase. Therefore, the earlier washes of low salt concentration had allowed the elution of impurities, leaving the pure apoenzyme to elute from the higher salt concentration washes. All fractions were also assayed for activity as described in Materials and Methods. The porphobilinogen deaminase activity of the fractions corresponded to the presence of bands for the enzyme on the gel, and a graph of activity against fraction number is shown in figure 5.2.

Figure 5.1 Denaturing Polyacrylamide Gel of Fractions Eluted from Affinity Chromatography of the Apoenzyme of Porphobilinogen Deaminase

The lane containing the marker is indicated with a 'Mk'
Lane 1 contains the fractions collected whilst loading the enzyme.
Lanes 2 and 3 contain the fractions eluted with 20mM Tris/HCl pH8.0, 5mM β-mercaptoethanol.
Lanes 4 and 5 contain the fractions eluted with 20mM Tris/HCl pH8.0, 5mM β-mercaptoethanol and 100mM NaCl.
Lanes 6 and 7 contain the fractions eluted with 20mM Tris/HCl pH8.0, 5mM β-mercaptoethanol and 250mM NaCl.
Lanes 8 and 9 contain the fractions eluted with 20mM Tris/HCl pH8.0, 5mM β-mercaptoethanol and 500mM NaCl.
Lanes 10 and 11 contain the fractions eluted with 20mM Tris/HCl pH8.0, 5mM β-mercaptoethanol and 1M NaCl.

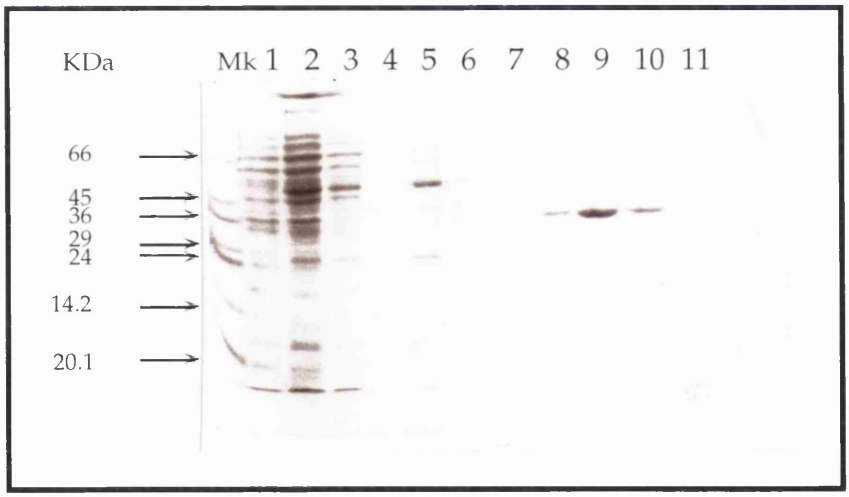

Figure 5.2 Activity of Fractions Eluted from Affinity Chromatography of the Apoenzyme of Porphobilinogen Deaminase using a Mimetic Orange A6XL Column

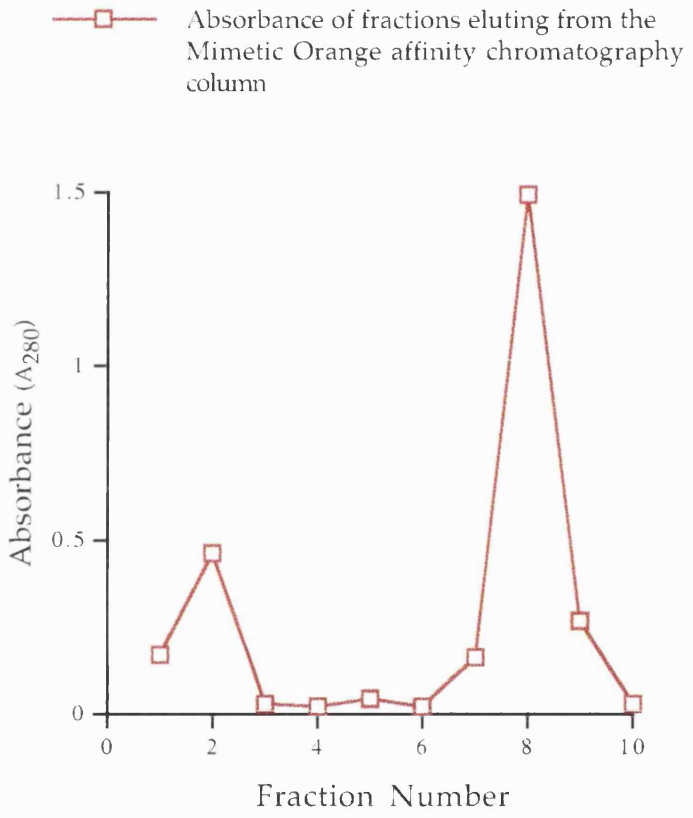

The gel and graph in figures 5.1 and 5.2 show that the fractions eluting in buffer containing 500mM NaCl and 1M Nacl (lanes 8, 9 and 10) contained protein bands which migrated to the same distance as the 36kDa standard on the molecular weight marker, and corresponded to the peak of deaminase activity (fractions 8, 9 and 10). The porphobilinogen deaminase containing fractions were then concentrated by ultrafiltration on a PM10 membrane and desalted *via* gel filtration into 1mM Tris/HCl buffer pH 7.5 containing 2mM dithiothreitol. The purified apoenzyme was then freeze-dried and stored at -20°C. Approximately 30mg of protein could be obtained per preparation from 2L media.

5.2.1.3 Reconstitution of Holoenzyme from Apoenzyme

5.2.1.3.1 Recovery of Activity from Apoenzyme - Preliminary Studies

The apoenzyme was preincubated with a two molar equivalent of porphobilinogen at 4°C for thirty minutes to reconstitute some of the activity of the holoenzyme. The preincubation was then assayed for activity as described in Materials and Methods, together with apoenzyme which had not been preincubated with substrate. The recovery of activity is shown in figure 5.3.

Figure 5.3 The Recovery of Activity from Apoenzyme, in the Presence and Absence of Preincubations with Porphobilinogen

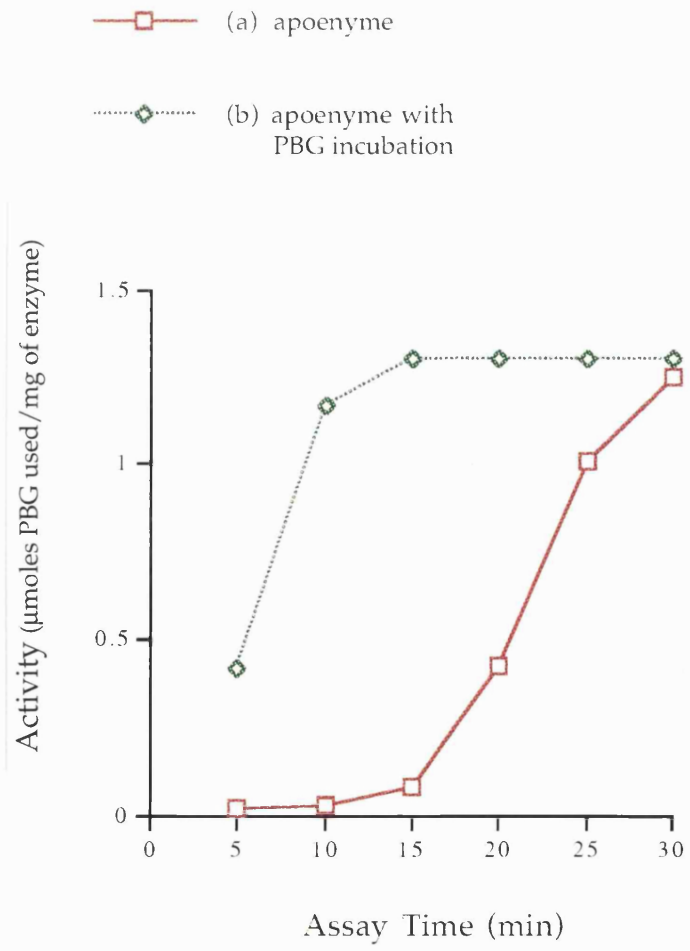

The graph in figure 5.3 shows that the apoenzyme which had been preincubated with a two molar equivalent of porphobilinogen (b) exhibited a linear increase in activity with time. The apoenzyme which had not been preincubated with substrate (a) exhibited first a lag phase of twenty minutes before showing a linear increase in activity.

The apoenzyme which had been preincubated with substrate was found to have recovered 12% of the activity of native holoenzyme as judged by determining the specific activity.

5.2.1.3.2 Recovery of Activity from Apoenzyme - Effect of Varying Time Length of Porphobilinogen Incubations

The apoenzyme was preincubated with a two molar equivalent of porphobilinogen at 4°C for different lengths of time up to thirty minutes. A graph showing the recovery of activity for the incubations is shown in figure 5.4.

The graph in figure 5.4 shows that the recovery of activity from apoenzyme increased in a linear fashion with time after a fifteen minute preincubation with a two molar equivalent of porphobilinogen at 4°C (d). The preincubation also appeared to be substrate concentration- and temperature-independant, as the gradient of activity increase was essentially the same for apoenzyme incubated with substrate at 4°C for twenty minutes (e), or at 37°C (during the assay) for twenty minutes (a). The trend for recovery of activity for apoenzyme was fairly consistent with each preparation, typically displaying a lag phase of between fifteen and twenty-five minutes for apoenzyme without substrate preincubation (a).

Figure 5.4 The Recovery of Activity from Apoenzyme, Preincubated with Porphobilinogen for Varying Lengths of Time

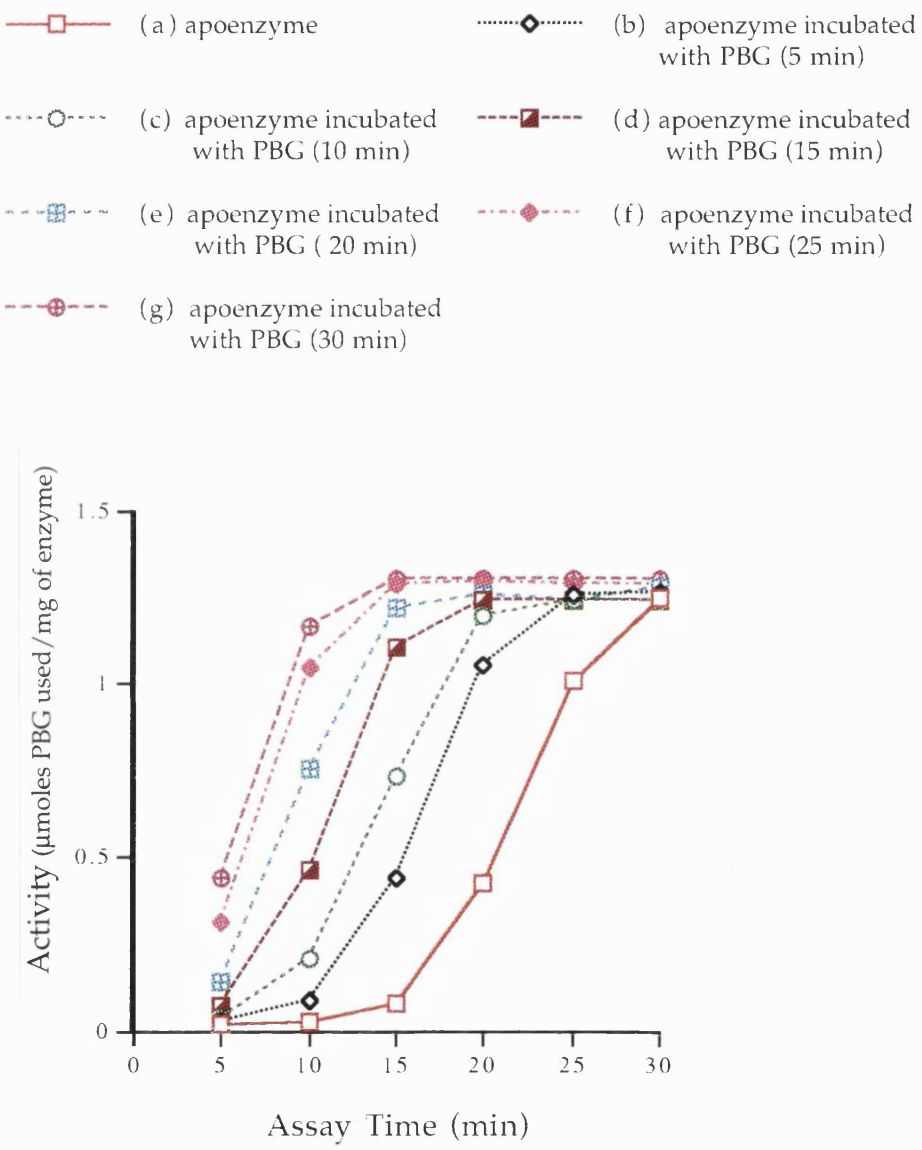

5.2.1.3.3 Recovery of Maximum Activity from Apoenzyme - Effect of Varying the Length of Porphobilinogen Incubations

Apoenzyme was incubated with a two molar equivalent of porphobilinogen at 37°C for up to three hours to recover maximum activity. The increase of activity with time is shown in figure 5.5.

Figure 5.5 The Maximum Recovery of Activity from Apoenzyme, Preincubated with Porphobilinogen for Up to Three Hours

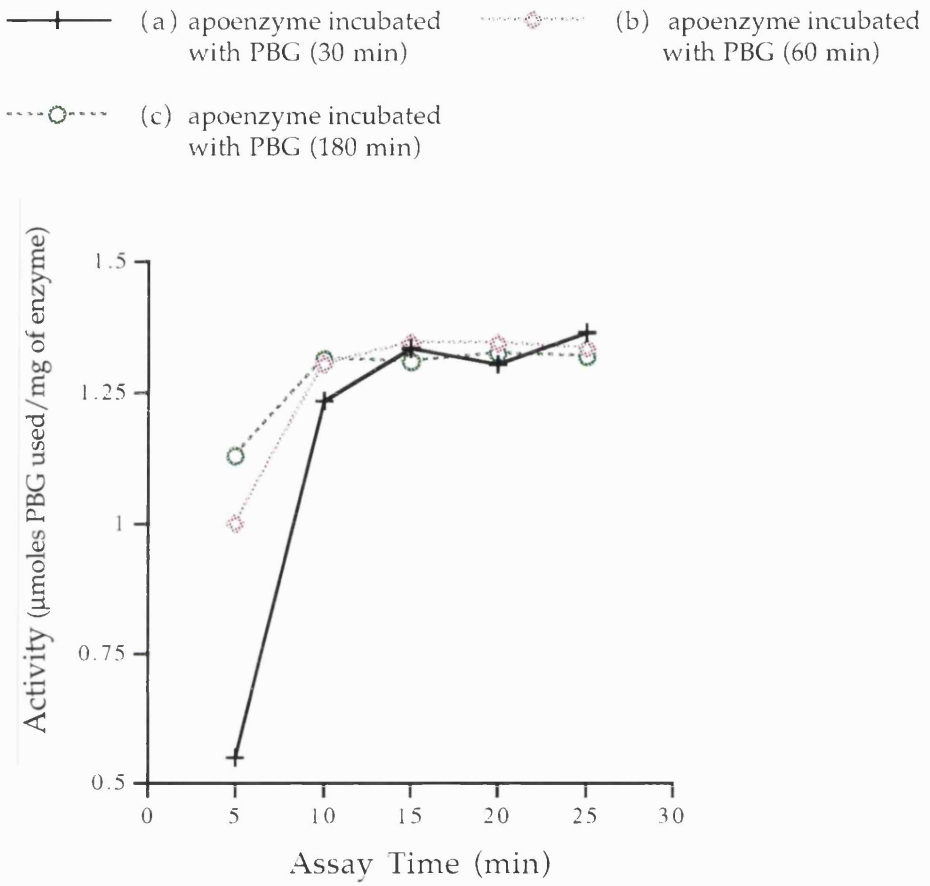

The graph in figure 5.5 shows that the activity recovered from apoenzyme increased with the length of substrate-incubation. The majority of the increase in activity occurred within one hour of incubation (b). After three hours (c), the apoenzyme had recovered 38% of the activity of holoenzyme, which is the typical maximum activity that can be recovered from apoenzyme using porphobilinogen incubation.

5.2.1.3.4 Visualisation of the Reconstitution of Holoenzyme from Apoenzyme By Polyacrylamide Gel Electrophoresis

Apoenzyme was incubated with a twenty molar excess of porphobilinogen at 37°C for 1 hour. The incubation was then subject to non

denaturing polyacrylamide gel electrophoresis for analysis, as shown in figure 5.6. For comparison, apoenzyme without substrate incubation and holoenzyme were also examined.

Figure 5.6 Non Denaturing Polyacrylamide Gel Showing the Reconstitution of Holoenzyme from Apoenzyme

Lane 1 contains wild-type apoenzyme.
Lane 2 contains substrate-incubated wild-type apoenzyme.
Lane 3 contains wild-type holoenzyme.

For clarity, the migrations of the apoenzyme and holoenzyme are marked in the figure.

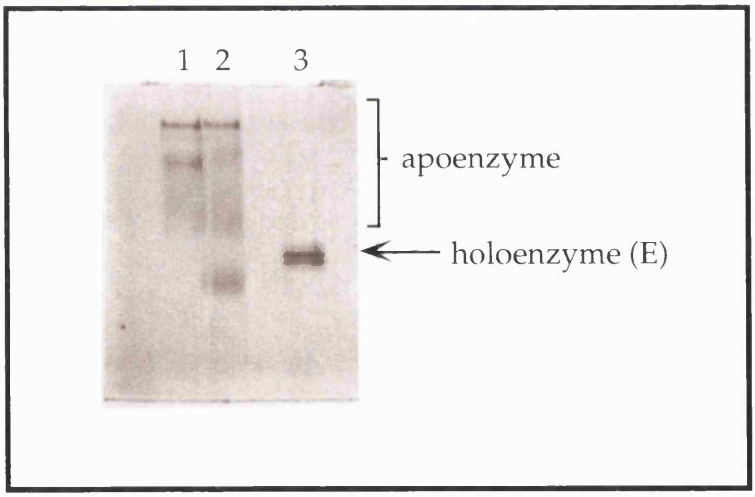

The gel in figure 5.6 shows that apoenzyme, without substrate incubation (lane 1), migrated as the characteristic ladder of bands. The apoenzyme which had been incubated with substrate (lane 2) also migrated as a ladder of bands, with an additional double band which migrated with a higher mobility than that of holoenzyme (lane 3). The non denaturing gel therefore indicated that, whilst some protein remained in the apoenzyme form, some had been reconstituted to form an enzyme-intermediate complex, most likely to be either ES, ES_2 or a mixture of both.

5.2.1.3.5 Recovery of Activity from Apoenzyme - Effect of Preincubation with Porphobilinogen in the Presence of Holoenzyme

The maximum activity recovered from preincubating apoenzyme with substrate was rarely above 50% of the specific activity of holoenzyme. A method was therefore devised to improve the recovery. It is certain that a minimum concentration of holoenzyme will always be present in all cells, and thus may act in some way to encourage the apoenzyme to reconstitute to the holoenzyme form in the presence of porphobilinogen.

Apoenzyme was therefore preincubated with a two molar equivalent of porphobilinogen in the presence of catalytic amounts (a one-fiftieth equivalent) of holoenzyme at 4°C for thirty minutes. The preincubation was assayed for activity. For comparison, four controls were also assayed: apoenzyme without preincubation; apoenzyme with the standard preincubation of a two molar equivalent of porphobilinogen at 4°C for thirty minutes; apoenzyme with a preincubation of a one-fiftieth equivalent of holoenzyme at 4°C for thirty minutes, in the absence of porphobilinogen; holoenzyme alone; a one-fiftieth equivalent of holoenzyme alone. The recovery of activity for all samples is shown in figure 5.7.

The graph in figure 5.7 shows that after five minutes of assay, the apoenzyme which had been preincubated with a two molar excess of porphobilinogen in the presence of a one-fiftieth equivalent of holoenzyme (d) was found to display 25% of the activity of holoenzyme, whereas apoenzyme with the standard preincubation of porphobilinogen alone (b) regained 5% of the activity of holoenzyme. Apoenzyme preincubated with a one-fiftieth equivalent of holoenzyme only (c) displayed a lag time of fifteen minutes before recovering activity with a linear increase. The graph shows that the small percentage of holoenzyme alone (e) has only a very slight gradient for activity increase, and therefore the raised rate of increased activity of the apoenzyme preincubated with both porphobilinogen and a one-fiftieth equivalent of holoenzyme (d) was unlikely to be due to the activity of holoenzyme alone, but the combined effect of substrate and holoenzyme preincubation with apoenzyme. Apoenzyme without preincubation failed to recover activity within twenty five minutes (a).

Figure 5.7 The Recovery of Activity from Apoenzyme with Various Preincubations, In the Presence and Absence of a One-Fiftieth Molar Equivalent of Holoenzyme

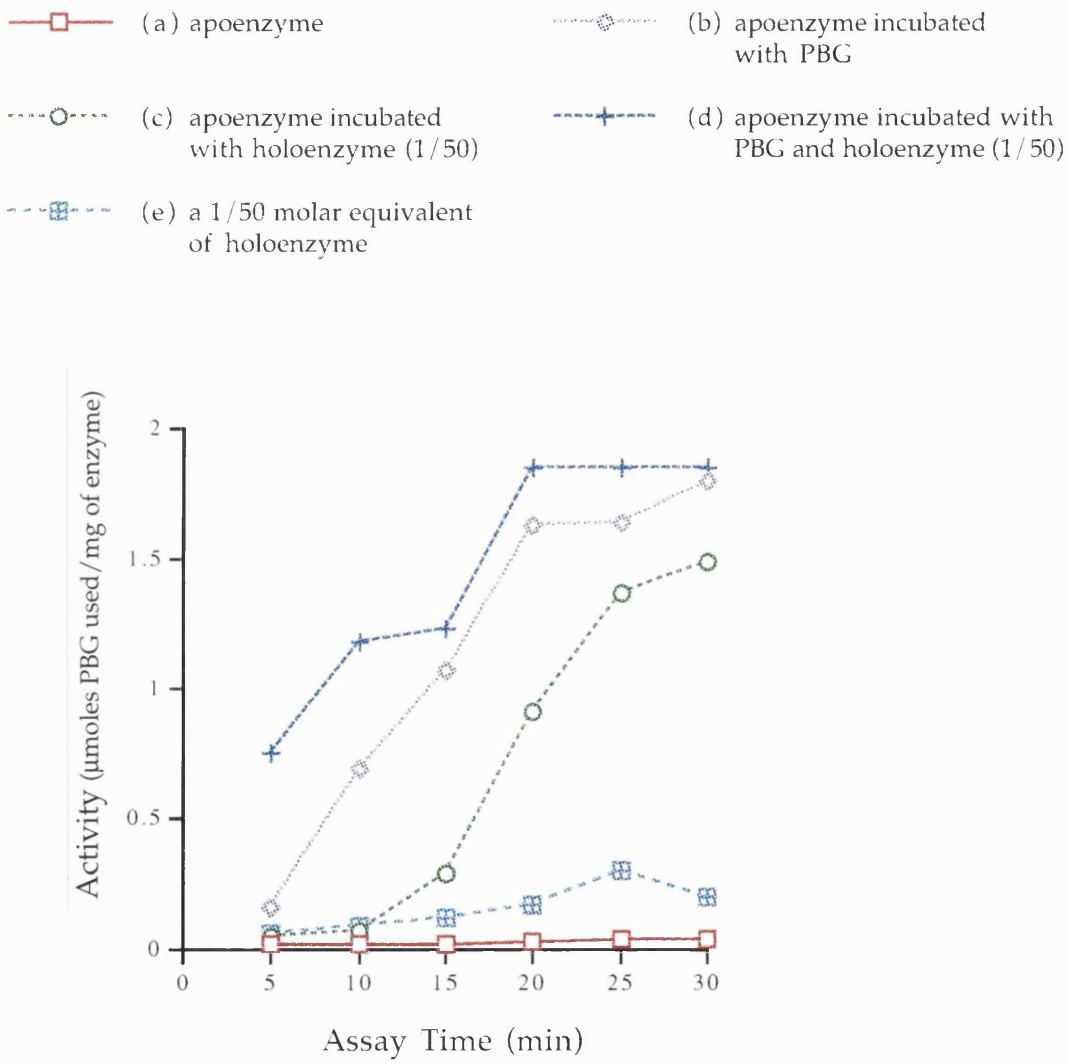

Thus, the presence of a small percentage of holoenzyme as a "catalyst" in the standard preincubation with substrate raised the rate at which the activity could be recovered.

5.2.1.3.6 Visualisation of the Reconstitution of Holoenzyme from Apoenzyme, in the Presence of a Small Molar Equivalent of Holoenzyme, by Polyacrylamide Gel Electrophoresis

Apoenzyme was mixed with a fifty molar excess of porphobilinogen in the presence and absence of a one-fiftieth molar equivalent of holoenzyme and immediately examined by non denaturing polyacrylamide gel electrophoresis, together with apoenzyme, holoenzyme, and a mixture of substrate and a one-fiftieth molar equivalent of holoenzyme for comparison. The non denaturing gel is shown in figure 5.8.

The gel in figure 5.8 shows that apoenzyme (lane 1) and holoenzyme (lane 4) migrated in a characteristic manner. The addition of substrate to apoenzyme (lane 2) gave rise to faint additional protein bands which migrated just beyond those of holoenzyme (lane 4). However, the addition of substrate to apoenzyme in the presence of a one-fiftieth molar equivalent of holoenzyme (lane 3) gave rise to strong bands which migrated just beyond those of holoenzyme (lane 4), in the manner of an ES_2 complex. The lane containing the addition of substrate to a one-fiftieth molar equivalent of holoenzyme (lane 5) only gave rise to extremely faint protein bands, indicating that the small equivalent of holoenzyme was not responsible for the extra bands observed in the presence of apoenzyme (lane 3).

5.2.1.3.7 Recovery of Activity from Apoenzyme - Effect of Reaction with Preuroporphyrinogen

The increased rate of the recovery of activity from apoenzyme and porphobilinogen in the presence of a one-fiftieth molar equivalent of holoenzyme suggested the possibility that preuroporphyrinogen, not porphobilinogen, may be serving as the preferred substrate for the reconstitution process. Preuroporphyrinogen was therefore generated from wild-type holoenzyme and porphobilinogen as described in Materials and Methods, and the holoenzyme was separated from the preuroporphyrinogen by filtration. A ten molar equivalent of preuroporphyrinogen was immediately added to the apoenzyme, and left to incubate for up to thirty minutes. For comparison, apoenzyme was also incubated with a ten molar equivalent of porphobilinogen, in the presence and absence of a one-fiftieth

Figure 5.8 Non Denaturing Polyacrylamide Gel Showing the Effect of a One-Fiftieth Molar Equivalent of Holoenzyme on the Reconstitution of Holoenzyme from Apoenzyme

Lane 1 contains wild-type apoenzyme.
Lane 2 contains wild-type apoenzyme mixed with substrate.
Lane 3 contains wild-type apoenzyme mixed with substrate in the presence of a one-fiftieth molar equivalent of holoenzyme.
Lane 4 contains wild-type holoenzyme.
Lane 5 contains a one-fiftieth molar equivalent of holoenzyme mixed with substrate.

For clarity, the migrations of the apoenzyme and holoenzyme are marked in the figure.

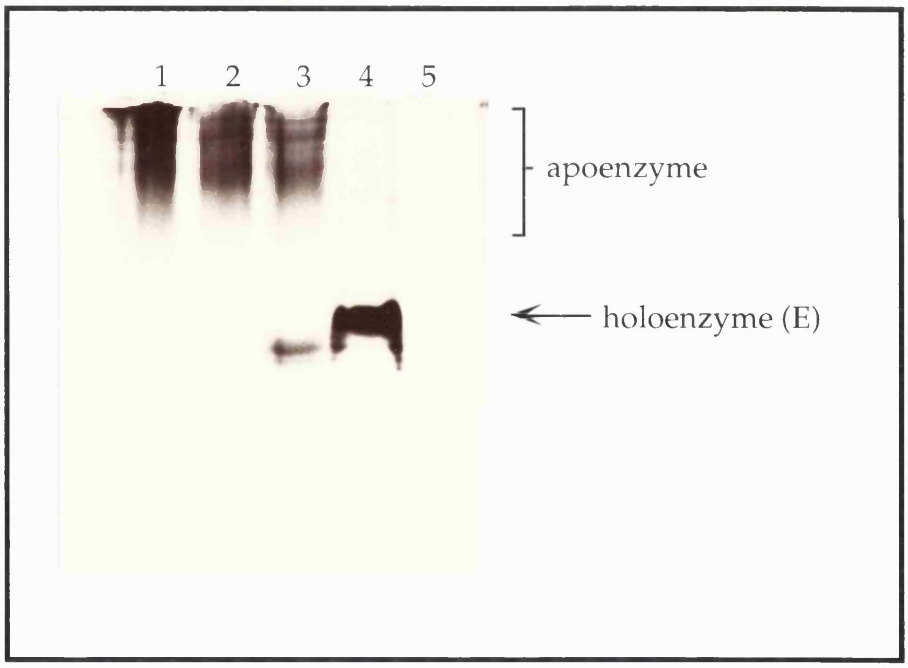

molar equivalent of holoenzyme. Preuroporphyrinogen, and a mixture of a one-fiftieth molar equivalent of holoenzyme and apoenzyme were also incubated as controls. Aliquots were removed at time intervals and assayed for recovery of activity, as shown in figure 5.9.

Figure 5.9 The Recovery of Activity from Apoenzyme with Various Preincubations, in Particular with Preuroporphyrinogen

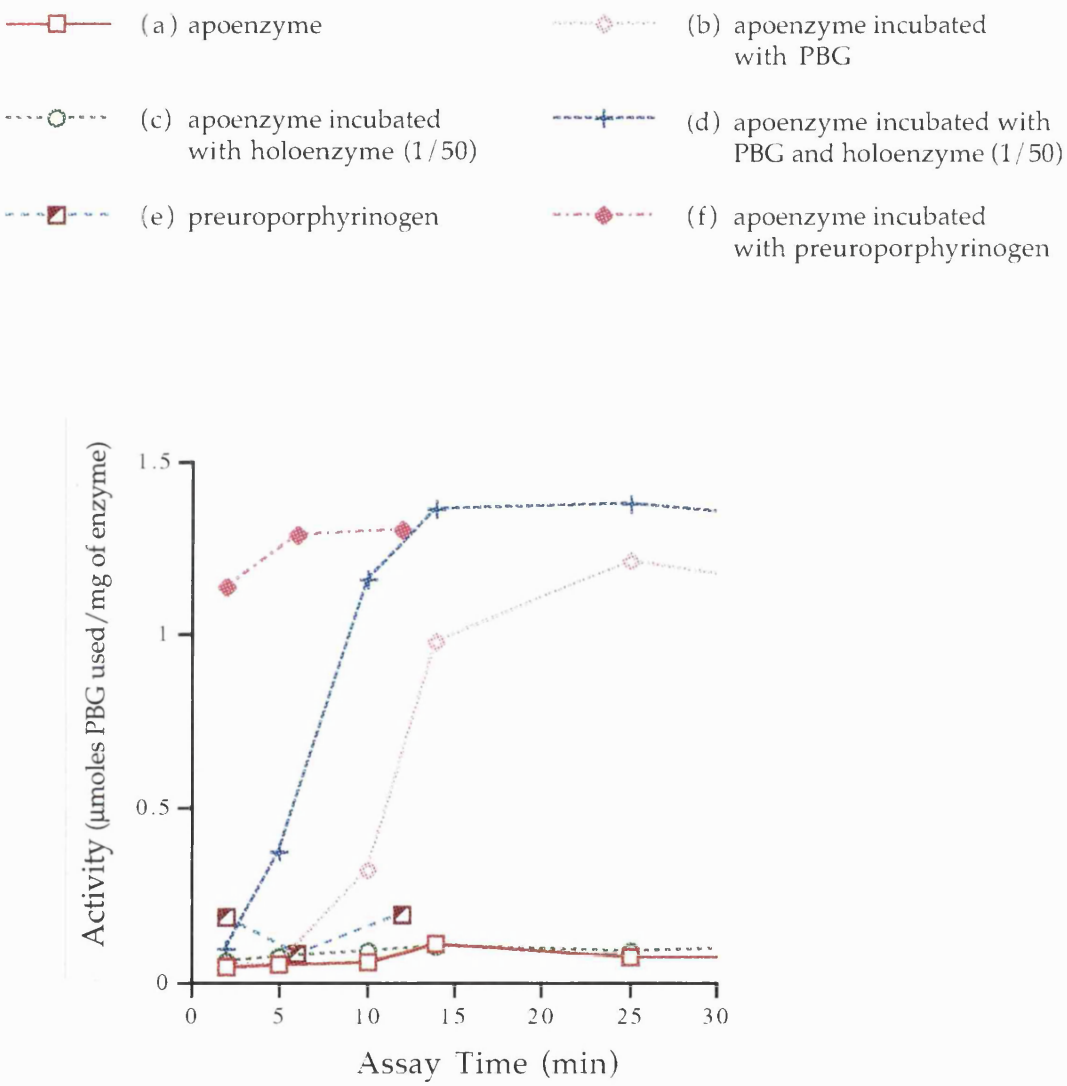

The graph in figure 5.9 shows that apoenzyme required a ten minute preincubation with porphobilinogen before activity could increase in a linear fashion with time (b). The addition of a one-fiftieth molar equivalent of holoenzyme to the mixture results in an increased recovery of activity that displays no lag phase (d). The addition of preuroporphyrinogen to the apoenzyme results in a greatly increased recovery of activity, that also displays no lag phase (f) . The graph for the addition of preuroporphyrinogen to the apoenzyme barely changes with time (e), and it is likely that all the preuroporphyrinogen will have cyclised within around five minutes.

The results strongly suggests that preuroporphyrinogen is the preferred substrate for apoenzyme to reconstitute the holoenzyme.

5.2.1.3.8 Visualisation of Reconstitution of Holoenzyme from Apoenzyme, in the Presence of Preuroporphyrinogen, by Polyacrylamide Gel Electrophoresis

Apoenzyme was mixed with a ten molar excess of pre-uroporphyrinogen and examined immediately by non-denaturing gel electrophoresis. For comparison, apoenzyme was also mixed with a ten molar excess of porphobilinogen and electrophoresed, together with apoenzyme and holoenzyme. The gel is shown in figure 5.10.

The gel in figure 5.10 shows that apoenzyme (lane 2) and holoenzyme (lane 1) migrated in a characteristic manner. Apoenzyme which had been mixed with porphobilinogen (lane 4) migrated similarly to apoenzyme in the absence of porphobilinogen (lane 2). Apoenzyme which had been mixed with preuroporphyrinogen (lane 3) migrated as a ladder of bands with additional bands which migrated with higher mobility than those of holoenzyme, in the manner of an ES_2 complex. The results appear to confirm the preference for preuroporphyrinogen as a substrate for apoenzyme. In the absence of porphobilinogen, the reaction of apoenzyme with preuroporphyrinogen accumulates at the ES_2 stage and is not carried further on to ES_3 or E under the conditions used. This suggests that the apoenzyme is binding intact preuroporphyrinogen, to produce a stable ES_2 complex.

Figure 5.10 Non-Denaturing Polyacrylamide Gel Showing the Effect of Preuroporphyrinogen on the Reconstitution of Holoenzyme from Apoenzyme

Lane 1 contains the wild-type holoenzyme.
Lane 2 contains wild-type apoenzyme.
Lane 3 contains wild-type apoenzyme mixed with preuroporphyrinogen.
Lane 4 contains wild-type apoenzyme mixed with porphobilinogen.

For clarity, the migrations of the apoenzyme and holoenzyme are marked in the figure.

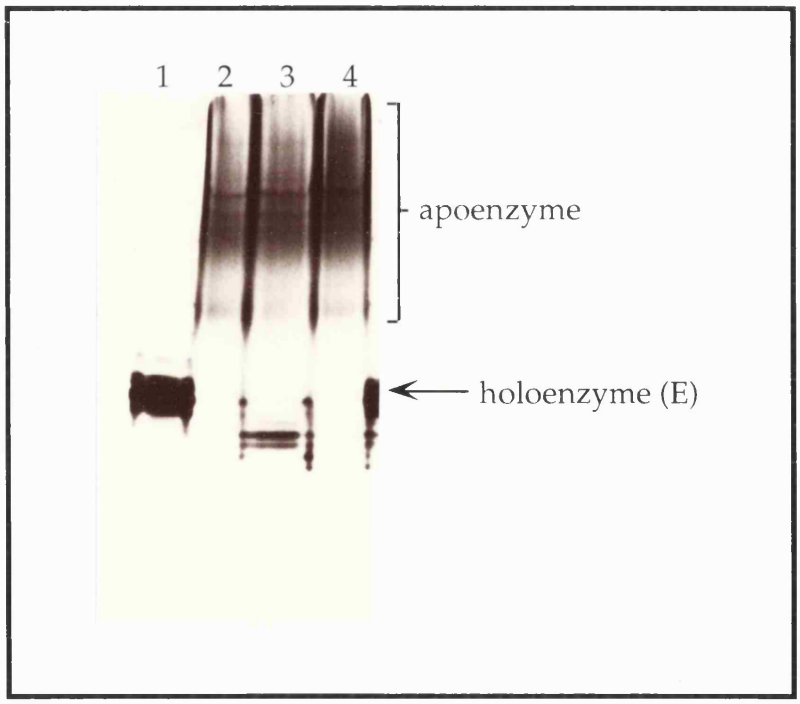

Apoenzyme was mixed with a ten molar excess of pre-uroporphyrinogen, heat treated at 60°C for ten minutes, cooled and examined immediately by non-denaturing gel electrophoresis. A sample of apoenzyme was also mixed with a ten molar excess of preuroporphyrinogen and not subjected to heat treatment. For further comparison, apoenzyme and holoenzyme were also examined before and after a similar heat treatment. The gel from these experiments is shown in figure 5.11.

Figure 5.11 Non-Denaturing Polyacrylamide Gel Showing the Effect of Heat-Treating an Incubation of Preuroporphyrinogen and Apoenzyme

Lane 1 contains the wild-type apoenzyme.
Lane 2 contains heat treated wild-type apoenzyme.
Lane 3 contains wild-type apoenzyme mixed with preuroporphyrinogen.
Lane 4 contains wild-type apoenzyme mixed with preuroporphyrinogen and heat treated.
Lane 5 contains wild-type holoenzyme.
Lane 6 contains heat treated wild-type holoenzyme.

For clarity, the migrations of the apoenzyme and holoenzyme are marked in the figure.

The gel in figure 5.11 shows that apoenzyme (lane 1) and holoenzyme (lane 5) migrated in a characteristic manner. On heat treatment, over half of the ladder of bands observed for apoenzyme were lost (lane 2). The heat treatment of holoenzyme, however, did not appear to affect the typical double band profile (lane 6). Apoenzyme which had been mixed with preuroporphyrinogen (lane 3) migrated as a ladder of bands with additional bands which migrated beyond those of holoenzyme (lane 5). The heated mixture of apoenzyme and preuroporphyrinogen (lane 4) showed that the

additional bands now migrated to the same distance and beyond those of holoenzyme (lane 5). Again, over half of the ladder of bands was also lost. The results indicated that the heat treatment, which is known to break down wild-type enzyme intermediate complexes (Warren and Jordan, 1988), had regenerated the free holoenzyme from ES_2 complex reconstituted from apoenzyme and preuroporphyrinogen. This provided additional evidence that the wild-type holoenzyme can be reconstituted from apoenzyme and preuroporphyrinogen. Whilst porphobilinogen can certainly act as a substrate for the apoenzyme and can regenerate the cofactor, it may play a relatively minor role *in vivo*.

The theory of reconstitution of holoenzyme by the addition of preuroporphyrinogen to apoenzyme was proposed during the last stages of the research. Therefore, the majority of results presented in the thesis were carried out on the basis of porphobilinogen serving as the natural ligand precursor for the cofactor assembly by the apoenzyme. The proceeding results all refer to reconstitution *via* the addition of porphobilinogen, and refer to porphobilinogen as the substrate. This may now infer that the experiments were not carried out under optimal conditions for cofactor assembly. However, it still remains that porphobilinogen does serve as a substrate for cofactor , and the lag phase observed in the reconstitution is likely to represent the time taken for preuroporphyrinogen to have been formed from the addition of porphobilinogen to apoenzyme. All proceeding experiments are therefore interpreted comparatively to the standard reconstitution from porphobilinogen and apoenzyme, and thus all conclusions are still regarded as valid.

5.2.1.3.9 Recovery of Activity from Apoenzyme in the Presence and Absence of Reducing Agents

After each purification, the final pure apoenzyme was desalted into 1mM Tris/HCl buffer pH 8.0 containing 2mM dithiothreitol. All standard assays for activity were carried out on protein resuspended in 100mM phosphate buffer containing 13mM β-mercaptoethanol. However, for a number of further experiments, apoenzyme was required in the absence of reducing agents, and therefore the ability of the apoenzyme to reconstitute holoenzyme in the absence of reducing agents was monitored.

Solid apoenzyme (~5mg) was resuspended in 20mM Tris/HCl buffer pH 8.0 and passed through a gel filtration into the same buffer, to remove the small dithiothreitol content from the protein. The apoenzyme was then assayed for activity in the presence and absence of the standard preincubation of a two molar equivalent of porphobilinogen at 37°C for two hours. For comparison, apoenzyme was assayed under the same conditions in the absence of 13mM β-mercaptoethanol present in all buffers. The recovery of activity for all samples is shown in figure 5.12.

Figure 5.12 The Recovery of Activity from Apoenzyme in the Presence and Absence of Reducing Agents

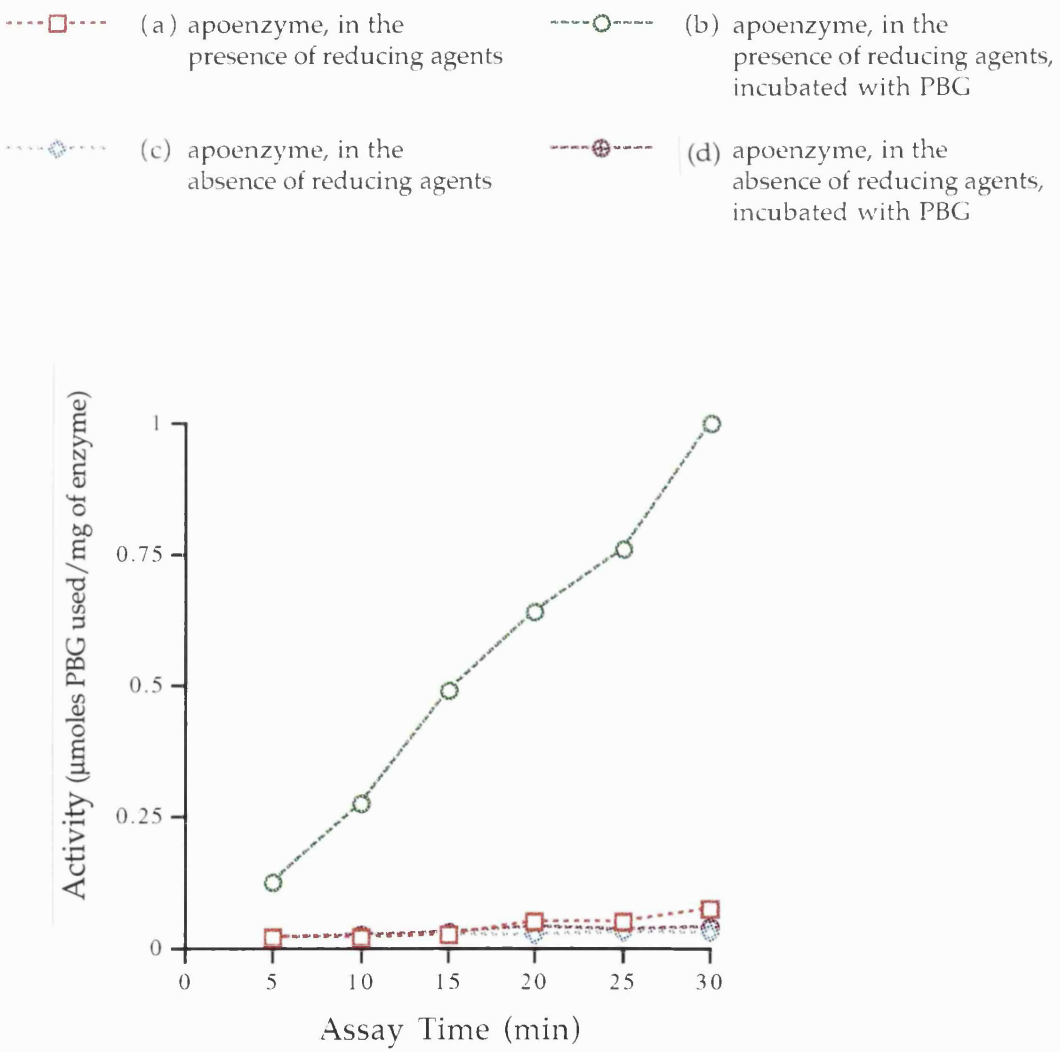

The graph in figure 5.12 shows that apoenzyme appeared to be inactive in the absence of reducing agents (c and d).

Longer preincubations of apoenzyme with substrate at 37°C for four hours were subsequently assayed. Apoenzyme in the absence of reducing agents was eventually able to recover a maximum activity of 25% of that of apoenzyme in the presence of reducing agents.

5.2.1.3.10 Activity of Holoenzyme in the Presence and Absence of Reducing Agents

To determine the nature of the drop in activity of apoenzyme in the absence of reducing agents, the holoenzyme was also assayed for activity in the absence of β-mercaptoethanol. Dithiothreitol was removed from the protein in the same manner as for apoenzyme using a gel filtration column. The activity of holoenzyme, in the presence and absence of reducing agents, is shown in figure 5.13.

The graph in figure 5.13 shows that the activity of holoenzyme appeared to be unchanged in the presence (b) or absence (a) of reducing agents, whilst the ability of apoenzyme to regenerate holoenzyme was significantly reduced in the absence of reducing agent. The increased susceptibility of apoenzyme to oxidation in the absence of reducing agents is likely to be due to the considerably exposed position of the key residue cysteine-242, to which the cofactor is bound. Oxidation of this residue may impede the chemistry required to covalently bind the cofactor. In the holoenzyme, the thiol residue is protected by the bound cofactor, and any loss of activity that may be observed for the holoenzyme is probably a result of oxidation of the dipyyromethane.

Figure 5.13 The Activity of Holoenzyme in the Presence and Absence of Reducing Agents

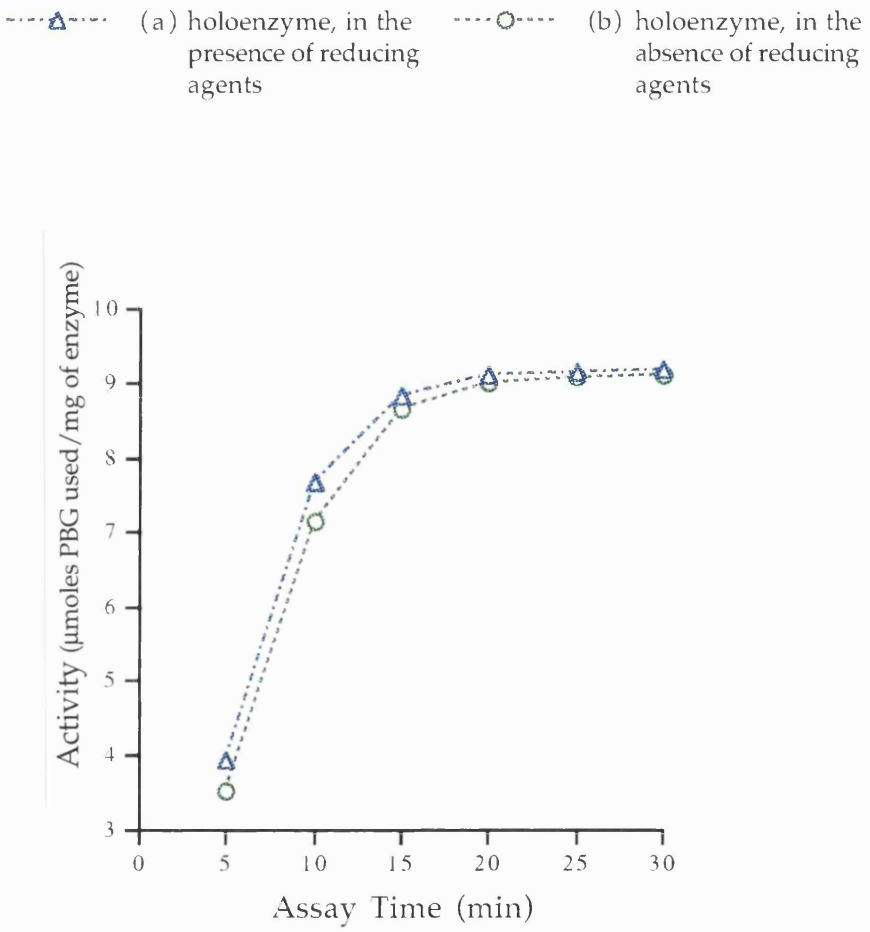

5.2.2 The Unstable Nature of Native Porphobilinogen Deaminase Apoenzyme

5.2.2.1 Susceptibility of Apoenzyme to Heat Treatment

5.2.2.1.1 Recovery of Activity from Apoenzyme - Effect of Heat Treatment

Apoenzyme is known to be unstable to heat treatment at 60°C, whereas holoenzyme is found to maintain its integrity. The stability upon heat treatment of apoenzyme, holoenzyme and holoenzyme reconstituted from apoenzyme was therefore monitored for comparison. (It was noted that in a crude extract the apoenzyme form of the mutant D84N was able to withstand heat treatment to some degree (Chapter 3, section 3.2.4.5). However, all studies on wild-type apoenzyme have been carried out on pure enzyme, for which there is less heat tolerance.)

Various incubations of apoenzyme were prepared to assay for activity after heat treatment at 60°C. All preincubations with substrate were carried out with the standard two molar equivalent of porphobilinogen at 37°C for an extended time of one hour. The incubations assayed for activity were as follows: apoenzyme preincubated with substrate; heat treated apoenzyme (no preincubations); apoenzyme preincubated with substrate and then heat treated; apoenzyme heat treated and then preincubated with substrate; holoenzyme; heat treated holoenzyme. The recovery of activity of all samples is shown in figure 5.14.

The graph in figure 5.14 shows that apoenzyme was found to be unstable to heat (b), and in the absence of a subsequent preincubation with substrate was not found to recover activity within thirty minutes of assay. However, a preincubation with substrate following heat treatment (e) did allow 25% of the normal activity of unheated substrate-preincubated apoenzyme (a) to be recovered. Heat treated apoenzyme which had been preincubated with substrate first (d) was found to remain as active as substrate-preincubated apoenzyme which had not been heat treated (c). Holoenzyme was unaffected by heat treatment (f and g).

Figure 5.14 The Recovery of Activity from Apoenzyme After Heat Treatment

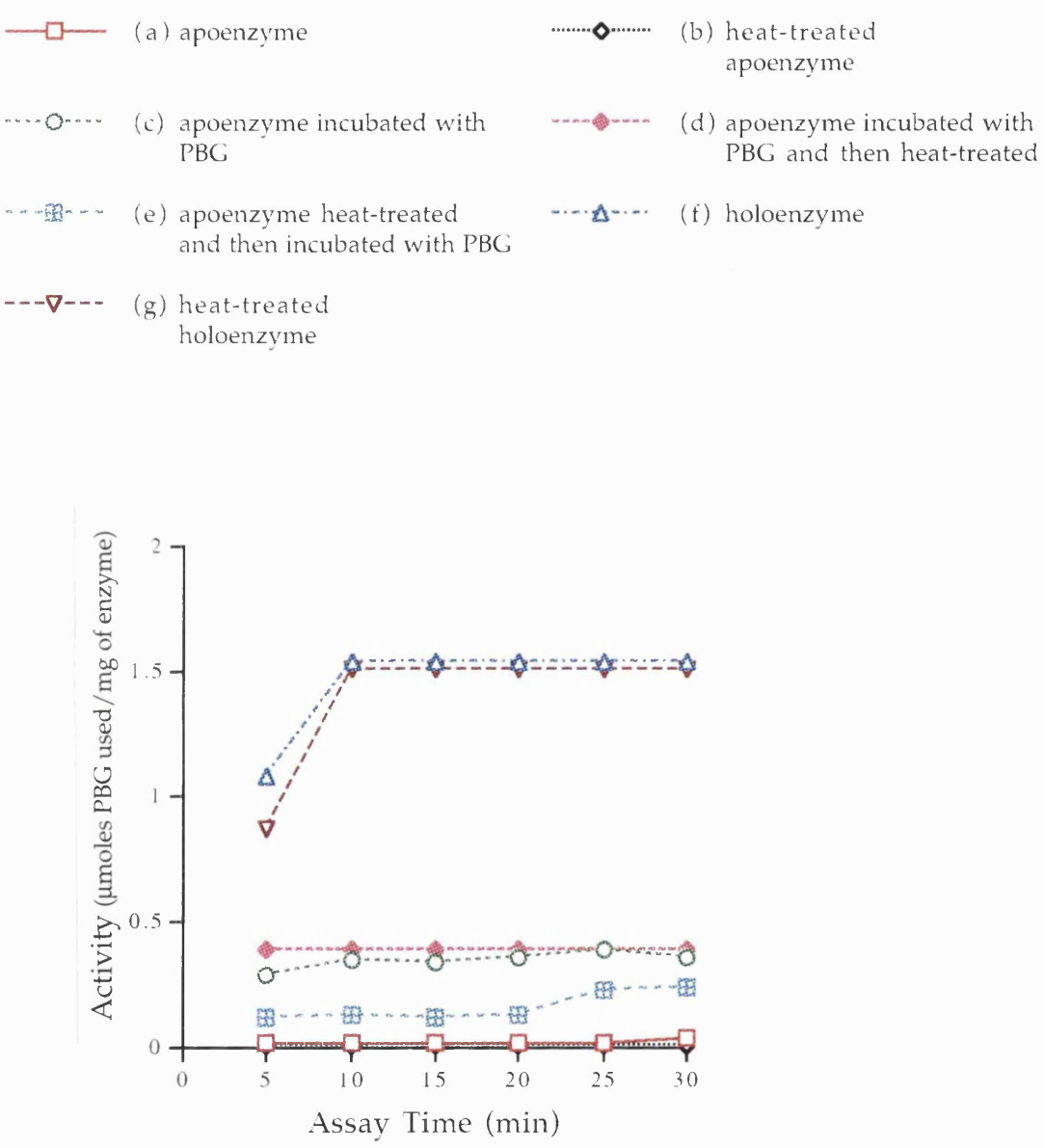

The percentage of apoenzyme which had reconstituted holoenzyme was therefore found to be as stable to heat treatment as native holoenzyme. Apoenzyme alone is found to be unstable to heat treatment, although some activity could be regained with an extended preincubation with substrate. The results supported the prediction of a less folded structure for the protein in the absence of cofactor (this is confirmed in Chapter 6).

5.2.2.1.2 Visualisation of the Reconstitution of Holoenzyme from Apoenzyme and the Effect of Heat Treatment, by Polyacrylamide Gel Electrophoresis

The susceptibility of apoenzyme to heat treatment was also analysed by non denaturing polyacrylamide gel electrophoresis. Apoenzyme alone and apoenzyme which had been preincubated with a fifty molar excess of porphobilinogen at 37°C for one hour were subjected to heat treatment at 60°C for ten minutes. Both samples, together with their unheated counterparts, were analysed on a non denaturing gel. For comparison, holoenzyme was also subject to the same conditions and analysed. The results of these assays were visualised by non denaturing polyacrylamide gel electrophoresis, as shown in figure 5.15.

The gel in figure 5.15 shows that the characteristic ladder of bands of apoenzyme (lane 5) was greatly reduced after heat treatment (lane 6). On preincubation with substrate (lane 7), the apoenzyme displayed the typical profile of a ladder of bands with additional bands migrating to the same distance and further than the double band of holoenzyme (lane 1). After heat treatment, the substrate-preincubated apoenzyme (lane 8) maintained the additional bands although the majority of the ladder was lost. Free holoenzyme (lane 1) displayed the typical double band profile, with additional bands migrating further appearing after incubation with substrate (lane 3). Both samples of holoenzyme appeared to be unaffected by heat treatment (lanes 2 and 4).

The results again confirmed that apoenzyme was unstable to heat treatment at 60°C. However, the banding pattern on the non denaturing gel clearly showed that apoenzyme which has reconstituted holoenzyme or enzyme-intermediate complexes remained stable to heat at this temperature, whilst any apoenzyme which did not reconstitute was lost. Thus holoenzyme is greatly stabilised by the presence of the cofactor.

Figure 5.15 Non-Denaturing Polyacrylamide Gel Showing the Susceptibilty of Apoenzyme to Heat Treatment

Lane 1 contains the wild-type holoenzyme.
Lane 2 contains heat treated wild-type holoenzyme.
Lane 3 contains wild-type holoenzyme, incubated with porphobilinogen.
Lane 4 contains wild-type holoenzyme, incubated with porphobilinogen and then heat-treated.

Lane 5 contains wild-type apoenzyme.
Lane 6 contains heat treated wild-type apoenzyme.
Lane 7 contains wild-type apoenzyme, incubated with porphobilinogen.
Lane 8 contains wild-type apoenzyme, incubated with porphobilinogen and then heat-treated.

For clarity, the migrations of the apoenzyme and holoenzyme are marked in the figure.

5.2.2.2 Susceptibility of Apoenzyme to Proteolytic Digestion

5.2.2.2.1 Visualisation of the Reconstitution of Holoenzyme from Apoenzyme and the Effect of Proteolytic Digestion, by Polyacrylamide Gel Electrophoresis

The apparent instability of apoenzyme to heat treatment suggests that it will also have an increased susceptibility to proteolytic digestion. Trypsin, a proteolytic enzyme which cleaves on the carboxyl side of arginine and lysine residues, is likely to have access to more residues in an unfolded structure than in a folded one. The susceptibility to trypsin digestion of apoenzyme, holoenzyme and holoenzyme reconstituted from apoenzyme was therefore monitored. Trypsin has previously been found to cleave the holoenzyme rapidly at lysine 64 in the sequence FVKELE.

Apoenzyme alone and apoenzyme which had been preincubated with a fifty molar excess of porphobilinogen at 37°C for one hour were subjected to trypsin digestion (1mg/ml) at 37°C for thirty minutes. Both samples, together with their undigested counterparts, were analysed by both denaturing and non denaturing gel electrophoresis. For comparison, holoenzyme was also subjected to the same conditions and analysed. The results are shown in figures 5.16 and 5.17.

The gel in figure 5.16 shows that the apoenzyme (lane 7), which in this case was not entirely pure, was seen as a band which migrated the same distance as the 36kDa standard on the molecular mass marker. On trypsin digestion (lane 8), the band was completely lost and replaced by two major bands, migrating to the same distance as the 24kDa and 12kDa standards on the molecular mass marker (representing a cleavage between arg-131 and arg-132). Further bands may have been present at molecular weights below 12kDa. Apoenzyme which had been substrate-preincubated and then subjected to trypsin digestion (lane 10), was seen to maintain the 36 KD band, with additional bands observed at 24kDa and 12kDa, and multiple bands between 30-36kDa and below 12kDa.

Holoenzyme which had not been subjected to digestion ran as a single band which migrated to the same distance as the 36kDa standard on the

Figure 5.16 Denaturing Polyacrylamide Gel Showing the Susceptibility of Holoenzyme and Apoenzyme to Trypsin Digestion

The lanes containing the marker are indicated with 'Mk'
Lane 1 contains the wild-type holoenzyme
Lane 2 contains trypsin-digested wild-type holoenzyme
Lane 3 contains wild-type holoenzyme, incubated with porphobilinogen
Lane 4 contains wild-type holoenzyme, incubated with porphobilinogen and then trypsin-digested

Lane 5 contains wild-type apoenzyme
Lane 6 contains trypsin-digested wild-type apoenzyme
Lane 7 contains wild-type apoenzyme, incubated with porphobilinogen
Lane 8 contains wild-type apoenzyme, incubated with porphobilinogen and then trypsin-digested

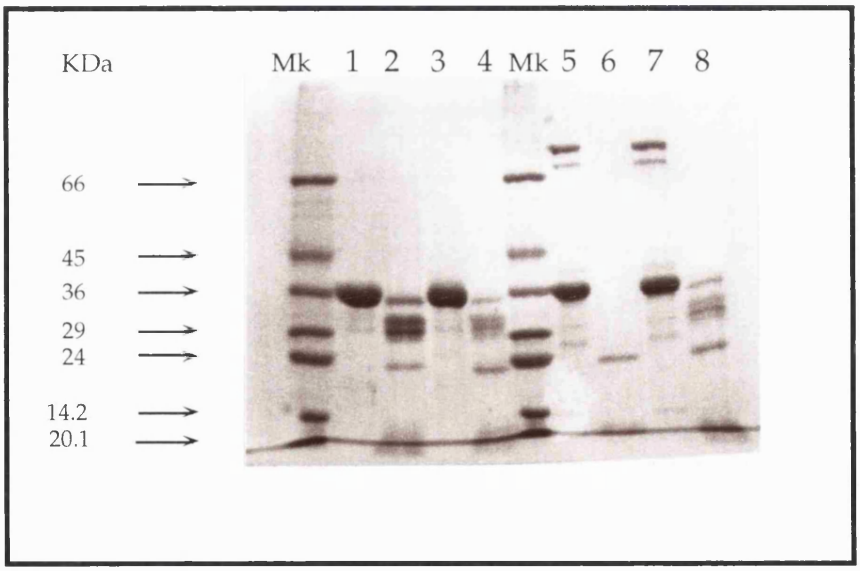

molecular weight marker for both the free enzyme (lane 2) and substrate-preincubated enzyme (lane 4). Both samples behaved similarly upon trypsin digestion (lanes 3 and 5), displaying the same banding pattern as for digested substrate-preincubated apoenzyme (lane 10).

The free apoenzyme is therefore unable to maintain the tertiary structure upon trypsin digestion, in contrast to holoenzyme. The

apoenzyme has clearly been digested to numerous low molecular mass fragments. However, reconstituted apoenzyme is seen to display an identical pattern of bands to that of holoenzyme and thus must be adopting a more tightly folded native conformation.

Figure 5.17 Non Denaturing Polyacrylamide Gel Showing the Susceptibility of Apoenzyme to Trypsin Digestion

Lane 1 contains the wild-type holoenzyme.
Lane 2 contains trypsin-digested wild-type holoenzyme.
Lane 3 contains wild-type holoenzyme, incubated with porphobilinogen .
Lane 4 contains wild-type holoenzyme, incubated with porphobilinogen and then trypsin-digested.

Lane 5 contains wild-type apoenzyme.
Lane 6 contains trypsin-digested wild-type apoenzyme.
Lane 7 contains wild-type apoenzyme, incubated with porphobilinogen.
Lane 8 contains wild-type apoenzyme, incubated with porphobilinogen and then trypsin-digested.

For clarity, the migrations of the apoenzyme and holoenzyme are marked in the figure.

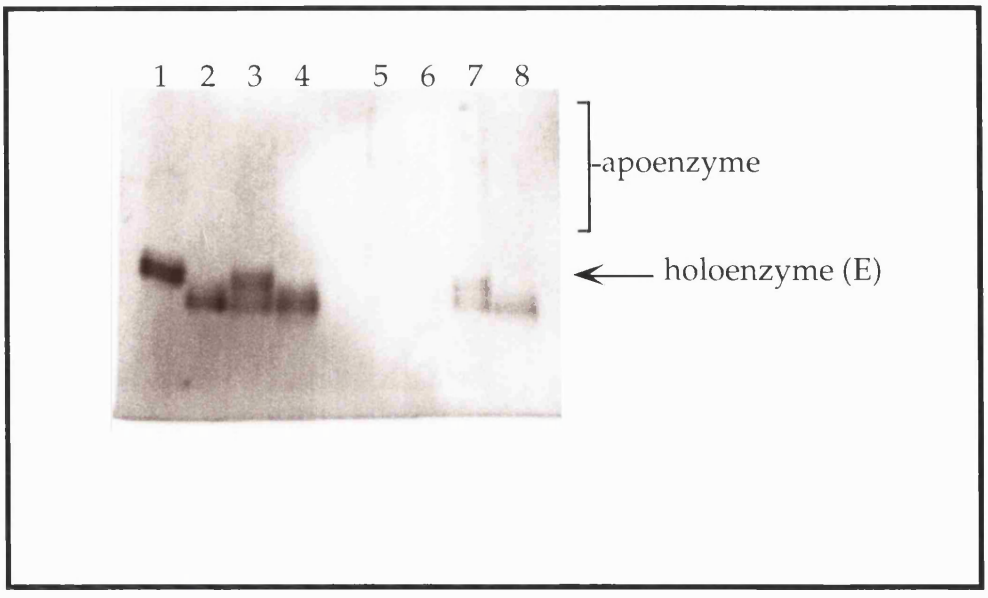

The gel in figure 5.17 shows that the holoenzyme, upon trypsin digestion (lane 2), ran as a double band migrating further than that of untreated holoenzyme. Substrate-preincubated holoenzyme (lane 3)migrated as multiple bands migrating to the same distance and beyond that of untreated holoenzyme (lane 1), although on trypsin digestion (lane 4) only the bands migrating beyond untreated holoenzyme were observed. The characteristic ladder of bands of apoenzyme (lane 5) were lost on trypsin digestion for apoenzyme (lane 6). Substrate-preincubated apoenzyme (lane 7) gave rise to a typical profile of a ladder with additional bands migrating further than those of free holoenzyme. On trypsin digestion, the ladder of substrate-preincubated apoenzyme was lost (lane 8) giving rise to a banding pattern similar to that of trypsin-digested holoenzyme.

The migration of the holoenzyme after trypsin digestion has been previously observed (Warren , 1988). The migration is similar to that of an enzyme-intermediate ES_2 complex and results from the loss of a 6kDa fragment from the N-terminus of the protein, due to a cleavage after lysine-64. The free apoenzyme appears to have broken down on trypsin digestion, although apoenzyme which has reconstituted the holoenzyme is seen to behave as trypsin digested holoenzyme. The results again confirm the less folded nature of apoenzyme in comparison to holoenzyme.

5.2.2.3 Molecular Sizing of Apoenzyme and Holoenzyme

The technique of dynamic light scattering allows the molecular size of an enzyme to be estimated. As the unstable nature of apoenzyme is attributed to an open flexible conformation in which the domains are minimally held together, it would be anticipated therefore that the apoenzyme would have a larger radius than that of the compact morphology of holoenzyme. Preliminary experiments were carried out, in which both apoenzyme and holoenzyme were examined by dynamic light scattering techniques.

Examination of holoenzyme gave reliable results with low noise figures. The sample was assigned as being monomeric, with a radius of 2.88 nm and an estimated molecular mass of 38 kDa. The apoenzyme, however, gave unreliable results when interpreted as a monodisperse sample. The average radius of the sample appeared to be 15 nm, with an estimated molecular

weight of 2200 kDa. The apoenzyme was then analysed instead as a polydisperse sample, and was found to give a better resolution after bi-modal regression (i.e., fitting two components with the raw data). The results now appeared to suggest two populations for apoenzyme, of radii 9.84 nm and 28.44 nm, and estimated molecular mass of 754 kDa and 9995 kDa respectively.

The results for holoenzyme appear to approximately fit with all previous observations for a compact structure. The crystal strucure of porphobilinogen deaminase holoenzyme reveals dimensions of 57x43x32Å. The estmation by light scattering, of 28.8Å, is in the same order but slighlty low. Similarly, the estimated molecular mass determination of 38kDa is close to that determined by electrospray (~34kDa), but shows some discrepancy. The apoenzyme, however, has not been well analysed by light scattering, as suggested by the clearly inaccurate molecular weight determinations. The results do indicate, however, that the apoenzyme is not a compact structure, and therefore has not been able to scatter light in the same manner as holoenzyme.

5.2.3 Properties of Apoenzyme Synthesised by the Cleavage of Cofactor from Native Porphobilinogen Deaminase Holoenzyme

5.2.3.1 The Purification of Apoenzyme by Cleavage of Cofactor

Native porphobilinogen deaminase holoenzyme was purified as described in Materials and Methods. The cofactor was cleaved from the holoenzyme using a minor modification of the protocol given by Hart *et al.*, 1988, as described in Methods. Approximately 6mg of apoenzyme was recovered from the initial 10mg of holoenzyme used in the experiment.

5.2.3.2 Comparison of Apoenzyme Purified by Two Distinct Routes

5.2.3.2.1 Recovery of Activity of Apoenzyme from Both Sources

Two samples of apoenzyme, one synthesised from the *hem B* strain and one from the chemical cleavage of cofactor, were assayed for activity. Both samples were assayed in the presence and absence of a two molar equivalent of porphobilinogen at 37°C for thirty minutes. The recovery of activity for all samples is shown in figure 5.18.

The graph in figure 5.18 shows that the apoenzyme prepared from the acidic cleavage of cofactor from holoenzyme (c and d) displayed a very close pattern of recovery to that of apoenzyme synthesised *via* the *hem B st*rain (a and b). Both samples, without preincubation (a and c), showed a typical lag time of around twenty minutes before recovering activity with a linear increase, and both were able to recover around 10% of the activity of native holoenzyme after a preincubation with substrate (b and d). A longer preincubation at 37°C showed that apoenzymes from both sources were able to recover a maximum activity of 50% of the native holoenzyme.

Figure 5.18 The Recovery of Activity from Apoenzyme Synthesised by Two Distinct Routes

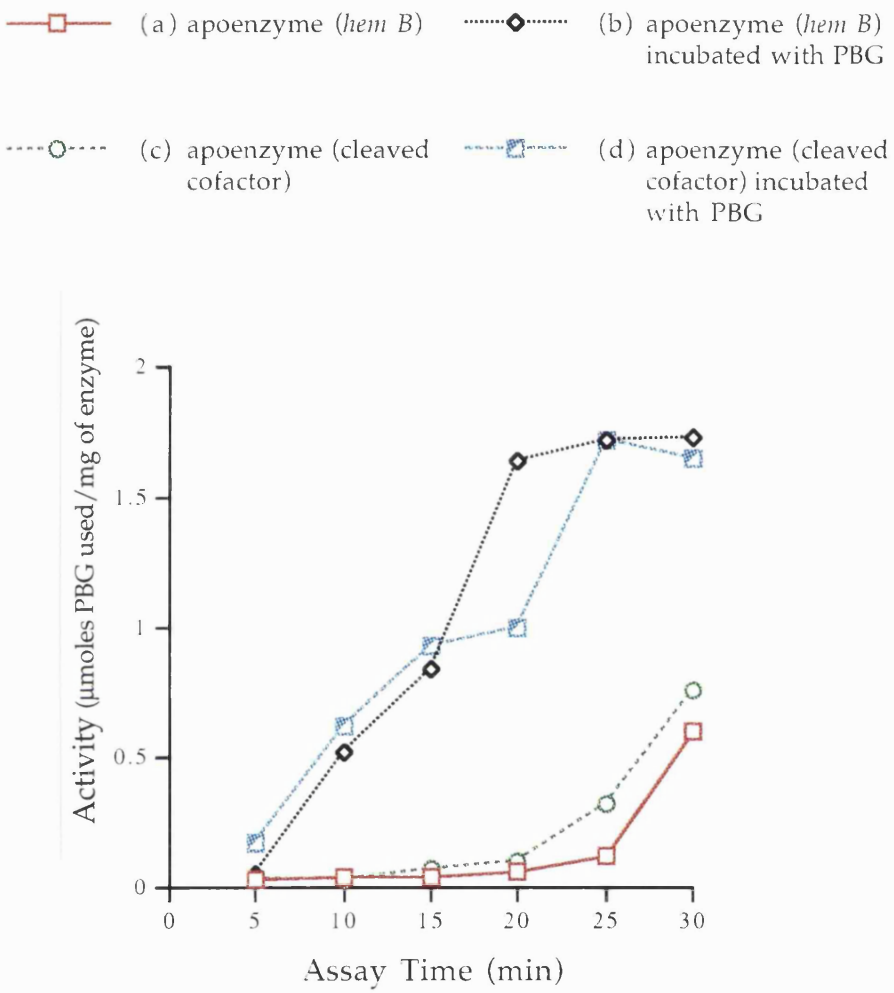

5.2.3.2.2 Visualisation of Reconstitution of Holoenzyme from Apoenzyme, from Both Sources, by Polyacrylamide Gel Electrophoresis

Apoenzyme samples obtained by both routes were incubated with a 50 molar excess of porphobilinogen and analysed by non denaturing gel electrophoresis after incubations. For comparison, apoenzyme alone and holoenzyme alone were also analysed. All apoenzyme samples were also heat treated at 60°C for ten minutes and analysed. The gel is shown in figure 5.19.

Figure 5.19 Non Denaturing Polyacrylamide Gel of Reconstitution of Holoenzyme from Apoenzyme Synthesised by Two Distinct Routes

Lanes 1-4 contain wild-type apoenzyme purified from the *hem B* strain.
Lane 5 contains wild-type holoenzyme.
Lane 6-9 contains wild-type apoenzyme purified from acidic cleavage of cofactor from holoenzyme.

Lanes 1 and 6 contain apoenzyme.
Lanes 2 and 7 contain heat-treated apoenzyme.
Lanes 3 and 8 contain apoenzyme incubated with porphobilinogen.
Lanes 4 and 9 contain apoenzyme incubated with porphobilinogen and then heat-treated.

For clarity, the migrations of holoenzyme and apoenzyme are marked in the figure.

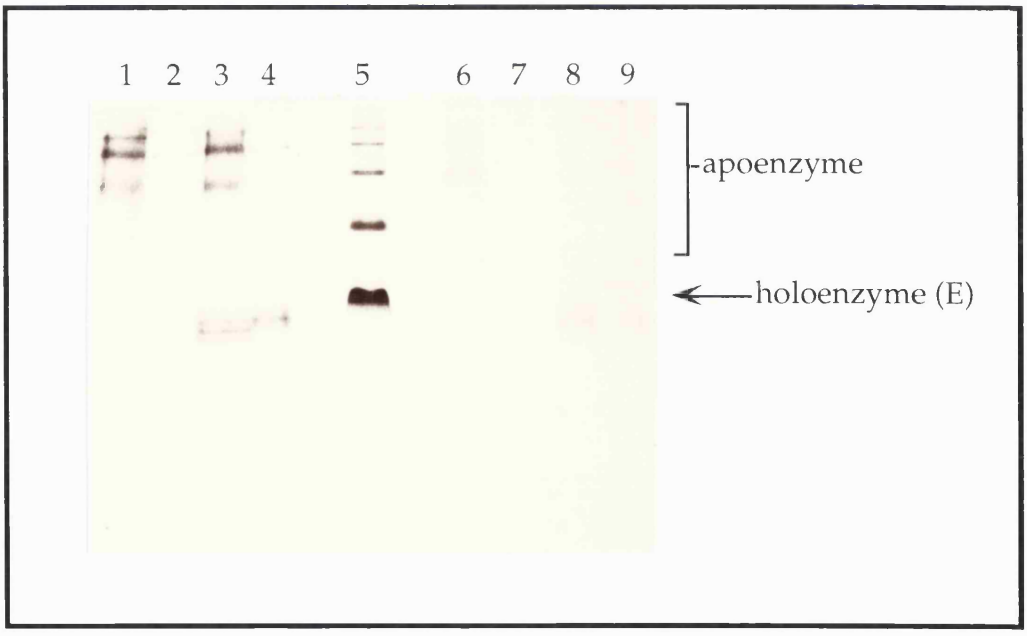

The gel in figure 5.19 shows that the apoenzyme samples from both sources behaved in similar ways. The holoenzyme used as a standard was found to have aggregated (lane 5); the double band which migrated furthest was taken as the monomeric form for reference.

The apoenzyme migrated as the characteristic ladder of bands (lanes 1 and 6), which largely disappeared on heat treatment (lanes 2 and 7). The apoenzyme which had been incubated with substrate (lanes 3 and 8) migrated also as the characteristic ladder of bands, with additional bands which migrated beyond the double band of holoenzyme (lane 5). Upon heat treatment (lanes 4 and 9), the majority of the ladder was seen to have disappeared, as well as the lower migrating of the additional bands.

These experiments showed that apoenzyme obtained by the cleavage of cofactor from holoenzyme appeared to behave identically to the apoenzyme isolated from the *hem B* strain. However, for all further studies the apoenzyme synthesised via the *hem B* strain was used, as this route was less time consuming and required fewer purification stages for isolation.

5.2.4 Inhibition Studies of the Regeneration of Holoenzyme from the Apoenzyme of Native Porphobilinogen Deaminase

5.2.4.1 Inhibition of Apoenzyme by the Substrate Analogue BromoPorphobilinogen

The reagent 2-bromoporphobilinogen is a substrate analogue and differs from porphobilinogen only by having bromine at the key α-position, as shown in figure 5.20. Bromoporphobilinogen (BrPBG) leads to a rapid inactivation (ca. 90%) of the native porphobilinogen deaminase holoenzyme when added in excess, although the presence of the substrate porphobilinogen greatly reduces the rate of inactivation (Warren and Jordan, 1988). Enzyme-BrPBG complexes EB, ESB and ES_2B can be isolated by the f.p.l.c. system. The reaction of BrPBG with ES_3 leads to the production of bromopreuro-porphyrinogen and enzyme.

Figure 5.20 The Chemical Structure of Bromoporphobilinogen

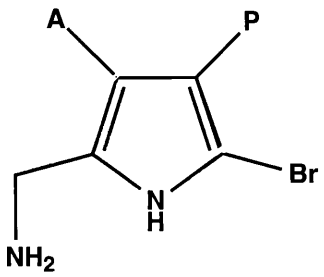

BrPBG acts as a suicide inhibitor of the deaminase since it is recognised by the catalytic site as a substrate and it is deaminated and coupled either to the cofactor or to any of the enzyme-intermediate complexes. Once bound, the presence of the Br atom at the α-position blocks further reaction with both the substrate and any additional BrPBG, and thus leaves the enzyme inactivated. Treatment of EB, ESB or ES_2B with 0.2M hydroxylamine or heat leads to the liberation of the bound Br-intermediate complex and complete restoration of the activity of the enzyme. The blocked α-position of the enzyme-BrPBG

complexes EB, ESB or ES_2B abolishes the typical dipyrromethane cofactor reaction of the enzyme with Ehrlich's reagent, providing powerful evidence that it is the cofactor that forms the covalent link with the substrate.

It is now known that apoenzyme assembles the cofactor preferentially by the addition of preuroporphyrinogen. However, the cofactor can also be assembled very slowly by the addition of porphobilinogen. It was therefore intended to investigate the impact of porphobilinogen analogues, such as BrPBG, on the process of the regeneration of holoenzyme. The reaction of holoenzyme with such an analogue was also studied. If the recovery of activity of apoenzyme was inhibited to the same degree as the activity of holoenzyme by BrPBG, it may suggest a similar mechanism for the molecular recognition of porphobilinogen by apoenzyme and holoenzyme.

Both apoenzyme and holoenzyme were incubated with five, twenty and fifty molar excesses of BrPBG at 4°C for fifteen minutes. Duplicate samples were then subjected to a further incubation of the same molar excesses of porphobilinogen at 4°C for fifteen minutes. All samples were assayed for activity, along with standard incubations of apoenzyme in the absence and presence of a two molar equivalent of porphobilinogen, and holoenzyme. The recovery of activity of apoenzyme is shown in figure 5.21 and the activity of holoenzyme is shown in figure 5.22.

The graphs in figures 5.21 and 5.22 show that the equivalent addition of porphobilinogen after BrPBG preincubation made little difference to the inhibition of activity caused by BrPBG. For clarity of comparison between apoenzyme and holoenzyme, the activity of samples in the absence of additional porphobilinogen is summarised in Table 5.1 The apoenzyme and holoenzyme in the absence of preincubations are shown as having an activity of 100% .

Figure 5.21 The Recovery of Activity of Apoenzyme after Incubation with BrPBG

(a) apoenzyme

(b) apoenzyme incubated with PBG

(c) apoenzyme incubated with BrPBG (1:2)

(d) apoenzyme incubated with BrPBG (1:2) and then PBG

(e) apoenzyme incubated with BrPBG (1:5)

(f) apoenzyme incubated with BrPBG (1:5) and then PBG

(g) apoenzyme incubated with BrPBG (1:20)

(h) apoenzyme incubated with BrPBG (1:20) andthen PBG

(i) apoenzyme incubated with BrPBG (1:50)

(j) apoenzyme incubated with BrPBG (1:50) and then PBG

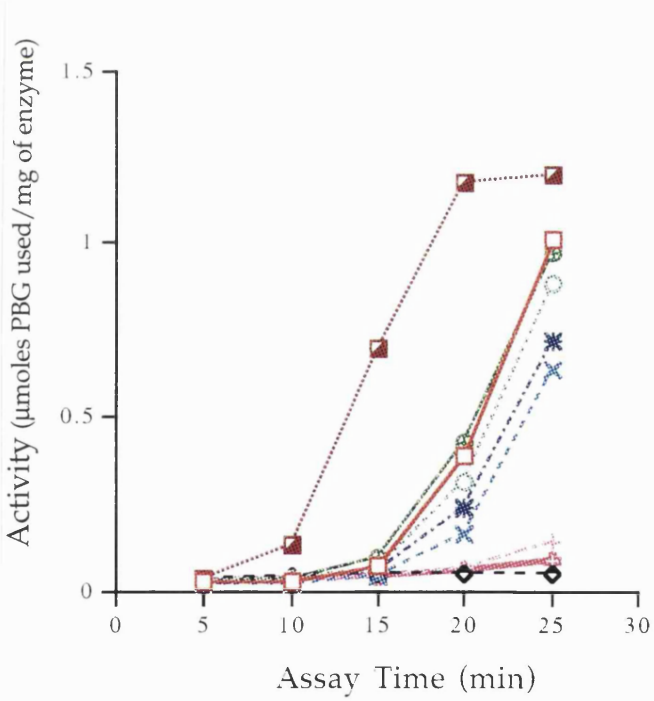

Figure 5.22 Activity of Holoenzyme after Incubation with BrPBG

(a) Holoenzyme

(b) Holoenzyme incubated with BrPBG (1:5)

(c) Holoenzyme incubated with BrPBG (1:5) and then PBG

(d) Holoenzyme incubated with BrPBG (1:20) and then PBG

(e) Holoenzyme incubated with BrPBG (1:20) and then PBG

(f) Holoenzyme incubated with BrPBG (1:50)

(g) Holoenzyme incubated with BrPBG (1:50) and then PBG

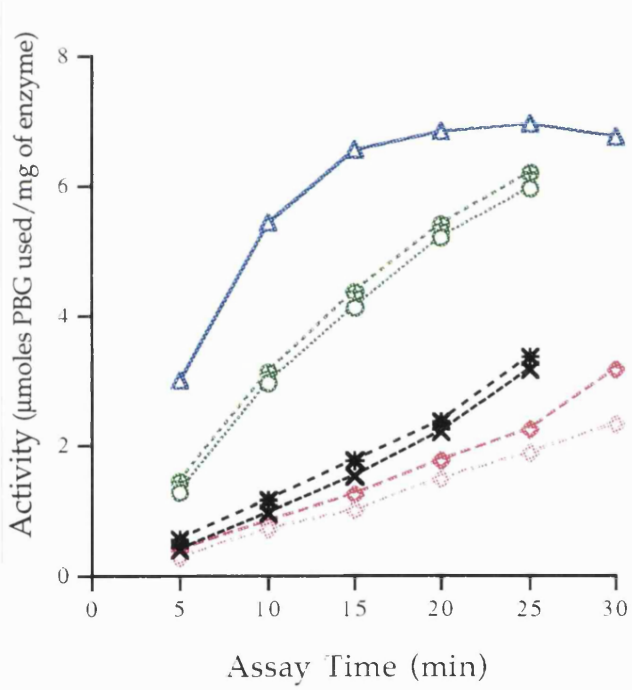

Table 5.1 Summary of Acitvity Retained by Apoenzyme and Holoenzyme After Incubation with BrPBG

Molar Excess of BrPBG	Apoenzyme (% Activity)	Holoenzyme (%Activity)
0	100	100
5	50	56
20	16	20
50	19	12

Table 5.1 shows that the inhibition of apoenzyme and holoenzyme by BrPBG appeared to be very similar, i.e. they are both inhibited to the same degree. This would suggest that BrPBG blocks the further addition of porphobilinogen in the same way, whether bound to apoenzyme or holoenzyme. It may also suggest that a similar mechanism is employed by both apoenzyme and holoenzyme for porphobilinogen incorporation.

5.2.4.2 Inhibition of Apoenzyme by the Substrate Analogue α-Fluoroporphobilinogen

A new susbstrate analogue was recently synthesised by Scott's group at Texas. The analogue, 2-fluoroporphobilinogen "aldehyde" required reduction to the alcohol (FPBG) with sodium borohydride for reaction with porphobilinogen deaminase. Once reduced, the product was unstable and therefore it was essential to carry out all experiments within two hours, although once covalently attached to deaminase the alcohol was believed to be stable. The alcohol was likely to serve as a good substrate for deaminase as a similar structure, hydroxyporphobilinogen, has previously been shown to be incorporated by the enzyme at around one-third the rate of porphobilinogen (Battersby *et al.*, 1979). It was determined by Scott's group that an enzyme-inhibitor (E-I) complex could be formed upon addition of the 2-fluoroporpho-bilinogen alcohol to enzyme. The 2-fluoro porphobilinogen "aldehyde" and is shown in figure 5.23.

The inhibition of both apoenzyme and holoenzyme by the alcohol FPBG would, like BrPBG, give an indication of the similarities or differences of

Figure 5.23 2-Fluoro Porphobilinogen " Aldehyde" and Alcohol

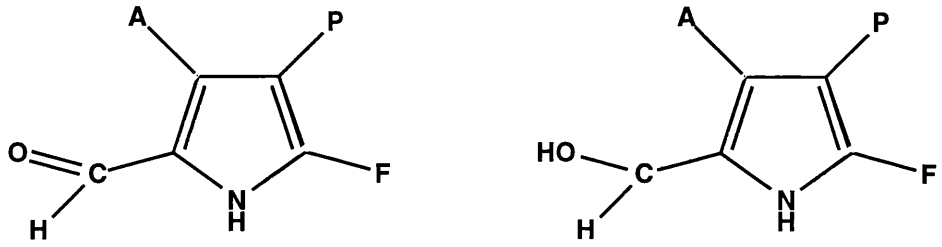

aldehyde alcohol

the mechanism by which porphobilinogen is bound to the apoenzyme and holoenzyme.

Both apoenzyme and holoenzyme were incubated with one, five and ten molar excesses of FPBG at 4°C for fifteen minutes. Due to the limited time over which the experiment could be carried out, samples involving both the absence and presence of further preincubation of substrate could not easily be assayed. In addition, the apparent indifference of the samples to a further preincubation with substrate after BrPBG preincubation implied that only one set of conditions need be sampled. All reactions were therefore subjected to a further incubation of the same molar excesses of porphobilinogen at 4°C for fifteen minutes. All samples were assayed for activity, along with standard incubations of apoenzyme in the absence and presence of a two molar equivalent of porphobilinogen, and holoenzyme. The recovery of activity of apoenzyme is shown in figure 5.24 and the activity of holoenzyme is shown in figure 5.25.

Figure 5.24 Recovery of Activity of Apoenzyme after Incubation with FPBG

(a) apoenzyme

(b) apoenzyme incubated with PBG

(c) apoenzyme incubated with FPBG (1:1) and then PBG

(d) apoenzyme incubated with FPBG (1:5) and then PBG

(e) apoenzyme incubated with FPBG (1:10) and then PBG

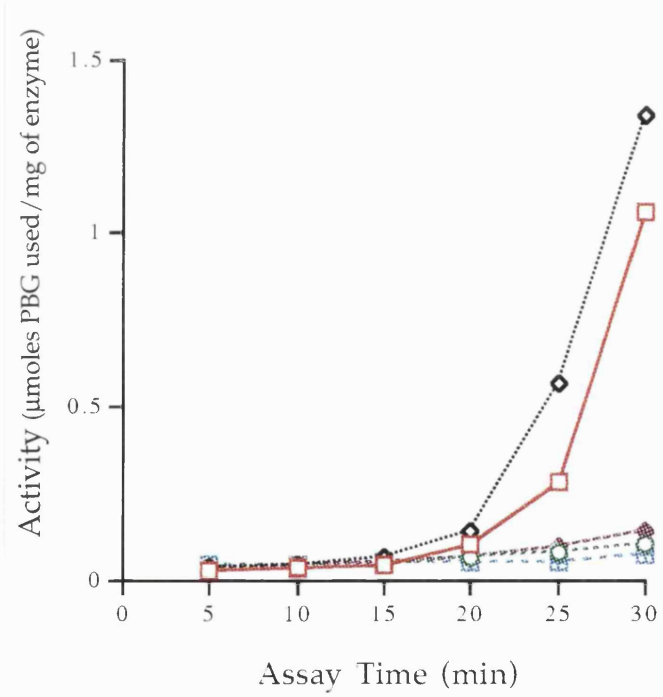

Figure 5.25 Activity of Holoenzyme after Incubation with FPBG

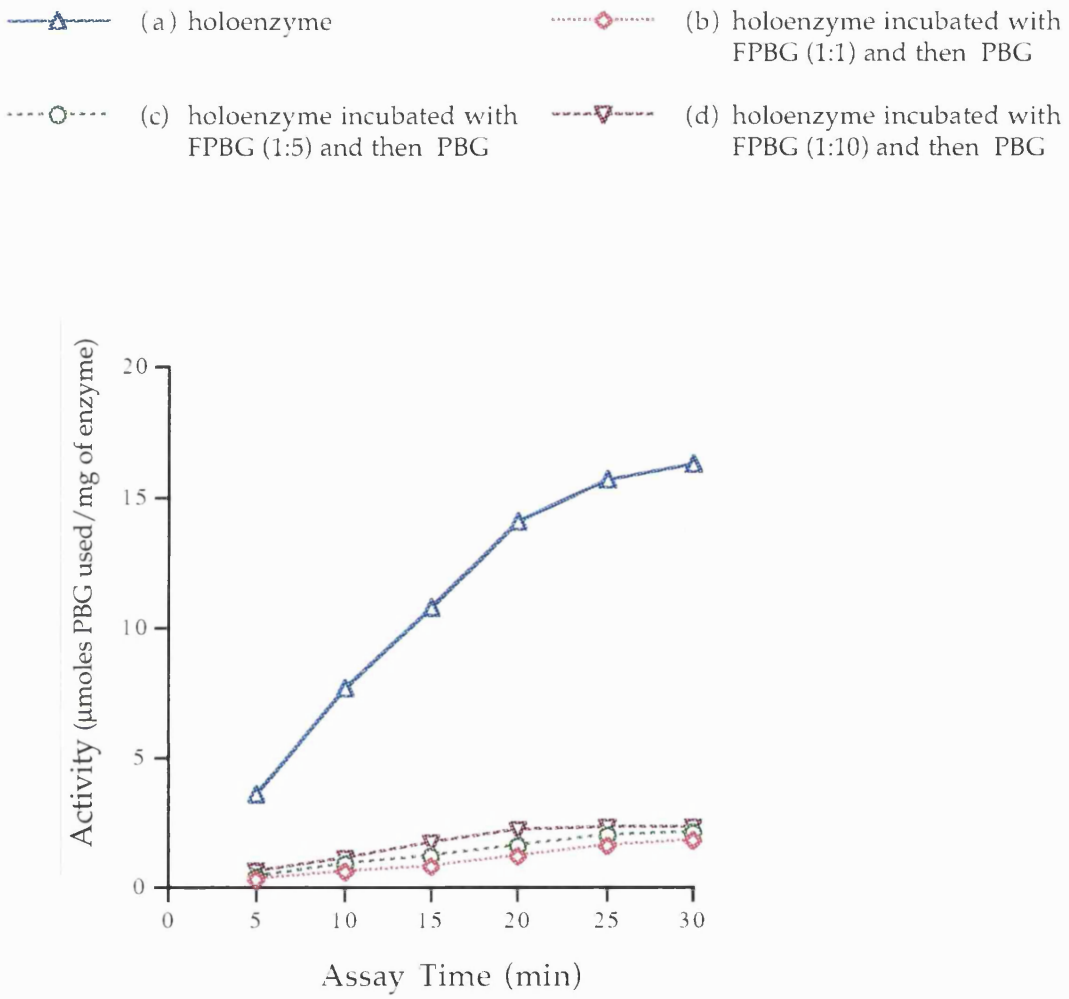

The graphs in figures 5.24 and 5.25 show that all the samples preincubated with FPBG (c-e for apoenzyme; b-d for holoenzyme) appeared to have a reduced activity of around 10% of those without inhibitor preincubation (a and b for apoenzyme; c for holoenzyme). The increased concentration of FPBG did not appear to increase inhibition of the samples.

The results would confirm those of the inhibition by BrPBG, which indicated that both apoenzyme and holoenzyme were inhibited to the same degree and so may well bind porphobilinogen by the same mechanism.

5.2.4.3 Inhibition of the Regeneration of Holoenzyme from Apoenzyme by the Sulfhydryl Reagent N-Ethylmaleimide

The presence of cysteine residues in the enzyme structure of porphobilinogen deaminase has long been known from inhibition studies of the enzyme by sulphydryl reagents (Russell and Rockwell, 1980). The susceptibility to sulphydryl reagents appears to be dependant on the number of porphobilinogen rings that the enzyme has bound. Thus the free *E. coli* holoenzyme appears rather unreactive to the sulphydryl reagents unless high concentrations of the inhibitor are used, while enzyme-intermediate complexes, on exposure to sulphydryl reagents, are found to show a marked increase in their susceptibility to inhibition (Warren and Jordan, 1988). The inhibition is dependant on the length of the chain of the enzyme-intermediate complexes, with a further increase in activation corresponding to the increase in the number of bound substrate molecules. The results therefore suggest that conformational changes are occurring in the protein to cause a previously unreactive sulphydryl group to become accessible to the reagent. The sulphydryl reagents, such as N-ethylmaleimide and 5,5'-dithiobis (2-nitrobenzoic acid), also exhibit time-dependant inhibition/inactivation on *E. coli* deaminase.

The elucidation of the three-dimensional crystal structure of *E. coli* porphobilinogen deaminase (Louie *et al.*, 1992) allows the inhibition of the enzyme by N-ethylmaleimide (NEM) to be better interpreted. The enzyme is known to possess four cysteine residues, occurring at positions 99, 134, 205 and 242 (Thomas and Jordan, 1986). The position of these residues in relation to the tertiary structure can be seen in figure 5.26. Cysteine-99 occupies a partially exposed position between domains 1 and 3 whereas cysteine-134 is located at the domain 2/3 interface. Both residues are therefore potentially susceptible to major environmental changes during the reaction. The environment of the remaining two cysteine residues is likely to remain more stable: cysteine 205 is located within domain 1 and is expected to maintain the same partially exposed position throughout the catalytic cycle; cysteine 242 is blocked in the form of a thioether due to its role as the covalent attachment site for the dipyrromethane cofactor.

The nature of enzyme inactivation by NEM was further studied by the generation of three site-directed mutants in which the cysteine residues at

positions 99, 134 and 242 were mutated to structurally related serine residues (Warren *et al.*, 1995). All three mutants, C99S, C134S and C242S, were purified and assayed for activity. The mutants C99S and C134S were found to have a similar specific activity to that of the wild-type enzyme. However, C242S appeared to have only about a third the activity of wild-type and was found to exist largely in an apoenzyme form. The mutants were also assayed for their susceptibility to NEM. The mutant C99S was found to behave in a similar manner to native enzyme and indicated therefore that cysteine-99 was not key cysteine residue affected. The mutant C242S, on assembling the cofactor, was also found to display a similar suscebtibility to NEM to that of wild-type. However, the mutant C134S was found to be completely insensitive to inhibition by NEM, despite the addition of the substrate. Cysteine-134 is therefore the likely site at which NEM modification leads to inactivation of the *E.coli* porphobilinogen deaminase.

The susceptibilty of apoenzyme to sulfyhdryl reagents has not previously been studied. The lack of cofactor in the apoenzyme, normally bound through the sulphur atom of the residue cysteine-242, would render the cysteine-242 exposed, and therefore it would be anticipated that the apoenzyme would show a marked decrease in its capacity to regenerate holoenzyme in comparison to the holoenzyme activity on exposure to sulfhydryl reagents.

The measure of susceptibility was not straightforward. The assay for the recovery of activity of apoenzyme in the presence of sulfhydryl reagents required the absence of reducing agents. It had been noted that apoenzyme was far less active in the absence of reducing agents, and therefore a longer preincubation with substrate was necessary to record the effects of the sulfhydryl reagent.

5.2.4.3.1 Recovery of Activity from Apoenzyme in the Presence of N-Ethylmaleimide

Solid apoenzyme was resuspended in 20mM Tris/ HCl buffer pH8.0 and passed through a gel filtration column into the same buffer, to remove the small dithiothreitol content from the protein. Reducing agents were removed from holoenzyme in the same way. Both apoenzyme and holoenzyme were

Figure 5.26 The Position of the Cysteine Residues in Native Porphobilinogen Deaminase

The residue cysteine-242, which is not labelled in the picture, is positioned on the mobile loop and links the cofactor (depicted in yellow) to the enzyme.

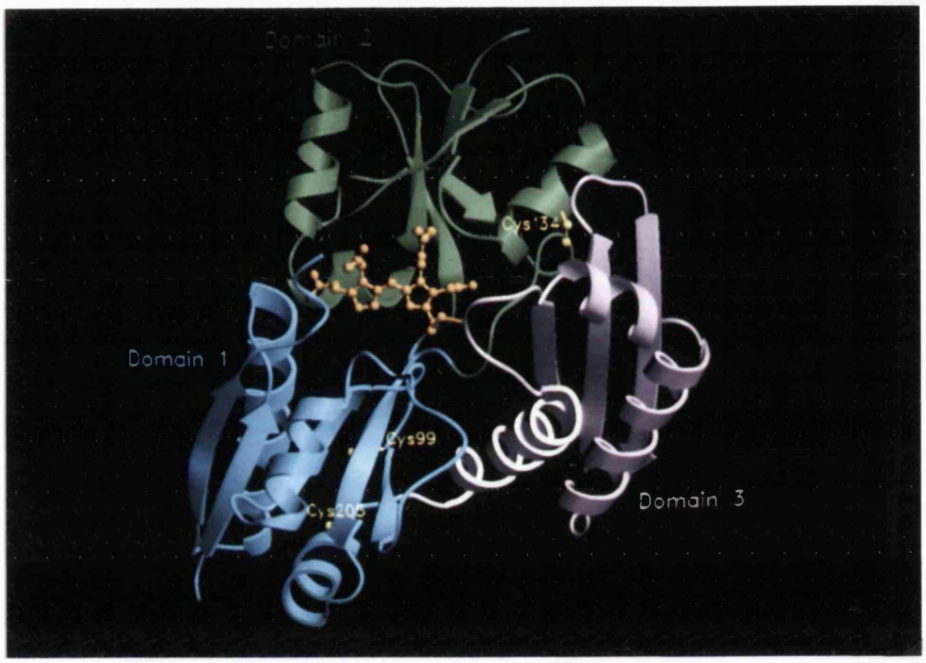

then preincubated with the sulfhydryl reagent N-ethylmaleimide (NEM) at total concentrations of 1, 5, 10 and 50mM at 37°C for ten minutes. The apoenzyme samples were then subjected to a preincubation with two molar equivalents of porphobilinogen at 37°C for four hours to attempt to regenerate the holoenzyme. All samples were assayed for activity, along with standard incubations of apoenzyme in the absence and presence of a two molar excess of porphobilinogen, and holoenzyme. The recovery of activity of apoenzyme is shown in figure 5.27 and the activity of holoenzyme is shown in figure 5.28.

Figure 5.27 Recovery of Activity of Apoenzyme in the Presence of NEM

(a) apoenzyme

(b) apoenzyme incubated with PBG

(c) apoenzyme incubated with NEM (1mM) and then PBG

(d) apoenzyme incubated with NEM (5mM) and then PBG

(e) apoenzyme incubated with NEM (10mM) and then PBG

(f) apoenzyme incubated with NEM (50mM) and then PBG

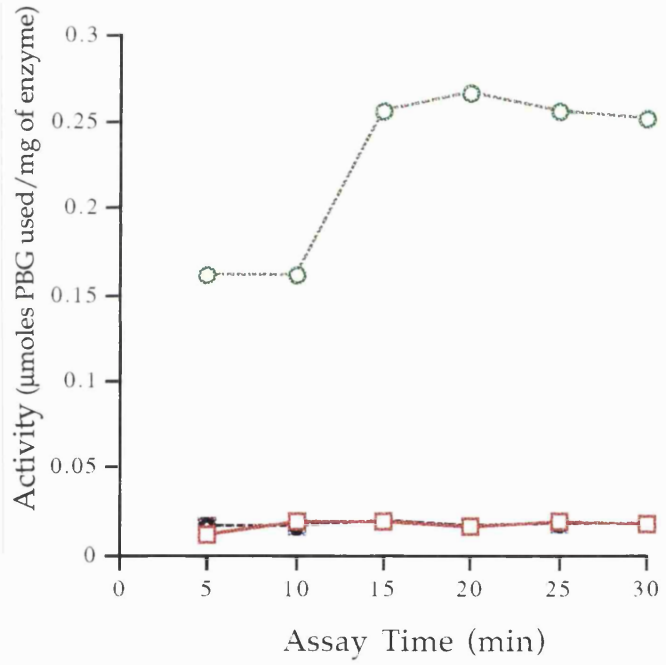

Figure 5.28 Activity of Holoenzyme in the Presence of NEM

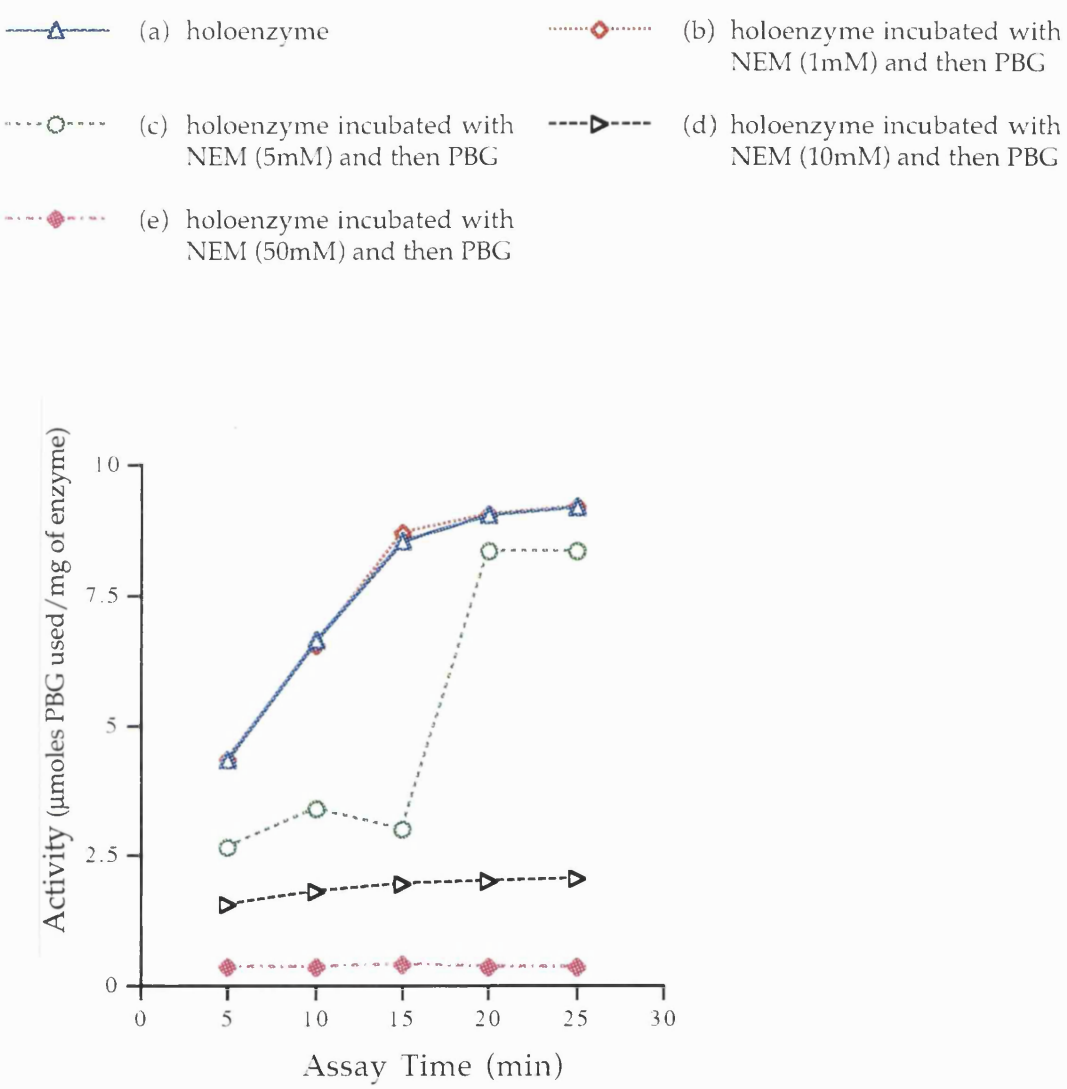

The graph in figure 5.27 shows that the apoenzyme in the absence of preincubation with substrate (a) appeared to be unable to recover any activity within thirty minutes of assay. Apoenzyme which had been preincubated with substrate only (b) was able to recover around 25% of its normal activity, i.e. of that in the presence of reducing agents. Apoenzyme which had been incubated with NEM appeared to have been completely inhibited (c-f), despite the subsequent long preincubation with substrate. Therefore, one or more of the cysteine residues had evidently been modified by the sulphydryl reagent, the most likely of these being the exposed cysteine-242. However, the possible contribution to inactivation from the other three cysteine residues cannot be

ignored, although it could not be predicted from these results alone whether the residues cysteine-99, -134 or -205 are exposed in the apoenzyme form.

The graph shown in figure 5.28 showed that the holoenzyme displayed a concentration -dependant inactivation by NEM, becoming completely modified by 50mM NEM (e). The inactivation also increased with time, presumably as more substrate rings became bound, bringing about the exposure of the residue cysteine-134. The inactivation profile of holoenzyme was typical and in keeping with those previously observed (Warren and Jordan, 1988).

5.2.4.3.2 Visualisation of the Reconstitution of Holoenzyme from Apoenzyme, After Modification by the Sulfhydryl Reagent N-Ethylmaleimide, by Polyacrylamide Gel Electrophoresis

The wild-type apoenzyme was also analysed for suscebtibilty to NEM by non denaturing polyacrylamide gel electrophoresis. Apoenzyme was incubated with a total concentration of 15mM NEM at 37°C for ten minutes, in the absence and presence of a subsequent incubation with a fifty molar excess of porphobilinogen at 37°C for one hour. Apoenzyme was also incubated with substrate only. All samples were analysed by non denaturing polyacrylamide gel electrophoresis, as shown in figure 5.29.

The gel in figure 5.29 shows that the apoenzyme (lane 1), in the presence of NEM alone, displayed the typical ladder of bands. Apoenzyme which had been incubated with substrate alone (lane 3) gave rise to additional bands which migrated beyond the ladder, characteristic of those seen when apoenzyme has reconstituted to form enzyme-intermediate complexes. Despite the reduced activity for this sample on assay, the percentage reconstituted as estimated from the gel is no less than that expected for the substrate-incubated apoenzyme in the presence of reducing agents.

The apoenzyme sample which had been incubated with both NEM and then substrate (lane 2) appeared to have become denatured as only a faint ladder of bands was observed for this sample. This result could be explained in light of the apparent susceptibilty of NEM-modified enzyme-intermediate complexes to heat treatment (Warren *et al.*, 1995). In contrast to the stability of free wild-type enzyme to heat treatment at 70°C, the NEM-modified enzyme is

Figure 5.29 Non Denaturing Gel of the Reconstitution of Holoenzyme from Apoenzyme, Showing the Susceptibility of Apoenzyme to NEM

Lane 1 contains wild-type apoenzyme incubated with NEM.
Lane 2 contains wild-type apoenzyme incubated with NEM and then porphobilinogen.
Lane 3 contains wild-type apoenzyme incubated with porphobilinogen.

For clarity, the migration of apoenzyme is marked in the figure.

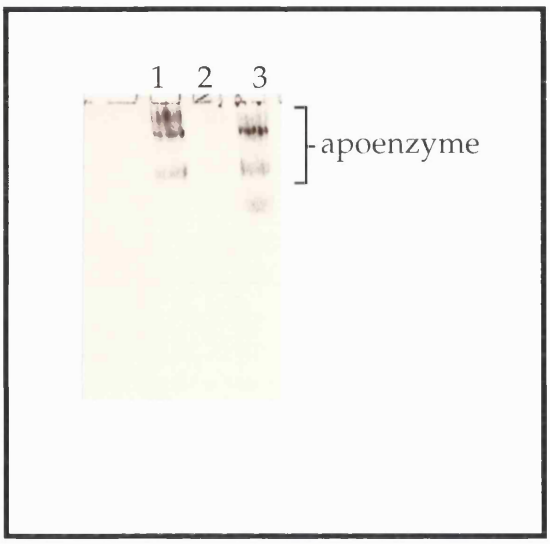

found to precipitate at only 40°C. It is suggested, therefore, that the NEM may have trapped the enzyme in a less stable conformation than that of the free enzyme, possibly because stabilising contacts between domains 2 and 3 are lost. In addition, the introduction of a hydrophobic ligand such as NEM to a position between two domains may have led to the instability. However, the observation that the stability of apoenzyme appeared only to be affected by the addition of substrate after NEM is more difficult to explain. It may be possible that the addition of porphobilinogen to the partially unfolded apoenzyme, which had already been trapped in an even more unstable form by the addition of NEM, brought about conformational changes which led to the denaturation of the structure.

5.2.5 The Mutants C134S and C242S of the Apoenzyme of Porphobilinogen Deaminase

5.2.5.1 Expression of the Cysteine Mutants of Apoenzyme

All DNA manipulations were carried out using standard techniques as described in Materials and Methods. The mutant deaminases C134S (strain 228) and C242S (strain219) were a gift from C. Roessner, Texas A & M, as described in Warren *et al.*, (1995). The cysteine mutants of apoenzyme were purified from *hem B*$^-$ derivatives of *E.coli* that has been transformed with the mutagenised plasmids.

5.2.5.2 Purification of the Cysteine Mutants C242S and C134S of Apoenzyme

The cysteine mutants of apoenzyme were isolated by the same method employed for the purification of wild-type apoenzyme. The *hem B* derivatives of *E.coli* transformed with the mutagenised plasmids were grown overnight in LB media containing ampicillin (100μg/ml) and hemin (5μg/ml) at 37°C. The presence of hemin was essential for growth due to the lack of the enzyme 5-aminolaevulinic acid dehydratase.

The cells were harvested by centrifugation, resuspended in 100mM phosphate buffer pH 8.0 containing 13mM β-mercaptoethanol and broken open by sonication. The sonicated cells were then centrifuged to remove cell debris and the supernatant was applied to a Mimetic Orange 1 A6XL column equilibriated in 20 mM Tris/HCl pH 7.5 containing 13mM β-mercaptoethanol. The protein was eluted using the same Tris buffer but containing increasing concentrations of NaCl as described in Materials and Methods. The fractions eluting from the column were examined by denaturing polyacrylamide gel electrophoresis and also assayed for activity. The activity was found to correspond to the bands identified for deaminase on the gel in the case of the C134S mutant enzyme. However, for the C242S mutant, the enzyme was not found to recover activity using the standard preincubation and assay, and therefore only the denaturing gel was used for analysis of fractions. Both mutants were found to elute pure in high salt concentrations. The

porphobilinogen deaminase containing fractions were concentrated by ultrafiltration on a PM10 membrane and desalted via gel filtration into 1mM Tris/HCl buffer pH 7.5 containing 2mM dithiothreitol. The purified apoenzyme of the cysteine mutants were then freeze-dried and stored at -20°C. Approximately 20mg of protein could be obtained per preparation from 2L media.

5.2.5.3 Reconstitution of Holoenzyme from the Cysteine Mutants of Apoenzyme

The recovery of activity of the cysteine mutants of apoenzyme would allow the importance of the residues cysteine-134 and cysteine-242 in the process of cofactor assembly and substrate binding to be established. When expressed in the usual overexpressing *hemC* derivatives of *E.coli*, the C134S mutant was found to display activity similar to that of wild-type enzyme, whereas the C242S mutant was found to have a specific activity of around 40% of the wild-type (Warren *et al.*, 1995). The reduced activity of the C242S mutant was explained by the fact that the enzyme existed largely in the apoenzyme form, although some holoenzyme was found to be present. The ability of the C242S mutant to assemble the cofactor at all was quite surprising since this would require the mostly unreactive serine OH to make an oxygen ether linkage with the C1 ring of the cofactor. The fact that the reaction could occur and yield approximately one-third of the C242S mutant as holoenzyme reflects the reactive nature of the enzyme. However, the discovery that preuroporphyrinogen is the preferred precursor of the apoenzyme makes the finding more understandable. The highly reactive OH group of the bilane would make the reaction more facile than that of apoenzyme and porphobilinogen.

It is anticipated that the C134S mutant of apoenzyme will have a similar activity of wild-type apoenzyme, as it is unlikely that the residue cysteine-134 plays a role in cofactor assembly. However, the C242S mutant is expected to show a dramatic loss of recovery of activity. Whilst the apoenzyme form has been seen to be able to reconstitute some holoenzyme *in vivo*, it is not anticipated that this task can be as easily performed *in vitro*. A lower activity of the cell has already been observed, has it has been seen that only around

40% of the apoenzyme can be reconstituted to holoenzyme *in vitro*, whilst *in vivo* the majority of the enzyme exists in the holoenzyme form.

5.2.5.3.1 Recovery of Activity of the C134S and C242S Mutants of Apoenzyme

The C134S and C242S mutants of apoenzyme were assayed for activity after the presence and absence of the standard preincubation with a two molar equivalent of porphobilinogen at 4°C for thirty minutes. For comparison, wild-type apoenzyme was also assayed after the presence and absence of the standard preincubation. The recovery of activity for the C134S and C242S mutants of apoenzyme is shown in figures 5.30 and 5.31.

The graph in figure 5.30 shows that the C134S mutant of apoenzyme was seen to display identical results to that of wild-type apoenzyme, both in the presence (b and d) and absence (a and c) of a preincubation with substrate. The graph shown in figure 5.31 showed that the C242S mutant of apoenzyme was unable to recover any activity within the thirty minutes of assay time (c and d).

In order to try and recover some activity from the C242S mutant of apoenzyme, longer preincuations with substrate and incubations with substrate in the presence of a one-fiftieth molar equivalent of holoenzyme were also assayed for activity. However, the apoenzyme still appeared to be unable to recover any activity. An alternative method of analysis was therefore required, and whilst polyacrylamide gel electrophoresis was unable to offer a readily quantitative measure of the constitution of the enzyme, a qualitative measure could be made and consequently the C242S mutant of apoenzyme was monitored by non denaturing gel electrophoresis.

Figure 5.30 Recovery of Activity from the C134S Mutant of Apoenzyme

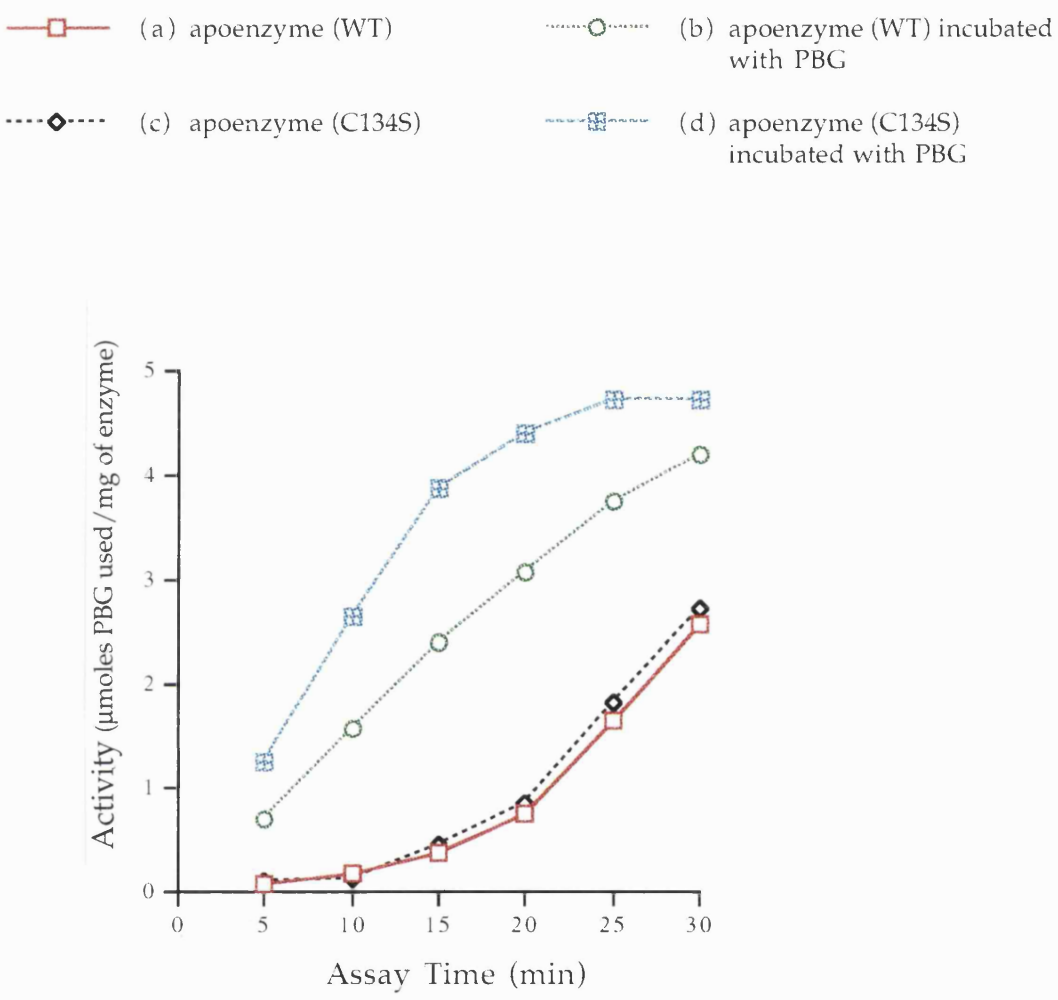

Figure 5.31 Recovery of Activity from the C242S Mutant of Apoenzyme

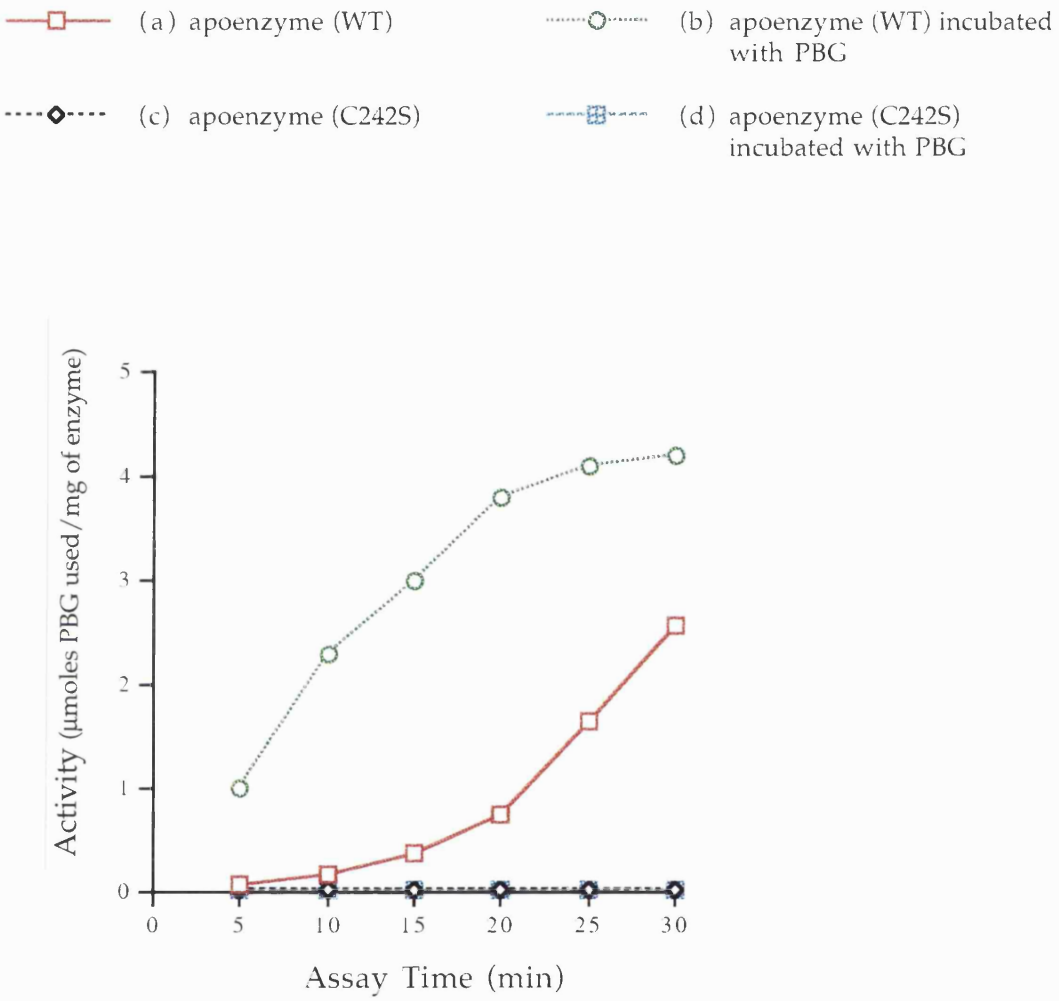

5.2.5.3.2 Visualisation of the Reconstitution of Holoenzyme from the Apoenzyme of the C242S Mutant

The C242S mutant of apoenzyme was incubated with a fifty molar excess of substrate at 37°C for one hour, in the absence and presence of a one-fiftieth molar equivalent of wild-type holoenzyme. Wild-type apoenzyme was also incubated under the same conditions. The incubations were analysed by non-denaturing polyacrylamide gel electrophoresis, alongside a one-fiftieth equivalent of holoenzyme, free apoenzyme (mutant and wild-type) and free wild-type holoenzyme. The non denaturing gel is shown in figure 5.32.

The gel in figure 5.32 shows that the wild-type apoenzyme which had been incubated with substrate in the absence of a one-fiftieth molar equivalent of holoenzyme (lane 2) migrated as a characteristic ladder of bands, with additional bands which migrated beyond that of holoenzyme (lane 4). The apoenzyme which had been incubated with both porphobilinogen and a one-fiftieth molar equivalent of holoenzyme (lane 3) migrated similarly, although the additional bands did not migrate as far as those in the absence of holoenzyme. Therefore, the presence of holoenzyme appeared to restrict slightly the accumulation of complexes (the presence of porphobilinogen is likely to have turned the reaction of apoenzyme with preuroporphyrinogen through to completion).

The C242S mutant of apoenzyme was found to behave similarly to wild-type apoenzyme. On incubation with substrate alone (lane 6), the enzyme was found to accumulate more as one particular enzyme-intermediate complex, likely to be the ES_2 complex. The presence of the one-fiftieth equivalent of holoenzyme (lane 7) also appeared to restrict the build up of complexes for the mutant of apoenzyme.

The C242S mutant of apoenzyme was therefore found to have recovered some activity, *in vitro* again demonstrating the highly reactive nature of the apoenzyme. The substrate-preincubated mutant, which appeared unable to recover activity when assayed for activity, was observed to have reconstituted to enzyme-intermediate complexes when examined by gel electrophoresis. Electrophoresis evidently provided a more sensitive method for judging the constitution of the enzyme.

Figure 5.32 Non Denaturing Polyacrylamide Gel of the Reconstitution of Holoenzyme from C242S Mutant Apoenzyme

Lane 1 contains wild-type apoenzyme.
Lane 2 contains porphobilinogen-incubated wild-type apoenzyme.
Lane 3 contains porphobilinogen-incubated with wild-type apoenzyme in the presence of a one-fiftieth equivalent of holoenzyme.
Lane 4 contains wild-type holoenzyme.

Lane 5 contains C242S mutant apoenzyme.
Lane 6 contains porphobilinogen-incubated C242S mutant apoenzyme.
Lane 7 contains porphobilinogen-incubated with C242S mutant apoenzyme in the presence of a one-fiftieth equivalent of holoenzyme.
Lane 8 contains wild-type holoenzyme.

For clarity, the migration of apoenzyme (wild-type) is marked in the figure.

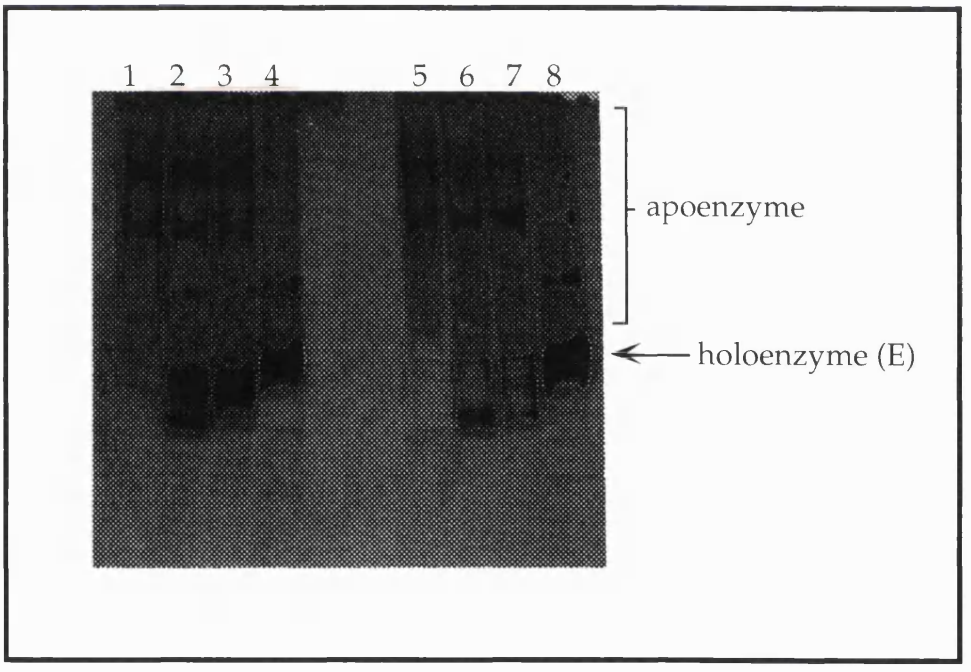

5.2.5.3.3 Recovery of Activity of the C134S Mutant of Apoenzyme in the Presence of the Sulfhydryl Reagent N-Ethylmaleimide

The modification of wild-type apoenzyme by N-ethylmaleimide (NEM) has been presented in this chapter. The possible target residues for the sulphydryl reagent are cysteines-99, 134, 205 and 242, although the most likely of these are cysteines-134 and 242. The exposed position of the C242S is an obvious site for modification by NEM, but the position of the cysteine-134 in the apoenzyme as a site for modification is uncertain. The recovery of activity for both these mutants after exposure to NEM will allow the relevance of these residues in cofactor assembly and substrate binding to be further clarified.

Solid samples of the C134S and C242S mutants of apoenzyme were resuspended in 20mM Tris buffer pH8.0 and passed through a gel filtration column (PD10) into the same buffer, to remove the small dithiothreitol content from the protein. As the C242S mutant had been observed to be unable to reconstitute holoenzyme as analysed by activity assay, the mutant was not monitored for inactivation by NEM by this method.

The C134S mutant was incubated with NEM (1mM) at 37°C for ten minutes, in the presence and absence of a further preincubation with a two molar equivalent of porphobilinogen at 37°C for four hours. All samples were assayed for activity, along with standard preincubations of wild-type apoenzyme in the absence and presence of a two molar excess of porphobilinogen (37°C for four hours). The recovery of activity of all apoenzyme samples is shown in figure 5.33.

The graph in figure 5.33 shows that the wild-type apoenzyme in the absence of preincubation with substrate (a) appeared to be unable to recover any activity within thirty minutes of assay. Apoenzyme which had been preincubated with substrate only (b) was able to recover around 25% of its normal activity, i.e. of that in the presence of reducing agents. All samples incubated with NEM (c and d) were found to be inactive.

The inactivation of the C134S mutant of apoenzyme would indicate the likelihood that the residue cysteine-242 has been modified by the sulphydryl reagent and thus is unable to participate in cofactor assembly or substrate binding.

Figure 5.33 Recovery of Activity of C134S and C242S Mutants of Apoenzyme and Wild-Type Apoenzyme in the Presence of NEM

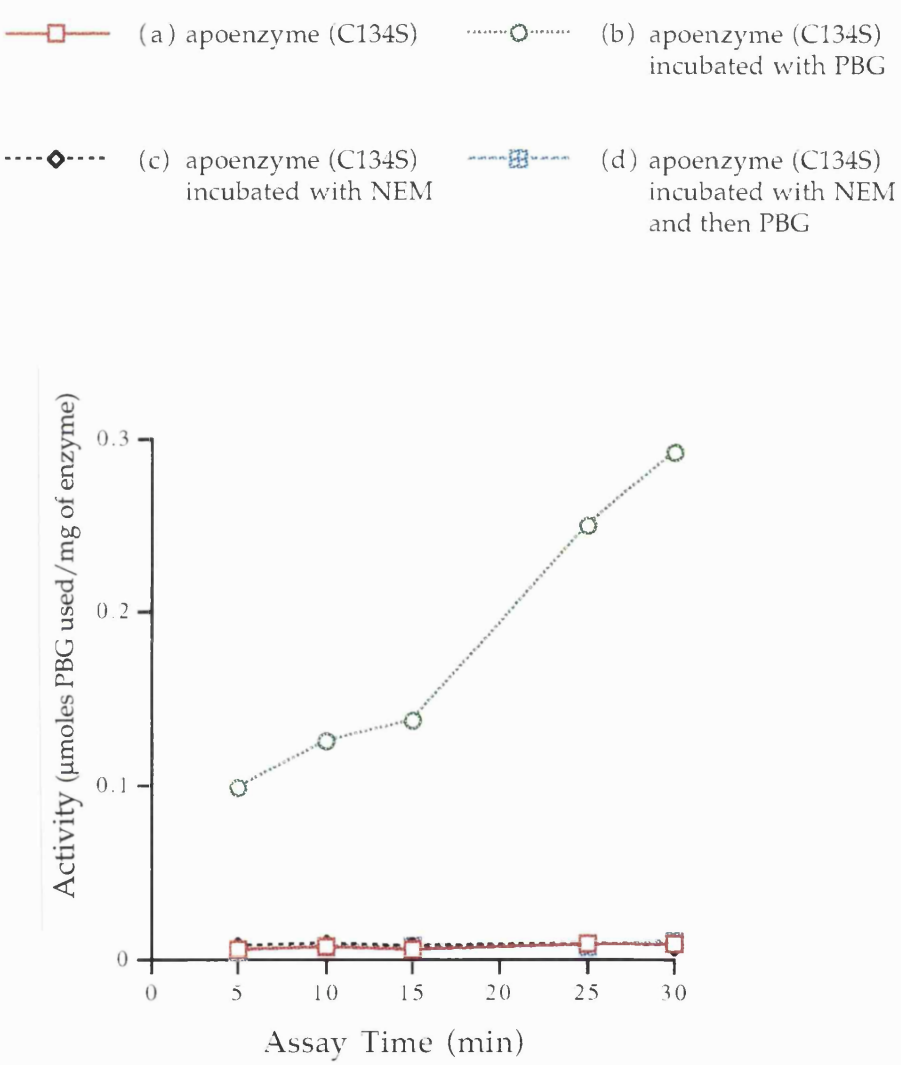

Similarly, the inactivation of the C242S mutant by NEM would be able to suggest that the cysteine-134 residue is also exposed in the apoenzyme form and has prevented the apoenzyme from regenerating the holoenzyme. However, as the C242S mutant apoenzyme was found to be inactive as determined by assay, even in the absence of NEM, it was necessary to examine the inhibition of the cysteine mutants of the apoenzyme by non denaturing polyacrylamide gel electrophoresis.

5.2.5.3.4 Visualisation of the Reconstitution of Holoenzyme from the Apoenzymes of the Cysteine Mutants, after Modification by the Sulfhydryl Reagent N-Ethylmaleimide, by Polyacrylamide Gel Electrophoresis

The C134S and C242S mutants of apoenzyme were incubated with a total concentration of 15mM NEM at 37°C for ten minutes, in the absence and presence of a subsequent incubation with a fifty molar excess of porphobilinogen at 37°C for one hour. Both samples were also incubated with substrate only. All samples were analysed by non denaturing polyacrylamide gel electrophoresis, as shown in figure 5.34.

The gel in figure 5.34 shows that the apoenzyme mutants, in the presence of NEM alone (lanes 1 and 4), displayed the typical ladder of bands. Apoenzyme mutants which had been incubated with substrate alone (lanes 3 and 6) gave rise to additional bands which migrated further than the ladder, characteristic of those seen when apoenzyme has reconstituted to form enzyme-intermediate complexes. The apoenzyme mutant samples which have been incubated with both NEM and then substrate (lanes 2 and 5) appeared to have denatured and only a faint ladder of bands was observed for these samples.

The C134S and C242S mutants of apoenzyme therefore appeared to behave similarly to wild-type apoenzyme on exposure to NEM. Both mutants, on exposure to NEM and then substrate, appeared to adopt unstable conformations, indicating that modification at either cysteine-134 or cysteine-242 may cause denaturation of the apoenzyme. As a result of the denaturation, neither mutant were able to engage in cofactor assembly or substrate binding.

The results indicate that both the cysteine-134 and cysteine-242 residues are exposed in the apoenzyme. However, the importance of these residues to cofactor assembly or substrate binding cannot be concluded from the results of NEM inhibition alone as its presence with substrate leads to the denaturation of the enzyme. The modification of cysteine-134 would be anticipated to affect the folding of the apoenzyme, and this may have been the cause of the precipitation of the apoenzyme. It is more surprising to find that modification of the cysteine-242 also causes the protein to precipitate. Nevertheless, the

Figure 5.34 Non Denaturing Gel of the Reconstitution of Holoenzyme from C134S ans C242S Mutants of Apoenzyme, Showing the Susceptibility of the Apoenzyme to NEM

Lane 1 contains C242S mutant apoenzyme incubated with NEM.
Lane 2 contains C242S mutant apoenzyme incubated with NEM and then porphobilinogen.
Lane 3 contains C242S mutant apoenzyme incubated with porphobilinogen.

Lane 4 contains C134S mutant apoenzyme incubated with NEM.
Lane 5 contains C134S mutant apoenzyme incubated with NEM and then porphobilinogen.
Lane 6 contains C134S mutant apoenzyme incubated with porphobilinogen.

For clarity, the migrations of the apoenzyme (mutants) are marked in the figure.

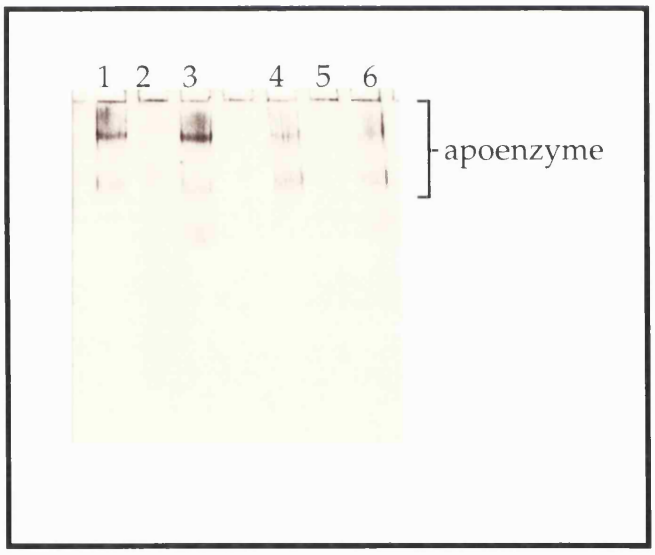

results do confirm the exposed position of cysteine-242 in the apoenzyme form.

The effect of modification on the exposed cysteine-134 is similar to results previously observed for this residue (Warren *et al.*, 1988). When wild

type holoenzyme is treated with NEM, it is noted that the enzyme-intermediate complexes are increasingly inhibited by the presence of the reagent as chain elongation occurs. It is now suggested that this is due to the exposure of the cysteine-134 residue during the polymerisation process (Warren *et al.*, 1995).

5.2.6 The Aspartate-84 Mutants of the Apoenzyme of Porphobilinogen Deaminase

The catalytic role of the residue aspartate-84 has previously been described (Woodcock and Jordan, 1994; see also chapter 3). The residue is found to be essential for catalytic activity by virtue of its hydrogen bonding to the pyrrole nitrogen hydrogens of the cofactor, and its provision of a negative charge to stabilise the positive charges created on the pyrrole nitrogens during the reaction. Site-directed mutants of this residue which highlight this role have been characterised, the residue being mutated to alanine (D84A), glutamate (D84E) and asparagine (D84N). All three mutants are found to have correctly inserted the cofactor. The mutant D84E is found to possess less than one percent of the activity of the wild-type enzyme, whilst the D84A and D84N mutants are found to be catalytically inactive.

Aspartate-84 is therefore seen to be responsible for the catalysis of the substrate to the cofactor but not for the catalysis of the cofactor assembly itself. This suggests that either a different mechanism is employed for cofactor assembly, or that cofactor assembly is aided by additional factors. It also appears possible that a certain amount of the mutant enzyme does exist in the apoenzyme form and may be unable to bind the cofactor easily, which would suggest that the cofactor assembly has been equally disrupted in these mutants. The apoenzyme form of these mutants may not have been easily detected as the purification procedure for the mutants involves a heat treatment step that would be expected to denature a large percentage of any apoenzyme present. The creation of the apoenzyme form of the aspartate-84 mutants would allow the kinetics of cofactor assembly to be monitored. A dramatic reduction in the rate of cofactor assembly by porphobilinogen addition would suggest a similar mechanism for cofactor assembly and chain elongation using porphobilinogen as a substrate. A similar rate of cofactor assembly for the mutant and wild-type apoenzyme would suggest an alternative or additional mechanism.

5.2.6.1 Expression of the Aspartate-84 Mutants of Apoenzyme

All DNA manipulations were carried out using standard techniques as described in Materials and Methods. The mutant deaminases D84A (strain SWD84A), D84E (strain SWD84E) and D84N (strain SWD84N) were generated by Woodcock and Jordan, (1994). The aspartate-84 mutants of apoenzyme were purified from *hemB* derivatives of *E.coli* transformed with the plasmids containing the mutagenised genes. Whilst the mutant D84E transformed easily *via* the use of $CaCl_2$ soaked cells, the mutants of D84A and D84N could only be transformed *via* electroporation. No obvious reason can be put forward to explain this.

5.2.6.2 Purification of the Apoenzyme of the Aspartate-84 Mutants

The *hemB* derivatives of *E.coli* transformed with the plasmids containing the mutagenised genes were grown overnight in LB media containing ampicillin (100μg/ml) and haemin (5μg/ml) at 37°C. The presence of haemin was essential for growth due to the lack of the enzyme 5-aminolaevulinic acid dehydratase. The cells were then harvested by centrifugation, resuspended in 100mM phosphate buffer pH 8.0 containing 13mM β-mercaptoethanol and broken by sonication.

The wild-type apoenzyme and all previous mutants of the apoenzyme had been successfully purified in a single step by affinity chromatography using Mimetic Orange 1 A6XL. However, the apoenzyme forms of the mutants D84A, D84E and D84N all appeared unable to bind to the Mimetic Orange column. The inability of the mutants to bind to the Mimetic Orange column was puzzling, and could only suggest that the structure of the apoenzyme mutants was considerably altered and likely to be more unfolded. Alternatively, the aspartate-84 may make an essential contact with the dye-ligand. The aspartate-84 mutants of the apoenzyme were then applied to other columns previously employed for isolation of porphobilinogen deaminase to seek a means of purification, including DEAE Sephacel anion exchange and a high resolution anion exchange MonoQ HR5/5 column attached to a Pharmacia f.p.l.c. system. However, the apoenzyme mutants were again found to be unable to bind to any of these columns.

Whilst it was surprising that a single mutation at the key catalytic residue would not only render the apoenzyme form inactive but also considerably altered in character, the apoenzyme mutants did appear to have been correctly expressed and therefore this result is genuine. However, the synthesis of these mutants by the *hemB strain* was abandoned as a more simple route for synthesising the apoenzyme form of the aspartate-84 mutants was available (Hart *et al.*, 1988). The isolation of the apoenzyme form of the aspartate-84 mutants was subsequently pursued *via* cleavage of the cofactor using dilute hydrochloric acid.

5.2.6.3 Purification of the Aspartate-84 Mutants and Cleavage of the Cofactor

The method for purification of the aspartate-84 mutants D84A, D84E and D84N has been previously described in Chapter 3. The mutants were not subjected to anion-exchange by the f.p.l.c. system, however, as the enzyme-intermediate complexes of the mutants were equally as accessible for cleavage of cofactor as free enzyme. The cofactor was cleaved from each mutant as described for wild-type enzyme. All solid samples of the mutant were white after freeze-drying, and did not react with Ehrlich's Reagent.

5.2.6.4 Visualisation of the Reconstitution of Holoenzyme from the Apoenzyme of the Aspartate-84 Mutants

The relative inactivity of the asp-84 mutants, even in the holoenzyme form, required that all analysis be carried out using non-denaturing gel electrophoresis. The inactivity of the mutants also necessitated that a lengthy incubation with substrate be used.

Samples of the wild-type and aspartate-84 mutant apoenzyme were incubated with a 50 molar excess of porphobilinogen at 37°C for up to forty eight hours. Aliquots of the incubations were analysed by non-denaturing polyacrylamide gel electrophoresis immediately, after four hours, after twenty four hours and after forty eight hours. For comparison, samples of the mutants before and after cofactor cleavage in the absence of any preincubations were also analysed. The gels are shown in figures 5.35-5.38.

Figure 5.35 Non Denaturing Gel of the Reconstitution of Holoenzyme from the Aspartate-84 Mutants of Apoenzyme

Lane 1 contains wild-type apoenzyme.
Lane 2 contains porphobilinogen-incubated wild-type apoenzyme.
Lane 3 contains wild-type holoenzyme.

Lane 4 contains D84A mutant apoenzyme.
Lane 5 contains porphobilinogen-incubated D84A mutant apoenzyme.
Lane 6 contains D84A mutant holoenzyme.

Lane 7 contains D84E mutant apoenzyme.
Lane 8 contains porphobilinogen-incubated D84E mutant apoenzyme.
Lane 9 contains D84E mutant holoenzyme.

Lane 10 contains D84N mutant apoenzyme.
Lane 11 contains porphobilinogen-incubated D84N mutant apoenzyme.
Lane 12 contains D84N mutant holoenzyme.

For clarity, the migrations of the apoenzyme and holoenzyme (wild-type) are marked in the figure.

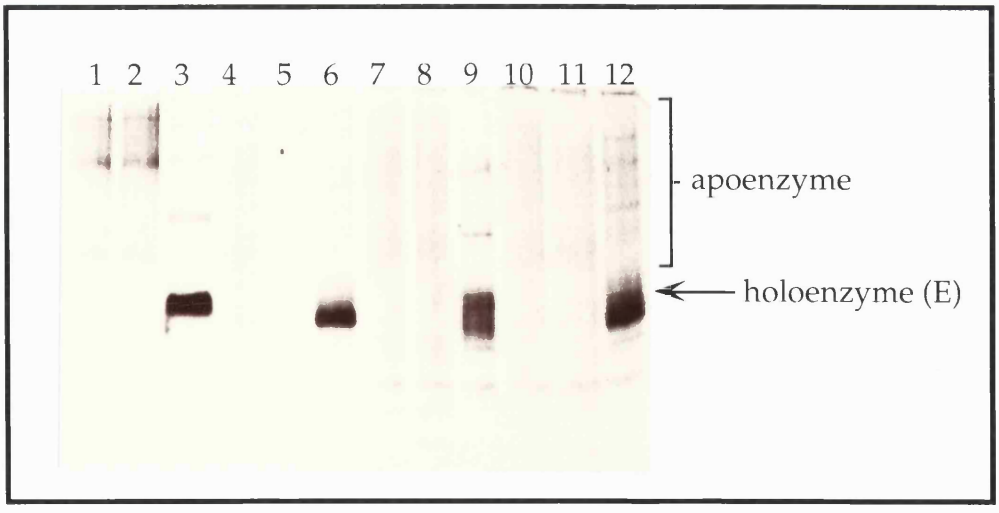

Figure 5.36 Non Denaturing Gel of the Reconstitution of Holoenzyme from the Aspartate-84 Mutants of Apoenzyme , After 4 Hours Porphobilinogen Incubation

The lanes are labelled as for figure 5.35.

Figure 5.37 Non Denaturing Gel of the Reconstitution of Holoenzyme from the Aspartate-84 Mutants of Apoenzyme , After 24 Hours Porphobilinogen Incubation

The lanes are labelled as for figure 5.35.

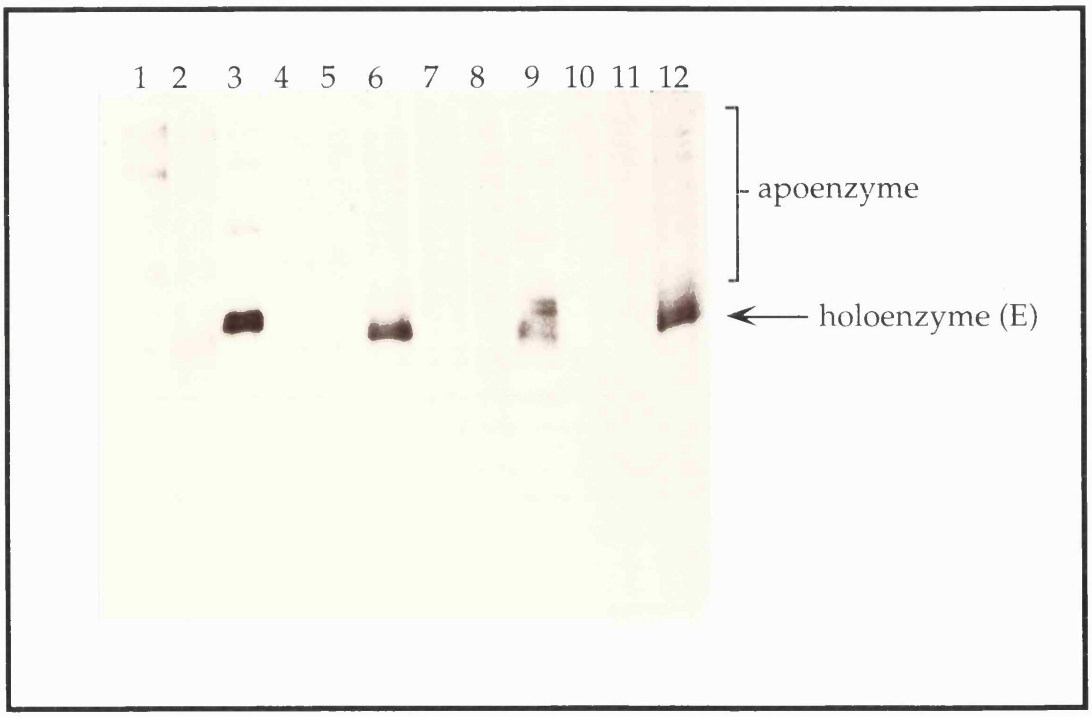

Figure 5.38 Non Denaturing Gel of the Reconstitution of Holoenzyme from the Aspartate-84 Mutants of Apoenzyme , After 48 Hours Porphobilinogen Incubation

The lanes are labelled as for figure 5.35.

The gels in figures 5.35-5.38 show that the samples of the aspartate-84 mutant apoenzyme without substrate incubation (lanes 4, 7, 10) all migrated as the characteristic ladders of bands. All samples of the aspartate-84 mutant holoenzyme before cofactor cleavage displayed bands which migrated beyond the ladder, typical of holoenzyme and enzyme-intermediate complexes (lanes 6, 9, 12). The mutants, before cleavage, also displayed a ladders of bands characteristic of apoenzyme bands.

The wild-type apoenzyme which had been incubated with substrate (lane 2) migrated as a ladder with additional bands migrating beyond holoenzyme (lane 3), as observed for samples which had reconstituted the holoenzyme and made enzyme-intermediate complexes. The substrate incubated D84E apoenzyme (lane 8) was also seen to reconstitute a small percentage of holoenzyme and enzyme-intermediate complexes, for the gel

run immediately on incubation with substrate. The substrate incubated D84A apoenzyme (lane 5) was seen to have reconstituted a small percentage of holoenzyme after twenty four hours. The substrate incubated D84N apoenzyme (lane 11) was observed to display a faint band for holoenzyme, but only after forty eight hours.

The rate of reconstitution of holoenzyme and enzyme-intermediate complexes had therefore been greatly reduced for all three apoenzyme mutants of aspartate-84. The results would suggest therefore that the same mechanism is employed for molecular recognition of porphobilinogen by apoenzyme as for recognition of porphobilinogen by holoenzyme. The marginally increased rate of reconstitution for the D84E mutant apoenzyme, which has a slightly higher specific activity than the other mutants, is consistent with this theory.

Throughout the thesis, 'CD-UV' should read 'UV-CD'.

5.3 Conclusions

The aim for this chapter was to characterise fully the apoenzyme of porphobilinogen deaminase. In particular, cofactor assembly was of interest, as were comparisons between apoenzyme and holoenzyme. The first step towards achieving the characterisation was the introduction of a highly efficient purification step of affinity chromatography, which allowed the apoenzyme to be purified from the *hemB* strain in a single step. It was interesting to note that apoenzyme purified in this way had identical characteristics to apoenzyme generated from the acidic cleavage of the cofactor from holoenzyme.

Investigation of the reconstitution of holoenzyme from apoenzyme led to the hypothesis of a new theory for cofactor assembly. The interpretation of results presented in this chapter in conjunction with observations from the D84A and D84N mutants (Chapter 3) suggested that preuroporphyrinogen was the preferred substrate for apoenzyme. Apoenzyme was also able to assemble the cofactor from porphobilinogen, although a lag in activity was observed of around 15 minutes. It now appears likely that this lag represents the time required to generate a small amount of holoenzyme, which in turn then generates preuroporphyrinogen.

Apoenzyme was observed to be considerably more susceptible to degradation by heat and proteolysis than holoenzyme. This was a predicted result, and confirmed that cofactor absence led to a more open, flexible tertiary structure. However, only pure apoenzyme was examined for its stability to heat; it has been noted for mutant forms that the apoenzyme can withstand heat treatment to some degree in a crude extract (see Chapter 3).

Inhibition studies using substrate analogues were also carried out on apoenzyme and holoenzyme. Inactivation by BrPBG pointed towards a similar mechanism for incorporation of porphobilinogen being employed for both cofactor assembly and chain elongation. The inhibition studies using FPBG reached the same conclusion. Whilst we now know that preuroporphyrinogen is in fact the preferred substrate for apoenzyme, the binding of porphobilinogen to the apoenzyme is still likely to occur using the same catalytic machinery. The results therefore indicate that the cofactor and polypyrrole chain may be assembled using the same catalytic groups.

Apoenzyme forms of the cysteine mutants, C242S and C134S, were also generated and isolated by the same methods. Surprisingly, some cofactor assembly could be achieved for the C242S mutant apoenzyme when analysed by non denaturing gel electrophoresis. The C134S mutant apoenzyme displayed similar characteristics to wild-type apoenzyme, suggesting that the residue cysteine-134 was not directly important for cofactor assembly. The results of the inhibition of these mutants by NEM were difficult to confirm, due to the lack of activity of apoenzyme in the absence of reducing agent. However, the results appeared to suggest that both cysteine-242 and -134 were exposed in the apoenzyme form. Additionally, modification of these residues led to inactivation of the enzyme, probably due to destabilisation of the structure.

Apoenzyme forms of the aspartate-84 mutants, D84A, D84E and D84N were also generated. It was surprising that none of these mutant apoenzymes generated from the *hemB* strains could be purified by affinity chromatography. The mutation of a single residue appeared to greatly affect the binding capacity. All three mutants were subsequently generated from their corresponding holoenzyme forms by acidic cleavage of the cofactor and were examined for cofactor assembly using porphobilinogen as a substrate. All three mutants appeared unable to assemble the cofactor within forty-eight hours, unlike the wild-type apoenzyme which had assembled the cofactor within four hours as examined by non denaturing gel electrophoresis. The slow rate of cofactor assembly for these mutants was comparable to their slow rate of catalysis. These results suggest that the aspartate-84 residue is likely to have an important role in cofactor assembly as well as chain elongation.

A more informative experiment may have been the study of the addition of preuroporphyrinogen to apoenzyme. A comparison of the rate of binding by the apoenzyme forms of the wild-type and the aspartate-84 mutants would have allowed the role of aspartate-84 in cofactor assembly to be better examined. Preliminary experiments of this nature were carried out (data not shown). It appeared, however, that the apoenzyme forms of the aspartate-84 mutants were unable to convincingly bind preuroporphyrinogen *in vitro*. These result, if confirmed, would suggest that the aspartate-84 residue is important for cofactor assembly. However, the reaction must be able to take place or it would not be possible to isolate the enzyme-intermediate complexes for the D84A and D84N mutants. An interpretation of these results may be

that the reaction is considerably slower for the aspartate-84 mutants *in vivo*, but due to the constant level of preuroporphyrinogen in the cell the mutants are able to generate a proportion of holoenzyme and enzyme-intermediate complexes, which can then be isolated. The observed presence of the apoenzyme form of the D84A and D84N mutants in crude extract supports this theory. Similar concentrations of preuroporphyrinogen would be difficult to generate in vitro, as preuroporphyrinogen is highly unstable with a half-life of only about 5 minutes at 37°C, pH 8.0 (Jordan *et al.*, 1979).

Chapter 6

Circular Dichroism Spectroscopy Study of *E. coli* Wild-Type and Mutant Porphobilinogen Deaminase

6.1 Introduction

The significant improvements in circular dichroism (CD) spectroscopy during recent years have made it possible to analyse the spectrum of a protein for secondary structure with high reliability (Johnson, 1990).

The initial protocol for the analysis of the CD spectra of proteins was produced during the groundbreaking work of Greenfield and Fasman in the late 1960's, who fitted the CD spectra of proteins with the spectra of various known individual secondary structures such as 100% α-helix and 100% β-sheet. However, due to the number of factors that contributed to the CD of a protein it was necessary to devise an alternative method, which is now more commonly used. The current method employs the use of reference spectra derived from the CD of proteins with known secondary structure (e.g. derived from X-ray crystallography).

The CD data recorded in the far CD-UV region (185-250nm) represents the backbone secondary structure of the protein. The CD of proteins is primarily the CD of the amide chromophore, and thus the secondary structure is measured by counting amide-amide interactions. Further information can be obtained from the protein by examining the near CD-UV region (250-320nm), which measures the local tertiary structure of aromatic amino acid residues (Strickland, 1974) and disulphide bonds (Siligardi, 1991).

Three residues contribute to the near CD-UV region, namely tryptophan (290nm), tyrosine (275nm), and phenylalanine (260nm), as well as disulphide bonds. Whilst *E. coli* porphobilinogen deaminase does not have any disulphide bonds, it has two tryptophans, five tyrosines and three phenylalanine residues. From the crystal structure of the *E. coli* isolated enzyme in which the cofactor is oxidised, it is known that one phenylalanine residue, phenylalanine-62, is located in the active site and is stacked against the second ring of the cofactor (Louie *et al.*, 1992). In the structure of the reduced cofactor enzyme, the phenylalanine-62 is seen to be stacked against the proposed substrate binding site (Hadener *et al.*, 1992). Whilst the contributions of the phenylalanine residues to the near CD-UV region carry the least weight of all the residues, it is still conceivable that

the local environment of this residue will change the most significantly in the course of any reaction, and therefore may serve as an active site marker.

In the absence of a structure for the apoenzyme of porphobilinogen deaminase, the work presented in this chapter was performed in order to investigate the changes in structure associated with the transformation of apoenzyme to holoenzyme. Furthermore, the studies were used to confirm that the structure of the holoenzyme at pH 5.1, the pH at which the enzyme is crystallised, is similar to that of enzyme at pH 8.0. The mutants of residue aspartate-84 were also examined.

The studies were carried out at Birkbeck College, London, which provides the National EPSRC Facility for Chiroptical Spectroscopy. Thanks are extended to Alexander Drake, and in particular Guiliano Siligardi.

6.2 Results and Discussion

All CD spectra were collected on either a JASCO J-720 or J-600 spectropolarimeter, according to the Materials and Methods. Secondary structure predictions were made using the "Grams" Multiple Component Analysis Software.

6.2.1 Comparison between Apoenzyme and Holoenzyme

The introduction section in Chapter 5 dealt with the properties and characteristics of apoenzyme. In general, the apoenzyme is found to be less stable than the holoenzyme, and this instability has been attributed to a less folded structure. A structure in which the domains are not held tightly together could easily be explained by the lack of the dipyrromethane cofactor in the apoenzyme, which provides a number of salt links and hydrogen bonds to the protein to induce the enzyme into a compact stable tertiary holoenzyme structure (Louie *et al.*, 1992). However, a structure for the apoenzyme in which the protein is totally unfolded has also been proposed and supported by NMR studies (Scott *et al.*, 1989). It would be more difficult to accept, though, that the addition of a cofactor would first lead to folding in the protein, and then a closing of the domains around it.

6.2.1.1 Far CD-UV

The spectra of apoenzyme and holoenzyme measured in the far CD-UV region are overlaid in figure 6.1. The secondary structure predictions from these spectra are given in Table 6.1. The secondary structure determinations for holoenzyme, derived from the x-ray crystal structure, are also given for comparison.

The spectra in figure 6.1 and predictions in table 6.1 suggest that the apoenzyme was not unfolded and, whilst the apoenzyme contained 5% less helical structure than the holoenzyme, it also contained 2.5% more β-sheet. The crystal structure of the holoenzyme has shown that there are few contacts between the three domains of the protein, and the majority of contacts that stabilise the association between the three domains of the

Figure 6.1 Far CD-UV Spectra Showing Apoenzyme and Holoenzyme

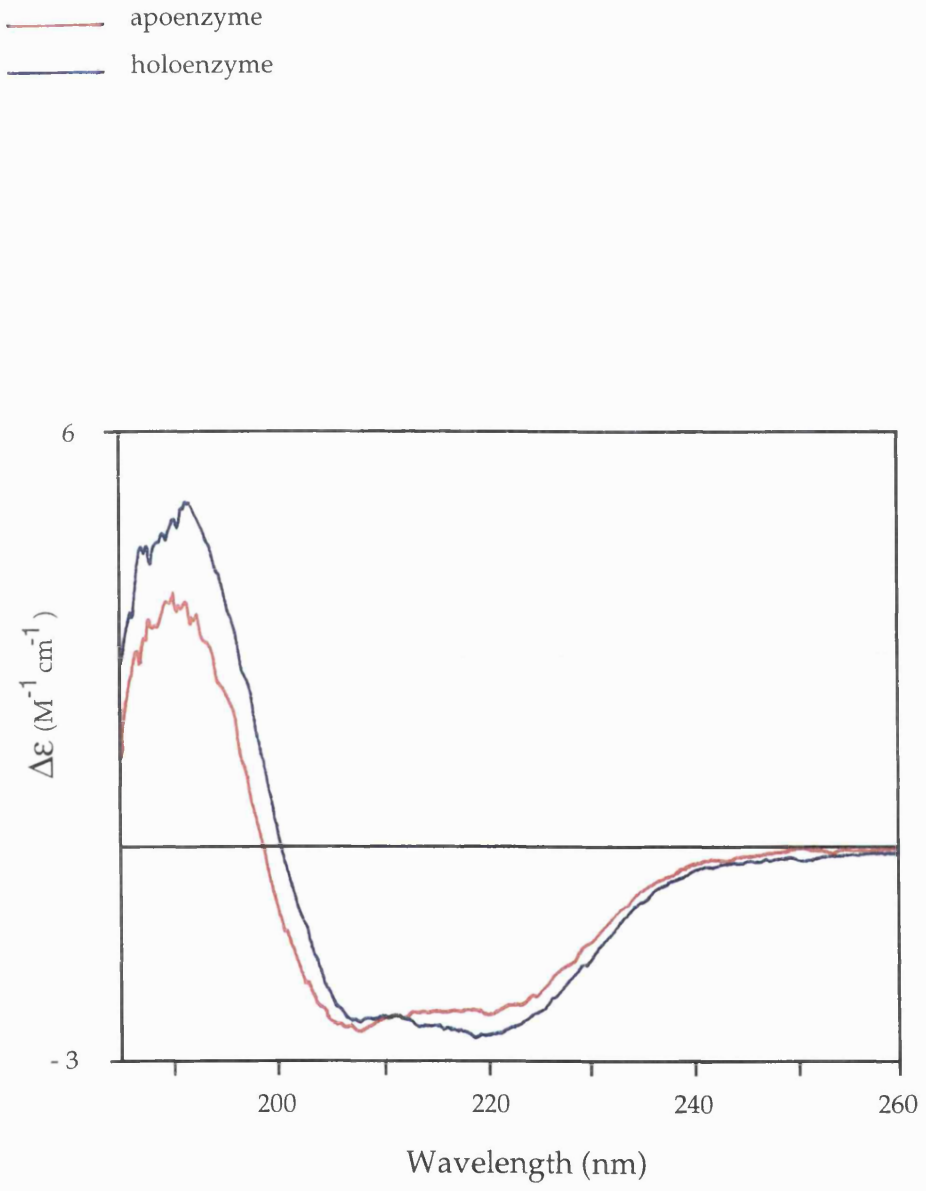

Table 6.1 Secondary Structure Predictions of Apoenzyme and Holoenzyme by CD Spectroscopy

Protein	Method of Structure Prediction	Conformation (%)		
		α	β	Other
Apoenzyme	CD	17.6	30.2	52.2
Holoenzyme	CD	22.7	27.7	49.6
Holoenzyme	X-ray	38.0	33.0	29.0

protein are formed between the enzyme and the cofactor. Therefore, it appears likely that the apoenzyme is folded, but mobile around the interdomain segments, leaving the protein with greater flexibility and therefore susceptibility to thermal denaturation and proteolytic degradation.

The comparison between the secondary structure predictions for holoenzyme made by CD spectroscopy and X-ray crystallography show considerable differences. The structure prediction made by CD spectroscopy had been calculated for enzyme which had been resuspended in 20mM Tris/ HCl buffer, pH 8.0, containing 13mM β-mercaptoethanol. The crystallisation, however, had been achieved in 100mM sodium acetate buffer, at pH 5.0. Therefore, the holoenzyme was instead resuspended in 20mM sodium acetate buffer, at both pH 5.1 and 7.4, and the spectra again measured in the far CD-UV region (the experiment and the spectra are described in detail later in section 6.2.5). The structure predictions at both pHs were very similar, 31 % α conformation, 32% β conformation and 37% other, and these predictions were much closer to that of the X-ray derived determination. The results therefore indicated that the holoenzyme adopted different conformations in the two buffers. However, the enzyme is known to be more active in Tris/ HCl buffer (Warren, 1988), and therefore the use of Tris was continued for subsequent experiments.

6.2.1.2 Near CD-UV

The spectra of apoenzyme and holoenzyme measured in the near CD-UV region are overlaid in figure 6.2.

Figure 6.2 shows significant, measurable differences in the local environment of the residues tyrosine and phenylalanine. The spectra of apoenzyme and holoenzyme provided a reference to which subsequent spectra could be compared and thus could be used to study the conversion of apoenzyme to holoenzyme.

Figure 6.2 Near CD-UV Spectra Showing Apoenzyme and Holoenzyme

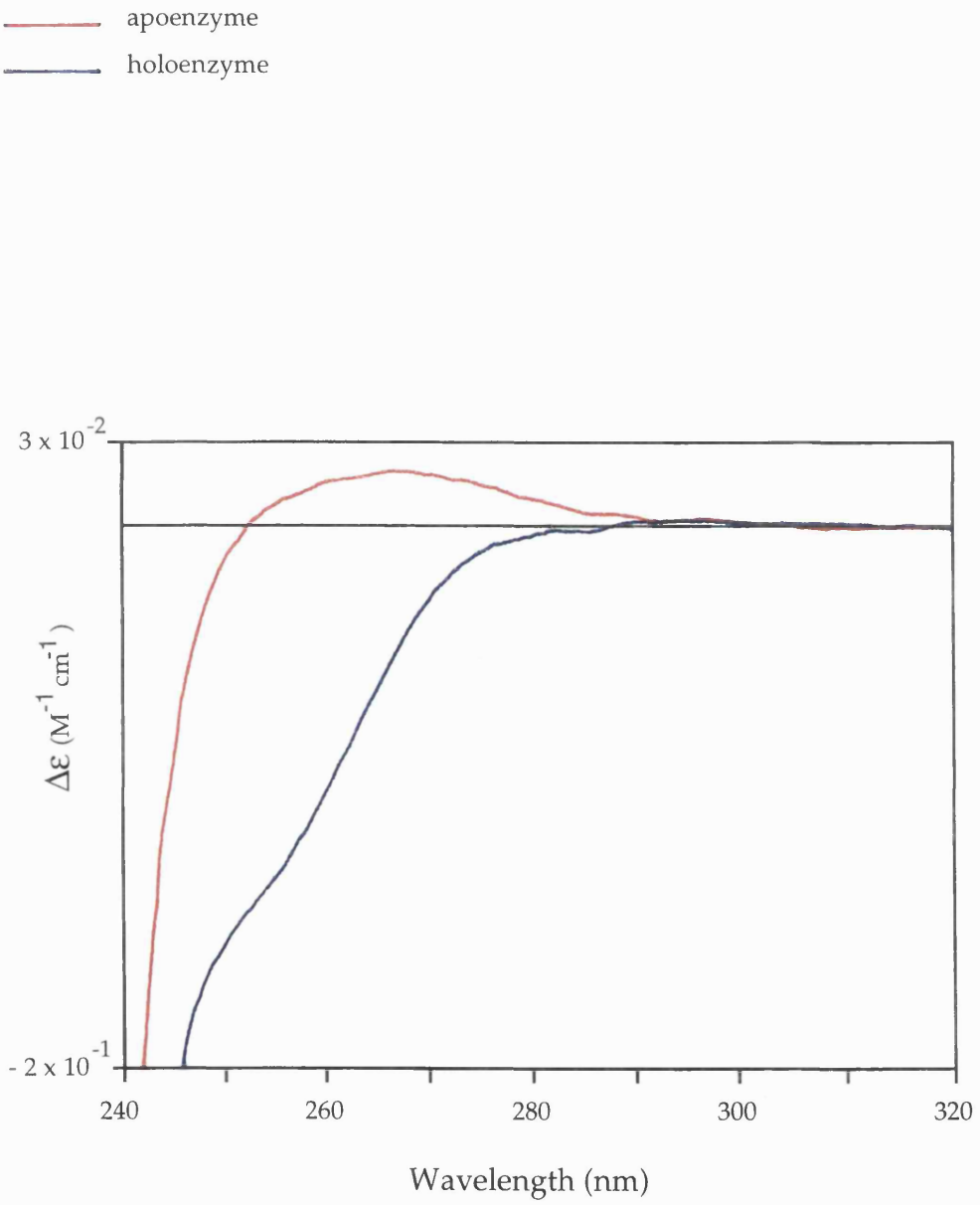

6.2.2 Substrate Binding - The Addition of Porphobilinogen to Holoenzyme

The binding of substrate to wild-type holoenzyme was examined by CD spectroscopy.

The temperature of the protein was first raised from room temperature, 20°C, to the incubation temperature of 37°C. Porphobilinogen was then added, and the spectra monitored over a period of time.

6.2.2.1 Far CD-UV

The spectra of holoenzyme and substrate-incubated holoenzyme are overlaid in figure 6.3. The secondary structure of holoenzyme appears unchanged on adding an excess of substrate. However, it is known that conformational changes do take place on adding substrate to holoenzyme (Warren and Jordan, 1988, Warren *et al.*, 1995), and it may be that the changes are too subtle to be detected by CD spectroscopy. The conformational change of reconstituting holoenzyme from apoenzyme is considered to be a more dramatic change and, yet, only small differences are observed in the backbone structures between the two. Therefore, it is not surprising that changes cannot be detected on adding substrate to holoenzyme.

6.2.2.2 Near CD-UV

Spectra were also recorded in the near CD-UV region for the addition of substrate to holoenzyme. In this region, it was anticipated that more meaningful changes could be recorded. The positioning of phenylalanine-62 against the predicted substrate-binding site would suggest that the local environment of this residue may change during the catalytic cycle of the enzyme. A four molar equivalent of porphobilinogen was added to the holoenzyme, the temperature of the protein was raised to 37°C for the incubation and, after a period of time, again reduced to room

Figure 6.3 Far CD-UV Spectra Showing the Effect of the Addition of Porphobilinogen to Holoenzyme

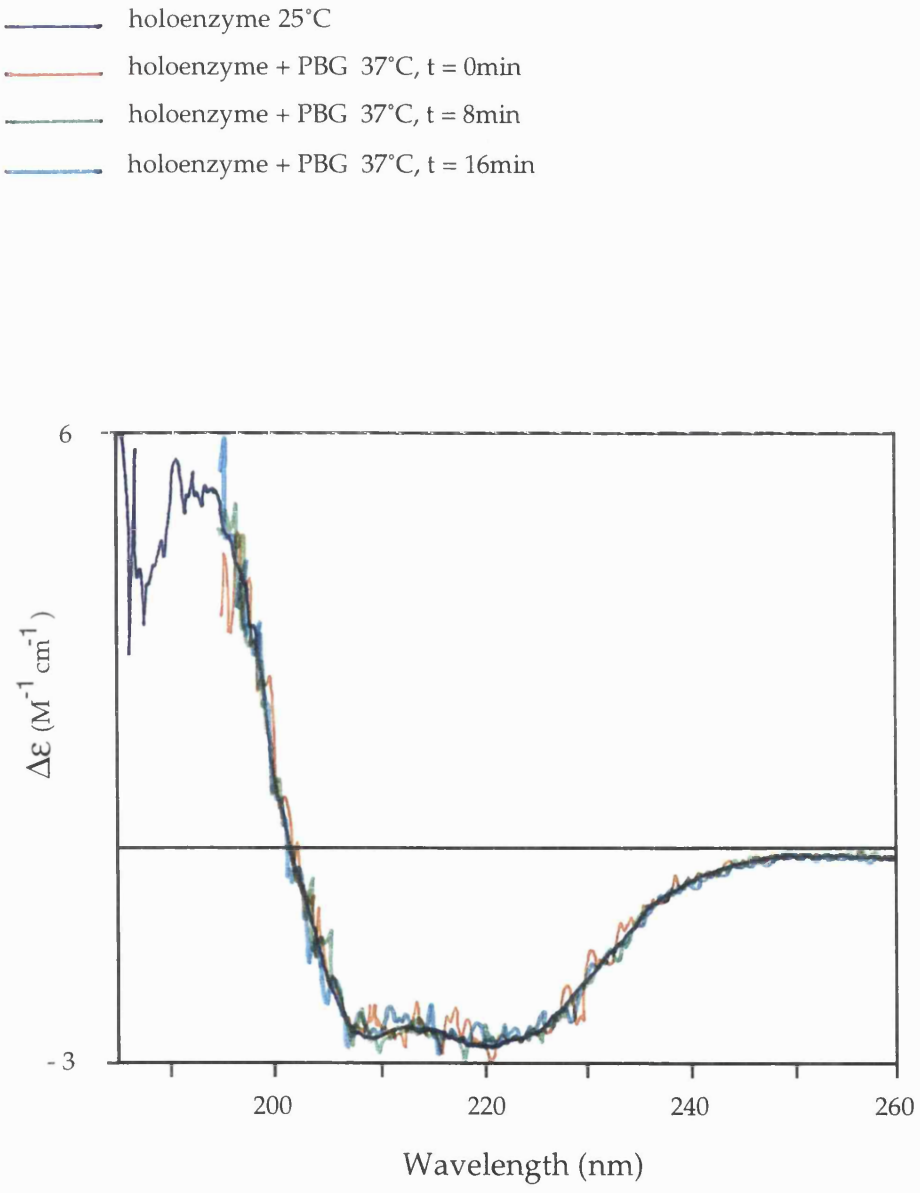

temperature. The spectra of holoenzyme and substrate-incubated holoenzyme can be seen in figure 6.4.

The initial raising of the temperature of holoenzyme in the absence of substrate had no effect on the spectra shown in figure 6.4. However, the addition of substrate had an immediate effect and the spectra showed changes in the environment of all three aromatic residues. Subsequently, with time, the environment of the tryptophan and tyrosine residues did not appear to change, but the environment of the phenylalanine appeared to be fluctuating slightly. Finally, dropping the temperature of the incubation also brought about changes in the phenylalanine environment, but this is likely to be due to the continuing effect of the substrate.

The majority of the change had occured immediately, with only slight fluctuations still observed after eight minutes. This is not surprising, as the holoenzyme would be expected to turn over such a small excess of porphobilinogen within the first eight minutes.

Figure 6.4 Near CD-UV Spectra Showing the Effect of the Addition of Porphobilinogen to Holoenzyme

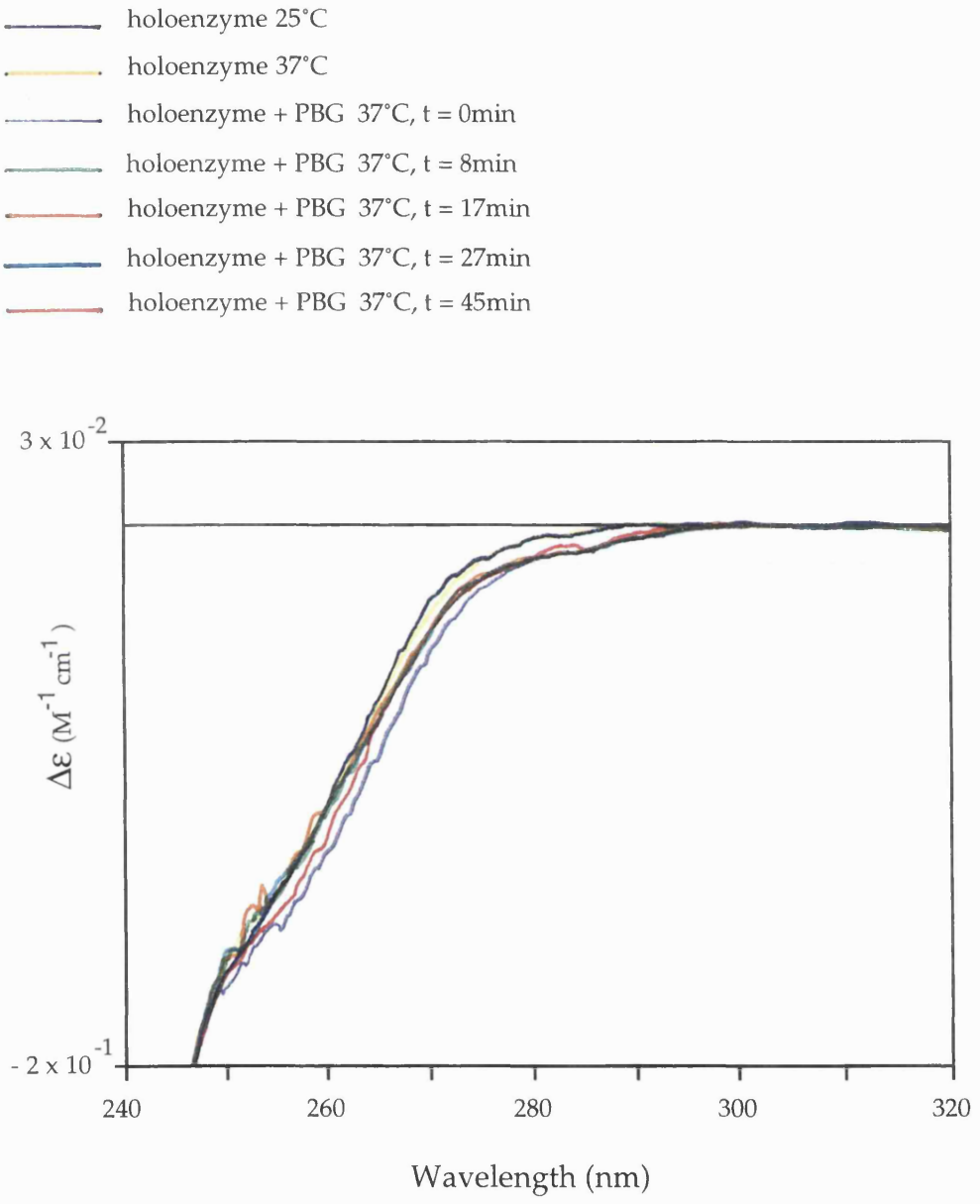

6.2.3 Reconstitution of Holoenzyme - The Addition of Porphobilinogen to Apoenzyme

The apoenzyme can be converted to holoenzyme *in vitro* with a yield of about 40% by incubation of apoenzyme with porphobilinogen (Scott *et al.*, 1989; Hart *et al.*, 1988; see also Chapter 5). The conversion of apoenzyme to holoenzyme is seen to display a lag phase of around thirty minutes, after which time the conversion is observed at a faster rate. It is now suggested that this lag phase is the time required to generate some active holoenzyme with which preuroporphyrinogen will be quickly generated to serve as the cofactor precursor for apoenzyme. The addition of porphobilinogen or preuroporphyrinogen to apoenzyme is predicted to bring about conformational changes, as the pyrrole rings are incorporated into the protein to form the dipyrromethane cofactor. In the case of the addition of preuroporphyrinogen, two substrate rings will also be added. Once formed, the interactions of the cofactor with the three domains allows the protein to form a stable tertiary structure. The reconstitution of holoenzyme from apoenzyme was monitored by CD spectroscopy. As previously explained, the discovery that preuroporphyrinogen was the preferrential substrate for apoenzyme came from the last results of the research, and therefore the majority of experiments presented in this chapter were carried out with porphobilinogen only.

6.2.3.1 Far CD-UV

Apoenzyme was incubated with a two molar equivalent of porphobilinogen at 37°C for two hours, and the far CD-UV region recorded. The region was not monitored with time. The overlaid spectra for apoenzyme, substrate-incubated apoenzyme and holoenzyme can be seen in figure 6.5. The secondary structure predictions for the three spectra can be seen in Table 6.2.

The spectra in figure 6.5 and predictions in table 6.2 show that the α-helical content of apoenzyme had increased a small amount on adding porphobilinogen, but the β-sheet content remained unchanged. The other conformations had also dropped on the addition of porphobilinogen.

Figure 6.5 Far CD-UV Spectra Showing the Effect of the Addition of Porphobilinogen to Apoenzyme

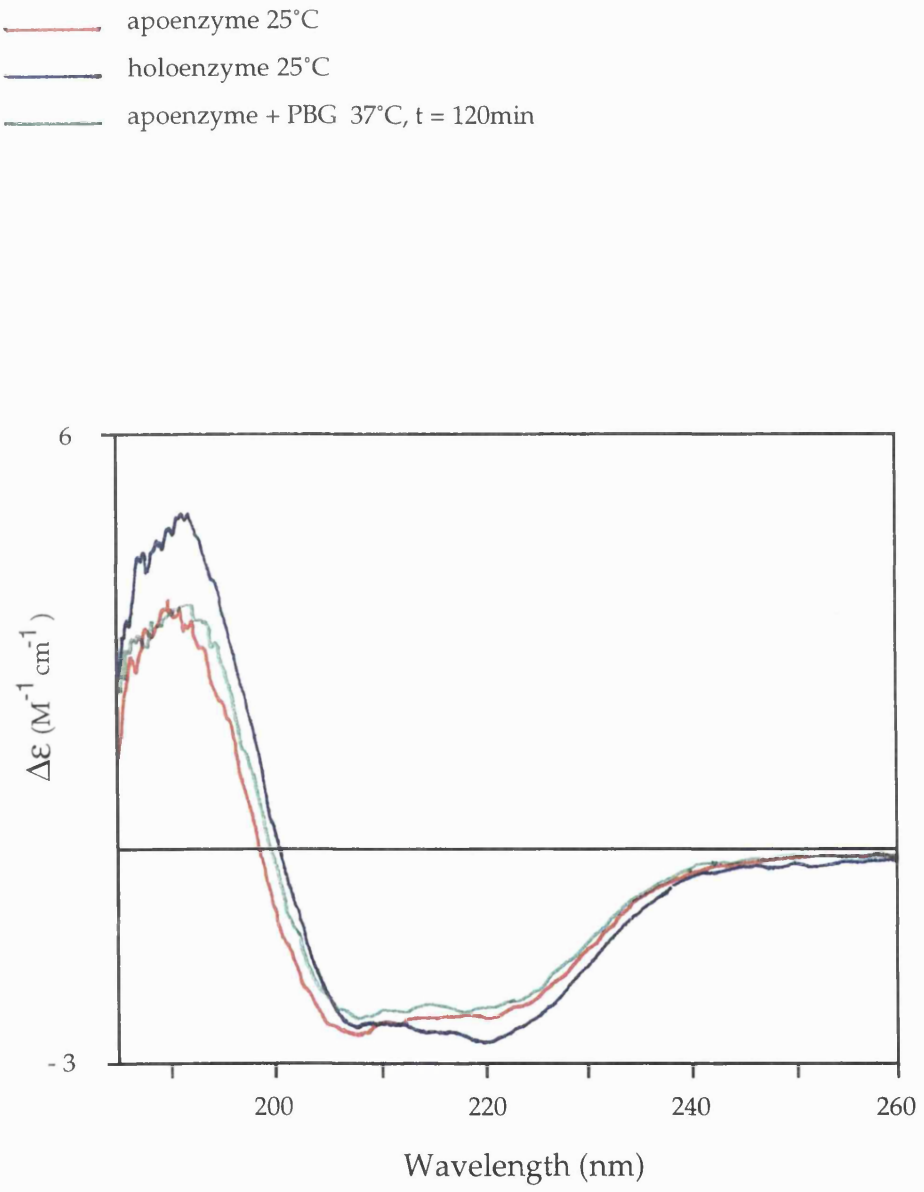

Table 6.2 Secondary Structure Predictions of Apoenzyme, Substrate-Incubated Apoenzyme and Holoenzyme by CD Spectroscopy

Protein	Conformation (%)		
	α	β	Other
Apoenzyme	17.6	30.2	52.2
Substrate-Incubated Apoenzyme	18.9	30.6	50.5
Holoenzyme	22.7	27.7	49.6

Therefore, the apoenzyme structure could be seen to become slightly more ordered (~25%) upon incubation with porphobilinogen.

6.2.3.2 Near CD-UV

The reconstitution of holoenzyme was anticipated as being most successfully examined in the near CD-UV region as it was hoped that phenylalanine-62 would serve as a suitable marker for the active site changes.

A two molar equivalent of porphobilinogen was added to the apoenzyme, to allow the cofactor to be bound by the apoenzyme. The temperature of the apoenzyme was raised from room temperature (20°C) to the incubation temperature of 37°C. Substrate was then added, and the mixture monitored with time. Finally, the temperature was again dropped to 20°C. The overlaid spectra for apoenzyme, substrate-incubated apoenzyme and native holoenzyme can be seen in figure 6.6, with the breakdown of changes given, for clarity, in figure 6.7.

The raising of the temperature of apoenzyme from 20°C to 37°C gave slight differences in the phenylalanine environment of the spectra shown in figures 6.6 and 6.7. The addition of substrate as monitored with

Figure 6.6 Near CD-UV Spectra Showing the Effect of the Addition of Porphobilinogen to Apoenzyme

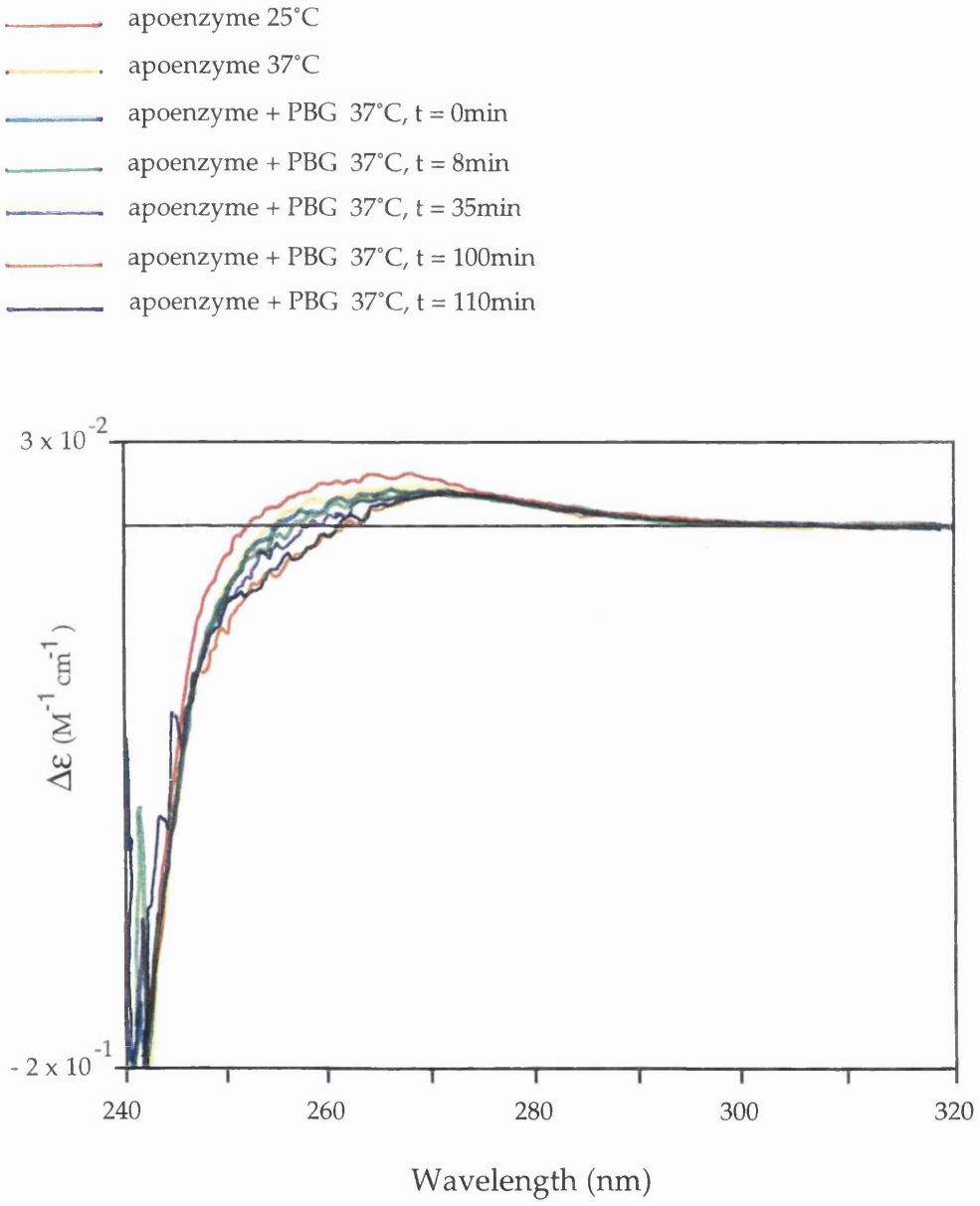

Figure 6.7 Near CD-UV Spectra Showing a Breakdown of the Changes Occurring Upon the Addition of Porphobilinogen to Apoenzyme

Colours are as given in figure 6.6

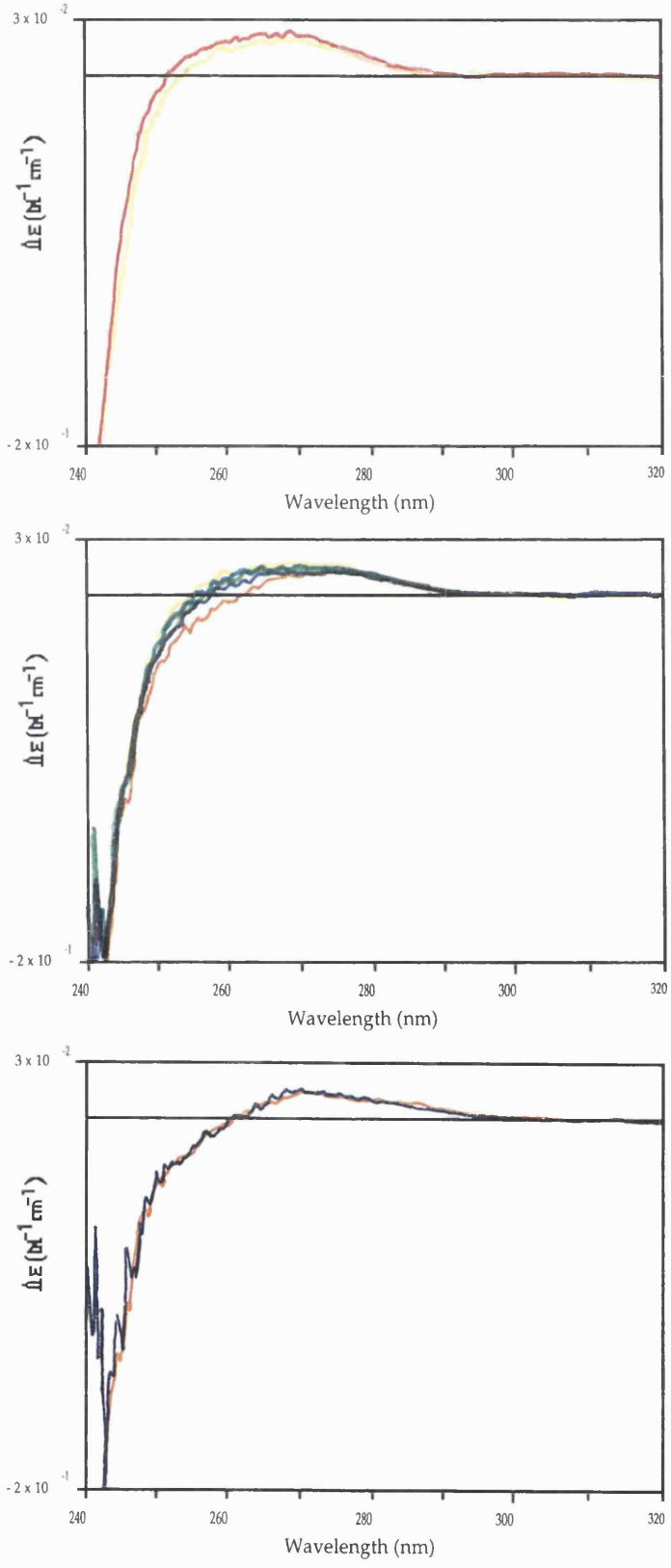

time gave gradual changes in the phenylalanine environment, as the local surroundings of the phenylalanine moved slowly towards that of holoenzyme. Lowering the temperature brought about no significant variance, and it appeared therefore that the reaction had been completed.

The substrate-incubated apoenzyme was monitored again after a further two hours, and no further changes were observed. The final spectra of apoenzyme, substrate-incubated apoenzyme and holoenzyme are given in figure 6.8.

6.2.3.3 Reconstitution of Holoenzyme - The Effect of Adding a One-Fiftieth Equivalent of Holoenzyme

The addition of a one-fiftieth molar equivalent of holoenzyme to apoenzyme, in conjunction with porphobilinogen, has been observed to give a more rapid and complete conversion of apoenzyme to holoenzyme. The reasons for this, namely, the preferential binding of preuroporphyrinogen to apoenzyme, are given in Chapter 5. The effect of a one-fiftieth molar equivalent of holoenzyme in the reconstitution of holoenzyme from apoenzyme was therefore monitored by CD.

6.2.3.3.1 Far CD-UV

Apoenzyme was incubated with a two-molar equivalent of porphobilinogen, in the presence and absence of a one-fiftieth molar equivalent of holoenzyme at 37°C for two hours. The overlaid spectra of apoenzyme, substrate-incubated apoenzyme, substrate/holoenzyme-preincubated apoenzyme and holoenzyme are given in figure 6.9.

Figure 6.9 shows that the additional presence of a one-fiftieth molar equivalent of holoenzyme had not affected the backbone spectra significantly more than the addition of porphobilinogen alone to the apoenzyme.

Figure 6.8 Near CD-UV Spectra Showing the Effect of a Long Incubation of Porphobilinogen with Apoenzyme

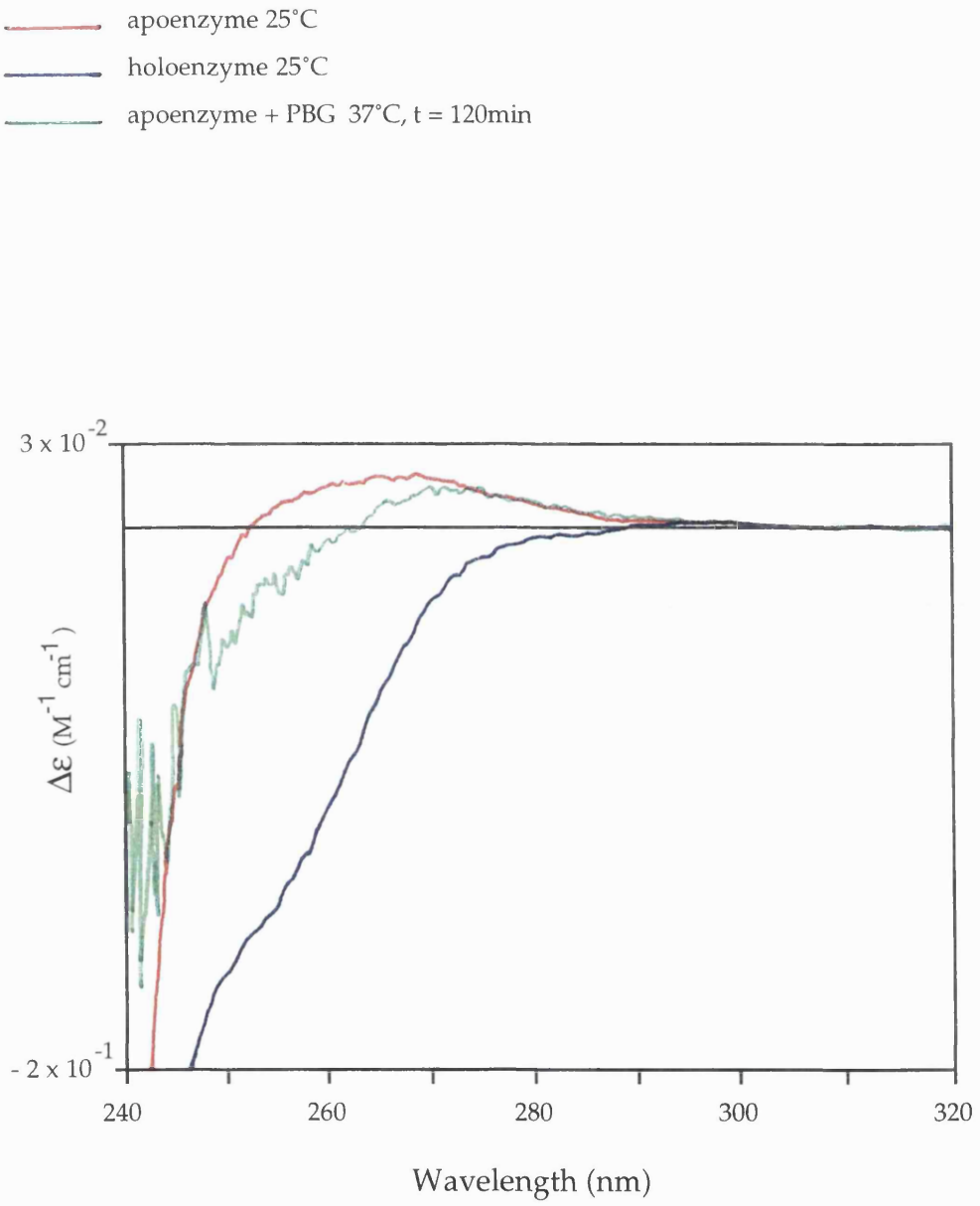

Figure 6.9 Far CD-UV Spectra Showing the Effect of the Addition of Both Porphobilinogen and a One-Fiftieth Molar Equivalent of Holoenzyme to Apoenzyme

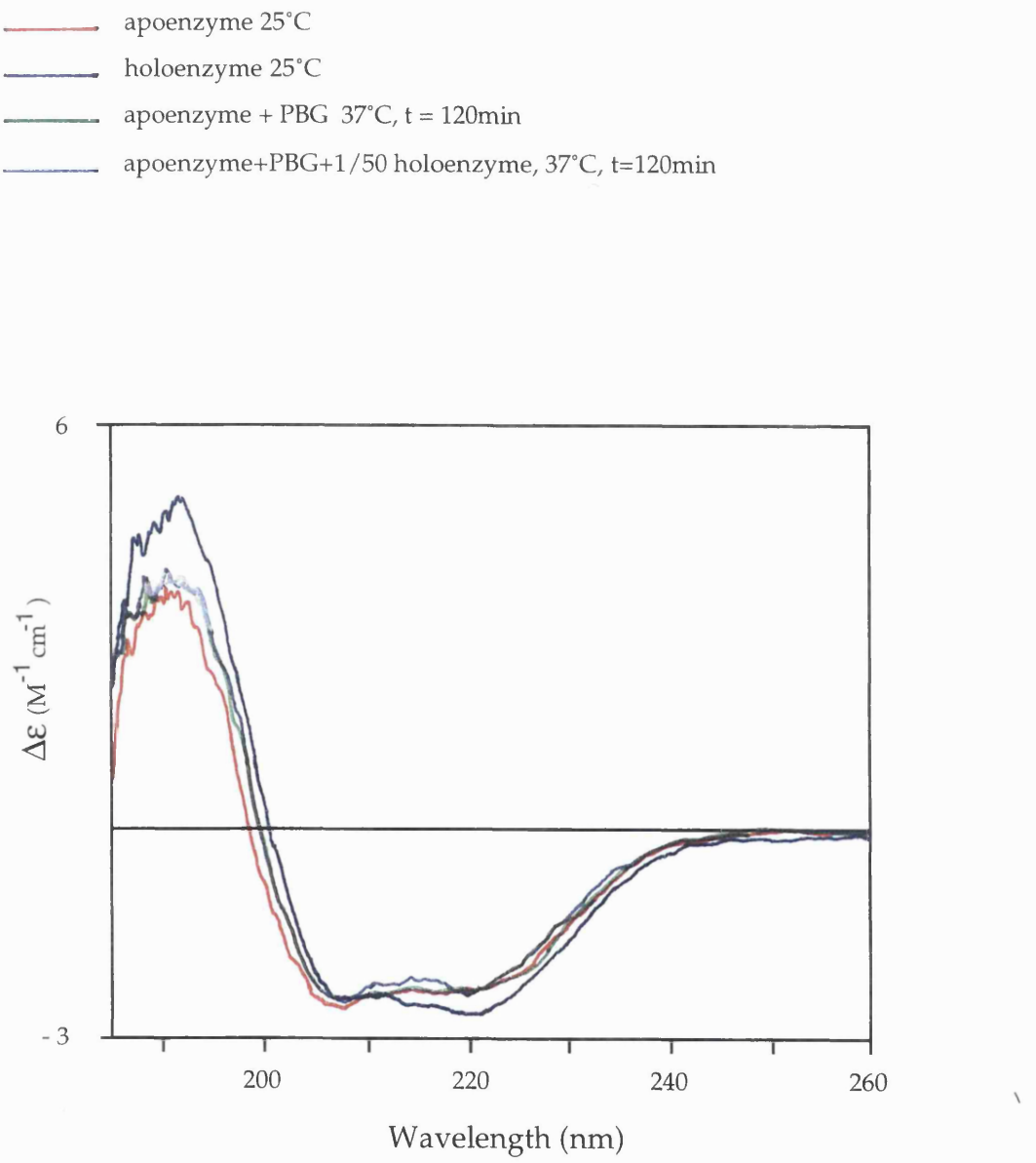

6.2.3.3.2 Near CD-UV

Apoenzyme was incubated with a two-molar equivalent of porphobilinogen, in the presence and absence of a one-fiftieth molar equivalent of holoenzyme at 37°C for two hours. The overlaid spectra of apoenzyme, substrate-incubated apoenzyme, substrate/holoenzyme-preincubated apoenzyme and holoenzyme are given in figure 6.10.

Figure 6.10 shows that the presence of a one-fiftieth molar equivalent of holoenzyme had no additional effect to that of substrate only-incubated apoenzyme. From comparing these results to the effect the small equivalent of holoenzyme has on activity, it is likely that the difference in results has arisen from the different conditions used during enzyme assay. The enzyme assay requires that, subsequent to the preincubation of apoenzyme with a small molar equivalent of substrate, a large excess of porphobilinogen is added. The CD spectroscopy studies have not included such an excess, due to signal : noise restrictions and the dilution factor. Therefore it may be the case that the porphobilinogen had been turned over and exhausted before the apoenzyme has maximally reconstituted to holoenzyme. The effect of the one-fiftieth molar equivalent of holoenzyme was probably in allowing a more rapid conversion of apoenzyme to holoenzyme, which would have occurred in minutes and not hours.

6.2.3.4 The Maximum Reconstitution of Holoenzyme from Apoenzyme

6.2.3.4.1 -By the Addition of Porphobilinogen - Near CD-UV

The maximum reconstitution of holoenzyme from the addition of porphobilinogen to apoenzyme is generally observed to be around 40%, as determined by the monitoring of activity (Chapter 5). To examine the maximum reconstitution that could be obtained, apoenzyme was incubated with a ten molar excess of porphobilinogen at 4°C and spectra were collected at short time intervals. Apoenzyme was also incubated with a ten molar excess of porphobilinogen at 37°C for 3 hours and the

Figure 6.10 Near CD-UV Spectra Showing the Effect of the Addition of Both Porphobilinogen and a One-Fiftieth Molar Equivalent of Holoenzyme to Apoenzyme

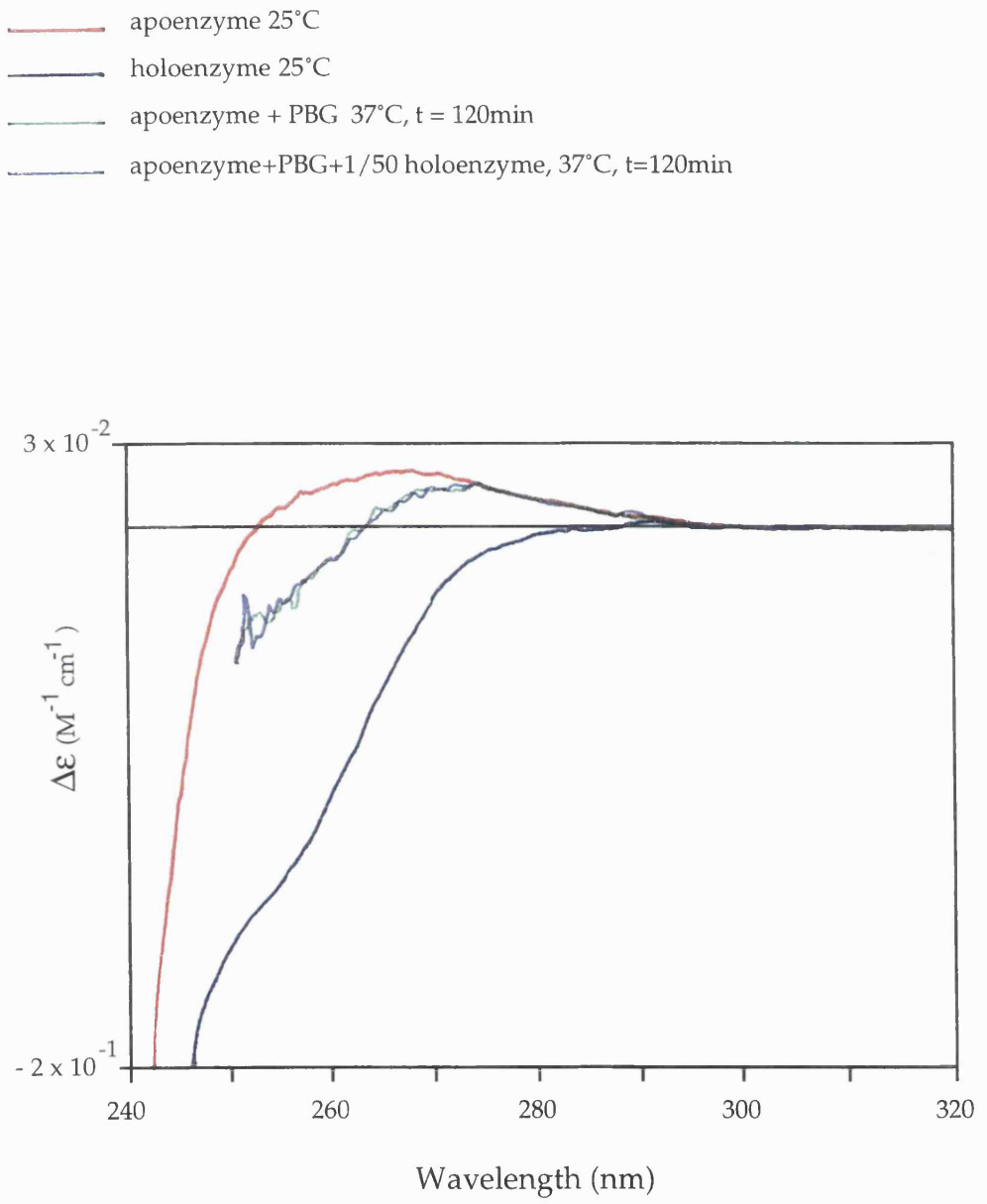

spectrum recorded. The spectra of apoenzyme, substrate-incubated apoenzyme at 4°C and holoenzyme can be seen in figure 6.11. The spectra of apoenzyme, substrate-incubated apoenzyme at 37°C and holoenzyme are shown in figure 6.12.

Simulated spectrum of apoenzyme and holoenzyme mixes had been found to correlate well with the spectra of apoenzyme and holoenzyme which had been physically mixed. Simulations were therefore made to fit with the recorded spectra of holoenzyme reconstitution.

Figures 6.11 and 6.12 show that, upon substrate incubation at 4°C, the environment of the phenylalanine residue would change slowly and move towards that of holoenzyme. The change appeared to be more rapid at 37°C, as the phenylalanine and tyrosine environment had moved further towards that of holoenzyme in a similar time scale. The simulated spectrum showed that the incubation of apoenzyme with porphobilinogen at 37°C for 3 hours were close to the spectrum of a mix of apoenzyme (65%) and holoenzyme (35%).

6.2.3.4.2 -By the Addition of Preuroporphyrinogen - Near CD-UV

The reconstitution of holenzyme from apoenzyme has also been investigated by the addition of preuroporphyrinogen, and has been found to display no lag phase in the recovery of activity (see Chapter 5). Apoenzyme was therefore incubated with a ten molar excess of preuroporphrinogen (free from porphobilinogen and enzyme) at 4°C and spectra were collected at short time intervals. After a two hour incubation, the temperature was raised to 37°C to examine any effects. The spectra of apoenzyme, preuroporphyrinogen-incubated apoenzyme and holoenzyme can be seen in figure 6.13.

Figure 6.13 shows that upon the addition of preuroporphyrinogen to apoenzyme, there is an instant change in the environment of the phenylalanine and tyrosine residues. The change progresses with time, and after two hours at 4°C the spectra is close to that of holoenzyme. Raising the temperature brought a further change, but this may just be the

Figure 6.11 Near CD-UV Spectra Showing the Maximum Effect of the Addition of Porphobilinogen to Apoenzyme at 4°C

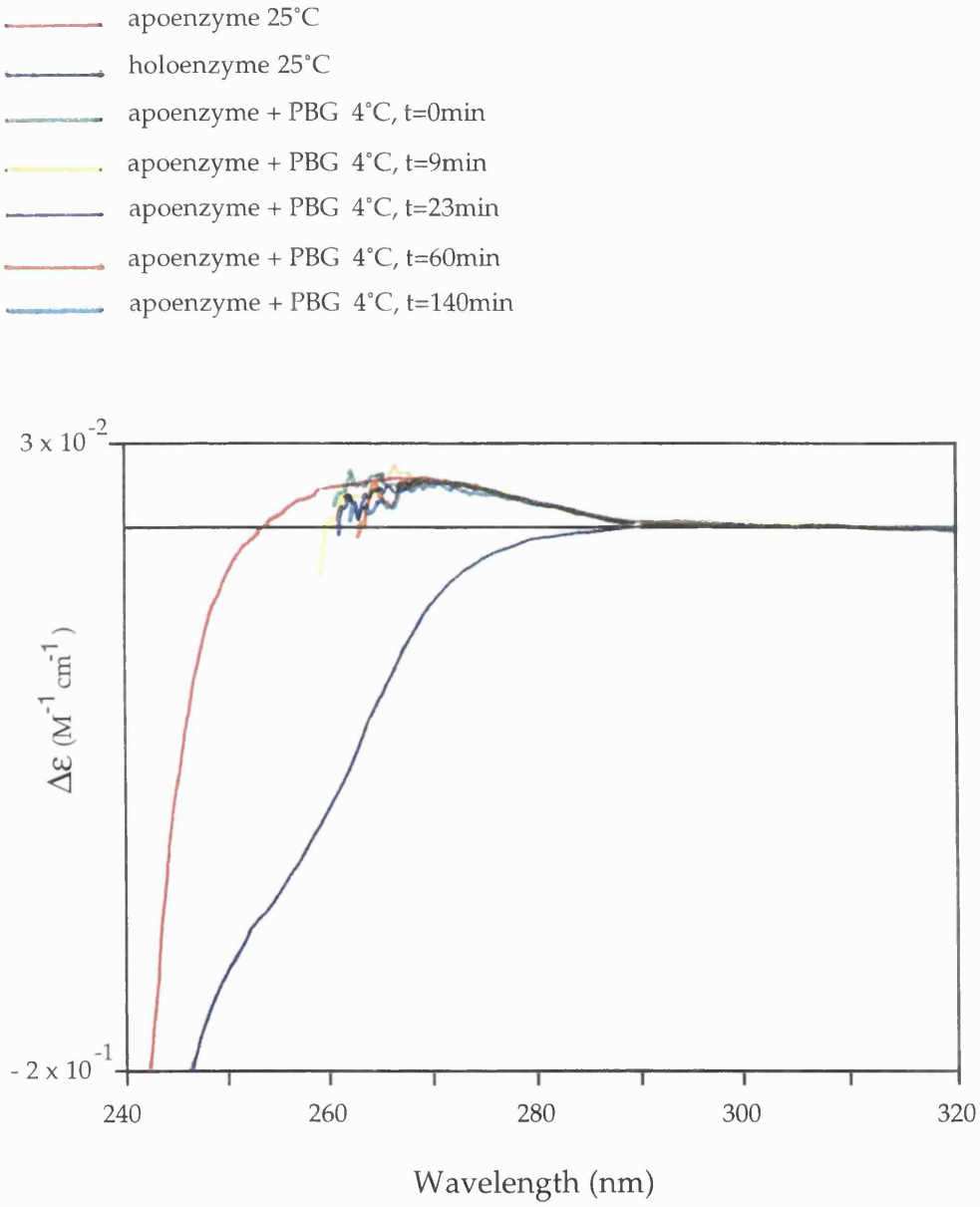

Figure 6.12 Near CD-UV Spectra Showing the Maximum Effect of the Addition of Porphobilinogen to Apoenzyme at 37°C

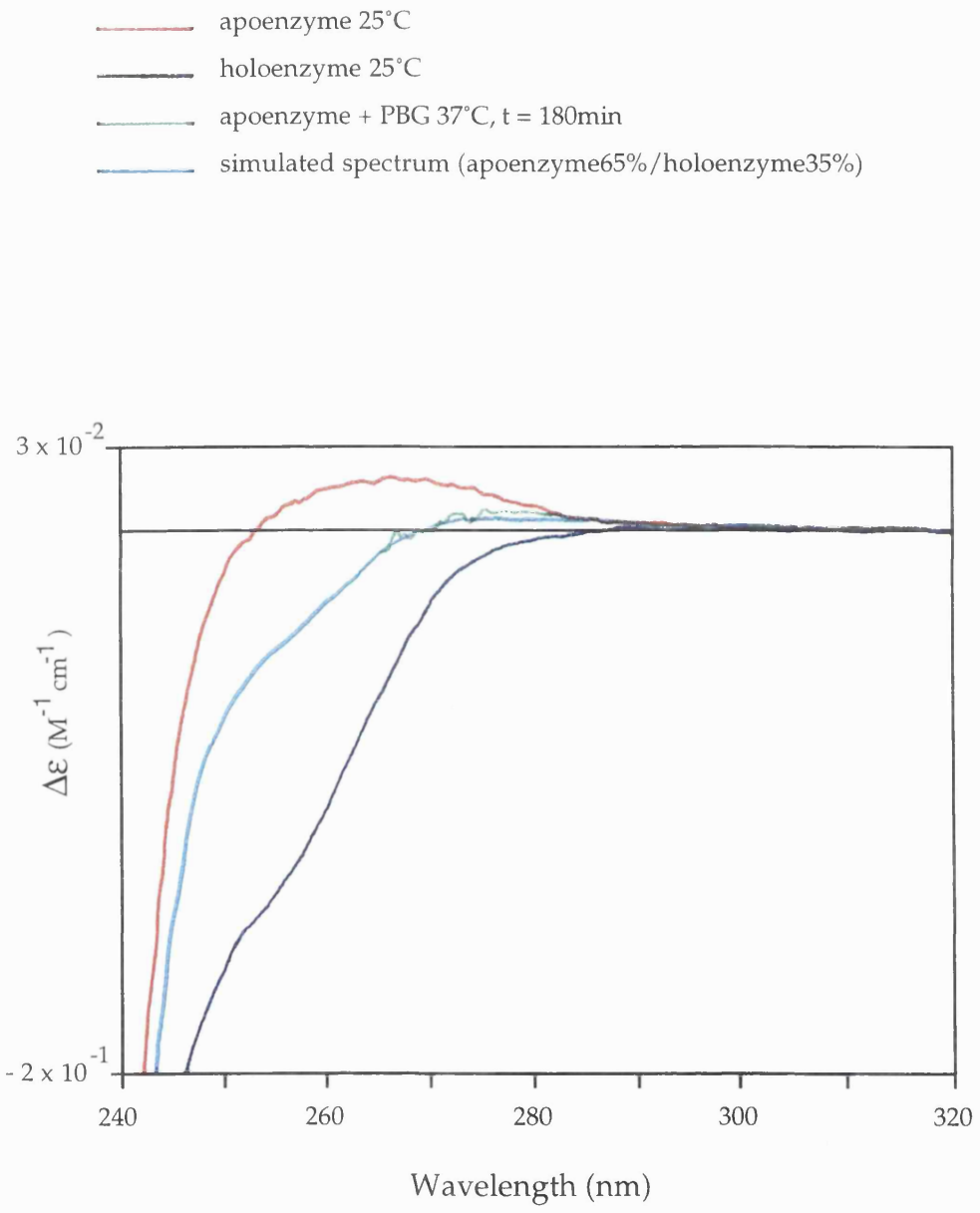

Figure 6.13 Near CD-UV Spectra Showing the Maximum Effect of the Addition of Preuroporphyrinogen to Apoenzyme

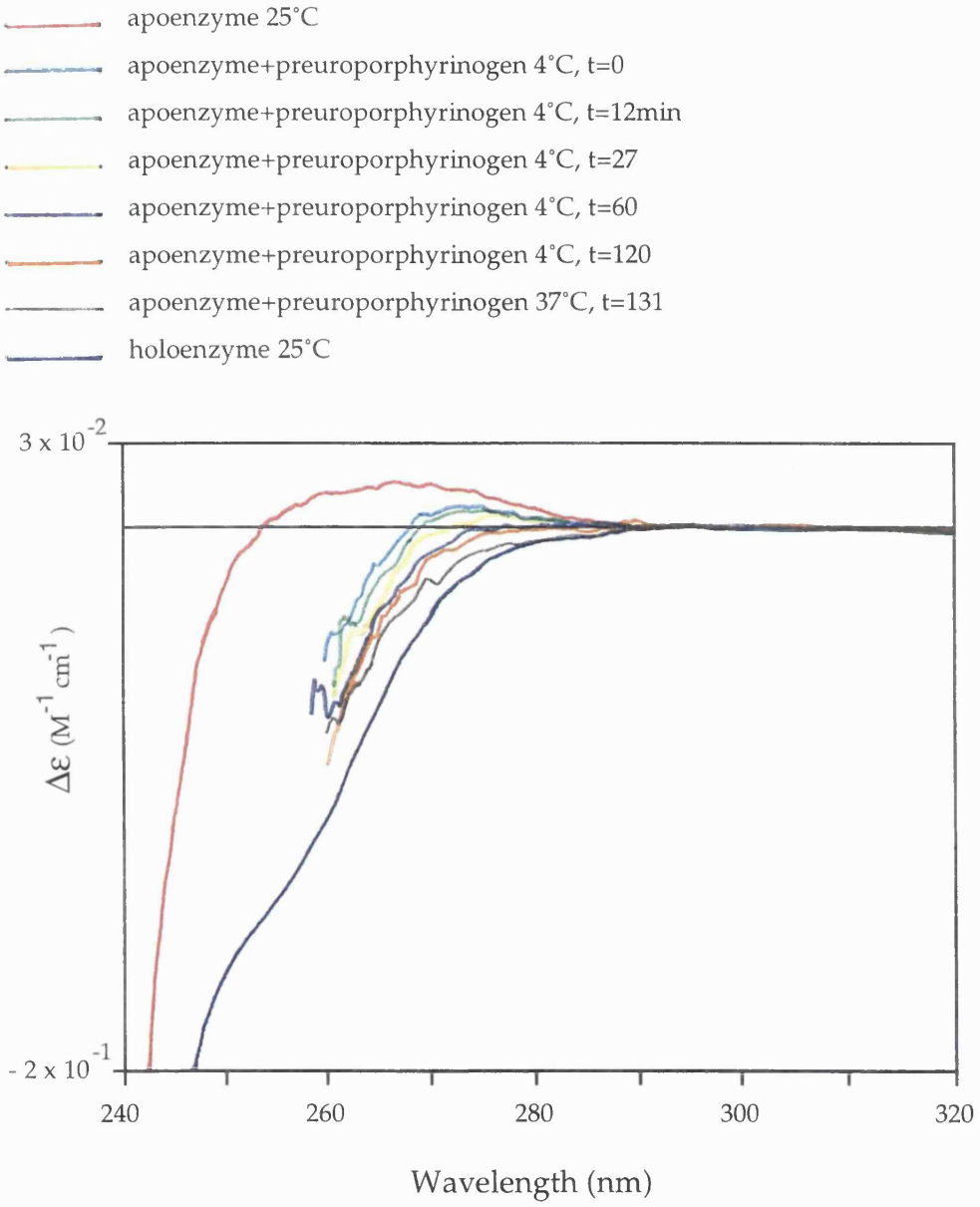

continuing effect of time. The incubation with preuroporphyrinogen shows the greatest conversion from apoenzyme to holoenzyme that has been observed. It is possible that the spectra may have have brought about additional changes with time, but time constraints did not allow the reaction to be monitored further.

The spectra of apoenzyme incubations with porphobilinogen and preuroporphyrinogen were overlaid for comparison, and are given in figure 6.14. Simulated spectra were composed to find the best fit with the recorded spectra. It can be seen that the spectra of apoenzyme incubated with preuroporphyrinogen at 4°C, at zero time, is similar to that of apoenzyme incubated with porphobilinogen at 37°C after three hours. These both match a simulated spectrum of a mix of apoenzyme (65%) and holoenzyme (35%). After two hours, the incubation of apoenzyme with preuroporphyrinogen has reached the spectrum of a mix of apoenzyme (30%) and holoenzyme (70%). These percentages confirm that preuroporphyrinogen is the preferred substrate of apoenzyme, leading to a relatively rapid conversion to holoenzyme. A conversion of 70% is the largest recorded reconstitution of holoenzyme from apoenzyme.

Figure 6.14 Near CD-UV Simulated Spectra, Comparing the Effects of Porphobilinogen and Preuroporphyrinogen Addition on Apoenzyme

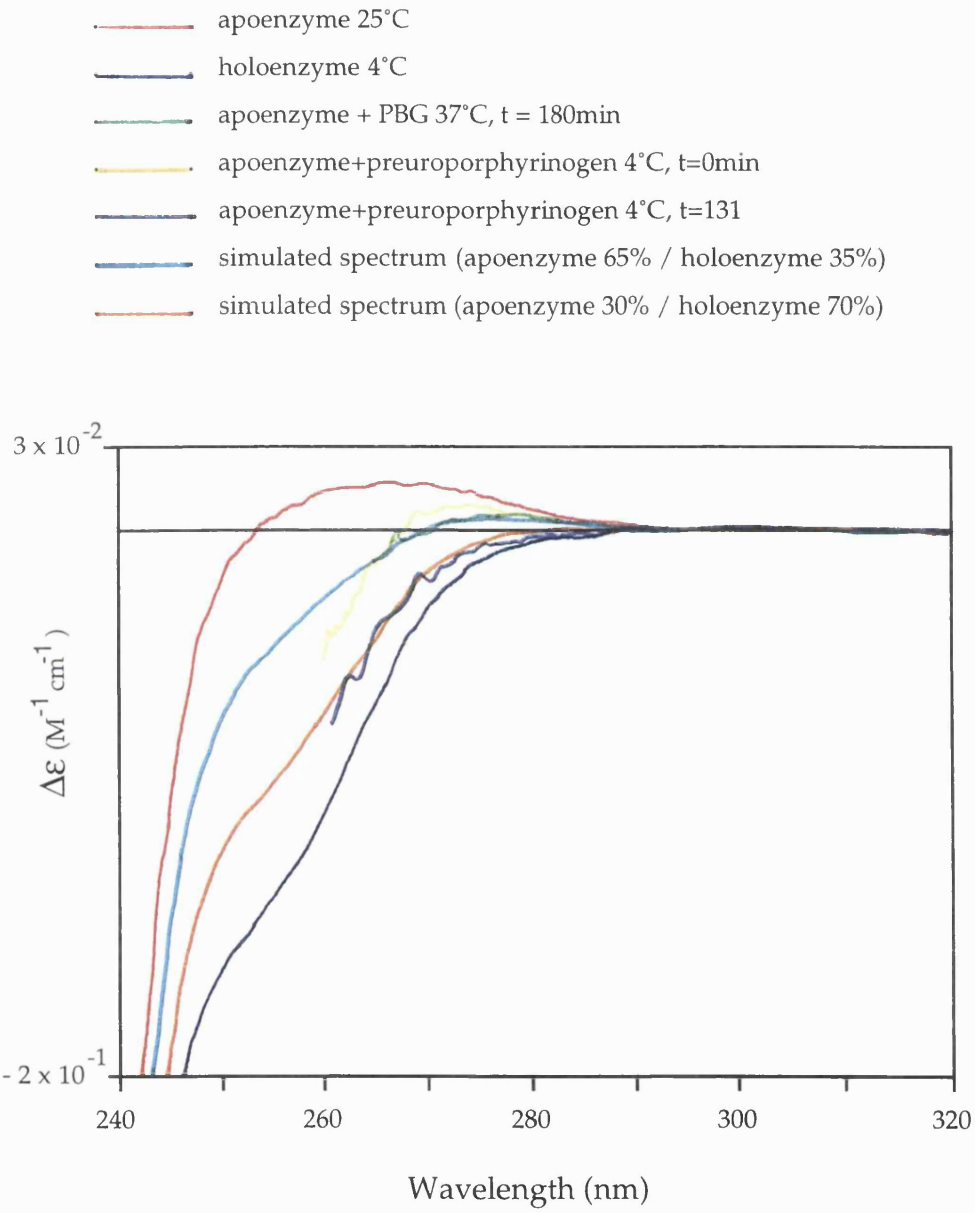

6.2.4 The Heat Treatment of Apoenzyme and Holoenzyme

The apoenzyme and holoenzyme have been observed to display distinctly different characteristics upon heat treatment (Scott *et al.*, 1989; Hart *et al.*, 1988; Chapter 5). In general, the holoenzyme has found to be stable to heat (Jordan *et al.*, 1988) and does not lose any of its secondary structure or activity after treatment at 60°C for ten minutes, as analysed both by gel electrophoresis and enzyme activity assay after cooling. The apoenzyme, however, analysed under the same conditions, showed a dramatic loss of activity and structure.

Heat treated apoenzyme was not observed to recover activity on assay. However, if the heat treated apoenzyme was allowed first to preincubate with a two molar equivalent of porphobilinogen at 37°C for one hour before assay, 25% of the activity of unheated substrate-preincubated apoenzyme could be recovered. Additionally, if the apoenzyme was first preincubated with substrate and then heat treated, normal recovery of activity as for unheated apoenzyme could be obtained. In other words, apoenzyme which had reconstituted to holoenzyme appeared to behave as native holoenzyme and was able to withstand the heat treatment. Analysis of incubations by non denaturing gel electrophoresis provided additional information. The bands corresponding to holoenzyme were still present after heat treatment, whereas the characteristic ladder of apoenzyme appeared to have been lost. In this case, both regions of near and far CD-UV were anticipated to be informative of the behaviour of apoenzyme and holoenzyme to heat treatment.

6.2.4.1 The Heat Treatment of Holoenzyme

6.2.4.1.1 Far CD-UV

The temperature of the holoenzyme was raised from 25°C to 60°C. Since each spectrum took eight minutes to record, the holoenzyme was first allowed to equilibriate at 60°C for five minutes, and then the spectrum was recorded at this temperature. Finally, the holoenzyme was

cooled down to room temperature and allowed to equilibrate for twenty minutes before the spectrum was again recorded. The overlaid spectra for holoenzyme can be seen in figure 6.15.

The spectra in figure 6.15 show that at 60°C, the holoenzyme secondary structure was lost or, at least, disrupted, but on cooling the native structure was recovered.

6.2.4.1.2 Near CD-UV

The near CD-UV spectra for the heat treatment of holoenzyme was recorded under the same conditions as for the far CD-UV region. The overlaid spectra can be seen in figure 6.16.

The spectra in figure 6.16 indicate that the environment of the aromatic residues was slightly changed at 60°C. However, on cooling, the environment of both tryptophan and tyrosine residues appeared to be as before heat treatment, whilst the phenylalanine spectrum had again slightly altered.

6.2.4.2 The Heat Treatment of Apoenzyme

6.2.4.2.1 Far CD-UV

The far CD-UV spectra for the heat treatment of apoenzyme were recorded under the same conditions as for the heat treatment of holoenzyme. The overlaid spectra can be seen in figure 6.17.

The spectra in figure 6.17 indicate that, similarly to holoenzyme, the secondary structure of apoenzyme was lost at 60°C. However, unlike holoenzyme, the structure did not appear to recover on cooling, but instead assumed a "new" secondary structure, somewhere between the two.

Figure 6.15 Far CD-UV Spectra Showing the Effect of Heat Treatment on Holoenzyme

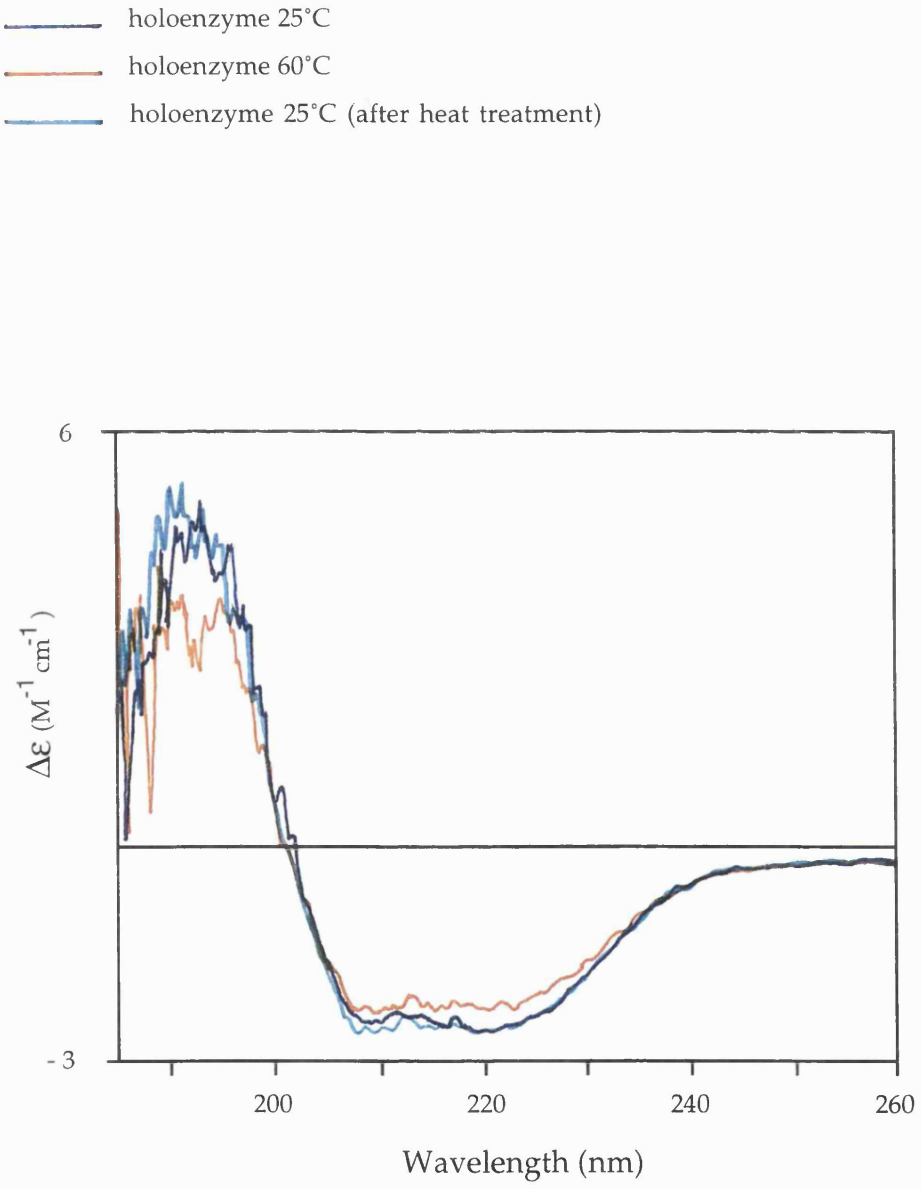

Figure 6.16 Near CD-UV Spectra Showing the Effect of Heat Treatment on Holoenzyme

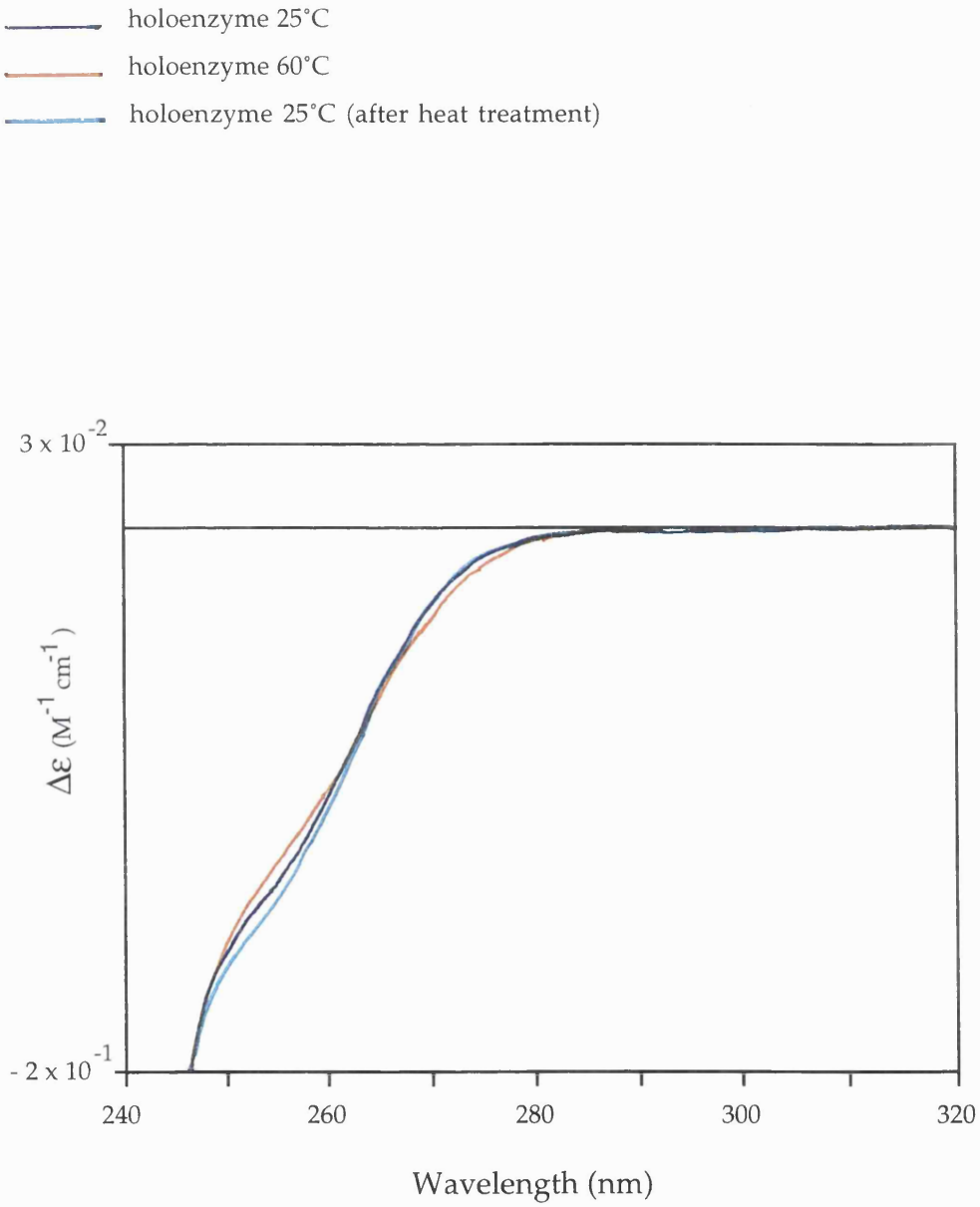

Figure 6.17 Far CD-UV Spectra Showing the Effect of Heat Treatment on Apoenzyme

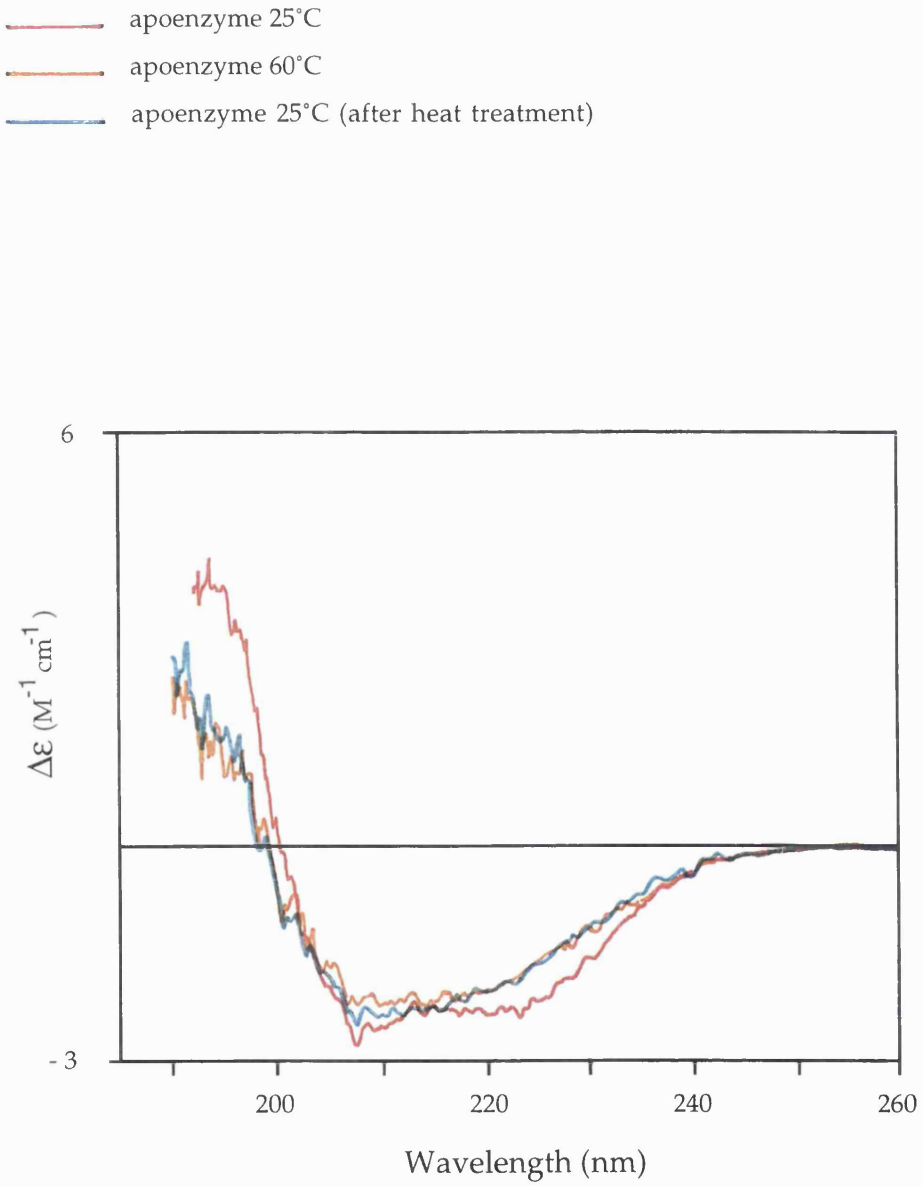

6.2.4.2.2 Near CD-UV

Again, the heat treatment of apoenzyme was recorded for the near CD-UV region, as for the holoenzyme. The overlaid spectra can be seen in figure 6.18.

The spectra in figure 6.18 indicate that the local tertiary environment of the aromatic residues was altered at 60°C, and on cooling the phenylalanine and tyrosine residues appeared in an environment which was between that of 25°C (unheated) and 60°C.

For further comparison, figure 6.19 displays the overlaid far CD-UV spectra of apoenzyme, substrate-incubated apoenzyme, holoenzyme, heat treated apoenzyme and heat treated holoenzyme. This figure shows that the structure of holoenzyme at 60°C is similar to that of substrate-incubated apoenzyme. However, as it is not possible to predict the percentage of reconstituted holoenzyme in the substrate-incubated apoenzyme mixture, it would be hard to interpret this comparison in a meaningful way.

6.2.4.3 The Addition of Substrate to Heat Treated Holoenzyme

These studies were only carried out on the near CD-UV region, since it had been previously observed in section 6.2.2.1. that the effect of substrate on the backbone region of holoenzyme was not detected in the far CD-UV region.

6.2.4.3.1 Near CD-UV

The holoenzyme was heated at 60°C for ten minutes and then cooled to room temperature. Spectra were recorded as for previous samples. The temperature was then raised to 37°C and an excess of porphobilinogen added.The changes in spectra were monitored at 37°C with time. The overlaid spectra can be seen in figure 6.20.

Figure 6.18 Near CD-UV Spectra Showing the Effect of Heat Treatment on Apoenzyme

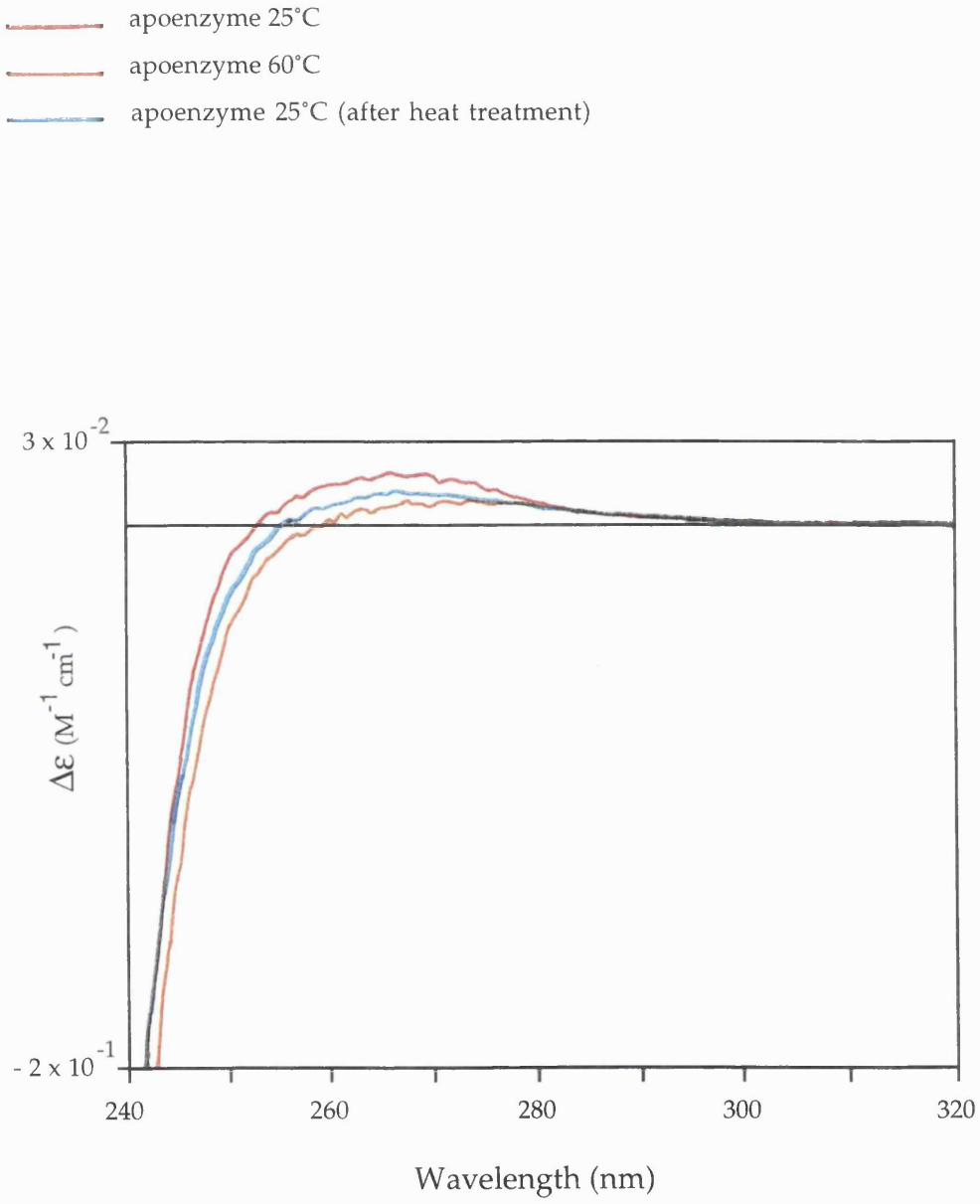

Figure 6.19 Far CD-UV Spectra, Comparing Various Conditions for Apoenzyme and Holoenzyme

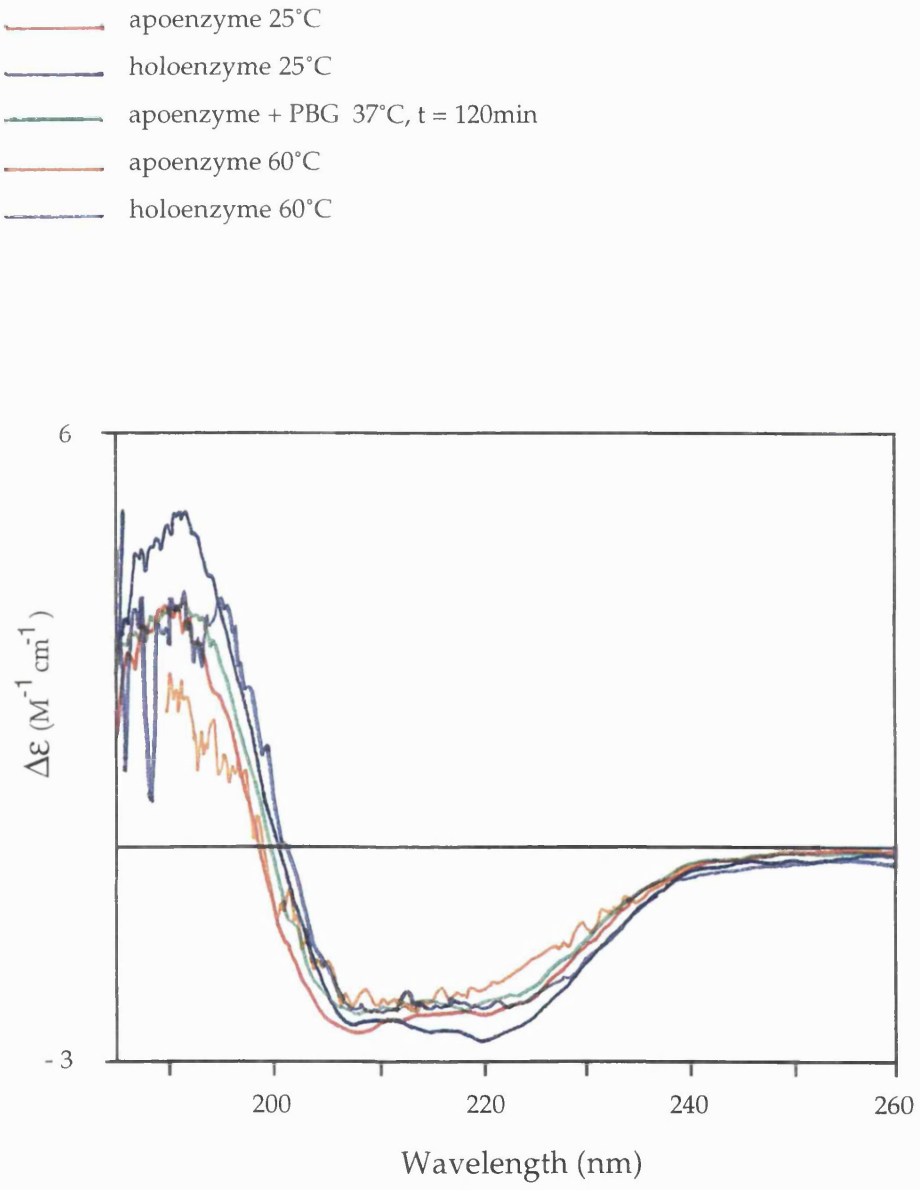

Figure 6.20 Near CD-UV Spectra Showing the Effect of the Addition of Porphobilinogen to Heat Treated Holoenzyme

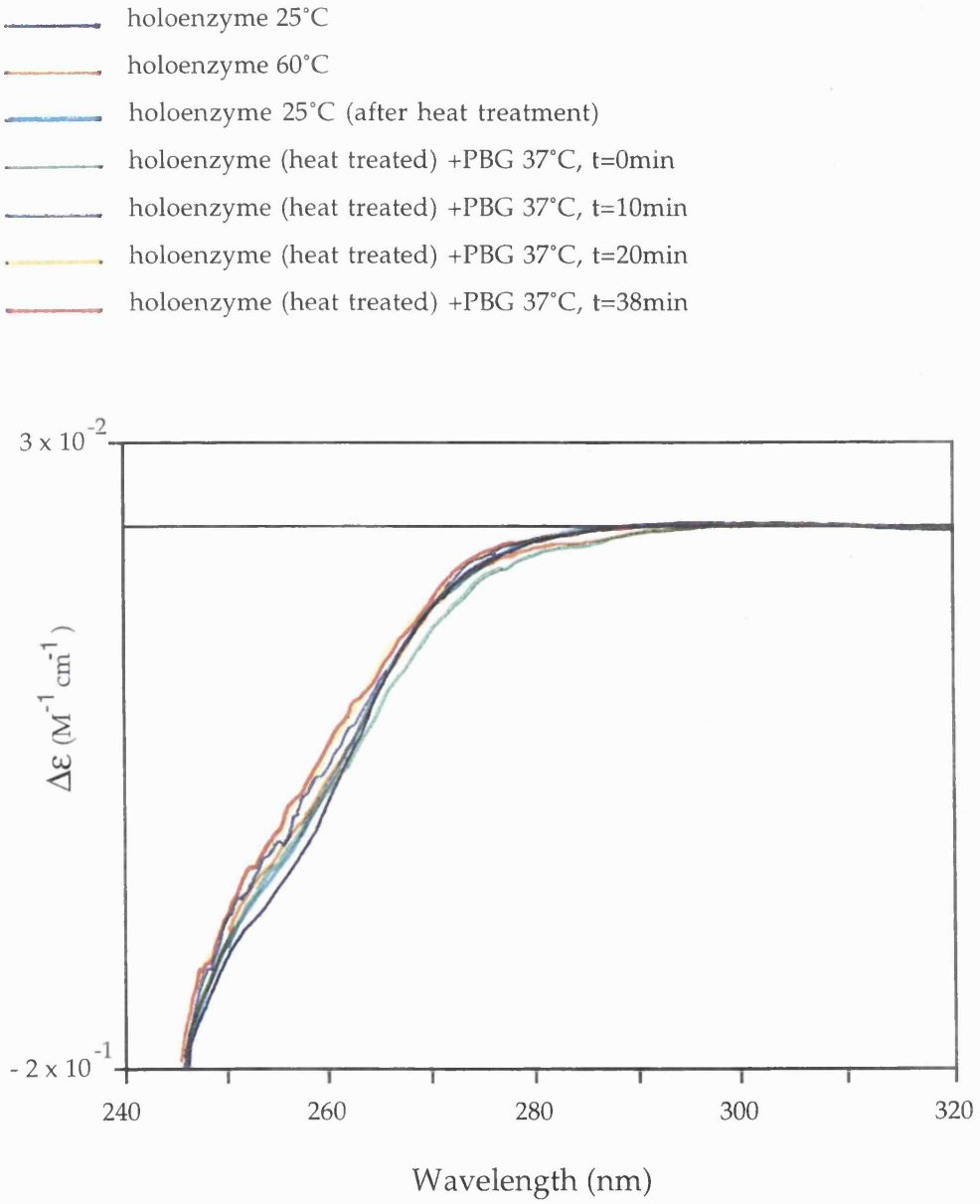

The spectra in figure 6.20 are similar to those of unheated holoenzyme with porphobilinogen. The excess of porphobilinogen would produce a longer reaction, and the tyrosine and particularly the phenylalanine regions were observed to fluctuate with time, evidently due to the continual changes in the environment of these residues upon PBG addition. The similar behaviour of the heated holoenzyme to unheated holoenzyme indicates that the holoenzyme is able to retain normal activity on heat treatment.

6.2.4.4 The Effect of Substrate on the Heat Treatment of Apoenzyme

6.2.4.4.1 Far CD-UV

The far CD-UV region was monitored to study the heat treatment of substrate-incubated apoenzyme. Changes in the far CD-UV region had previously been observed for the addition of substrate to apoenzyme and also for the heat treatment of apoenzyme. It was anticipated that reconstituted holoenzyme would be resistant to heat treatment.

The apoenzyme was preincubated with a two molar equivalent of porphobilinogen at 37°C for three hours and the spectrum recorded. The mixture was heated to 60°C for ten minutes, cooled to 25°C, and the spectrum again recorded. The overlaid spectra, including the spectrum of apoenzyme in the absence of substrate, can be seen in figure 6.21.

The spectra in figure 6.21 indicate that changes occured in the backbone of the protein on binding porphobilinogen, bringing the secondary structure closer to that of the holoenzyme. However, on heat treating the preincubation, the secondary structure appeared to have been more disrupted than that of unheated apoenzyme in the absence of substrate.

It was expected, from past observations, that preincubation with substrate would allow some holoenzyme to reconstitute, and therefore lessen the degree of disruption to the secondary structure upon heat treatment. The results here are therefore contradictory to this hypothesis.

Figure 6.21 Far CD-UV Spectra Showing the Effect of Heat Treating Porphobilinogen-Incubated Apoenzyme

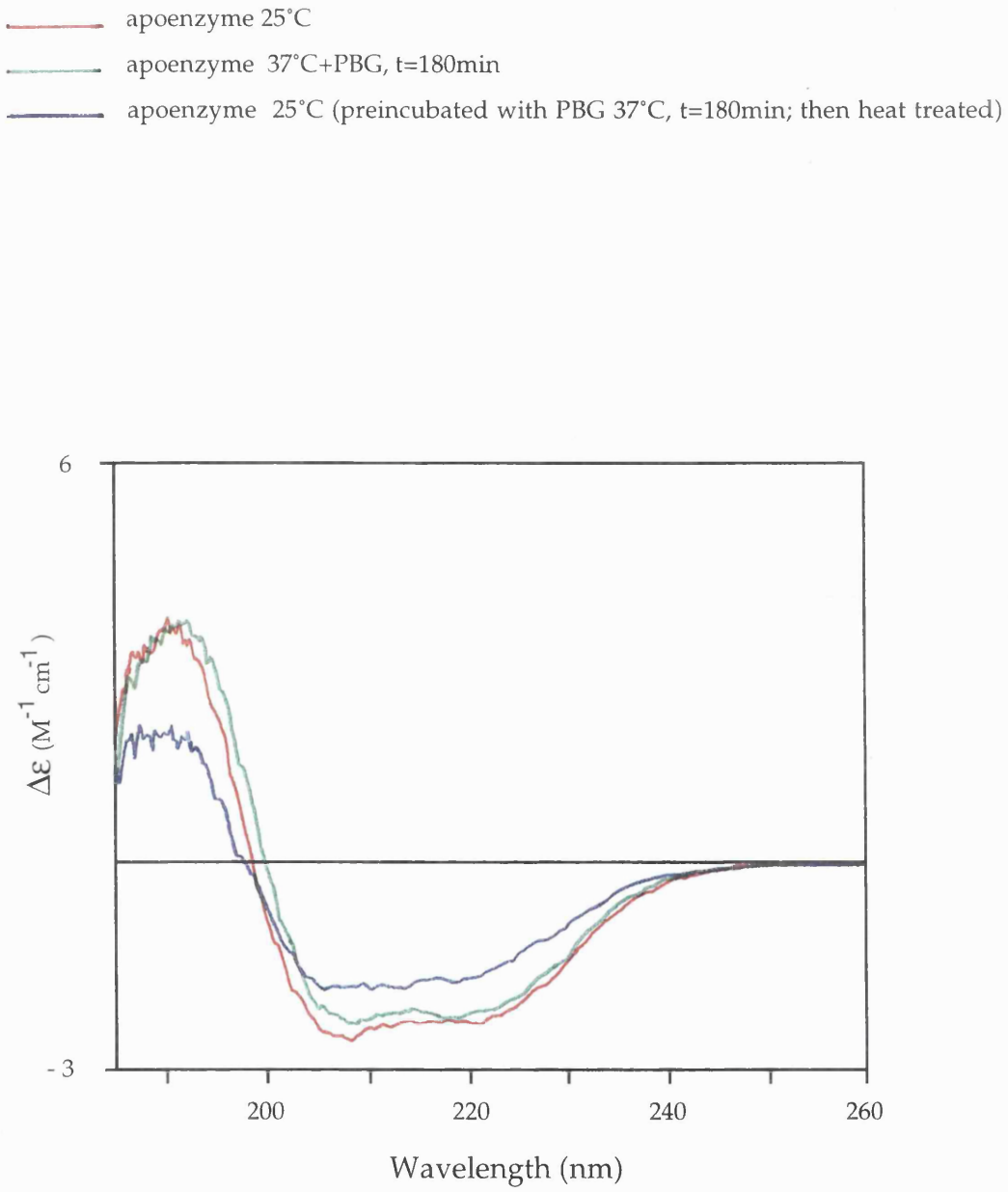

These results were obtained during preliminary experiments with CD spectroscopy, and the spectrum of substrate preincubated apoenzyme at 25°C after heat treatment was one in which the mixture was heated at 60°C for a full ten minutes before the spectrum was recorded. The total time at 60°C would then have been eighteen minutes, and the additional time of the heat treatment may have led to the further breakdown of structure. The experiment would have to be repeated before conclusive results could be drawn.

6.2.4.4.2 Near CD-UV

Several conditions were monitored for apoenzyme in the presence and absence of substrate preincubation and heat treatment in the near CD-UV region, to complement all the enzyme assay studies.

In the first, apoenzyme was heated at 60°C for ten minutes and cooled to room temperature. Spectra were recorded as for the previous samples. The temperature was raised to 37°C and a two molar equivalent of porphobilinogen added. The changes in spectra were monitored with time at 37°C. The overlaid spectra, along with holoenzyme for comparison, are given in figure 6.22.

The spectra in figure 6.22 show that, after heat treatment, the addition of porphobilinogen did not change the environment of any of the aromatic residues. In the case of unheated apoenzyme, the substrate-incubation would have caused the environment of the residues to change and the spectrum would move in the direction of the holoenzyme. In addition, when assayed for activity, heat treated apoenzyme will display 25% of the previous activity on incubation with substrate.

Again, the different results must be a consequence of the different conditions. Certainly the lack of alterations in the local environment of the aromatic residues of apoenzyme after heat treatment correlates with the results for heat treated apoenzyme as examined by gel electrophoresis.

Figure 6.22 Near CD-UV Spectra Showing the Effect of Porphobilinogen on Heat Treated Apoenzyme

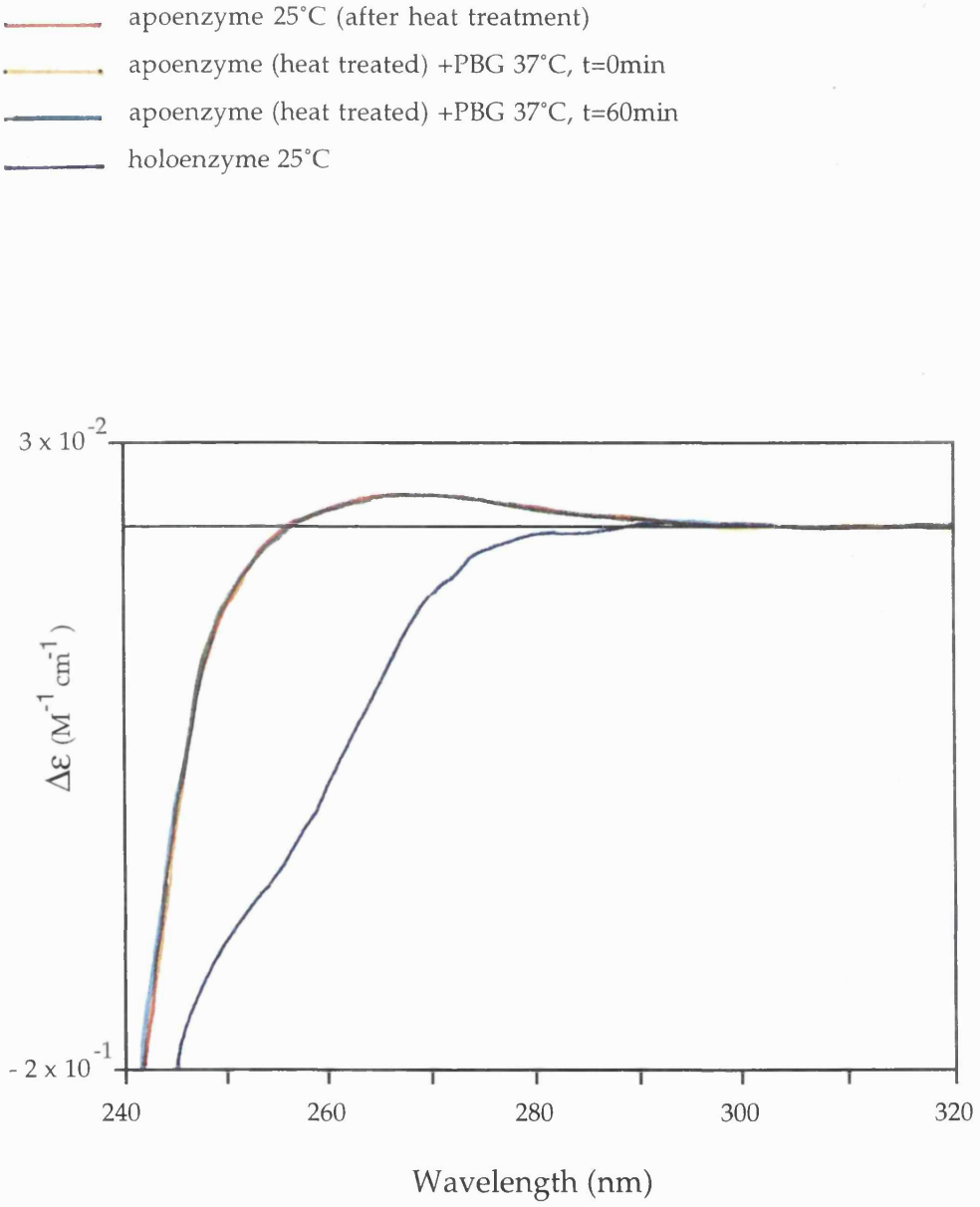

The apoenzyme was also monitored in the near CD-UV region for the effect of first preincubation with substrate and then heat treatment. Apoenzyme was preincubated with a two molar equivalent of substrate at 37°C for two hours and the spectrum was recorded. The temperature of the incubation was then raised to 60°C for ten minutes and then cooled down to room temperature, and the spectrum again recorded. The overlaid spectra, together with apoenzyme, heat treated apoenzyme and holoenzyme can be seen in figure 6.23.

Figure 6.23 shows that the spectrum of apoenzyme, on incubation with substrate, moves towards that of holoenzyme. However, heat treatment of the incubation brings the spectrum back to that of heat treated apoenzyme, i.e. that which has had no substrate incubation. Again, it would be anticipated that, on incubation with substrate, some apoenzyme would reconstitute to give holoenzyme. The reconstituted holoenzyme would then be expected to behave as native holoenzyme, and whilst any remaining apoenzyme would show behaviour typical of native apoenzyme on heat treatment, the reconstituted holoenzyme should also record some effect on the spectra.

The results therefore do not correlate with previous observations. There are two plausible explanations. One is that the spectra of heat treated substrate-incubated apoenzyme has not returned exactly to that of the heat treated apoenzyme, and that the reconstituted holoenzyme is showing its effect. This hypothesis could be confirmed if a mixture of holoenzyme (20%) and apoenzyme (80%) was subjected to heat treatment and the near CD-UV examined. A similar spectrum would resolve the matter.

However, it is also possible that the environment of the tyrosine and phenylalanine is altered in the same way as that of heated apoenzyme in the absence of substrate, because secondary structure not vital to the activity of the enzyme is lost in both cases. Already it has been seen from the far CD-UV region that some backbone structure is lost for both samples on heat treatment. The contribution to the near CD-UV region does not come from the active site phenylalanine alone, and losses in other regions containing aromatic residues may also be being identified here. In particular, the corresponding gel electrophoresis experiments suggest that apoenzyme does reconstitute some holoenzyme on substrate incubation,

Figure 6.23 Near CD-UV Spectra Showing the Effect of Heat Treating Porphobilinogen-Incubated Apoenzyme

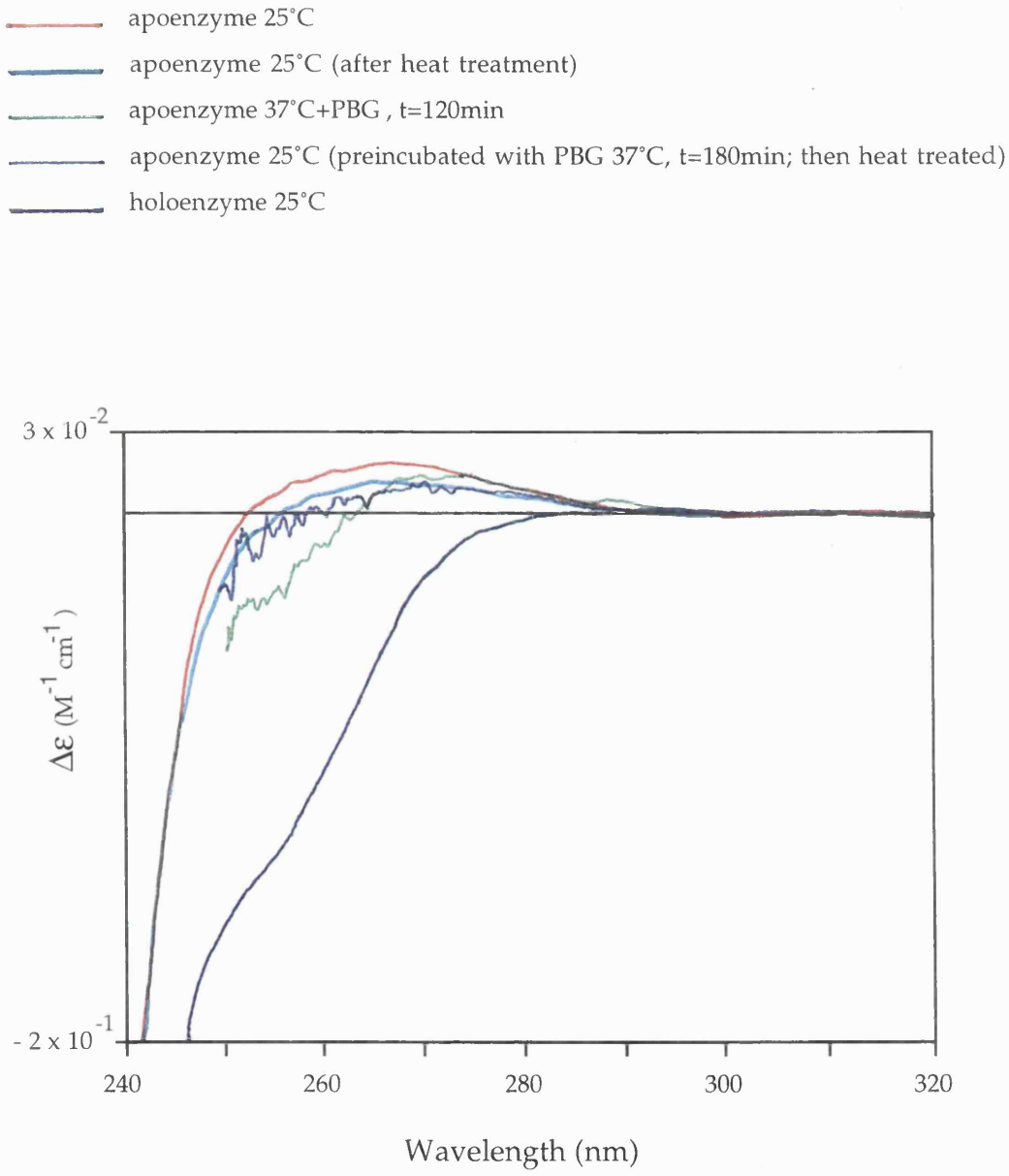

and this reconstituted holoenzyme is stable to heat. Whichever hypothesis is correct, it is unlikely that the apoenzyme, on reconstituting holoenzyme after incubation with substrate, is unstable to heat.

6.2.5 The Effect of Reducing the pH of the Holoenzyme Solution - the Viability of Crystallising the Enzyme at pH 5

Native *E.coli* porphobilinogen deaminase has an optimal activity around pH 8.5 (Jordan *et al.*, 1988). The enzyme is found to be inactive below pH 6.0 , and the inactivation is reversible unless the pH drops below pH 4.0. However, it has been observed that crystal growth for the enzyme is most effective in conditions at pH 5.0, and the structure currently available for porphobilinogen deaminase is one which has been resolved at pH 5.0. The validity of a structure obtained from porphobilinogen deaminase at a pH at which it was inactive was therefore investigated by CD spectroscopy.

It has also been noted that crystals of the native enzyme at pH 5.0 will shatter upon the addition of substrate, and this indicates that the crystals are able to interact with the substrate (Wood). It is possible that this interaction is a result of some residual activity, although this may be a consequence of a slight raising of pH upon the addition of excess substrate.

6.2.5.1 Far CD-UV

To investigate the effects of pH on structure, the holoenzyme was resuspended in sodium acetate buffer (20mM) at pH 7.4, and the spectrum recorded. Sodium acetate buffer was used for the experiment as it was the buffer in which crystallisation of the enzyme was achieved. The pH was then dropped by the addition of acetic acid, until the solution was at pH 5.1. The spectrum was again recorded, and the overlaid spectra are given in figure 6.24.

The far CD-UV spectrum of holoenzyme in figure 6.24 appeared unchanged at the lower pH. Therefore, the backbone of the protein was not in an altered conformation at pH 5.0. Thus porphobilinogen deaminase crystallised at pH 5.0 is likely to have an identical structure to enzyme crystallised at pH 7.4.

Figure 6.24 Far CD-UV Spectra Showing the Effect of Reducing the pH of the Holoenzyme Solution to pH 5

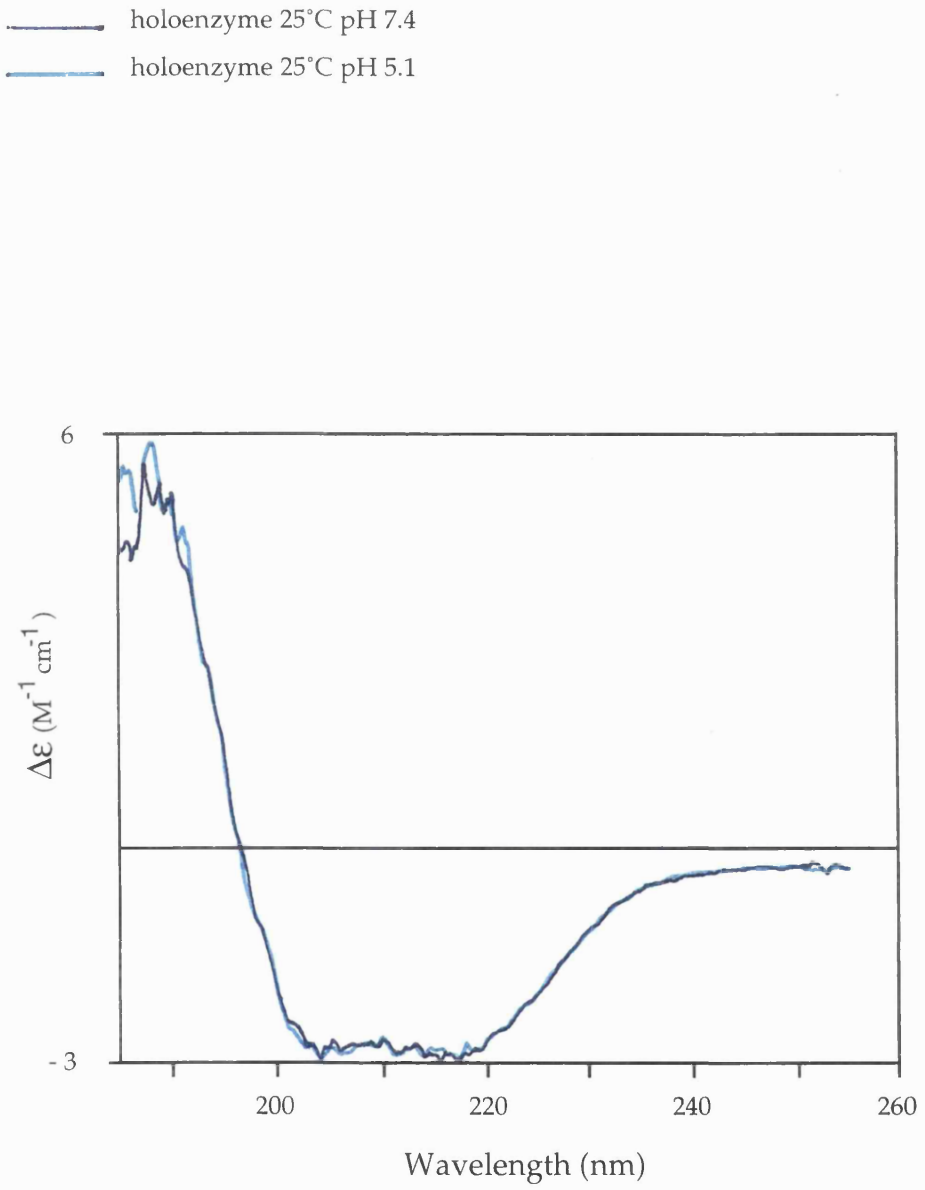

6.2.5.2 Near CD-UV

The holoenzyme was also monitored for the drop from pH 7.4 to pH 5.1 in the near CD-UV region under the same conditions. The two spectra can be seen in figure 6.25.

Again, the spectra in figure 6.25 show that the environment of the aromatic residues had not been altered by lowering the pH to 5.0. This further confirmed the validity of a porphobilinogen deaminase structure obtained at pH 5.0.

Figure 6.25 Near CD-UV Spectra Showing the Effect of Reducing the pH of the Holoenzyme Solution to pH 5

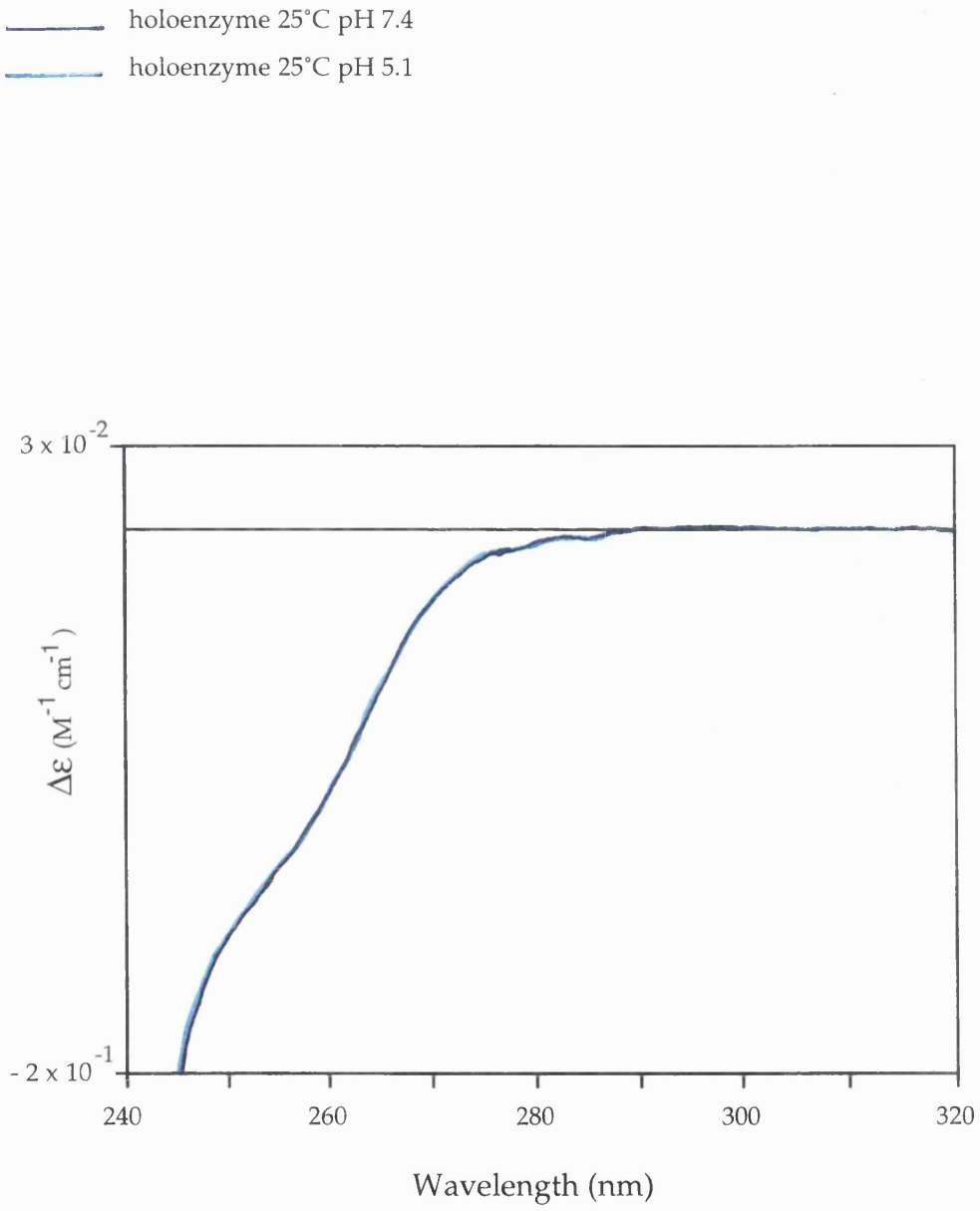

6.2.6 The Effect of Dropping the pH of the Holoenzyme Solution to pH 3.7

The holoenzyme is noted to become irreversibly inactivated below pH 4.0 (Jordan *et al.*, 1988). Such a loss of activity suggests that the holoenzyme may be denatured at pH 3.7. It would be anticipated, therefore, that some changes would be observed in either region at the lower pH.

6.2.6.1 Far CD-UV

The holoenzyme was resuspended in 20mM Tris/HCl buffer pH 7.4 containing 13mM β-mercaptoethanol and the spectrum was recorded. The pH was then dropped to pH 3.7 by the addition of hydrochloric acid, and the spectrum again recorded. The spectra of holoenzyme at both pHs is given in figure 6.26, overlaid with those of substrate-incubated apoenzyme, and holoenzyme at 60°C.

The spectra in figure 6.26 show that some secondary structure had been lost at pH 3.7. The spectrum of holoenzyme at pH 3.7 resembled that of holoenzyme at 60°C and also that of substrate-incubated apoenzyme.

6.2.6.2 Near CD-UV

The holoenzyme was resuspended in 20mM Tris/HCl buffer pH 7.4 containing 13mM β-mercaptoethanol and the spectrum recorded. The pH was then dropped to pH 3.7 by the addition of hydrochloric acid, and the spectrum was again recorded. The spectra of holoenzyme at both pHs is given in figure 6.27, overlaid with those of substrate-incubated apoenzyme, and holoenzyme at 60°C.

Figure 6.27 shows that the effect of dropping the pH of holoenzyme from pH 7.4 to 3.7 brought about changes in the local environment of the tyrosine and particularly the phenylalanine residues. A greater change was observed than for the effect of heating holoenzyme at 60°C. This may reflect the irreversibility of the low pH on the activity of the enzyme; the heat effect is reversible. It was also noted that whilst the substrate-

Figure 6.26 Far CD-UV Spectra Showing the Effect of Reducing the pH of the Holoenzyme Solution to pH 3.7

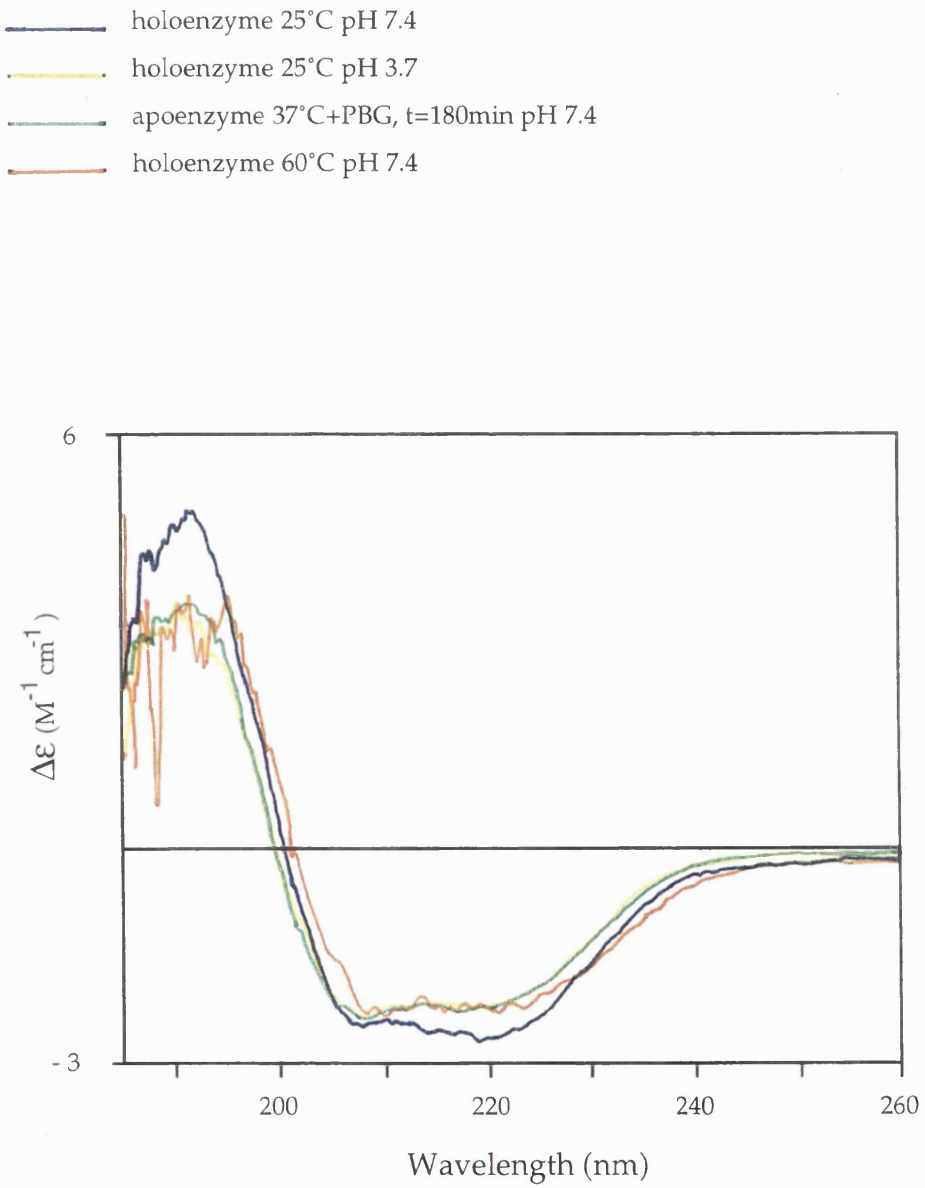

Figure 6.27 Near CD-UV Spectra Showing the Effect of Reducing the pH of the Holoenzyme Solution to pH 3.7

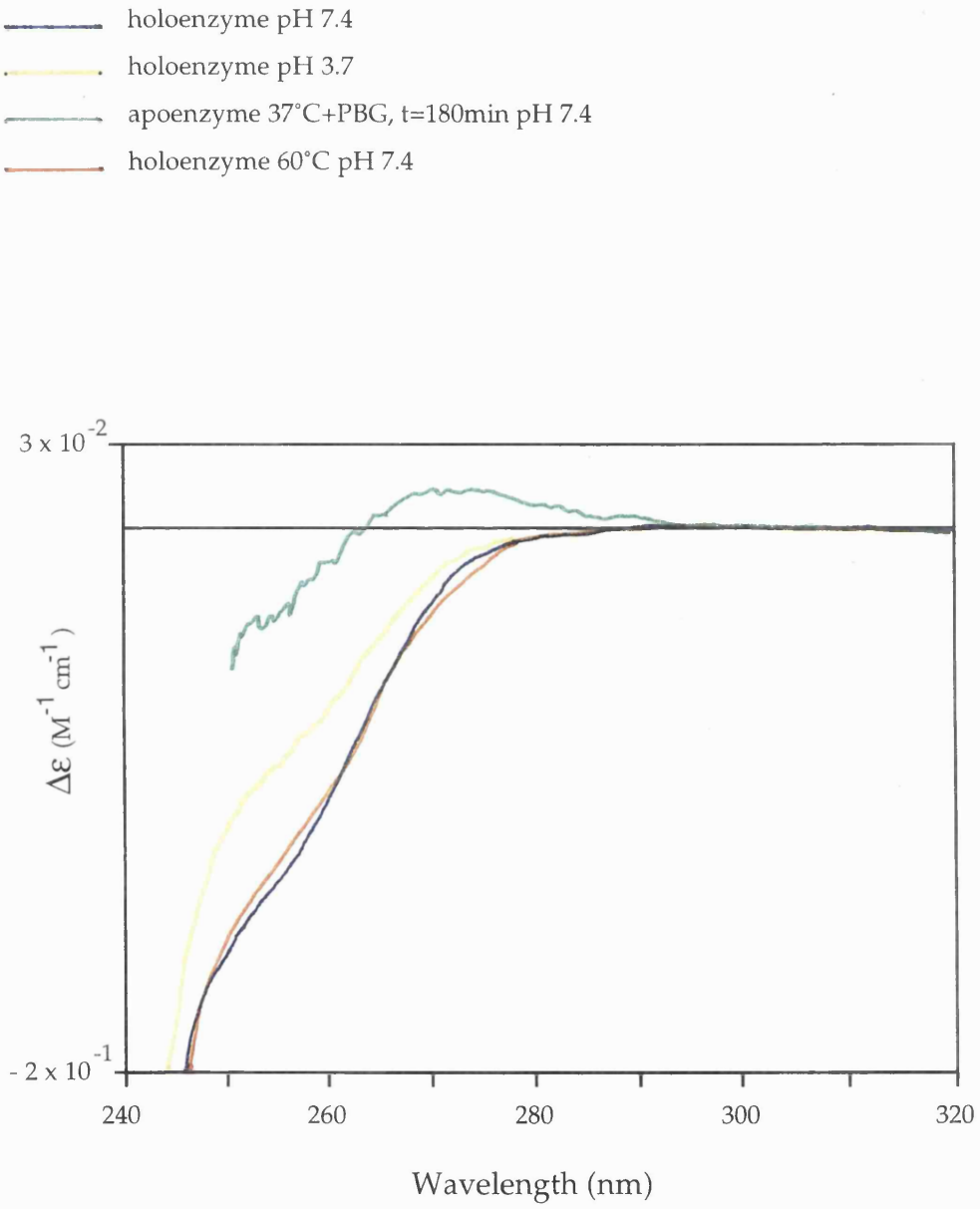

incubated apoenzyme resembled both holoenzyme at pH 3.7 and holoenzyme at 60°C in terms of secondary structure, it had an entirely different local environment of its tyrosine and phenylalanine residues.

Whilst the similarities of the spectra with substrate-incubated apoenzyme are noted, they are not considered further, as the composition of structures in the incubation are not known. It would be difficult to predict whether the mixture contains a percentage of apoenzyme and holoenzyme, or whether all the apoenzyme has reacted with porphobilinogen in some way but has not taken on the structure of holoenzyme. Speculations about the similarities would therefore be questionable.

The results suggest that both heat and low pH have the same overall effect on the secondary structure, and are likely to give rise to a more flexible and open conformation. The extreme drop in pH would cause an unfolding of the protein as bonds would begin to break, largely through the protonation of the side groups. The increase in temperature would also bring about a similar loss of change in conformation, as the entropic contributions would become raised making an unfolded state more favourable. The similar secondary structures brought on by the two effects suggests that the protein has unfolded in a specific way. The protein does not appear to have completely unfolded, as there is still a considerable amount of secondary structure. It is also unlikely that such an effect would then be reversible (as for heat treatment). The different local environments of the aromatic residues, however, may reflect the nature of the unfolding by the different techniques.

6.2.7 Study of the Aspartate-84 Mutants

The mutations of aspartate-84 to alanine (D84A), glutamate (D84E) and asparagine (D84N) have been described in some detail (Chapter 4). Aspartate-84 represents a key catalytic residue, and therefore the D84E mutant is found to maintain only 1% of the activity of the wild-type enzyme, whereas D84A and D84N are catalytically inactive (Woodcock and Jordan, 1994). All three mutants are found to have correctly inserted the cofactor. The experimental observations for the mutants D84A and D84N have been hard to reconcile as, whilst they are measured to be catalytically inactive, they also appear to have formed enzyme-intermediate complexes. The three purified mutants, before application to the f.p.l.c. system, are believed to exist as a mixture of free enzyme and enzyme-intermediate complexes. It was possible that CD could throw further light on the conformational states of the mutants, and therefore all three were studied in both the near and far CD-UV regions.

6.2.7.1.1 Far CD-UV

The spectra of the far CD-UV region of each of the mutants D84A, D84E and D84N were recorded. The overlaid spectra, together with those of apoenzyme and holoenzyme, are given in figure 6.28.

The spectra in figure 6.28 show that the backbone region of mutants D84E and D84N were very similar, and close to that of holoenzyme. The mutant D84A, however, appeared to show an increase in β-sheet structure. None of the mutants matched the spectrum of apoenzyme.

The difference in the secondary structure of any of the mutants to holoenzyme was surprising, as the mutation is made at a key catalytic residue and whilst the catalytic inactivity can be explained the mutations would not be predicted to bring about an altered secondary structure. In addition, the crystal structure of an enzyme-intermediate complex of D84E has been resolved and the backbone is not noted to be structurally different. Further, the presence of substrate has also been observed not to affect the backbone of holoenzyme. However, it is also noted that the mutants are pink and the colour suggests that the complexes may be

Figure 6.28 Far CD-UV Spectra Showing the Aspartate-84 Mutants

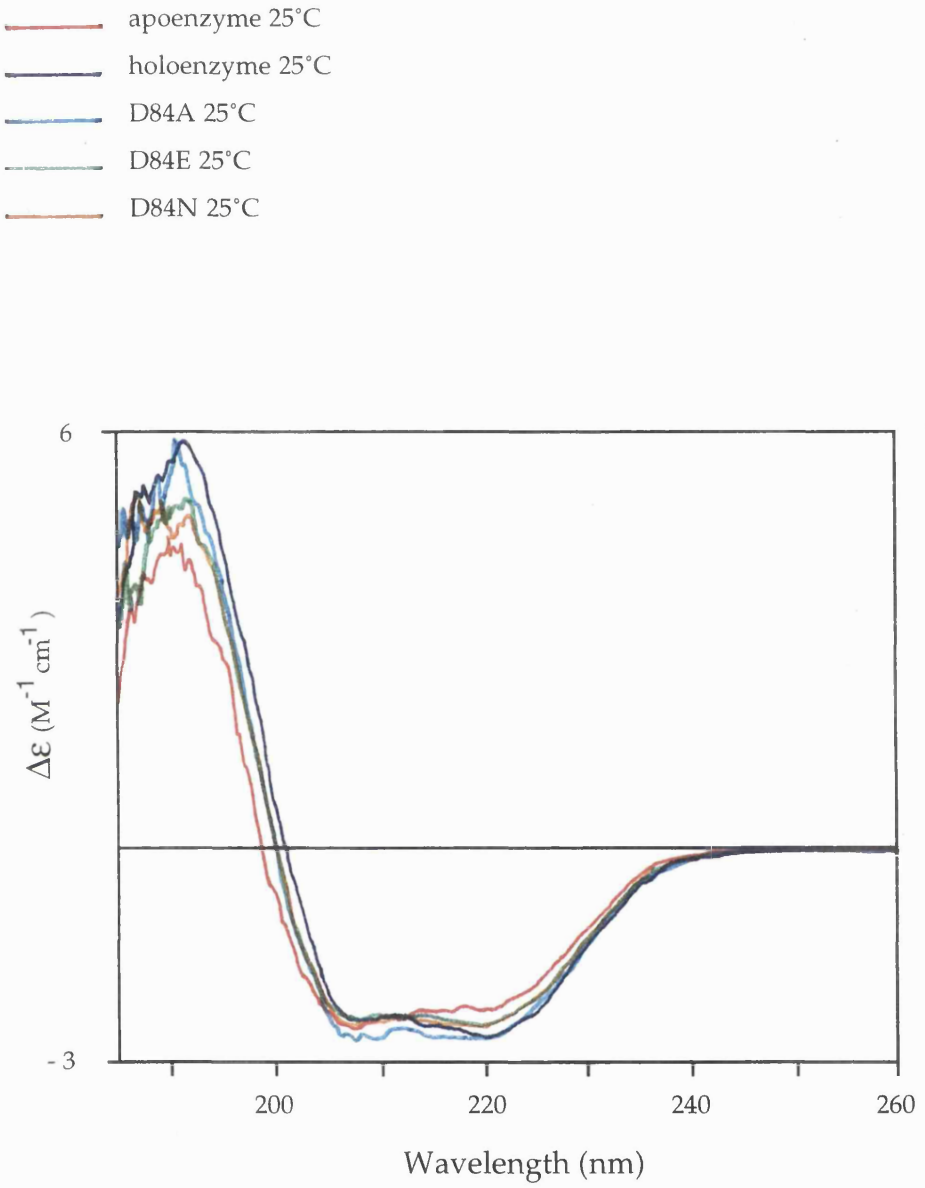

oxidised, which may mean that the complexes are in an alternative, strained conformation. The position of the D84E and D84N spectra also suggests that some loss of secondary structure had taken place in these two mutants.

6.2.7.1.2 Near CD-UV

The spectra of the near CD-UV region of each of the mutants D84A, D84E and D84N were recorded. The overlaid spectra, together with those of apoenzyme and holoenzyme, are given in figure 6.29.

The spectra in figure 6.29 show that the local environment of the aromatic residues tyrosine and phenylalanine were very similar for D84A and D84N, and close to that of D84E. The spectra appeared approximately midway between that of apoenzyme and holoenzyme. Interestingly, the spectra of the D84A and D84N mutants match exactly that of a mixture of apoenzyme (60%) and holoenzyme (40%).

Before these results are interpreted, it should be noted that the altered environment of the aromatic residues for all three mutants is likely to correspond, at least, to the altered environment of the residue phenylalanine-62, which is in the vicinity of the residue at 84. The mutations mean that the spectra cannot be directly compared with either the apoenzyme or the holoenzyme of the wild-type, as the signal at 260nm will undoubtably have been affected.

The near CD-UV spectra suggest that there is a percentage of the apoenzyme form present in the samples. This is a likely interpretation, as the mutants had not been purified using the f.p.l.c. system and such samples have previously been observed to contain apoenzyme forms (see Chapter 3). However, if such a large ratio of apoenzyme is present in the samples it would also be expected to have an effect on the far CD-UV. The far CD-UV spectra for these mutants does not indicate the presence of a large percent of apoenzyme.

Figure 6.29 Near CD-UV Spectra Showing the Aspartate-84 Mutants

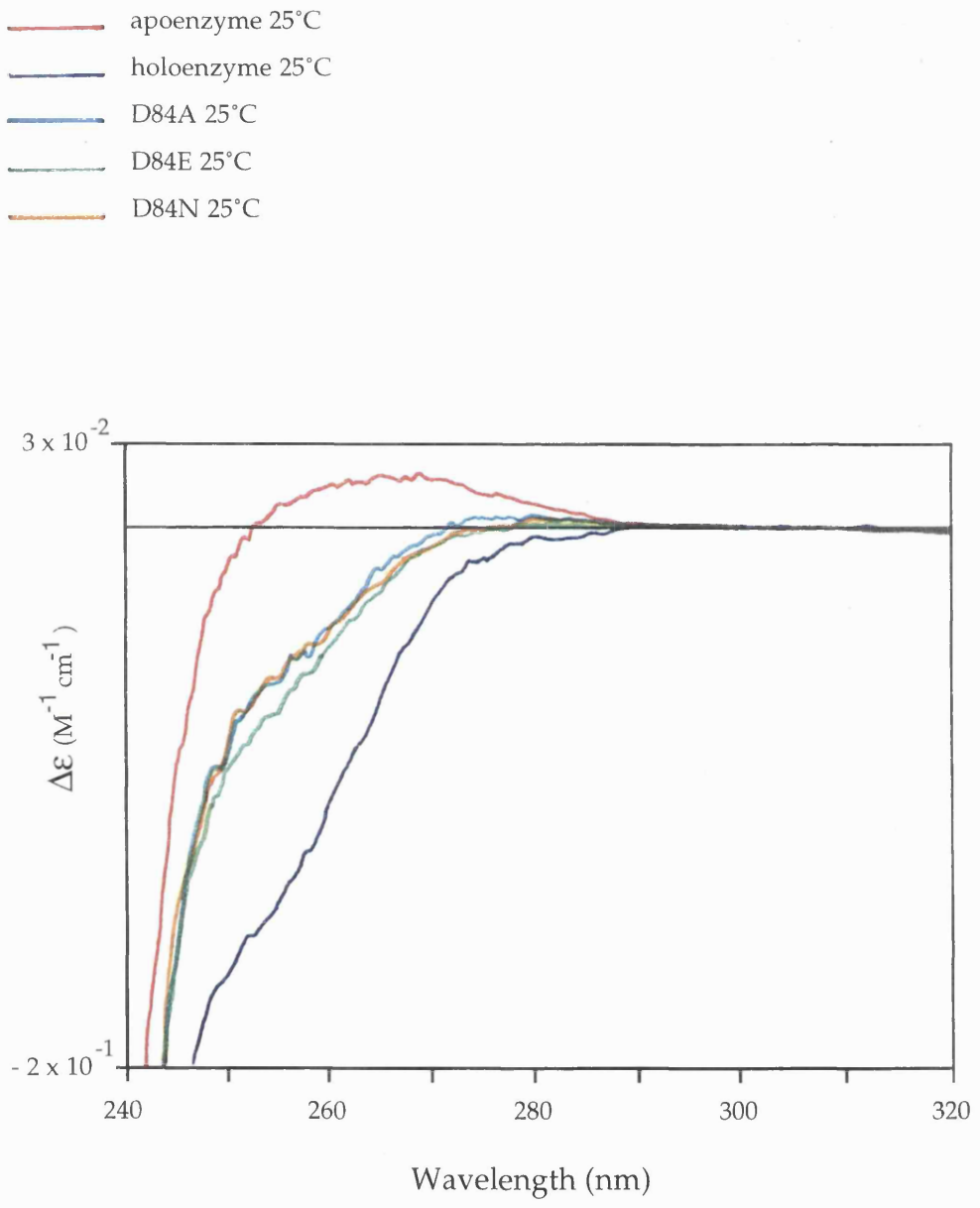

6.2.7.2 The Addition of Substrate to the Aspartate-84 Mutants

The mutant D84E would be expected to show differences, at least in the near CD-UV region, on the addition of substrate as it does retain some activity. However, it is anticipated that the spectra for the catalytically inactive mutants D84A and D84N will remain unchanged.

6.2.7.3.1 Far CD-UV

The mutants were incubated with a four to six molar equivalent of porphobilinogen at 37°C for up to forty minutes. The spectra for each were recorded, and the overlaid spectra, together with those of apoenzyme, substrate-incubated apoenzyme and holoenzyme, can be seen in figure 6.30.

The spectra in figure 6.30 show that no changes had taken place in the backbone of the mutants. As the effect of substrate had been previously observed to alter the backbone of apoenzyme only, the result was not surprising.

6.2.7.3.2 Near CD-UV

The mutants were incubated with a four to six molar equivalent of porphobilinogen at 37°C for up to forty minutes. The spectra for each were recorded, and the overlaid spectra together with those of apoenzyme, substrate-incubated apoenzyme and holoenzyme can be seen in figure 6.31.

Figure 6.31 shows that the D84A spectrum was observed to change for the phenylalanine environment on the raising of temperature from 20°C to 37°C (breakdown not shown). The change was surprising, as the spectrum moved away from that of holoenzyme. However, from then on the spectra remained unchanged, throughout the addition of porphobilinogen and the final dropping of temperature.

Figure 6.30 Far CD-UV Spectra Showing the Effect of the Addition of Porphobilinogen to the Aspartate-84 Mutants

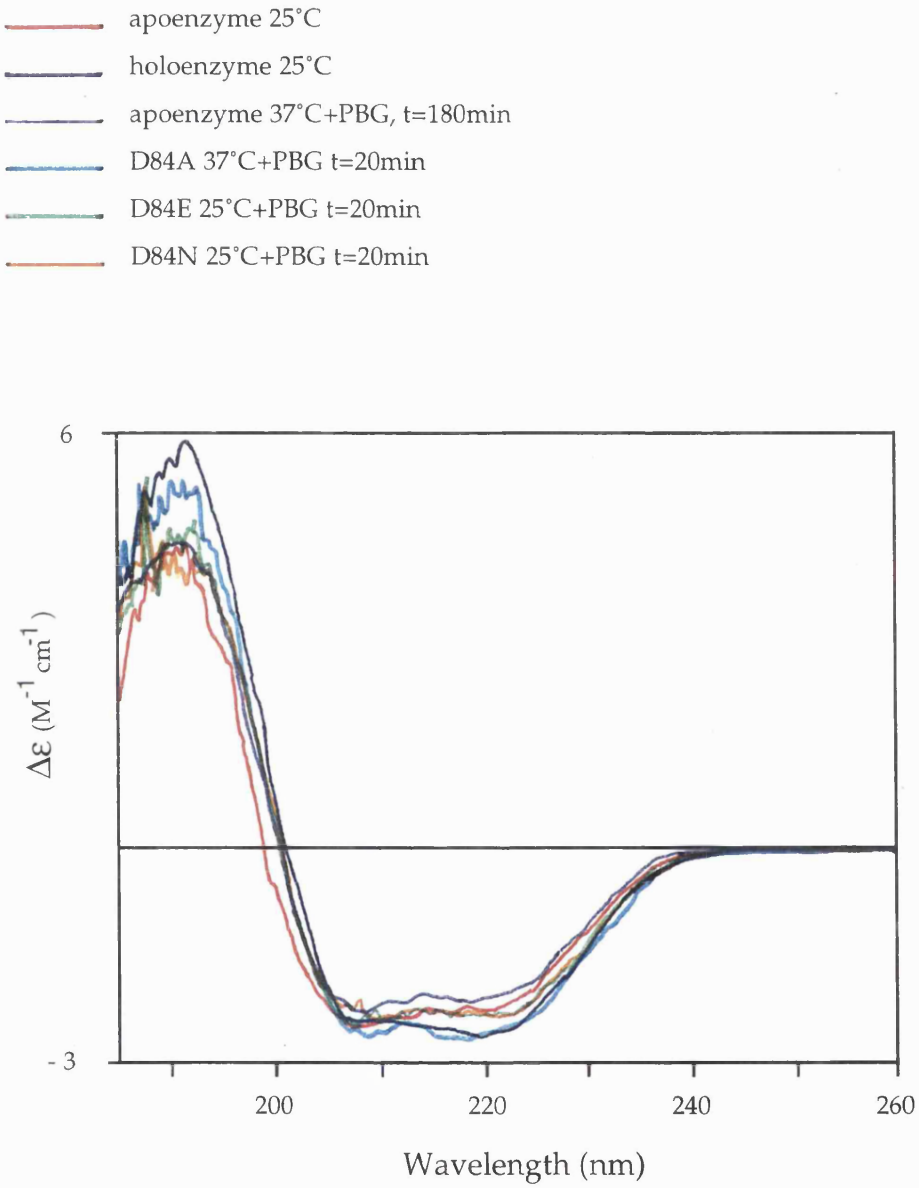

Figure 6.31 Near CD-UV Spectra Showing the Effect of the Addition of Porphobilinogen to the Aspartate-84 Mutants

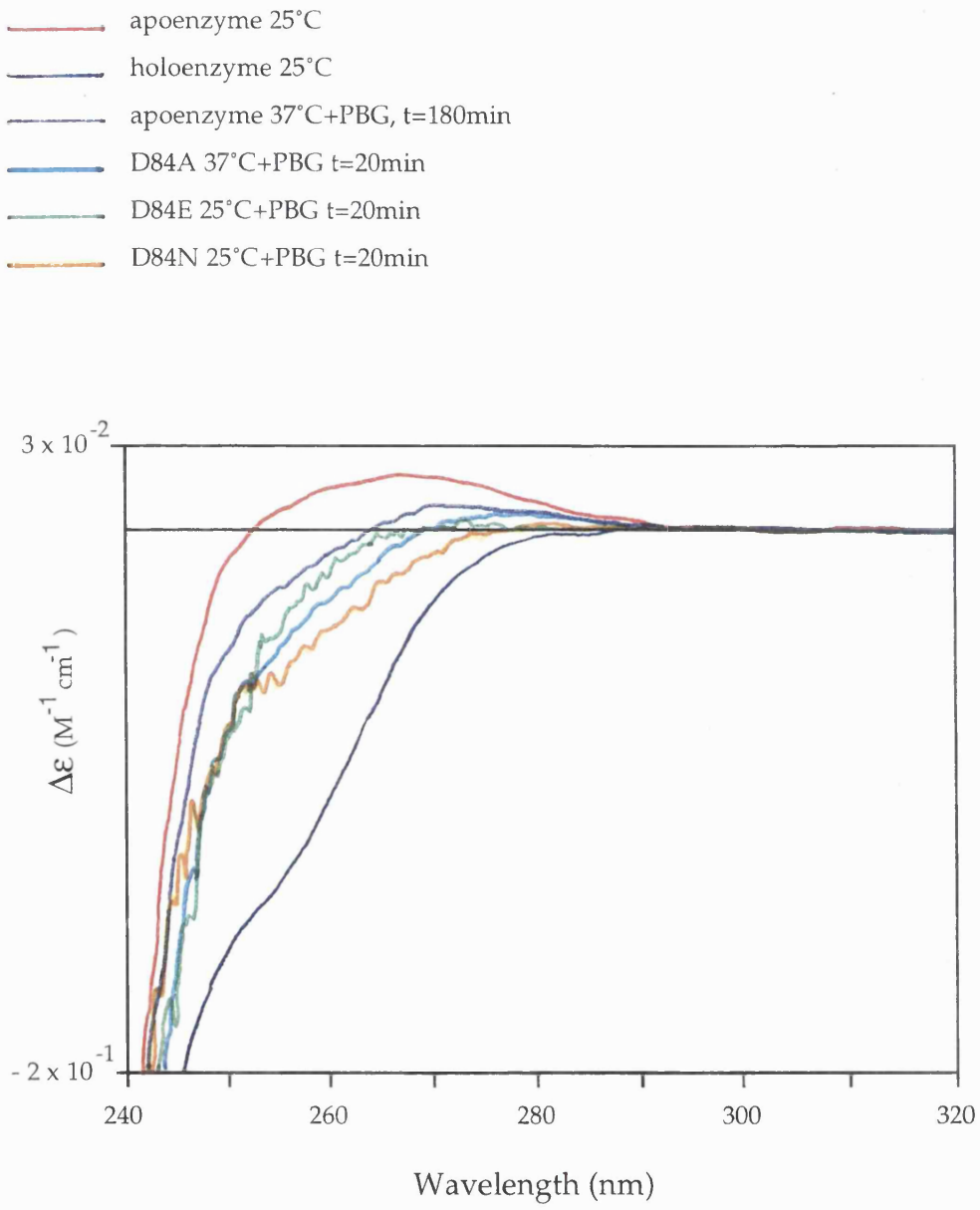

The D84E spectrum was observed to have changed in the phenylalanine environment on adding porphobilinogen at 37°C. The shift for the area of this residue was greater than that for D84A. However, as the effect of raising the temperature alone was not recorded, it could not be predicted which of the factors, temperature or substrate, had brought about the change. Again, it was surprising to observe that the change which took place moved the environment of the phenylalanine residue away from that of holoenzyme. Particularly interesting was the observation that the spectrum of substrate-incubated D84E moved very close to that of substrate-incubated apoenzyme. Subsequently, with time, no more differences in spectra were observed for D84E, and the spectra also remained unchanged on the dropping of temperature.

The D84N spectrum was observed to remain unchanged throughout this experiment.

The changes in spectra observed for these mutants on the raising of temperature and addition of porphobilinogen are difficult to interpret. The mutants D84A and D84N would be expected to behave similarly, and therefore the observation that the raising of temperature brought about a change for D84A and not D84N is surprising. The results are therefore treated as preliminary, and further experiments would be required to obtained an improved interpretation of the data.

6.3 Conclusions

The technique of CD spectroscopy has not been previously applied to porphobilinogen deaminase. The technique has proved successful, not only in confirming existing results but also in allowing different aspects of the enzyme to be studied. Whilst considerable detail of the tertiary structure of holoenzyme is known from X-ray crystallography (Louie *et al.*, 1992), the apoenzyme has been difficult to crystallise. The tool of CD spectroscopy was therefore useful in allowing the conformation of apoenzyme to be studied.

The apoenzyme has been reported to exist as an unfolded structure (Scott *et al.*, 1989). However, the CD spectroscopy studies have shown that the apoenzyme in fact contains a considerable amount of ordered secondary structure. This would suggest that the domains of apoenzyme are folded but, in the absence of cofactor, are flexible about the few contacts between them. Such an explanation would seem more likely, and the proposed open, flexible structure would still account for the unstable characteristics of apoenzyme.

The discovery that preuroporphyrinogen is the preferred substrate for apoenzyme was a major achievement of the research. In this case, CD spectroscopy studies provided an excellent means of confirming the finding. The technique allowed the conversion of apoenzyme to holoenzyme to be closely followed, and revealed that 70% reconstitution had been obtained using preuroporphyrinogen as the substrate for cofactor assembly. This percentage was the highest that had been observed for reconstitution of holoenzyme. The reconstitution was also much more rapid with preuroporphyrinogen.

The heat treatment of holoenzyme and apoenzyme was also studied. It was already known that whilst holoenzyme was heat stable at 60°C, apoenzyme was heat labile. CD spectroscopy provided the additional observation that it was not only apoenzyme that lost secondary structure at 60°C, but also holoenzyme. The difference in characteristics became apparent on cooling, when it was found that holoenzyme was able to recover its secondary structure after heat treatment. Apoenzyme was found to be unable to recover its secondary structure. It was unexpected to

find, however, that the preincubation of porphobilinogen with apoenzyme did not lessen the effects of heat treatment. It would have been anticipated that some holoenzyme would have reconstituted that would have been heat stable. The reason for the contradiction may well have been due to the different conditions used for CD spectroscopy. One of the drawbacks of the technique is the intolerance of a high concentration of porphobilinogen, which leads to high noise levels. This presented a continual problem in that the conditions used for the enzyme assay could not be faithfully represented in CD experiments, as a large excess of porphobilinogen could not be used.

The secondary structure predictions for holoenzyme examined by CD spectroscopy varied significantly in the different buffers monitored, Tris and sodium acetate. Whilst it was observed that the structure of the enzyme was 'unaltered' by the low pH of crystallisation, it appeared that the buffer of crystallisation had affected the conformation. As the enzyme has been found to be more active in Tris buffer (Warren, 1988), this finding could suggest that the crystal structure is not physiologically accurate. However, as neither buffer truly reflects *in vivo* conditions, the result remains an observation.

The structure of the holoenzyme was also examined at pH 3.7, which revealed a loss in secondary structure. It was interesting to observe that the spectra of the backbone of heated holoenzyme and holoenzyme at pH 3.7 were similar, suggesting that the enzyme had unfolded in a specific way.

Finally, the aspartate-84 mutants, D84A, D84E and D84N were also examined by CD spectroscopy. The results were unexpected in terms of the local environment of the aromatic residues, as they suggested spectra corresponding to a mix of apoenzyme and holoenzyme. The samples had all been purified by gel filtration, but had not been subjected to the f.p.l.c. system. This raised the possibilty that a percentage of the enzyme did exist as apoenzyme, as earlier observations had supported this hypothesis. The hypothesis did not, however, accommodate the far CD-UV data. The subsequent experiments of the addition of porphobilinogen to aspartate-84 mutants also gave rise to unexpected results, which were not interpreted due to their preliminary nature. These results may well prove valuable,

and therefore a fuller analysis of these mutants by CD spectroscopy would be worthwhile.

Chapter 7

Conclusions

7.1 Conclusions

The aims of this research were to : i) establish the mechanism of cofactor assembly by porphobilinogen deaminase and ii) gain insight into the manipulation of the growing polypyrrole chain by the enzyme.

The thorough characterisation of the apoenzyme allowed the first objective to be fully accomplished. As predicted, the apoenzyme is not observed to be unfolded (as reported by Scott *et al.*, 1989), but in fact found to contain a considerable percentage of secondary structure. The overall structure still appears to be open and susceptible to modification, and therefore it is likely that the domains of apoenzyme are folded, but flexible about interdomain hinges. Whilst the incorporation of the cofactor would serve to bring the three domains together through bonding, it is not expected to bring about any major conformational changes within the domains.

The most significant finding of the research is the discovery that apoenzyme preferentially binds preuroporphyrinogen rather than porphobilinogen as its substrate for cofactor assembly. On binding the hydroxymethylbilane, the enzyme-intermediate complex ES_2 is formed which can then proceed through the normal catalytic cycle to eventually yield the product, preuroporphyrinogen, and holoenzyme. The proposed mechanism of cofactor assembly is illustrated in figure 7.1.

The role of porphobilinogen for cofactor assembly is not dismissed. Initially, porphobilinogen must be used as a substrate by the apoenzyme until sufficient holoenzyme has been reconstituted. Once preuroporhyrinogen has been produced, however, the physiological role for porphobilinogen in terms of cofactor assembly is likely to be minimal. It is possible that porphobilinogen may even serve as an inhibitor of apoenzyme, competing with the hydroxymethylbilane for incorporation.

The results have suggested that porphobilinogen is bound by the apoenzyme using the same catalytic machinery as is employed by the holoenzyme. It is possible that the binding of preuroporphyrinogen is also catalysed by the same machinery. An argument against this could arise from the catalytic inactivity of the aspartate-84 mutants, D84A and D84N,

Figure 7.1 The Proposed Mechanism of the Cofactor Assembly of Porphobilinogen Deaminase

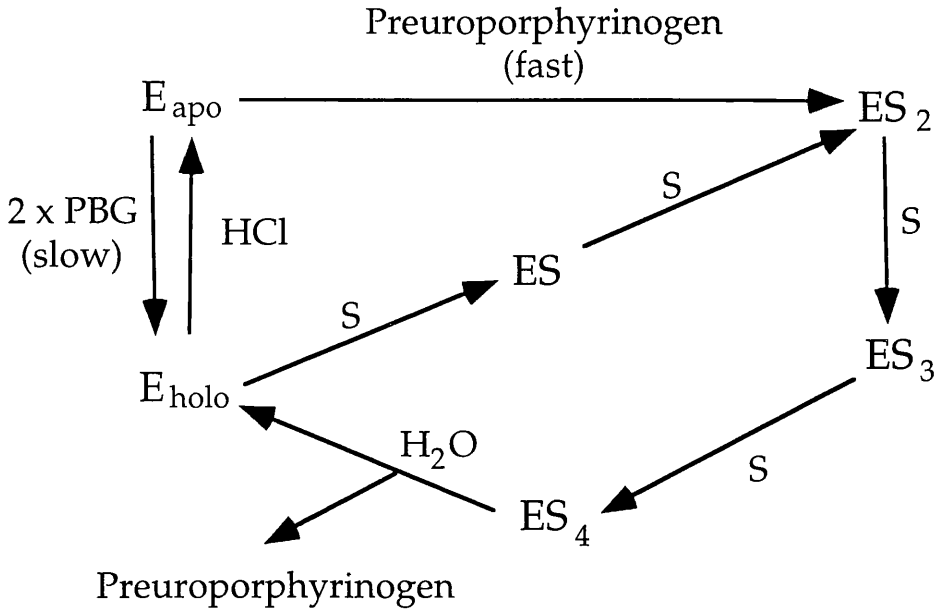

which have clearly bound preuroporphyrinogen. However, it is feasible that the binding of preuroporhyrinogen to these mutants has also been relatively low, and that it is only an artefact of the highly reactive nature of the hydroxymethylbilane that ES_2 complexes have been formed. It may well be that a large percentage of the mutants actually exist in the apoenzyme form, and therefore have not bound preuroporphyrinogen. If so, it is possible that these apoenzyme mutants would have been lost during the purification process.

It is interesting to consider why the preuroporphyrinogen is chosen as the preferred substrate for reconstituting holoenzyme. The obvious reason would appear to be that, for reaction with the residue cysteine-242, the hydroxy group serves as a better leaving group than the amino side chain of porphobilinogen. Additionally, the folding of apoenzyme around

four pyrrole rings rather than two would give the enzyme a higher chance of taking on the correct conformation. It may be that, on binding only one or two rings of porphobilinogen, the apoenzyme closes round incorrectly to yield an inactive or inefficient conformation (this may explain why no more than 40% of holoenzyme has been observed when reconstituting with porphobilinogen).

The second main aim of the research, to provide an insight into the mechanism by which the growing polypyrrole chain is accommodated by the enzyme, proved more difficult to fulfil. The model of the D84E mutant ES_2 complex was confidently modelled only for the two rings of cofactor and the first ring of substrate. If the modelling of the second ring was to be believed, however, it appeared that no conformational changes had yet taken place, although some movement would have to occur if another ring was to be accommodated. The positioning of the catalytic machinery also remained unchanged, and was not within hydrogen bonding distance of the second substrate ring. One explanation for this may have been that the constrainsts of crystallisation, such as the packing effect, may have 'forced' the enzyme into this conformation. Alternatively, the model may be physiologically correct, and this would at least explain the observation that the ES_2 complex is the most stable of the intermediates.

The commonly postulated theories for the manipulation of the polypyrrole chain include i) that the catalytic machinery moves along the chain during the elongation process and ii) that the chain itself moves, maintaining the penultimate bound ring and the incoming substrate in the vicinity of the catalytic groups. The current D84E ES_2 model does not favour either of these theories. The apparent mobility of the second substrate ring of an ES_2 complex has since been further confirmed by preliminary results of the cryocooling of the substrate-soaked D84E mutant enzyme (results not shown in thesis). The low temperatures were not found to improve the resolution for the second substrate ring. The second theory proposed for chain elongation involves the movement of the chain, suggesting that the last two rings of the polypyrrole would be bound by the arginines-131, -132, -11, -149 and -155. The mobility of the second substrate ring would make this theory less likely.

The model does, however, suggest an alternative theory. It is possible, although perhaps unlikely, that for each ring bound the

machinery moves to catalyse the binding and then returns to its original position. This would also leave the machinery in the correct place to catalyses the hydrolysis of the tetrapyrrole in the final step of the reaction. However, whilst this theory would be supported by the model, it can only be purely speculative until a confident model of an ES_2 or ES_3 enzyme-intermediate complex is obtained.

7.2 Further Work

The following experiments may provide further insights :

- A study of the rate of cofactor assembly for the D84A and D84N mutants, using preurophyrinogen as a substrate. Preliminary experiments have suggested that, *in vitro*, the hydroxymethylbilane is not incorporated by the apoenzyme mutants before the preuroporphyrinogen cyclises (results not shown in thesis). It would therefore be necessary to design a system in which preuroporphyrinogen is being constantly produced.

- Radiolabelling studies of the rate of cofactor assembly and substrate preference for wild-type apoenzyme. For this experiment, either the porphobilinogen or the preuroporphyrinogen could be labelled.

- A study of the fate of preuroporphyrinogen. It would be interesting to determine the rate at which apo-porphobilinogen deaminase competes with cosynthase for preuroporphyrinogen.

- Obtaining a crystal structure of the D84E ES_3 complex. However, the mobility of the substrate rings may present a continual problem in this area.

References

Acharya, R., Fry, E., Stuart, D., Fox, G., Rowlands, D. & Brown, F. (1989). The three-dimensional structure of foot-and-mouth disease virus at 2.9-Å resolution. *Nature*, **337**, 709-716.

Anderson, B. F., Baker, H. M., Norris, G. E., Rumball, S. V. & Baker, E. N. (1990). Apolactoferrin structure demonstrates ligand-induced conformational change in transferrins. *Nature*, **344**, 784-787.

Anderson, P. M. & Desnick, R. J. (1980). Purification and properties of uroporphyrinogen I synthase from human erythrocytes. Identification of stable enzyme-substrate intermediates. *J Biol Chem*, **255**, 1993-1999.

Aplin, R. T., Baldwin, J. E., Pichon, C., Roessner, C. A., Scott, A. I., Schofield, J., Stolowich, N. J. & Warren, M. J. (1991). Observation of enzyme bound intermediates in the biosynthesis of preuroporphyrinogen by pig deaminase. *Bioorg Medicinal Chem Lett*, **1**, 503-506.

Baker, E. N. & Lindley, P. F. (1992). New perspectives on the structure and function of transferrins. *J Inorg Biochem*, **47**, 147-160.

Baker, E. N., Rumball, S. V. & Anderson, B. F. (1987). Transferrins: insights into structure and function from studies on lactoferrin. *Trends Biochem Sci*, **12**, 350-353.

Battersby, A. R., Fookes, C. J. R., Gustafson-Potter, K. E., Matcham, G. W. J. & McDonald, E. (1979a). Proof by synthesis that unrearranged hydroxymethylbilane is the product from deaminase and the substrate for cosynthase in the biosynthesis of uro'gen III. *J Chem Soc Chem Commun*, 539-541.

Battersby, A. R., Fookes, C. J. R., Matcham, G. W. J. & McDonald, E. (1978). Biosynthesis of natural porphyrins. Enzymatic experiments on isomeric bilanes. *J Chem Soc Chem Commun*, 1064-1066.

Battersby, A. R., Fookes, C. J. R., Matcham, G. W. J. & McDonald, E. (1979b). Order of assembly of the four rings pyrrole during biosynthesis of the natural porphyrins. *J Chem Soc Chem Commun*, 539-541.

Battersby, A. R., Fookes, C. J. R., Matcham, G. W. J., McDonald, E. & Gustafson-Potter, K. E. (1979c). Biosynthesis of the natural porphyrins: experiments on the ring-closure steps with the hydroxy-analogue of porphobilinogen. *J Chem Soc Chem Commun*, 316-319.

Battersby, A. R. & Leeper, F. J. (1990). Biosynthesis of the pigments of life: mechanistic studies on the conversion of porphobilinogen to uroporphyrinogen III. *Chem Rev*, **90**, 1261-1274.

Battersby, A. R. & McDonald, E. (1976). Biosynthesis of porphyrins and corrins. *Philos Trans R Soc Lond B Biol Sci*, **273**, 161-180.

Beale, S. I. & Castelfranco, P. A. (1974). Biosynthesis of δ-aminolevulinic acid biosynthetic pathways among phototrophic bacterial groups. *Plant Physiol*, **53**, 297-303.

Beale, S. I., Foley, T. & Dzelzkalns, V. (1981). δ-Aminolevulinic acid synthase from *Euglena gracilis*. *Proc Natl Acad Sci U S A*, **78**, 1666-1669.

Beaumont, C., Porcher, C., Picat, C., Nordmann, Y. & Grandchamp, B. (1989). The mouse porphobilinogen deaminase gene. Structural organization, sequence, and transcriptional analysis. *J Biol Chem*, **264**, 14829-14834.

Billeter, M. (1992). Comparison of protein structures determined by NMR in solution and by X-ray diffraction in single crystals. *Q Rev Biophys*, **25**, 325-377.

Blacklow, S. C., Liu, K. D. & Knowles, J. R. (1991). Stepwise improvements in catalytic effectiveness: independence and interdependence in combinations of point mutations of a sluggish triosephosphate isomerase. *Biochemistry* , **30**, 8470-8476.

Blundell, T. L. & Johnson, L. (1976). *Protein crystallography*. Academic Press.

Bolivar, F., Rodriguez, R. L., Greene, P. J., Betlach, M. C., Heynaker, H. L., Boyer, H. W., Crosa, J. H. & Falkow, S. (1977). Construction and characterisation of new cloning vehicles. II. A multipurpose cloning system. *Gene*, **2**, 95-113.

Bottomley, S. S. (1982) Sideroblastic anaemia. *Clin Haematol*, **11**, 389-409.

Bottomley, S. S. & Muller-Eberhard, U. (1988). Pathophysiology of Heme Synthesis. *Semin Hematol*, **25**, 282-302.

Bradford, M. (1976). A rapid and sensitive method for the quantification of microgram quantities of protein utilising the principle of protein-dye binding. *Anal Biochem*, **72**, 248-254.

Brownlie, P. D., Lambert, R., Louie, G. V., Jordan, P. M., Blundell, T. L., Warren, M. J., Cooper, J. B. & Wood, S. P. (1994). The three-dimensional structures of mutants of porphobilinogen deaminase: toward an understanding of the structural basis of acute intermittent porphyria. *Protein Sci*, **3**, 1644-1650.

Chretien, S., Dubart, A., Beaupain, D., Raich, N., Grandchamp, B., Rosa, J., Goossens, M. & Romeo, P. H. (1988). Alternative transcription and splicing of the human porphobilinogen deaminase gene result either in tissue-specific or in housekeeping expression. *Proc Natl Acad Sci U S A*, **85**, 6-10.

Clemens, K. R., Pichon, C., Jacobson, A. R., Yon-Hin, P., Gonzalez, M. D. & Scott, A. I. (1994). Systematic specificity studies on porphobilinogen deaminase. *Bioorg Medicinal Chem Letter*, **4**, 521-524.

Correa-Garcia, S. R., Rossetti, M. V. & Batlle, A. M. (1991). Studies on porphobilinogen-deaminase from *Saccharomyces cerevisiae*. *Z Naturforsch C*, **46**, 1017-1023.

Danchin, A. & Lenzen, G. (1988). Structure and evolution of bacterial adenylate cyclase: comparison between *Escherichia coli* and *Erwina chrysanthemi*. *Second Messengers Phosphoproteins*, **12**, 7-28.

Davies, R. C. & Neuberger, A. (1973). Polypyrroles formed from porphobilinogen and amines by uroporphyrinogen synthetase of *Rhodopseudomonas spheroides*. *Biochem J*, **133**, 471-492.

Delfau, M. H., Picat, C., de-Rooij, F. W., Hamer, K., Bogard, M., Wilson, J. H., Deybach, J. C., Nordmann, Y. & Grandchamp, B. (1990). Two different point G to A mutations in exon 10 of the porphobilinogen deaminase gene are responsible for acute intermittent porphyria. *J Clin Invest*, **86**, 1511-1516.

Desnick, R. J., Ostasiewicz, L. T., Tishler, P. A. & Mustajoki, P. (1985). Acute intermittent porphyria: characterization of a novel mutation in the structural gene for porphobilinogen deaminase. Demonstration of noncatalytic enzyme intermediates stabilized by bound substrate. *J Clin Invest*, **76**, 865-874.

Eisenberg, D. & Hill, C. (1989). Protein crystallography: more surprises ahead. *Trends Biochem Sci*, **14**, 260-264.

Elder, G. H. (1982). Enzymatic defects in porphyria: an overview. *Semin Liver Dis*, **2**, 87-99.

Elder, G. H., Evans, J. O. & Thomas, N. (1976). The primary enzyme defect in hereditary coproporphyria. *Lancet*, **2**, 1217-1219.

Fabiano, E. & Golding, B. T. (1991). On the mechanism of pyrrole formation in the Knorr pyrrole synthesis and by porphobilinogen synthase. *J Chem Soc Perk Trans 1*, **12**, 3371-3375.

Frydman, B., Frydman, R. B., Valasinas, A., Levy, E. S. & Feinstein, G. (1976). Biosynthesis of uroporphyrinogens from porphobilinogen: mechanism and the nature of the process. *Philos Trans R Soc Lond B Biol Sci*, **273**, 137-160.

Frydman, R. B. & Feinstein, G. (1974). Studies on porphobilinogen deaminase and uroporphyrinogen III cosynthase from human erythrocytes. *Biochim Biophys Acta*, **350**, 358-373.

Frydman, R. B., Levy, E. S., Valasinas, A. & Frydman, B. (1978). Biosynthesis of uroporphyrinogens. Interaction among 2-aminomethyldipyrrylmethanes and the enzymatic system. *Biochemistry*, **17**, 110-120.

Fuesler, T. P., Castelfranco, P. A. & Wong, Y.-S. (1984). Formation of Mg-containing chlorophyll precursors from protoporphyrin IX, δ-aminolevulinic acid, and glutamate in isolated, photosyntheticallly competent, developing chloroplasts. *Plant Physiol*, **74**, 928-933.

Gacesa, P. & Ramji, D. P. (1994). *Vectors.* Chichester: Wiley.

Grandchamp, B., De-Verneuil, H., Beaumont, C., Chretien, S., Walter, O. & Nordmann, Y. (1987). Tissue-specific expression of porphobilinogen deaminase. Two isoenzymes from a single gene. *Eur J Biochem*, **162**, 105-110.

Greenfield, N. & Fasman, G. (1969). Computed circular dichroism spectra for the evaluation of protein conformation. *Biochemistry*, **8**, 4108-4116

Hadener, A., Alefounder, P. R., Hart, G. J., Abell, C. & Battersby, A. R. (1990). Investigation of putative active-site lysine residues in hydroxymethylbilane synthase. Preparation and characterization of mutants in which (a) Lys-55, (b) Lys-59 and (c) both Lys-55 and Lys-59 have been replaced by glutamine. *Biochem J*, **271**, 487-491.

Hadener, A., Matzinger, P. K., Malashkevich, V. N., Louie, G. V., Wood, S. P., Oliver, P., Alefounder, P. R., Pitt, A. R., Abell, C. & Battersby, A. R. (1992). Purification, characterisation, crystallisation and X-ray analysis of selenomethionyl hydroxymethylbilane synthase from *Escherichia coli*. *Eur J Biochem*, **211**, 615-624.

Hamfelt, A. & Wetterberg, L. (1969). Pyridoxal phosphate in acute intermittent porphyria. *Ann NY Acad Sci*, **166**, 361-364.

Hart, G. J., Abell, C. & Battersby, A. R. (1986). Purification, N-terminal amino acid sequence and properties of hydroxymethylbilane synthase (porphobilinogen deaminase) from *Escherichia coli. Biochem J*, **240**, 273-276.

Hart, G. J., Leeper, F. J. & Battersby, A. R. (1984). Modification of hydroxymethylbilane synthase (porphobilinogen deaminase) by pyridoxal 5'-phosphate. Demonstration of an essential lysine residue. *Biochem J*, **222**, 93-102.

Hart, G. J., Miller, A. D. & Battersby, A. R. (1988). Evidence that the pyrromethane cofactor of hydroxymethylbilane synthase (porphobilinogen deaminase) is bound through the sulphur atom of a cysteine residue. *Biochem J*, **252**, 909-912.

Hart, G. J., Miller, A. D., Leeper, F. J. & Battersby, A. R. (1987). Biosynthesis of the natural porphyrins: proof that hydroxymethylbilane synthase (porphobilinogen deaminase) uses a novel binding group in its catalytic action. *J Chem Soc Chem Commun*, 1762-1765.

Hayashi, N. (1987). Heme biosynthesis and its regulation. *Tanpakushitsu Kakusan Koso*, **32**, 797-814.

Higuchi, M. & Bogorad, L. (1975). The purification and properties of uroporphyrinogen I synthases and uroporphyrinogen III cosynthase. Interactions between the enzymes. *Ann N Y Acad Sci*, **244**, 401-418.

Jencks, W. P. (1975). Binding energy, specificity, and enzymic catalysis: the Circe Effect. *Adv Enzymol Relat Areas Mol Biol*, **43**, 219-410.

Johnson, W. C. (1990). Protein structure and circular dichroism : a practical guide. *Proteins*, **7**, 205-214.

Jones, R. M. & Jordan, P. M. (1994). Purification and properties of porphobilinogen deaminase from *Arabidopsis thaliana. Biochem J*, **299**, 895-902.

Jordan, P. M. (1991). *Biosynthesis of Tetrapyrroles*. Amsterdam: Elsevier.

Jordan, P. M. & Berry, A. (1980). Preuroporphyrinogen, a universal intermediate in the biosynthesis of uroporphyrinogen III. *Febs Lett*, **112**, 86-88.

Jordan, P. M. & Berry, A. (1981). Mechanism of action of porphobilinogen deaminase. The participation of stable enzyme substrate covalent intermediates between porphobilinogen and the porphobilinogen deaminase from *Rhodopseudomonas spheroides. Biochem J*, **195**, 177-181.

Jordan, P. M., Burton, G., Nordlov, H., Schneider, M. M., Pryde, L. M. & Scott, A. I. (1979). Preuroporphyrinogen, a substrate for uroporphyrinogen III cosynthase. *J Chem Soc Chem Comm*, 204-205.

Jordan, P. M. & Seehra, J. S. (1979). The biosynthesis of uroporphyrinogen III: order of assembly of the four porphobilinogen molecules in the formation of the tetrapyrrole ring. *Febs Lett*, **104**, 364-366.

Jordan, P. M. & Seehra, J. S. (1986). Purification of porphobilinogen synthase from bovine liver. *Methods Enzymol*, **123**, 427-434.

Jordan, P. M. & Shemin, D. (1973). Purification and properties of uroporphyrinogen I synthetase from *Rhodopseudomonas spheroides*. *J Biol Chem*, **248**, 1019-1024.

Jordan, P. M., Thomas, S. D. & Warren, M. J. (1988). Purification, crystallization and properties of porphobilinogen deaminase from a recombinant strain of *Escherichia coli* K12. *Biochem J*, **254**, 427-435.

Jordan, P. M. & Warren, M. J. (1987). Evidence for a dipyrromethane cofactor at the catalytic site of *Escherichia coli* porphobilinogen deaminase. *FEBS Lett*, **225**, 87-92.

Jordan, P. M., Warren, M. J., Mgbeje, B. I., Wood, S. P., Cooper, J. B., Louie, G., Brownlie, P., Lambert, R. & Blundell, T. L. (1992). Crystallization and preliminary X-ray investigation of *Escherichia coli* porphobilinogen deaminase. *J Mol Biol*, **224**, 269-271.

Jordan, P. M. & Woodcock, S. C. (1991). Mutagenesis of arginine residues in the catalytic cleft of *Escherichia coli* porphobilinogen deaminase that affects dipyrromethane cofactor assembly and tetrapyrrole chain initiation and elongation. *Biochem J*, **280**, 445-449.

Kannangara, C. G., Gough, S. P., Bruyant, P., Hoober, J. K., Kahn, A. & von-Wettstein, D. (1988). $tRNA^{Glu}$ as a cofactor in δ-aminolevulinate biosynthesis: steps that regulate chlorophyll synthesis. *Trends Biochem Sci*, **13**, 139-143.

Keng, T., Richard, C. & Larocque, R. (1991). Structure and regulation of yeast *HEMS'* the gene for porphobilinogen deaminase. *Mol Gen Genetics*, **234**, 233-243.

Kunkel, T.A., Roberts, J.D. & Zakour, R.A. (1987). Rapid and efficient site-specific mutagenesis without phenotypic selection. *Methods Enzymol*, **154**, 367-382.

Knowles, J. R. (1991). To build an enzyme.... *Phil Trans Roy Soc Lon*, **332**, 115-121.

Lander, M., Pitt, A. R., Alefounder, P. R., Bardy, D., Abell, C. & Battersby, A. R. (1991). Studies on the mechanism of hydroxymethylbilane synthase concerning the role of arginine residues in substrate binding. *Biochem J*, **275**, 447-452.

Leeper, F. J. (1985). The biosynthesis of porphyrins, chlorophylls, and vitamin B12. *Nat Prod Rep*, **2**, 561-580.

Lennox, E. S. (1955). Transduction of linked genetic characters of the host by bacteriophage PI. *Virology*, **1**, 190-206.

Li, J. M., Umanoff, H., Proenca, R., Russell, C. S. & Cosloy, S. D. (1988). Cloning of the *Escherichia coli* K-12 hemB gene. *J Bacteriol*, **170**, 1021-1025.

Llewellyn, D. H., Scobie, G. A., Urquhart, A. J., Harrison, P. R. & Elder, G. H. (1992). Splice-defective mutations of the porphobilinogen deaminase gene responsible for acute intermittent porphyria. *Neth J Med*, **42**, A28.

Louie, G. V. (1993). Porphobilinogen deaminase and its structural similarity to the periplasmic binding protein. *Curr Opin Struct Biol*, **3**, 401-408.

Louie, G. V. & Brayer, G. D. (1990). High-resolution refinement of yeast iso-1cytochrome c and comparisons with other eukaryotic cytochromes c. *J Mol Biol*, **214**, 527-555.

Louie, G. V., Brownlie, P. D., Lambert, R., Cooper, J. B., Blundell, T. L., Wood, S. P., Warren, M. J. & Jordan, P. M. (1996). The three-dimensional structure of *Escherichia coli* porphobilinogen deaminase at 1.76-Å resolution. *Proteins*, **25**, 48-78.

Louie, G. V., Brownlie, P. D., Lambert, R., Cooper, J. B., Blundell, T. L., Wood, S. P., Warren, M. J., Woodcock, S. C. & Jordan, P. M. (1992). Structure of porphobilinogen deaminase reveals a flexible multidomain polymerase with a single catalytic site. *Nature*, **359**, 33-39.

Mauzerall, D. & Granick, S. (1956). The occurrence and determination of δ-aminolevulinic acid and porphobilinogen in urine. *J Biol Chem*, **219**, 435-446.

Mazzetti, M. B. & Tomio, J. M. (1990). Kinetic and molecular parameters of human hepatic porphobilinogen deaminase. *Biochem Int*, **21**, 463-471.

Mgbeje, B.I.A. (1990). *Molecular biology and enzymology of the hemD locus of Escherichia coli K-12*. PhD Thesis. University of Southampton.

McPherson, A. (1982). Preparation and analysis of protein crystals. New York: Wiley.

Meisler, M., Wanner, L., Eddy, R. E. & Shows, T. B. (1980). The UPS locus encoding uroporphyrinogen I synthase is located on human chromosome 11. *Biochem Biophys Res Commun*, **95**, 170-176.

Messing, J. (1983). "New M13 vectors for cloning" *Methods Enzymol*, **101**, 20-78.

Mgone, C. S., Lanyon, W. G., Moore, M. R. & Connor, J. M. (1992). Detection of seven point mutations in the porphobilinogen deaminase gene in patients with acute intermittent porphyria, by direct sequencing of in vitro amplified cDNA. *Hum Genet*, **90**, 12-16.

Miller, A. D., Hart, G. J., Packman, L. C. & Battersby, A. R. (1988). Evidence that the pyrromethane cofactor of hydroxymethylbilane synthase (porphobilinogen deaminase) is bound to the protein through the sulphur atom of cysteine-242. *Biochem J*, **254**, 915-918.

Miller, A. D., Packman, L. C., Hart, G. J., Alefounder, P. R., Abell, C. & Battersby, A. R. (1989). Evidence that pyridoxal phosphate modification of lysine residues (Lys-55 and Lys-59) causes inactivation of hydroxymethylbilane synthase (porphobilinogen deaminase). *Biochem J*, **262**, 119-124.

Nordmann, Y., de-Verneuil, H., Deybach, J. C., Delfau, M. H. & Grandchamp, B. (1990). Molecular genetics of porphyrias. *Ann Med*, **22**, 387-391.

Oh, B.-H., Pandit, J., Kang, C.-H., Nikaido, K., Gokcen, S., Ames, G. F.-L. & Kim, S.-H. (1993). Three-dimensional structures of the periplasmic lysine/arginine/ornithine-binding protein with and without a ligand. *J Biol Chem*, **268**, 11348-11355.

Petricek, M., Rutberg, L., Schroder, I. & Hederstedt, L. (1990). Cloning and characterization of the hemA region of the *Bacillus subtilis* chromosome. *J Bacteriol*, **172**, 2250-2258.

Petsko, G. A. (1975). Protein crystallography at sub-zero temperatures: cryo-protective mother liquors for protein crystals. *J Mol Biol*, **96**, 381-392.

Picat, C., Bourgeois, F. & Grandchamp, B. (1991). PCR detection of a C/T polymorphism in exon 1 of the porphobilinogen deaminase gene (PBGD). *Nucleic Acids Res*, **19**, 5099-5099.

Pichon, C., Clemens, K. R., Jacobsen, A. R. & Scott, A. I. (1992). On the mechanism of porphobilinogen deaminase: design, synthesis, and enzymatic reactions of novel porphobilinogen analogues. *Tetrahedron*, **23**, 4687-4712.

Plusec, J. & Bogorad, L. (1970). A dipyrrolic intermediate in the enzymatic synthesis of uroporphyrinogen. *Biochemistry*, **9**, 4736-4743.

Quiochio, F. A. (1991). Atomic structures and function of periplasmic receptors for active transport and chemotaxis. *Curr Opin Struct Biol*, **1**, 922-933.

Radmer, R. & Bogorad, L. (1972). A tetrapyrrylmethane intermediate in the enzymatic synthesis of uroporphyrinogen. *Biochemistry*, **11**, 904-910.

Raich, N., Romeo, P. H., Dubart, A., Beaupain, D., Cohen-Solal, M. & Goossens, M. (1986). Molecular cloning and complete primary sequence of human erythrocyte porphobilinogen deaminase. *Nucleic Acids Res*, **14**, 5955-5968.

Rhodes, G. (1993). *Crystallography made crystal clear*. London: Academic Press.

Rosenberg, J. M. (1991). Structure and function of restriction endonucleases. *Curr Opin Struct Biol*, **1**, 104-113.

Russell, C. S. & Rockwell, P. (1980). The effects of sulfhydryl reagents on the activity of wheat germ uroporphyrinogen I synthase. *Febs Lett*, **116**, 199-202.

Sack, J. S., Trakhanov, S. D., Tsigannik, I. H. & Quiocho, F. A. (1989). Structure of the L-leucine-binding protein refined at 2.4 Å resolution and comparison with the Leu/Ile/Val-binding protein structure. *J Mol Biol*, **206**, 193-207.

Scobie, G. A., Urquhart, A. J., Elder, G. H., Kalsheker, N. A., Llewellyn, D. H., Smyth, J. & Harrison, P. R. (1990). Linkage disequilibrium between DNA polymorphisms within the porphobilinogen deaminase gene. *Hum Genet*, **85**, 157-159.

Scott, A. I., Clemens, K. R., Stolowich, N. J., Santander, P. J., Gonzalez, M. D. & Roessner, C. A. (1989). Reconstitution of apo-porphobilinogen deaminase: structural changes induced by cofactor binding. *Febs Lett*, **242**, 319-324.

Scott, A. I., Roessner, C. A., Stolowich, N. J., Karuso, P., Williams, H. J., Grant, S. K., Gonzalez, M. D. & Hoshino, T. (1988). Site-directed mutagenesis and high-resolution NMR spectroscopy of the active site of porphobilinogen deaminase. *Biochemistry*, **27**, 7984-7990.

Sharif, A. L., Smith, A. G. & Abell, C. (1989). Isolation and characterisation of a cDNA clone for a chlorophyll synthesis enzyme from *Euglena gracilis*. The chloroplast enzyme hydroxymethylbilane synthase (porphobilinogen deaminase) is synthesised with a very long transit peptide in *Euglena*. *Eur J Biochem*, **184**, 353-359.

Shashidhara, L. S., Lim, S. H., Shackleton, J. B., Robinson, C. & Smith, A. G. (1992). Protein targeting across the three membranes of the *Euglena* chloroplast envelope. *J Biol Chem*, **267**, 12885-12891.

Shashidhara, L. S. & Smith, A. G. (1991). Expression and subcellular location of the tetrapyrrole synthesis enzyme porphobilinogen deaminase in light-grown *Euglena gracilis* and three nonchlorophyllous cell lines. *Proc Natl Acad Sci U S A*, **88**, 63-67.

Shemin, S. & Rittenberg, D. (1945). Utilization of glycine for synthesis of porphyrin. *J Biol Chem*, **159**, 567-568.

Shioi, Y., Nagamine, M., Kuroki, M. & Sasa, T. (1980). Purification by affinity chromatography and properties of uroporphyrinogen I synthetase from *Chlorella regularis*. *Biochim Biophys Acta*, **616**, 300-309.

Siligardi, G., Drake, A. F., Mascagni, P., Rowlands, D., Brown, F. & Gibbons, W. A. (1991). Correlations between the conformations elucidated by CD spectroscopy and the antigenic properties of four peptides of the foot-and-mouth disease virus. *Eur J Biochem*, **199**, 545-551.

Spano, A. J. & Timko, M. P. (1991). Isolation, characterization and partial amino acid sequence of a chloroplast-localized porphobilinogen deaminase from pea (*Pisum sativum L.*). *Biochim Biophys Acta*, **1076**, 29-36.

Spurlino, J., Lu, G.-Y. & Quiocho, F. A. (1991). The 2.3-Å resolution structure of the maltose- or maltodextrin-binding protein, a primary receptor of bacterial active transport and chemotaxis. *J Biol Chem*, **266**, 5202-5219.

Strand, L. J., Meyer, U. A., Felsher, B. F., Redeker, A. G. & Marver, H. S. (1972). Decreased red cell uroporphyrinogen I synthase activity in intermittent acute porphyria. *J Clin Invest*, **51**, 2530-2536.

Strickland, E. H. (1974). Aromatic contributions to circular dichroism spectra of proteins. *Crit Rev Biochem*, **2**, 113-175.

Stubnicer, A. C., Picat, C. & Grandchamp, B. (1988). Rat porphobilinogen deaminase cDNA: nucleotide sequence of the erythropoietic form. *Nucleic Acids Res*, **16**, 3102.

Sweeney, V. P., Pathak, M. A. & Asbury, A. K. (1970). Acute intermittent porphyria. Increased ALA-synthetase activity during an acute attack. *Brain*, **93**, 369-380.

Thomas, S. D. & Jordan, P. M. (1986). Nucleotide sequence of the *hem*C locus encoding porphobilinogen deaminase of *Escherichia coli* K12. *Nucleic Acids Res*, 14, 6215-6226.

Tunnacliffe, A. & McGuire, R. S. (1990). A physical linkage group in human chromosome band 11q23 covering a region implicated in leukocyte neoplasia. *Genomics*, **8**, 447-453.

Wang, A. L., Arredondo-Vega, F. X., Giampietro, P. F., Smith, M., Anderson, W. F. & Desnick, R. J. (1981). Regional gene assignment of human porphobilinogen deaminase and esterase A4 to chromosome 11q23 leads to 11qter. *Proc Natl Acad Sci U S A*, **78**, 5734-5738.

Warren, M.J. (1988). *Investigations into the mechanism of porphobilinogen deaminase*. PhD Thesis. University of Southampton.

Warren, M. J., Gul, S., Aplin, R. T., Scott, A. I., Roessner, C. A., O'Grady, P. & Shoolingin-Jordan, P. M. (1995). Evidence for conformational changes in *Escherichia coli* porphobilinogen deaminase during stepwise pyrrole chain elongation monitored by increased reactivity of cysteine-134 to alkylation by N-ethylmaleimide. *Biochemistry*, **34**, 11288-11295.

Warren, M. J. & Jordan, P. M. (1988). Investigation into the nature of substrate binding to the dipyrromethane cofactor of *Escherichia coli* porphobilinogen deaminase. *Biochemistry*, **27**, 9020-9030.

Warren, M. J. & Scott, A. I. (1990). Tetrapyrrole assembly and modification into the ligands of biologically functional cofactors. *Trends Biochem Sci*, **15**, 486-491.

Weinstein, J. D. & Beale, S. I. (1983). Separate physiological roles and subcellular compartments for two tetrapyrrole biosynthetic pathways in *Euglena gracilis*. *J Biol Chem*, **258**, 6799-6807.

Williams, D. C., Morgan, G. S., McDonald, E. & Battersby, A. R. (1981). Purification of porphobilinogen deaminase from *Euglena gracilis* and studies of its kinetics. *Biochem J*, **193**, 301-310.

Witty, M., Wallace-Cook, A. D., Albrecht, H., Spano, A. J., Michel, H., Shabanowitz, J., Hunt, D. F., Timko, M. P. & Smith, A. G. (1993). Structure and expression of chloroplast-localized porphobilinogen deaminase from pea (*Pisum sativum L.*) isolated by redundant polymerase chain reaction. *Plant Physiol*, **103**, 139-147.

Woodcock, S.C. (1992). *Studies on the mechanism of porphobilinogen deaminase using site directed mutagenesis*. PhD Thesis. University of Southampton.

Woodcock, S. C. & Jordan, P. M. (1994). Evidence for participation of aspartate-84 as a catalytic group at the active site of porphobilinogen deaminase obtained by site-directed mutagenesis of the *hem*C gene from *Escherichia coli*. *Biochemistry*, **33**, 2688-2695.

Yoo, H. W., Warner, C. A., Chen, C. H. & Desnick, R. J. (1993). Hydroxymethylbilane synthase: complete genomic sequence and amplifiable polymorphisms in the human gene. *Genomics*, **15**, 21-29.